DOT/FAA/AR-10/15

Air Traffic Organization
NextGen & Operations Planning
Office of Research and
Technology Development
Washington, DC 20591

The Evaluation of Red-Dye Contamination in Jet Fuel and the Identification of a Screening Method for Thermal Stability Issues

July 2010

Final Report

This document is available to the U.S. public through the National Technical Information Services (NTIS), Springfield, Virginia 22161.

This document is also available from the Federal Aviation Administration William J. Hughes Technical Center at actlibrary.tc.faa.gov.

U.S. Department of Transportation
Federal Aviation Administration

NOTICE

Technical Report Documentation Page

1. Report No.	2. Government Accession No.	3. Recipient's Catalog No.
DOT/FAA/AR-10/15		

4. Title and Subtitle	5. Report Date
THE EVALUATION OF RED-DYE CONTAMINATION IN JET FUEL AND THE IDENTIFICATION OF A SCREENING METHOD FOR THERMAL STABILITY ISSUES	July 2010
	6. Performing Organization Code

7. Author(s)	8. Performing Organization Report No.
Clifford A. Moses, Ph.D., George Wilson, and James Johnson	

9. Performing Organization Name and Address	10. Work Unit No. (TRAIS)
Fuels and Lubricants Technology Department Southwest Research Institute® 6220 Culebra Road San Antonio, TX 78238	11. Contract or Grant No.

12. Sponsoring Agency Name and Address	13. Type of Report and Period Covered
U.S. Department of Transportation Federal Aviation Administration Air Traffic Organization NextGen & Operations Planning Office of Research and Technology Development Washington, DC 20591	Final Report
	14. Sponsoring Agency Code ANE-110

15. Supplementary Notes

The Federal Aviation Administration Airport and Aircraft Safety R&D Division COTR was Skip Byrnes.

16. Abstract

An experimental study was conducted to quantify the effects of red-dye contamination on the thermal stability of jet fuel and subsequent fouling rates of critical fuel system components. The effect of red-dye contamination on fouling rate is linear, but each nozzle has a different slope. A concentration of 0.55 mg/L caused a four-fold increase in the fouling rate of the most sensitive nozzle. The effect of a concentration just above the visible level, 0.055 mg/L, was measurable. The results are to be used by the aircraft engine manufacturers to define the minimum acceptable level of red-dye contamination in jet fuel.

A methodology was developed based on the determination of the fouling rate of fuel nozzles, which can be used to evaluate the effect of additives and contaminants.

17. Key Words	18. Distribution Statement
Jet fuel contamination, Thermal stability, Red dye	This document is available to the U.S. public through the National Technical Information Service (NTIS), Springfield, Virginia 22161. This document is also available from the Federal Aviation Administration William J. Hughes Technical Center at actlibrary.tc.faa.gov.

19. Security Classif. (of this report)	20. Security Classif. (of this page)	21. No. of Pages	22. Price
Unclassified	Unclassified	144	

ACKNOWLEDGMENTS

This work was supported by the U.S. Federal Aviation Administration, Airworthiness Assurance Branch, Atlantic City International Airport, N.J. under contract DTFA03-98-C-00028, with Mr. Skip Byrnes serving as the technical monitor. Significant funding for this program was also provided by the U.S. Defense Energy Support Center, the U.S. Internal Revenue Service, the Airline Transport Association, the American Petroleum Institute, and the original equipment manufacturers Boeing, General Electric, Honeywell, Pratt & Whitney, and Rolls-Royce. The test fuels for the hardware fouling tests were provided by the U.S. Defense Energy Support Center.

The authors wish to thank the following oil companies for providing the fuel samples used in this evaluation:

- Amoco Corporation
- Atlantic Richfield Company
- Ashland, Inc.
- BP, p.l.c.
- Chevron Corporation
- Citgo Petroleum Corporation
- Exxon Mobil Corporation
- Conoco Phillips Company
- Shell - Royal Dutch Shell p.l.c.
- Sunoco, Inc.

(Note: Some of these companies have merged and/or changed names between the time of the sample collection and the time of this writing.)

The authors wish also to thank the many technicians who set up and conducted the hardware tests for their valuable contributions. In particular, Chad Vollmer was instrumental in setting up the nozzle fouling tests and the data acquisition programs. Clay Davis and Mike Gass worked out many of the problems of modifying and instrumenting the fuel nozzles. Jay Johnson worked out many of the problems in setting up the spool valve and filter test rigs. Other technicians worked evening and night shifts for many months to conduct the hundreds of tests.

A special thanks to Wendy Mills for putting the report in final form.

TABLE OF CONTENTS

LIST OF FIGURES

LIST OF TABLES

LIST OF ACRONYMS

APU	Auxiliary power unit
CRC	Coordinating Research Council
DLA	Diesel lubricity additives
ETA	Elipsometric Tube Analyzer
FAME	Fatty-acid methyl esters
FIA	Fluorescence Indicator Absorption
FN	Flow number
FR	Fouling rate
GE	General Electric
HSDSR	High-sulfur diesel reference fuel
JFTOT	Jet Fuel Thermal Oxidation Tester
OEM	Original equipment manufacturer
PAC	Program Advisory Committee
SFC	Super-critical chromatography
SwRI	Southwest Research Institute®

EXECUTIVE SUMMARY

An experimental study of the effect of diesel fuel red-dye contamination on the thermal stability of jet fuel was performed by the Federal Aviation Administration with multiple sponsorships, including the U.S. Defense Energy Support Center, the Airline Transport Association, the engine and airframe manufacturers, and the American Petroleum Institute. The program had two objectives:

- To quantify the effect of red-dye contamination on fuel thermal stability
- To identify and validate a methodology for evaluating thermal stability issues

The effort to meet the first objective consisted of two phases:

- A screening effort to identify and select a test fuel that had a thermal stability that was sensitive to red dye

- A series of fuel system hardware tests to quantify the effect of red dye on fouling life

This report summarizes the results of fouling tests on critical fuel system components, i.e., fuel nozzles, fuel control spool valves, and torque motor filter screens. Nine different types of fuel nozzles were involved, representing large and small engines from commercial and military aircraft.

Test results showed that 0.55 mg/L of red dye can lower the Jet Fuel Thermal Oxidation Tester breakpoint by 10° to 15°C and cause as much as a four-fold increase in the fouling rate of fuel nozzles. This is the concentration of dye that would be present if the jet fuel were contaminated with 5% fully dyed diesel fuel. Supplemental tests showed the increase in fouling rate was linear with red-dye concentration. A concentration of 0.055 mg/L, i.e., just above the visible limit, caused a measurable increase in fouling rate in the most sensitive nozzle.

It is recommended that the aircraft engine manufacturers use the results presented on the effect of red-dye concentration on nozzle fouling rates to develop an industry consensus on the minimum acceptable level of red-dye contamination in jet fuel.

This project has demonstrated that the fouling rates of fuel nozzles, as well as other components of the fuel system, can be quantified and correlated with the thermal stability of the jet fuel. This methodology has provided a basis for evaluating the effect of red-dye contamination on the fouling rate of the hardware. The same methodology can be applied to evaluating future thermal stability issues with other fuel contaminants or in the qualification of new fuel additives.

1. INTRODUCTION.

Since 1994, the United States Internal Revenue Service has required that nontaxed diesel fuel, including home heating oil, be dyed with a strong red dye to differentiate nontaxable fuel from taxable diesel fuel used on the highways. In the United States, diesel fuel and home heating oil are transported through multiproduct pipelines that also carry jet fuel. The pipeline companies vigorously attempt to avoid contamination of the jet fuel shipment with other products, but occasionally accidental contaminations occur. Sometimes these accidental contaminations go undetected because the fuel properties that the airport evaluates remain within specification limits. However, contamination by red-dyed diesel fuel can be detected visually due to the pink color of the fuel during the standard "white bucket test" (ASTM D 6986).

Normally, this pink color would be associated with a contamination by diesel fuel/fuel oil, but there could be situations where the dye was accidentally added to a batch of jet fuel. In either case, pink fuel suggests a contaminated product. However, there are two situations in which a fuel exhibits a pink color that is not caused by red-dye contamination: (1) refinery carry-overs can temporarily give jet fuel a pinkish color; this coloring disappears when exposed to light and (2) aging can also cause discoloration that does not disappear under strong light and can be interpreted as containing red coloration.

Red-dye levels as low as 0.040 mg/L are visible to the naked eye, although there can be individual sensitivities and color biases. Several test methods have been developed to measure red-dye concentration. The most commonly used is the Petrospec JT100.

Once the fuel is known to be contaminated, it is no longer acceptable as jet fuel and must be downgraded, i.e., reclassified to a nonaviation fuel. As the pipelines only transport fuel in one direction, the fuel must be transported from the airport via truck.

The following reported contaminations have been identified at recent meetings of the Coordinating Research Council (CRC) Aviation Fuels, Lubricants, and Equipment Committee:

- July 1995: Dulles—1.5 million gallons
- February 1996: La Guardia—200 thousand gallons
- March 1996: La Guardia—60 thousand gallons
- April 1996: Miami—600 thousand gallons
- August 1996: Seattle—6 planes defueled; passengers disembarked
- November 1996: Miami—800 thousand gallons
- September 1998: Hartford—200 thousand gallons

With the exception of the Seattle incident, all contaminations were discovered in the bulk storage tank before the contaminated fuel entered the airport distribution system; the contaminated tank was isolated, and the fuel was transported from the airport and downgraded. In the Hartford incident, there was an insufficient supply of uncontaminated fuel. The airport was not forced to shutdown, but over a 3-day period, some flights were canceled while others came in with additional fuel to avoid refueling.

The potential problem is that contaminated fuel will get into the airport fuel distribution system. Under current regulations, if this happens, the airport will have to be shutdown while the hydrant system is flushed out. To avoid this, the airlines asked the engine and airframe companies for a level of contamination under which they would be allowed to fly on the contaminated fuel. This would allow cleaning out the airport fuel distribution system and avoid a shutdown. While offering some guidance, the airframe companies deferred to the engine companies for a technical solution.

The CRC conducted an investigation of the potential effects of red dye on various aspects of aircraft and engine performance and durability. The conclusion was that thermal stability was the only problem area. The presence of red dye was found to reduce the breakpoint temperature of about half the fuels tested, but it was not possible to identify any factors that were common to the sensitive fuels. A full engine test by General Electric (GE) verified the impact of red dye on the fouling of fuel nozzles (Strauss, 1997).

The engine companies were not able to provide an allowable level because no test protocol exists for evaluating such contaminations short of conducting engine endurance tests, and no bench-scale deposition tests exist that have been correlated with fouling rates of actual engine hardware. Engine endurance tests would cost on the order of $2 million each. Parametric costs that derive from the individual manufacturers drive the cost further upward. Additionally, both large and small engines, e.g., commuter and business aircraft, would have to be evaluated since they have different operating temperatures and dimensions of fuel-flow passages.

An experimental program was developed to quantify the effect of red-dye contamination on the performance of fuel system components by placing selected hardware in a thermal environment typical of actual engine installation.

This concept was based on a project conducted by Southwest Research Institute® (SwRI) for the U.S. Navy to evaluate the effect of blending small amounts of diesel fuel into jet fuel; such an action might be used as a temporary means of extending the supply of jet fuel if an air-capable ship, such as a frigate or destroyer, began to run short of jet fuel and was unable to get replenished (Moses, et al., 1984). That study was based on work by GE during the U.S. Air Force program in the late 1970s and early 1980s to evaluate the effect of synthetic fuels and broad specification fuels on engine performance and durability. In these programs, fuel nozzles were placed in a heated air stream to simulate engine installation; elevated fuel temperatures were used to accelerate the tests, and the time to obtain a 10-percent increase in the pressure drop across the fuel nozzle was determined. It was demonstrated that this “fouling life” could be related to the fuel temperature and the Jet Fuel Thermal Oxidation Tester (JFTOT) breakpoint temperature. Supplemental tests, detailed in appendix J, showed the increase in fouling rate was linear with red-dye concentration.

This approach was proposed to the engine manufacturers as a means of quantifying the effect of red-dye contamination without the expense of engine tests.

2. OBJECTIVES AND SCOPE.

The two technical objectives for this research were

- to determine the allowable concentration of red-dye contamination in jet fuel, both commercial and military.

- to identify and validate a methodology for evaluating thermal stability issues with jet fuel that may arise from contamination or as part of a protocol for qualifying new additives.

The first objective was intended to prevent airport shutdowns in the event of accidental contamination without compromising safety and airworthiness. To address this objective, SwRI is developing experimental data quantifying the effect of red-dye concentration on the fouling rates of selected fuel system components. This data will be given to the respective engine companies for their use in establishing a common industry consensus on the allowable red-dye concentration for unrestricted use.

The second objective addressed the current inability to quantify the effects of additives and contaminants on fuel thermal stability in a manner that can be related to engine performance and durability. The purpose of this methodology would be to reduce the amount of combustor and/or engine tests necessary to approve additives and to study the effect of fuel contaminants.

3. APPROACH.

3.1 OVERVIEW.

This program is being conducted in three phases:

- Phase 1: Selection of test fuels
- Phase 2: Fouling tests on selected fuel system components
- Phase 3: Evaluation of test methodology(s) for addressing thermal stability issues

The first two phases address the first program objective. The first phase will define the test fuels. The second phase will use those test fuels to quantify the effect of red dye on performance degradation of selected fuel system hardware. The results from these component tests will be used by the aircraft turbine engine manufacturers to determine the allowable safe level of red-dye contamination in jet fuel. The third phase addresses the second program objective by developing correlations between the fuel system component tests and bench-scale deposition tests.

Phase 1 has been completed and is summarized in section 4 of this report. The progress to date on Phase 2 is summarized in section 5. No formal work has been done on Phase 3 as of this writing.

3.2 PROGRAM ADVISORY COMMITTEE.

A Program Advisory Committee (PAC) oversees this effort. The PAC is comprised of representatives from the aircraft engine companies, several sponsoring organizations, and an independent consultant, who is knowledgeable of jet fuels and refining practices. The members of the PAC and their affiliation are listed in table 1.

Table 1. Program Advisory Committee

Name of PAC Member	Affiliation
Fred Barnes	American Petroleum Institute
Tedd Biddle	Pratt & Whitney
Skip Byrnes	Federal Aviation Administration
Gerry Chambers	Airline Transport Association
Oren Hadaller	Boeing Airplane Company
Chris Lewis	Rolls Royce
Pam Serino	Defense Energy Support Center
Stan Seto	General Electric Aircraft Engines
Kurt Strauss	Consultant

During Phase 1, the two primary functions of PAC were

- to assist in selecting and securing test fuels to screen for sensitivity to red dye.
- to review the results of the screening process and assist in the selection of the test fuels for Phase 2.

During Phase 2, the engine companies have the most active role because they were responsible for

- the selection of the test hardware.
- the determination of the test conditions and instrumentation of the test hardware.
- the review of the fouling test results.
- the development of a unified industry decision on the allowable safe concentration of red dye.

4. PHASE 1: SELECTION OF TEST FUELS.

4.1 OBJECTIVE.

The primary objective of Phase 1 was to identify a jet fuel that had a thermal stability that was sensitive to red-dye contamination. It was also desirable to identify fuel characteristics that caused the thermal stability to be sensitive to red dye.

4.2 APPROACH.

4.2.1 Test Fuels.

One of the major difficulties in selecting a fuel for large-scale tests is duplicating the certain specific properties/characteristics of that fuel for future tests at a later date. In this case, the desirable characteristic was a thermal stability that was degraded by the presence of red dye.

Because it was unknown which characteristics caused jet fuels to be sensitive to red dye, fuels were obtained that represented a broad range of fuels available across the United States that addressed issues of crude source and refining techniques. In the simplest terms, crude oils can be characterized as either heavy or light and sweet or sour. Jet fuel can be processed from crude oil by simple distillation with or without sweetening or with increasing severity of hydrotreating to reduce sulfur and aromatics. In the extreme, the kerosene yield of heavy crude oils can be increased by hydrocracking or thermal cracking. Figure 1 shows a matrix representing viable combinations of crude source and processing for which samples were sought from various oil companies and refineries around the continental United States. (The shaded areas are not reasonable combinations for jet fuel production.)

PROCESSING	LIGHT CRUDE		MIXED CRUDE	HEAVY CRUDE	
	SWEET	SOUR		SOUR	SWEET
Straight-Run, No Treatment	2				
Straight-Run, Sweetened Merox™ treated Bender treated Doctor Sweetened	 3 1 1				
Straight-Run, Hydrotreated	1	2	1	2	1*
Hydrocracked			2	2	
Thermal Cracked, Hydrotreated			1		

*Contains syncrude from Canadian tar sands

Figure 1. Matrix of Crude Sources and Refining Processes for Making Jet Fuel

A total of 19 fuel samples were obtained representing refineries from all producing regions of the United States, i.e., East Coast, Gulf Coast, Mid-Continent, and West Coast. Figure 1 shows the number of samples obtained for each element of the matrix. Two 55-gallon drums of each fuel were obtained to retain each sample after the thermal stability evaluations were completed. A third 55-gallon sample of each fuel was shipped to the Air Force Fuels Branch at Wright-

Patterson Air Force Base, Dayton, Ohio, for thermal stability evaluations using unique test hardware developed there.

All test fuels were samples of production-run Jet-A fuels and therefore were assumed to meet the specifications for Jet-A. The test fuels, however, were analyzed for a selected set of properties considered relevant to thermal stability, i.e., hydrocarbon chemistry, sulfur, boiling point distribution, hydrogen content, and JFTOT. These results are summarized in table 2 with the exception of the boiling point distribution, which is more easily evaluated graphically (figure 2). The test fuels highlighted in table 2 were found to have thermal stability sensitive to red dye at 0.55 mg/L and were therefore candidates for the test fuel in Phase 2.

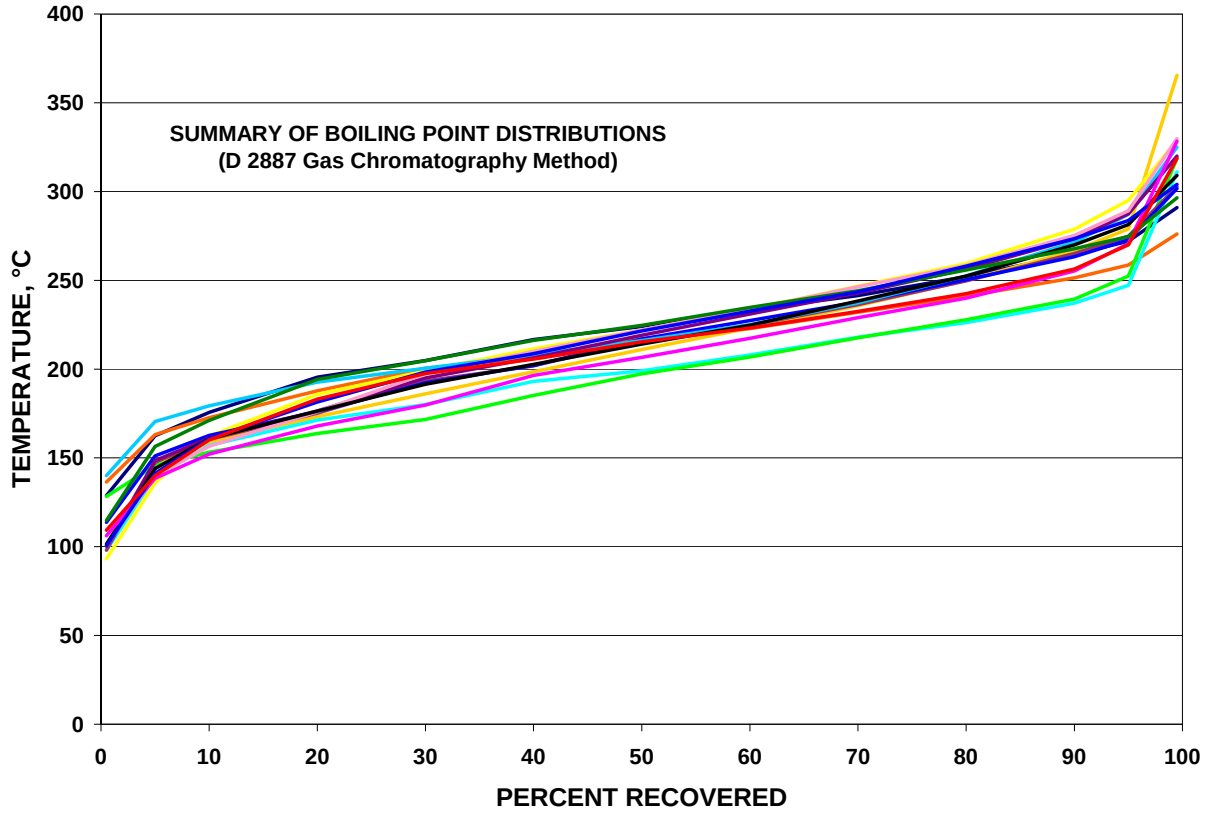

Figure 2. Boiling Point Distributions of Test Fuels in Phase 1

The specification test for aromatics, ASTM D 1319 fluorescence indicator absorption (FIA), does not provide information about the specific aromatics that are present in the fuel. For this reason, a second method using super-critical chromatography (SFC) was used to separate the single-ring, double-ring, and polyaromatic compounds. Hydrogen content was determined by ASTM D 5291. Total sulfur content was determined by x-ray fluorescence (XRF) in accordance with ASTM D 2622, while the mercaptan sulfur was determined by ASTM D 3227.

Nothing unusual was found in any of the properties of the test fuels. All the properties in table 2 met the ASTM D 1655 fuel specification for those tests included in that specification. All the fuels have well-behaved boiling point distributions as well.

Table 2. Properties and Characteristics of Test Fuels Screened for Sensitivity to Red Dye in Phase 1

Test Fuel No. 1	Fuel Description		Composition by FIA			SFC Aromatics				Hydrogen	Sulfur, m%		JFTOT, °C	
	Crude	Refining	Aromatics	Olefins	Sat.	% Mono-	% Di-	% Poly-	Total	wt%	Total	Mercaptan	Tbp - neat[2]	Tbp + RD[3]
RDTF-1	Heavy, sweet[1]	Straight-run, hydrotreated	23.9	1.3	74.8	24.4	1.7	0.1	26.2	13.46	0.020	0.0003	270	255
RDTF-2	Light, sour	Straight-run, hydrotreated	21.7	1.1	77.2	22.5	2.5	0.1	25.1	13.73	0.007	0.0003	280	285
RDTF-3	Mixed crude	Straight-run, hydrotreated	17.6	1.5	80.9	18.5	1.6	0.1	20.2	13.90	0.012	0.0003	290	290
RDTF-4	Heavy, sour	Straight-run, hydrotreated	21.9	1.1	77.0	22.4	1.6	0.2	24.2	13.69	0.018	0.0000	305	305
RDTF-5	Light, sweet	Straight-run, no sweetening	15.0	1.0	84.0	16.4	1.3	0.1	17.8	14.04	0.024	0.0001	290	285
RDTF-6	Light, sweet	Straight-run, clay treated	16.6	0.9	82.5	18.5	1.5	<0.01	20.0	13.64	0.016	0.0004	280	285
RDTF-7	Light, sweet	Straight-run, Merox treated	15.8	1.0	83.2	15	2.5	0.1	17.6	13.77	0.063	0.0005	280	280
RDTF-8	Light, sweet	Straight-run, doctor sweet	18.5	1.0	80.5	17.1	3.5	<0.01	20.6	13.86	0.055	0.0003	295	290
RDTF-9	Light, sweet	Straight-run, hydrotreated	17.7	1.0	81.3	17.6	2.3	0.1	20.0	13.11	0.010	0.0000	295	295
RDTF-10	Mixed crude	Hydrocracked	21.8	1.7	76.5	22.2	0.06	0.1	22.9	13.29	<0.001	0.0002	280	275
RDTF-11	Mixed crude	Contains therm crack	22.0	1.0	77.0	21.2	2.6	0.2	24.1	13.61	0.184	0.0002	285	285
RDTF-12	Heavy, sour	Hydrocracked and hydrotreated	21.9	1.1	77.0	21.6	3.1	0.1	24.8	13.24	0.119	0.0004	255	260
RDTF-13	Mixed crude	Contains hydrocracked	18.1	0.9	81.0	19.3	1.8	0.3	21.3	13.94	0.188	0.0012	315	315
RDTF-14	Light, sweet	Straight-run, Merox	17.4	1.0	81.6	17.6	1.8	0.2	19.6	13.89	0.164	0.0016	340	330
RDTF-15	Light, sweet	Straight-run, Bender Swtn	15.3	4.7	80	19.7	2.1	0.2	22	13.65	0.225	0.0018	335	340
RDTF-16	Light, sweet	Straight-run, Merox treated	18.7	1.2	80.1	18.9	2.2	0.1	21.3	13.80	0.094	0.0007	285	285
RDTF-17	L-M, sour	Med. hydrotreatment	16.4	1.0	82.6	16.4	2.2	0.2	18.8	13.82	0.043	0.0006	290	290
RDTF-18	Heavy, sour	Contains hydrocracked	17.3	1.5	81.3	17.0	0.4	0.2	17.6	13.37	<0.001		370	335
RDTF-19	Heavy, sour	Hydrotreated	18.5	2.2	79.4	18.0	1.9	0.2	20.1	13.76	0.104		300	290

Notes: [1]Highlighted fuels were found to have thermal stability sensitive to red dye.
[2]JFTOT breakpoint temperature of uncontaminated fuel.
[3]JFTOT breakpoint temperature of fuel contaminated with 0.55 mg/L of red dye.

4.2.2 Evaluation Tools for Thermal Stability.

The test fuels were evaluated for the effect of red dye on thermal stability by using the ASTM D 3241 JFTOT. Two methods were used to quantify the results from the JFTOT tests.

The primary method was to determine the JFTOT breakpoint temperature of the test fuels with and without red-dye contamination. The breakpoint temperature is the highest temperature at which a fuel still passes the JFTOT visual deposit rating; the methodology is described in ASTM D 3241, Appendix X.2. A change of 5°C is not considered significant in evaluating JFTOT breakpoints; given past experience with this procedure, it was decided that a change of at least 10°C was necessary for this program.

In recent years, a method of measuring the deposit thickness on JFTOT tubes was developed using laser optics based on concepts for measuring the thickness of thin films in the semi-conductor industry. This technology, the JFTOT Elipsometric Tube Analyzer (ETA), is capable of measuring deposit thicknesses in the range of 10 to 2000 nm (David, et al., 1997). More recently, Phillips Analytical has commercialized this system and renamed it the Fuel Qualifier.

Figure 3 presents a typical map of deposit thickness as determined by the ETA. Deposit thickness is mapped in two dimensions—axially and circumferentially. The direction of flow is from left to right in this figure. The deposit is very thin at the entrance on the left where the tube temperature is low. In this example, the deposit thickness remains thin and then increases to about 90 nm before falling off toward the end of the test section where the temperature of the tube decreases due to conduction. It is possible to calculate deposit volume by integrating the area under this surface, but for this work, the maximum deposit depth was used as the metric, believing it is more closely related to the conventional visual rating based on deposit color. This information was very useful for interpreting the results from the standard visual-rating procedure and confirming the effects of red-dye contamination on JFTOT deposits.

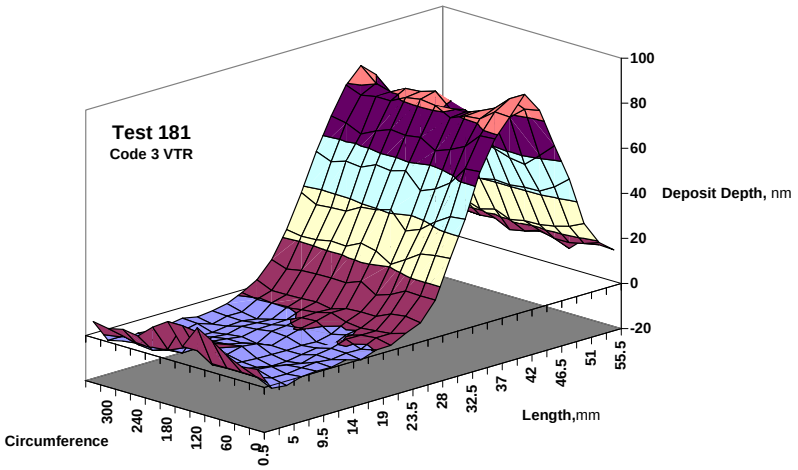

Figure 3. Map of Deposit Thickness on JFTOT Tube Using ETA

4.2.3 Red-Dye Contaminant.

The effect of red dye on fuel thermal stability was evaluated by comparing the breakpoints of the neat fuel and two concentrations of red dye: 0.55 mg/L and 0.27 mg/L. The higher concentration represents the amount of dye that would be present if the jet fuel were contaminated by 5 percent of fully dyed diesel fuel. It is believed that 5 percent represents a practical maximum contamination that could occur without detection by fuel tests normally conducted at an airport, e.g., freezing point. The rationale then became that if a fuel did not show a sensitivity at this concentration, it would not be important. The lower concentration is simply half of the higher level. The lower concentration was only evaluated with the fuels that were found to be sensitive at the 0.55 mg/L level; in every case tested, the effect was insignificant at the lower concentration.

Only three manufacturers produce red dye that is approved for use in diesel fuel. The chemistry of the dyes is proprietary, but is known to differ only slightly. All three dyes were evaluated for their effect on the breakpoint of several of the test fuels and were found to have the same effect. The one that seems to be most dominant in the market was chosen as the contaminant for the program.

4.3 RESULTS.

Figure 4 shows the distribution of breakpoint temperatures of the test fuels showing a broad distribution averaging about 280°C (536°F). This agrees well with the fact that many refineries actually require that their jet fuel pass the JFTOT at 275°C (527°F) rather than 260°C (500°F) to provide some margin for error and contamination during transport (DESC, 2000). Six fuels exhibited very high thermal stabilities with breakpoints of 300°C (572°F) or more. The inset in figure 4 shows the corresponding distribution of breakpoints when 0.55 mg/L of red dye is added to each fuel. The average breakpoint remains about the same, but several of the fuels were shifted to lower values.

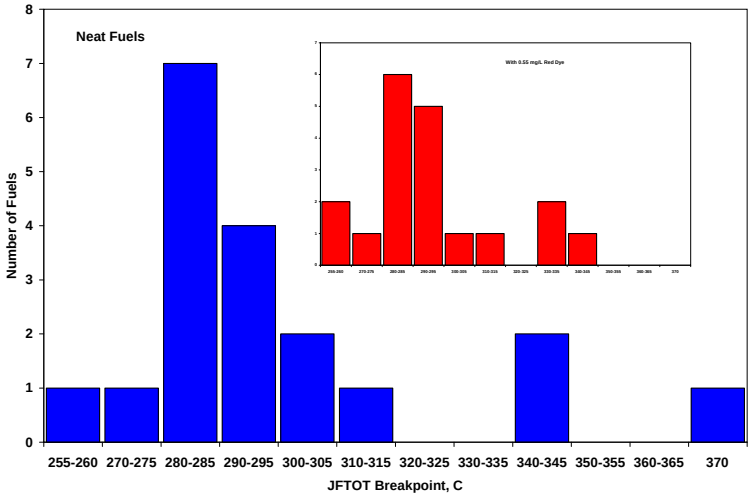

Figure 4. Distribution of JFTOT Breakpoint Temperatures for Phase 1 Test Fuels

Of the 19 fuels evaluated, 4 fuels demonstrated sensitivity to red dye at the concentration of 0.55 mg/L, i.e., the JFTOT breakpoint temperature was decreased by at least 10°C. None of the fuels were sensitive at the lower concentration. Four other fuels also showed an increase in deposit thickness at the breakpoint temperature; however, the breakpoint itself was not reduced by 10°C or more. For another 4 of the 19 fuels, the breakpoint temperature actually increased in the presence of 0.55 mg/L of red dye, but this was only 5°C in all cases and not considered significant; this is confirmed by the fact that the deposit thicknesses were not reduced.

Figure 5 shows the effects of 0.55 mg/L of red dye on breakpoint temperature. Presented in order of increasing breakpoint temperature, it is clear that the fuels that are sensitive to red dye can have either marginal breakpoint temperatures, i.e., close to 260°C (403°F), or very high breakpoint temperatures.

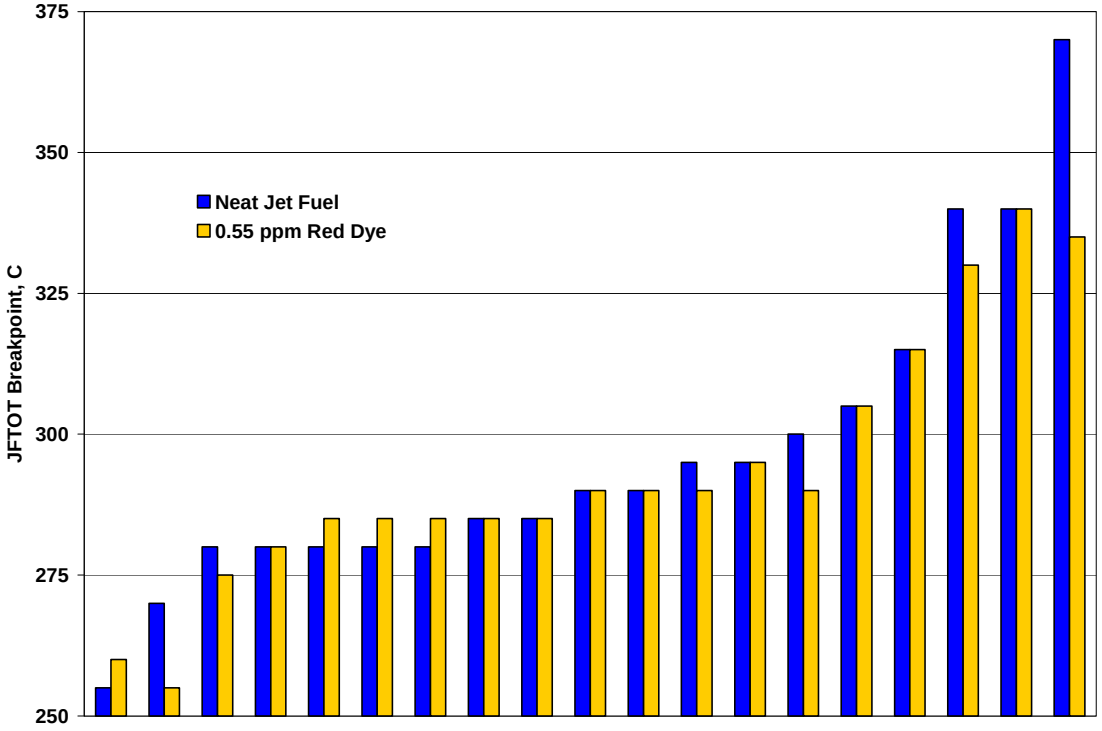

Figure 5. Effect of 0.55 mg/L of Red Dye on JFTOT Breakpoint Temperatures

Figure 6 presents the same data grouped according to crude source. This demonstrates that fuels from both light and heavy crude oils may have thermal stabilities that are sensitive to red dye. Moreover, the data show that the thermal stability, as measured by breakpoint temperature, is independent of crude source, i.e., fuels from both heavy and light crudes, and either sweet or sour crudes, can have either marginal or very good thermal stability.

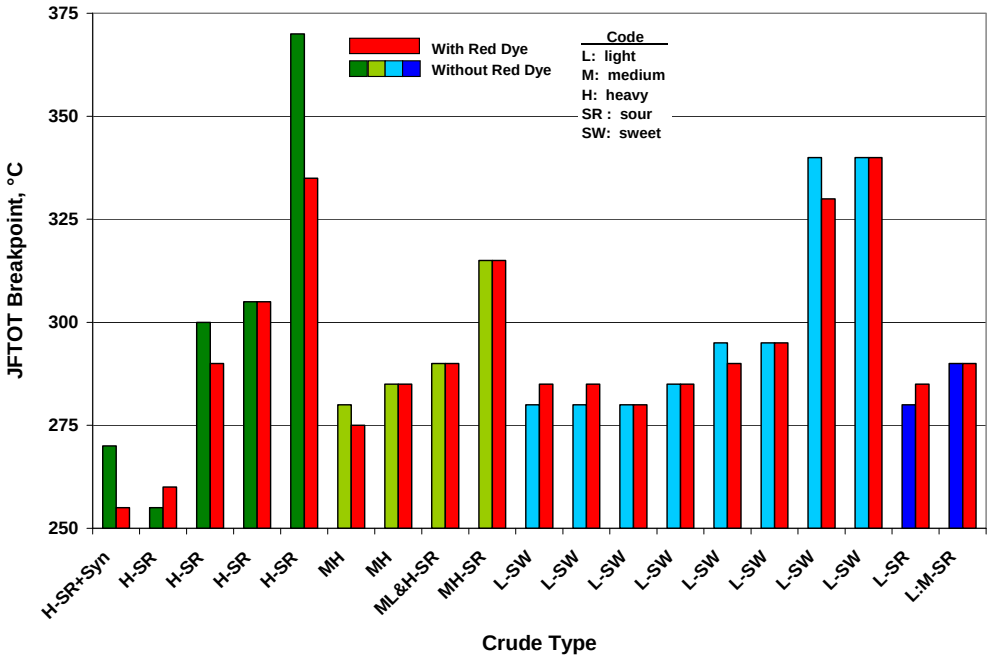

Figure 6. Effect of 0.55 mg/L of Red Dye on Breakpoint by Crude Source Characteristic

Figure 7 presents the same data, now grouped according to refining process. Again, the fuels that are sensitive to red dye are distributed among the processes. This grouping demonstrates that fuels with high breakpoint temperature are independent of processing; they can be either hydrotreated or straight-run.

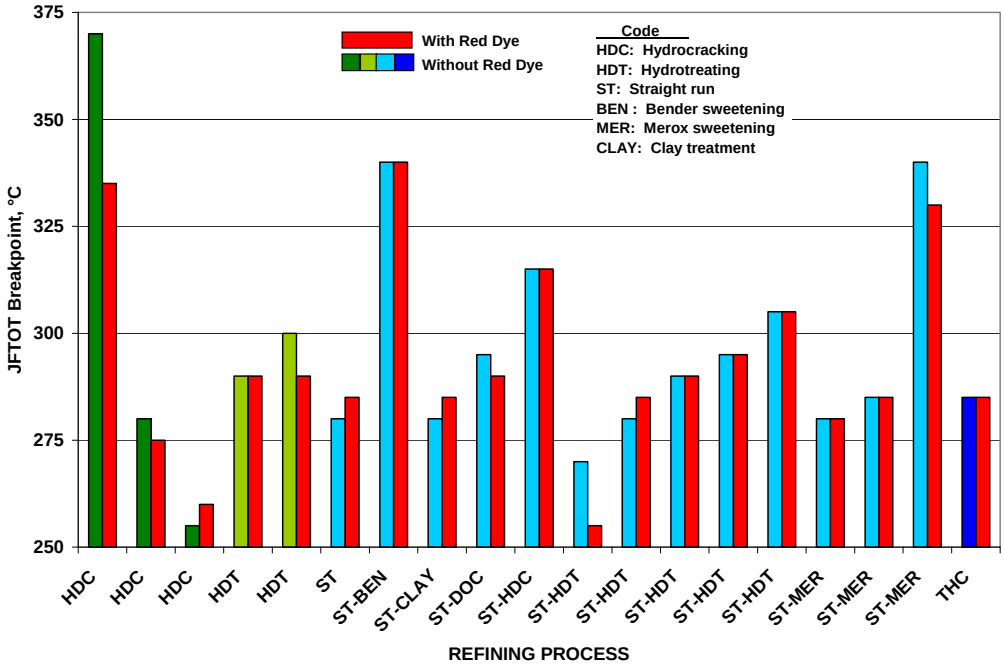

Figure 7. Effect of 0.55 mg/L of Red Dye on Breakpoint by Refining Process

Figure 8(a) and (b) present two examples of the effect of red dye on the deposit thickness as determined by the ETA analyses. The horizontal axis is the temperature at which the JFTOT test was conducted. The vertical axis is the maximum deposit depth measured with the ETA. The numbers next to the data points are the visual rating of the deposit. For all fuels, as the temperature of the JFTOT test increases, the deposit thicknesses increase, as does the visual-rating code; and adding the red dye increases the deposit thickness at all temperatures. There is a significant difference, however. In figure 8(a), the presence of the red dye caused the breakpoint to drop from 270° to 255°C (132° to 491°F). In figure 8(b), the red dye does not change the breakpoint, 280°C (138°F) for both fuels, but the deposit at the breakpoint is 1.73 times as thick with the dyed fuel. These may be important considerations when correlating the effect of fuel thermal stability to fuel nozzle fouling rates.

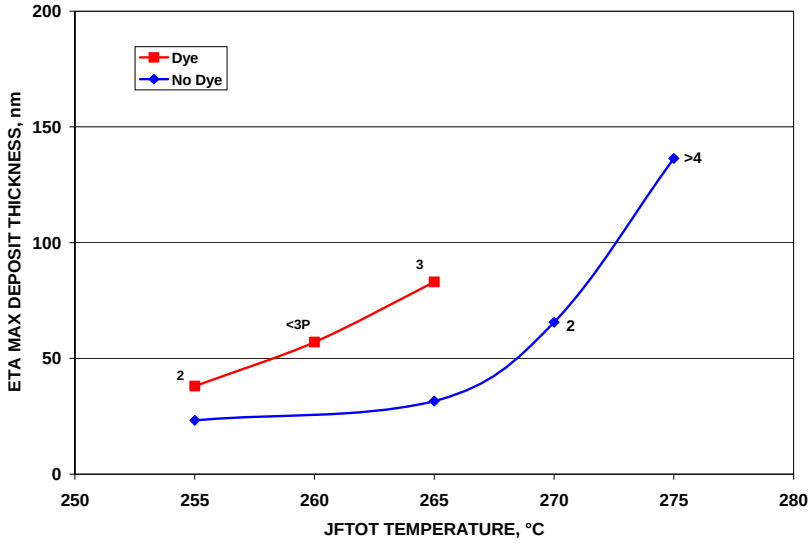

(a)

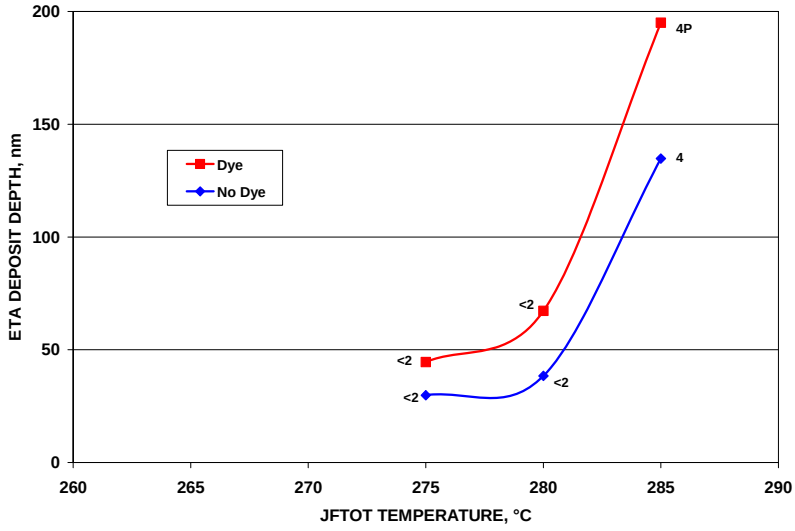

(b)

Figure 8. Effect of 0.55 mg/L of Red Dye on JFTOT Deposit Thickness by Ellipsometry

Figure 9 presents a summary of the eight fuels that exhibited sensitivity to red dye in the JFTOT test, showing the effect of the red dye on the deposit thickness at the breakpoint temperature of the undyed fuel. The impact of the dye on deposit rate varies with the fuel but is more than 200% greater for four fuels. Since the fuels are ordered according to the breakpoint temperature of the undyed fuel, it is clear that the effect of red dye is not related to the thermal stability of the base fuel.

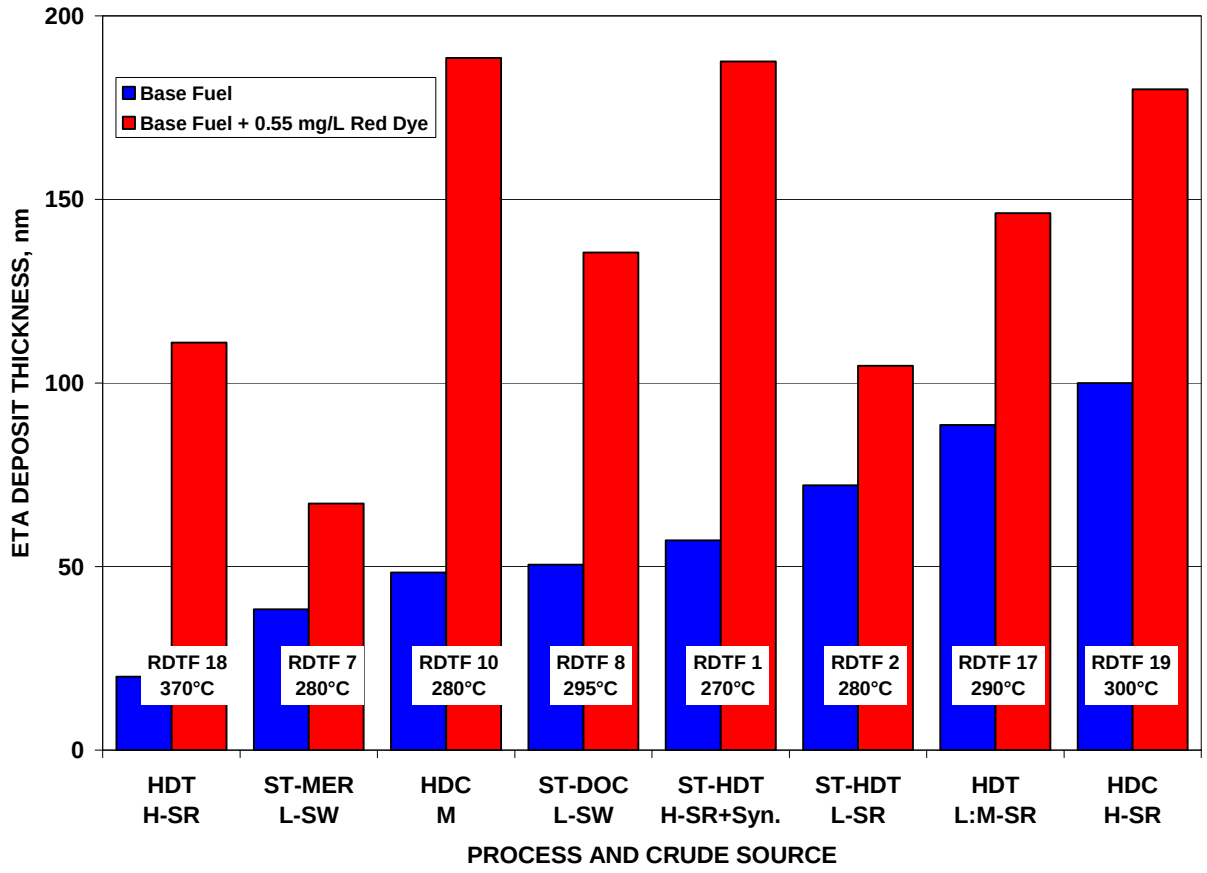

Figure 9. Effect of 0.55 mg/L of Red Dye on JFTOT Deposit Thickness at the JFTOT Breakpoint Temperature

Figure 10 presents the fuel matrix of figure 1, again showing which fuels were sensitive to red dye and which ones were not. This is really just another way of showing the results presented in figures 6 and 7, confirming that a pattern for sensitivity to red dye based on refining practices was not found.

PROCESSING	LIGHT CRUDE		MIXED CRUDE	HEAVY CRUDE	
	SWEET	SOUR		SOUR	SWEET
Straight-Run, No Treatment	RDTF-5 RDTF-6				
Straight-Run, Sweetened					
Merox treated	RDTF-7				
Merox treated	RDTF-14				
Merox treated	RDTF-16				
Bender treated	RDTF-15				
Doctor Sweetened	RDTF-8				
Straight-Run, Hydrotreated	RDTF-9	RDTF-2 RDTF-17	RDTF-3	RDTF-4 RDTF-19	RDTF-1
Hydrocracked			RDTF-10 RDTF-13	RDTF-12 RDTF-19	
Thermal Cracked, Hydrotreated			RDTF-11		

Figure 10. Fuel Source Matrix Showing Fuels Sensitive to 0.55 mg/L of Red Dye (highlighted in red)

4.4 FUEL CORRELATIONS.

It is evident that the fuels sensitive to red dye did not correlate with processing, crude source, or thermal stability of the base fuel. Correlations were made between the breakpoint temperature of the test fuels and each of the various chemical properties provided in table 2 for both the fuels that were sensitive to red dye and those that were not. Figures 11 to 13 present correlations with sulfur content, single- and double-ring aromatics, and olefins. Figure 11 shows that fuels with a high sulfur content can have very good thermal stabilities. The correlations in figure 12 show that thermal stability, i.e., breakpoint temperature, generally decreased with aromatic content, but the correlation coefficients are very poor. Figure 13 shows there was no correlation between thermal stability and olefin content. In all three figures, the sensitive fuels are scattered amongst the nonsensitive fuels so that none of these metrics for bulk chemistry is related to the sensitivity of thermal stability to red dye. It appears that trace chemistry determines thermal stability as well as sensitivity to red dye.

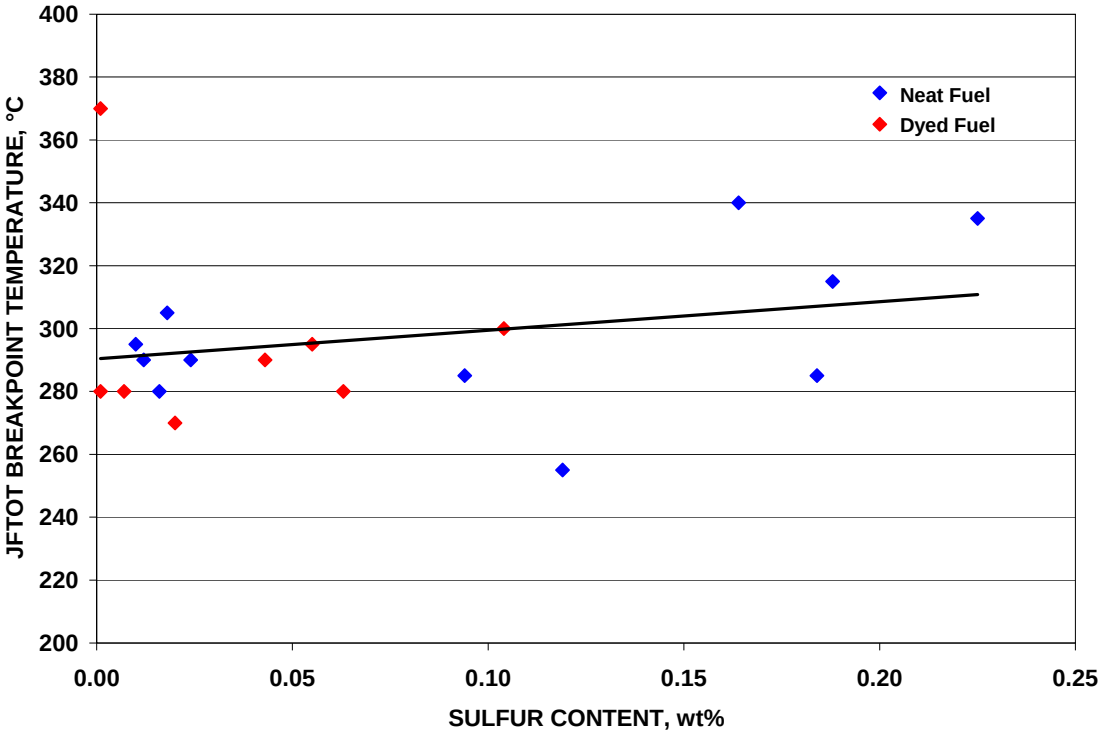

Figure 11. Correlation of JFTOT Breakpoint With Sulfur Content

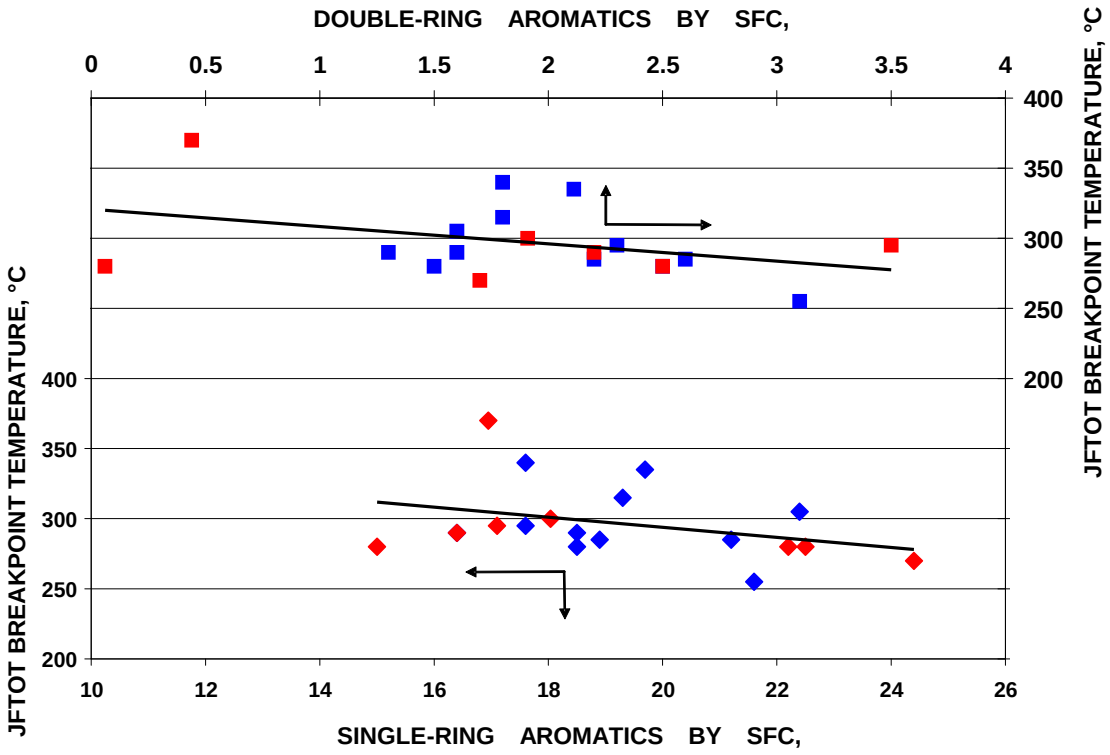

Figure 12. Correlation of JFTOT Breakpoint With Aromatic Content

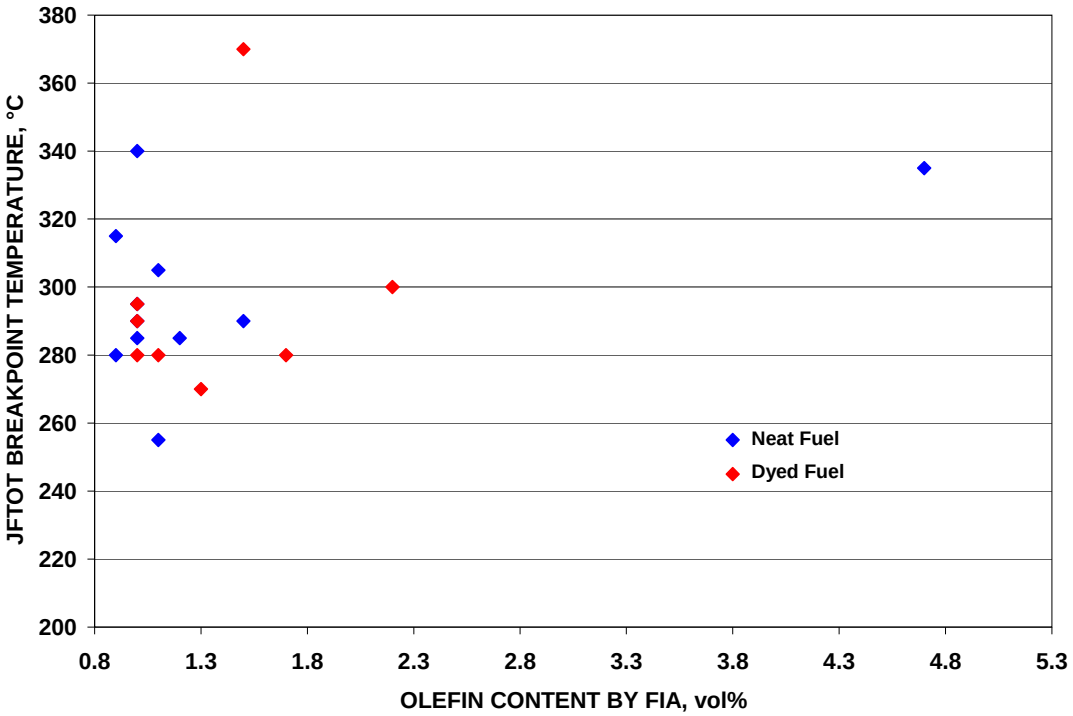

Figure 13. Correlation of JFTOT Breakpoint With Olefin Content

4.5 TEST FUEL SELECTION FOR PHASE 2 HARDWARE TESTING.

Upon review of the characteristics of the eight fuels found to be sensitive to red dye, five were selected as being the most likely candidates for the hardware testing of Phase 2.

The following gives the rationale for rejecting three of the test fuels found sensitive to red dye:

- RDTF-2 showed inconsistent effects of red dye upon retest of existing fuel sample.
- RDTF-8 showed failed JFTOT on pressure differential rather than deposition.
- RDTF-18 showed a very high breakpoint that was inconsistent.

The remaining five fuels had reasonable characteristics and are listed in order of desirability:

- RDTF-19 had a moderately high breakpoint, but it was consistent; this fuel was from a Gulf Coast refinery that was likely to have a consistent product and fed into a major pipeline to the East Coast.

- RDTF-17 red dye increased deposit thickness but did not change breakpoint; this fuel was from a Gulf Coast refinery feeding into a major pipeline to the East Coast.

- RDTF-1 showed a good response to red dye, but came from a small, rather isolated refinery.

- RDTF-10 showed a good response to red dye, but came from a West Coast refinery and is less likely to be exposed to red dye than RDTF-19 or -17.

4.6 EVALUATION OF DIESEL FUEL CONTAMINATION.

4.6.1 High-Sulfur Diesel Reference Fuel.

A study was conducted of the effect of diesel fuel contamination on the thermal stability and freezing point of jet fuel. This was needed to support the validity of the dye concentrations used and to provide guidance for selecting a diesel fuel to use as a contaminant in the Phase 2 hardware tests.

Red dye is used to mark high-sulfur diesel fuel and home heating oil. Of these, it seemed logical to use the high-sulfur diesel reference fuel (HSDRF) used for diesel engine sequence testing; this fuel is also known by the terminology Cat 1H. This fuel is fully compliant with the diesel fuel specification ASTM D 975. Moreover, as a reference fuel, it is formulated to maintain constant chemical characteristics and could be reproduced for use in future studies.

There was concern among the PAC as to whether this fuel was too unusual to represent a reasonable worst case. To address this question, the fuel was first reviewed by Mr. Steve Westbrook, Chairman of the ASTM Diesel Fuel Committee, and then by Mr. John Bacha of Chevron Products who is a recognized expert in diesel fuel characteristics and stability. Table 3 compares the properties of the HSDRF with the requirements of ASTM D 975 and three high-sulfur diesel fuels available on the commercial market.

Table 3. Comparison of Properties of HSDRF

Property	Units	Limit(s)	HSDRF	RS8189*	RS8039*	RS8032*
Flash point	°C	52, min	89	81	65	72
BS&W	%vol	0.05, max	<0.05	-	-	-
Distillation, 90%	°C	338, max	319	331	322	322
Viscosity at 40°C	cSt	1.9-4.1	3.1	2.9	2.4	3.2
Ash	%mass	0.01, max	0.006	-	-	-
Sulfur	%mass	0.50, max	0.41	0.47	0.40	0.20
Copper strip		#3, max	1A	-	-	-
Cetane number		40, min	52.6	-	-	-
Cetane index (ASTM D 4737)		-	-	44.1	45.4	54.0
Aromatics	%mass	-	29.2	35.2	33.8	23.4
Cloud point	°C	-	-8	-	-14	-13
Ramsbottom carbon	%mass	0.35, max	0.08	-	-	-

*Commercial high-sulfur diesel fuels: courtesy of Mr. John Bacha, Chevron Products

Having compared these fuels, Mr. Bacha provided the following conclusion:

> "I have compared the properties of your HS Ref Diesel with those of a number of commercial, red-dyed, high sulfur diesel fuels that I have examined over the last two years or so. Selected properties of three such fuels are presented in the attached file. Based on such comparison, I do not find that your HS Ref Diesel is particularly unusual. Thus, it should be suitable for use as a nominal worst case."

4.6.2 Effect of Diesel Fuel Contamination on Thermal Stability of Jet Fuel.

Regarding thermal stability, Mr. Bacha referred to work reported in IASH Newsletter #23 in which the results of JFTOT breakpoint tests on selected diesel fuels were compared to the new diesel fuel thermal stability test. The JFTOT breakpoint temperatures are compared in table 4. The breakpoint of the HSDRF is comparable to two of the three fuels. Of particular note is the fact that fuels A, B, and C were low-sulfur diesel fuels.

Table 4. Comparison of JFTOT Breakpoint Temperature of High-Sulfur Diesel Reference Fuel

Fuel Sample	JFTOT Breakpoint (°C)
HSDRF	210
Fuel A	>245
Fuel B	200
Fuel C	210

(Courtesy of John Bacha, Chevron Products)

Based on this information, the PAC concurred with the choice of the Cat 1H high-sulfur diesel reference fuel for evaluation as the diesel fuel contaminant for this program.

Figure 14 demonstrates the effect of diesel fuel contamination on the thermal stability of the five test fuels identified in section 4.5 as being the most desirable for use in the Phase 2 hardware testing; the fuel selected as the reference fuel was also evaluated. These data show that as little as 1% of HSDRF can cause a very good Jet A fuel to fail the JFTOT test. Figure 14 also shows that the effect is not the same for all fuels, as evidenced by the relatively small effect on the reference fuel, which has the lowest breakpoint when uncontaminated with HSDRF.

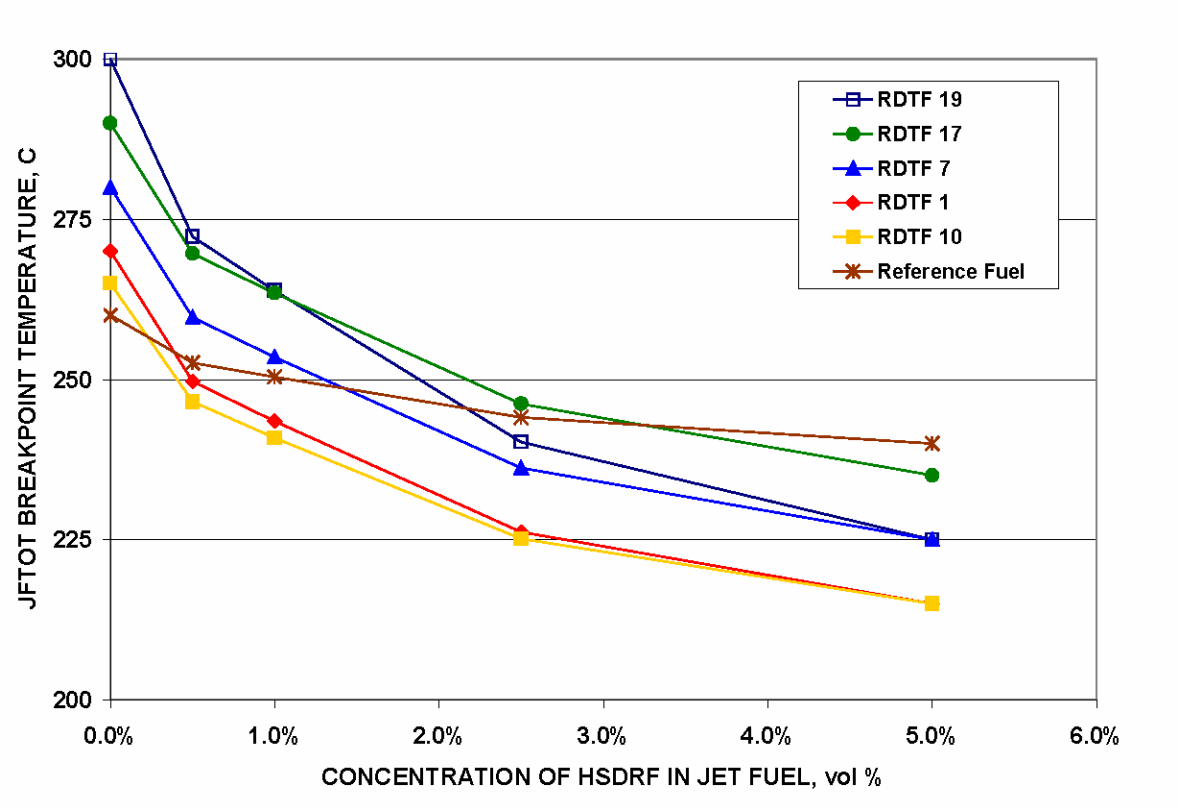

Figure 14. Effect of Diesel Fuel Contamination on the Thermal Stability of Jet Fuel

4.6.3 Effect of Diesel Fuel Contamination on Freezing Point of Jet Fuel.

The choice of 0.55 mg/L or red dye was selected, as discussed in section 4.2.3, because it is the amount of red dye that would be present if the jet fuel were contaminated with 5% fully dyed diesel fuel. It was assumed that more than 5% diesel fuel would cause the jet fuel to go off-specification on some other property commonly measured at the airport, such as freezing point.

This assumption was tested by determining the freezing point of 18 of the Phase 1 test fuels when contaminated with 5% of the HSDRF. These results are shown in figure 15. Of the 18 contaminated fuels, 7 still had a freezing point of -40°C or less. The presence of the diesel fuel only raised the freezing point of these fuels by a couple degrees or less. Like the effect on thermal stability, contamination does not affect all fuels in a similar manner. While 5% of the HSDRF was sufficient to cause most of the fuels to go off-specification on freezing point, it is certainly possible to have more than 5% and not fail this test.

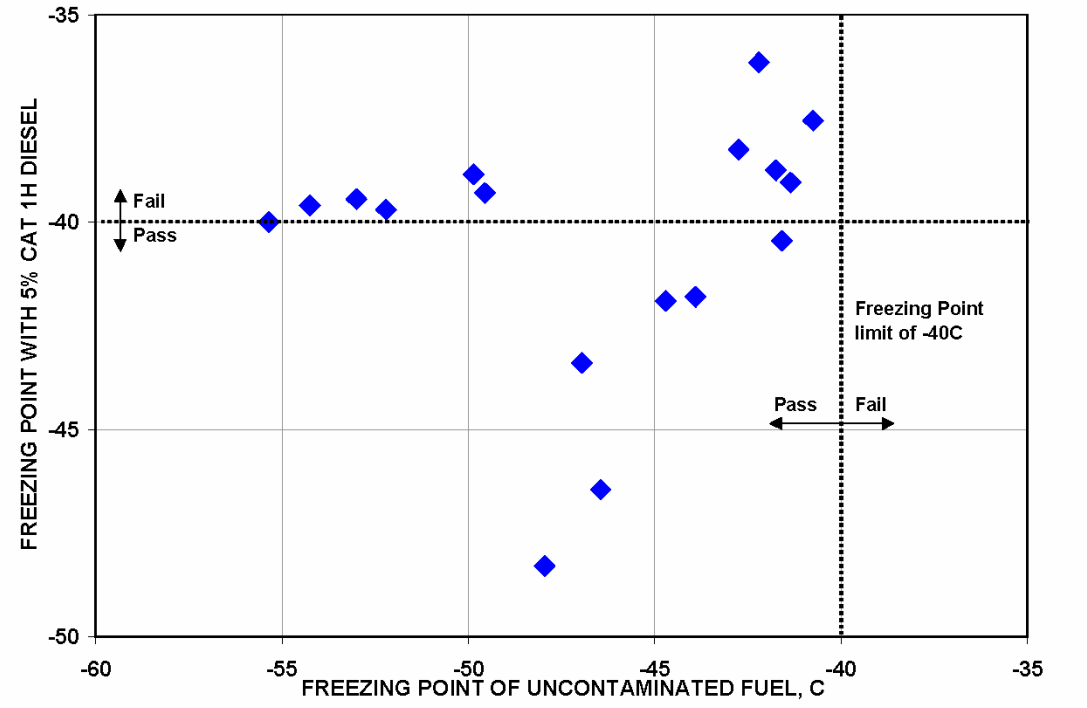

Figure 15. Effect of Diesel Fuel Contamination on the Freezing Point of Jet Fuel

From the results presented in figure 15, it is concluded that small amounts of undyed diesel fuel could be present in jet fuel without being detected at the airport. When compared to the results presented in figure 14, in which only 1% diesel fuel was sufficient to fail the JFTOT, a test that is not conducted at all airports.

These results strongly support the need for conducting tests in Phase 2 with diesel fuel contamination in addition to the red dye by itself.

4.7 PHASE 1 SUMMARY.

Nineteen fuels marketed in the United States as Jet A were sampled and evaluated to determine the effect of red-dye contamination on thermal stability as measured by the JFTOT. These fuels represented the full scope of crude sources and refining processes used in making jet fuels. The fuels were supplied from various refineries by 11 different oil companies. The fuels had a broad range of thermal stabilities, with breakpoint temperatures ranging from 255° to 375°C (491° to 707°F); the average was 280°C (536°F).

Two methods of quantifying the JFTOT results were used to evaluate the effect of red-dye contamination—the breakpoint temperature and the maximum deposit depth. The effect of red dye was tested at a concentration of 0.55 mg/L, the amount of red dye that would be present if the jet fuel were contaminated with 5% fully dyed diesel fuel, a concentration believed to be a practical maximum.

Eight test fuels were found to have thermal stability reduced by this concentration of red dye: four by at least a 10°C drop in breakpoint temperature and the other four fuels by an increase in deposit thickness at the breakpoint even though the breakpoint itself did not change. The increase in deposition rate caused by 0.55 mg/L of red dye ranged from 30 to 375 percent.

No correlations could be found between either breakpoint temperature or sensitivity to red dye and fuel chemistry. Also, there was no pattern as to which refining techniques or crude sources produced fuels that were sensitive to red dye.

A fuel was selected as the test fuel for Phase 2 that was sensitive to red dye and showed consistency in these characteristics upon evaluation of new samples from the refinery. Furthermore, the refinery that produced this fuel is known to produce very consistent jet fuel products.

5. PHASE 2: FUEL SYSTEM HARDWARE FOULING TESTS.

5.1 OBJECTIVE.

The objective of Phase 2 was to define and conduct tests to quantify the effect of red-dye contamination on the performance of fuel system hardware.

5.2 SCOPE.

5.2.1 Test Hardware.

The engine manufacturers considered three types of fuel system components to be critical for evaluating the effect of red dye on system performance: fuel nozzles, fuel control spool valves, and fine filter screens.

The fuel nozzles are the hottest part of the fuel system. The formation of deposits in fuel flow passages can cause a maldistribution of fuel among the nozzles; if significant, this can lead to a nonuniform temperature distribution in the turbine section, resulting in life reduction of rotating parts. Great care is taken in the designs to limit the fuel-wetted wall temperatures and to prevent the formation of fuel deposits, assuming the fuel meets the thermal stability limits of the fuel specification. Some hardware is already known to be marginal on thermal stability requirements, and any further reduction caused by contamination cannot be tolerated.

The spool valves are an important part of the engine fuel control system. They have very small clearances, which would be very susceptible to sticking if a deposit were to form. Such a deposit could prevent a pilot-commanded change in the fuel flow rate at a critical point in the flight.

The torque motor filter screens are last-chance filters to remove any particles from the fuel flows used to actuate circuits of the fuel control system. If they become fouled, they cannot be removed for cleaning or replacement without removing and dismantling the fuel control.

In selecting fuel nozzles for this program, it was necessary to allow for fuel nozzles from both large and small engines because of the different operating environments and design considerations. While many of the smaller engines operate with lower temperatures, the fuel flow passages are generally much smaller and, therefore, more sensitive to deposition. It was considered necessary to include the fuel nozzle from an auxiliary power unit (APU) because of their unique duty cycle and because they are "flight essential" on twin-engine aircraft flying over water. Fuel nozzles from two military fighter aircraft have been included as a basis for establishing an allowable red-dye contamination level for military aircraft refueling at commercial airports.

Each of the engine manufacturers recommended fuel injectors that represented the designs used in their current generation engines. The strategy in defining the nozzles was to provide for the various design technologies in both large and small atomizers, while at the same time, allowing for each manufacturer to identify a nozzle design upon which they were willing to base their decision on allowable red-dye concentration, i.e., a worst case and/or one to which other nozzle design could be related. The nozzles chosen included single- and dual-orifice pressure atomizers and several kinds of air blast atomizers, and some contained an integral flow divider valve.

The engines of the fuel nozzles chosen are identified in table 5, along with examples of the aircraft powered by each engine; some of the relevant design characteristics are also provided. A single spool valve and a torque motor filter screen were agreed upon by the engine manufacturers as representing the design technology of their engines.

Table 5. Summary of Test Hardware

Engine Manufacturer	Engine Model	Aircraft Used On	Atomizer Type	Flow Circuit
GE	CFM56	B737, A319	Pressure	Dual
GE	CT7/T700	Saab 340, various helicopters	Airblast	Single
GE	F414	F-18 (USN)	Pressure	Dual
Pratt & Whitney	PW2500-A5	B757	Airblast	Single
Pratt & Whitney	F100	F-15 (USAF)	Hybrid airblast	Dual
Pratt & Whitney (Canada)	PT6	Saab 2000, Cessna Citation 10	Pressure	Dual
Rolls-Royce	RB211-535	B757	Airblast	Single
Rolls-Royce	AE3007	Embraer 135/145	Hybrid airblast	Dual
Sundstrand	APU	A330, B767	Pressure	Single
Honeywell	Spool valve	Various		
Honeywell	Filter screen	Various		

USN = United States Navy
USAF = United States Air Force

The modification of the hardware for the purposes of testing is described in section 5.3.1.

5.2.2 Test Fuels.

Eight test fuels were used to conduct the hardware fouling tests. The "reference fuel" was a Jet A fuel that had marginal thermal stability, i.e., it just barely passed the JFTOT (ASTM D 3241) at 260°C (500°F), and represented a worst-case specification jet fuel. The "base fuel" was the fuel identified at the culmination of Phase 1 as having sensitivity to red dye.

The reason for using two different Jet A fuels to baseline the fuel nozzles was to establish the sensitivities of the nozzle designs to fuel thermal stability and fuel inlet temperature irrespective of the red dye and diesel fuel contamination. This was considered important because the JFTOT and bench-scale deposit tests were not expected to respond to these contaminations in the same manner as the fuel nozzles. Also, because one of the baseline fuels was a minimal thermal stability fuel, a scale was established for evaluating the effects of fuel contamination.

It was planned that six contaminated fuels would be made from the base fuel. The first two contaminations were red dye at two concentrations. The other four contaminations were diesel fuel at two concentrations and two concentrations of red dye and diesel fuel; however, financial constraints did not allow for tests to be conducted on these last four contaminations.

For future reference, the diesel contamination was to have been the Cat 1H high-sulfur diesel reference fuel. Generally, this fuel has a breakpoint temperature of approximately 200° to 220°C 392° to 428°F), which is thought to be about the worst case. The advantage of using this fuel is that it is a reference fuel and could theoretically be reproduced as opposed to using a commercial diesel fuel. The results of these tests are highly desirable, and additional tests will be conducted if future funding becomes available.

5.3 APPROACH—FUEL NOZZLE TEST.

5.3.1 Overview.

The basic approach to the fuel nozzle test was to reproduce the thermal and flow environments of the nozzles as if they were installed in the engine. The exact conditions for each fuel nozzle design were specified by the engine manufacturer and were different for each design. The test conditions specified included the fuel flow rate and a temperature on the outside surface of the test article; in the case of airblast atomizers, the airflow rate and temperature were also specified. These specified conditions remained constant for all tests of that specific hardware type.

Tests were conducted at three fuel temperatures to isolate the temperature sensitivity of fouling from the fuel thermal stability effects. The details of the environment and the modifications necessary to the test hardware are described below followed by the test results.

5.3.2 Test Environment.

The fuel nozzles under test were placed in a heated, fluidized sand bath to provide sufficient heat transfer to the hardware to simulate engine-installed conditions, i.e., skin temperatures, as defined by the manufacturer of the hardware. This is shown in figure 16 while figure 17 shows the entire flow system. The fuel was not recirculated and was not reused.

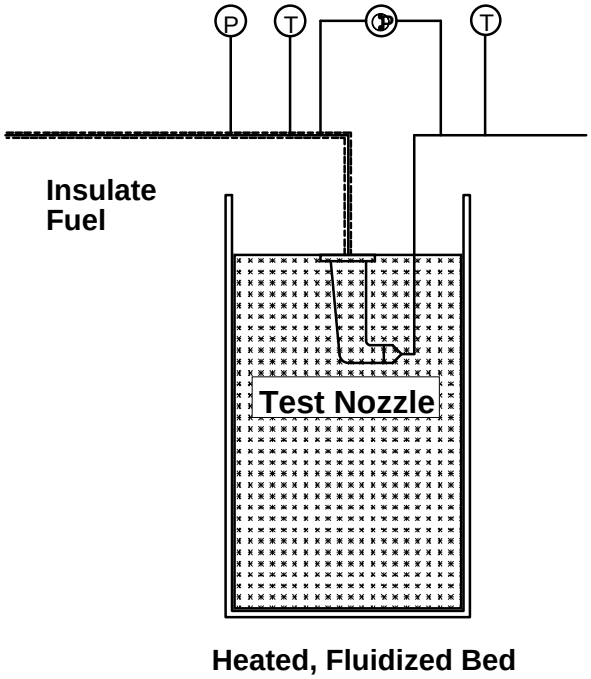

Figure 16. Heated, Fluidized Bed for Nozzle Fouling Tests

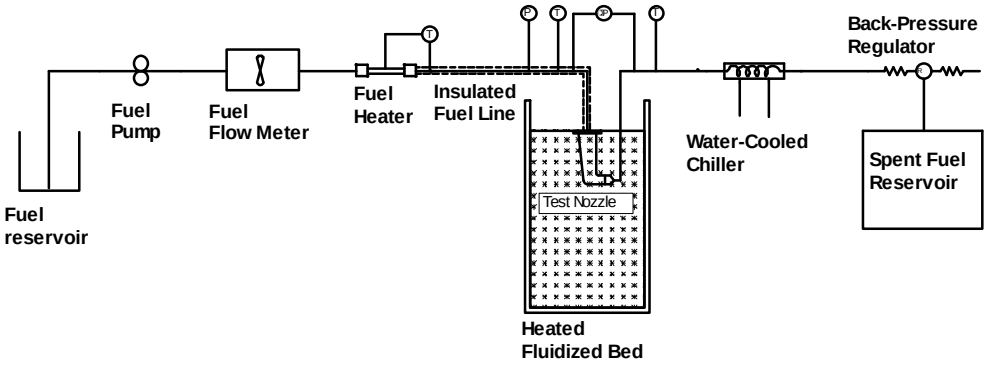

Figure 17. Flow System for Nozzle Fouling Tests

The inlet fuel temperatures were a compromise between reality and acceptable test lengths. The fuel temperatures must be elevated above actual operating temperatures to reduce testing time; however, they must not be too high so as to cause a change in deposition mechanisms. The test temperatures vary among the component and fuel combinations because the fuels have different thermal stabilities and each hardware type has unique temperature differences between the

outside surface and the fuel-wetted walls of the flow passages. The initial test temperature for each component on the baseline fuels was selected from past experience; the other two temperatures were higher or lower, depending upon the fouling rate of the initial test.

5.3.3 Modifications to Test Fuel Nozzles.

It was necessary to modify the fuel nozzles before the tests to capture the fuel as it exits the nozzle; this was necessary to prevent the hot fuel from spraying into the heated, fluidized bed and starting a fire. The modifications varied with the design features of the nozzle.

The fuel nozzles used in this program fall into four basic design categories:

- Single-orifice pressure atomizers, e.g., T700, Sundstrand APU
- Dual-orifice pressure atomizers, e.g., CFM56, F414, PT6
- Prefilming airblast atomizers, e.g., RB211, PW2040
- Hybrid airblast atomizers, e.g., AE3007, F100

With only two types of pressure atomizers, the modifications were straightforward and relatively easy. Figures 18 and 19 show the basic design features of single- and dual-orifice pressure atomizers and the modification. A capture cup was simply welded over the exit of the nozzle tip. Where present, air shrouds around the nozzle tip were removed to allow heat transfer to the surface beneath the shroud. Heated air normally flows between the shroud and the tip, but the fluidized bed would not force air through this passage; rather, it would just fill up with sand and become blocked. Therefore, it was necessary to remove the air shroud to obtain the correct temperature on the surface under the shroud.

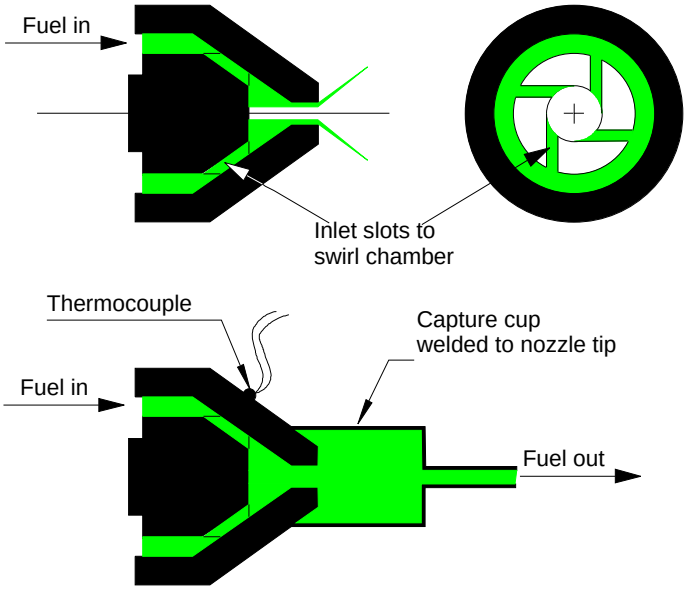

Figure 18. Single-Orifice Pressure Atomizers Test

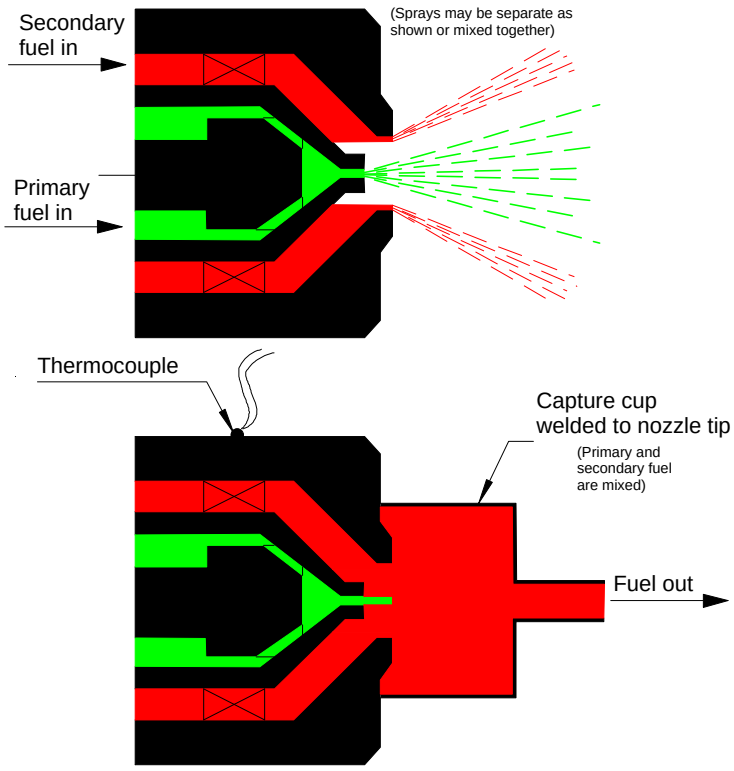

Figure 19. Dual-Orifice Pressure Atomizer Test

The two types of airblast atomizers presented unique problems. It was necessary to maintain the inner core airflow because it is a heat source for some of the fuel-wetted surfaces within the nozzle. At the same time, it was necessary to separate this airflow from the fuel flow at the exit.

For the prefilming airblast atomizers shown in figure 20, this was accomplished by silver-brazing a blocking plate at the exit of the core airflow. The heating normally provided by the core airflow was provided by forcing heated air through a tube placed inside the core; this air was forced to flow out of the core along the wall, but in the reverse direction. A thermocouple was placed in the airflow at the tube exit as a control. It was not possible to put a thermocouple on the wall of the core airflow. To get a correct convective heat transfer coefficient, it was only necessary to match the Reynold's number of the airflow through the annulus with that of the original core airflow. The outer air swirlers were also removed for reasons similar to the removal of the air shrouds on the pressure atomizers. A second control thermocouple was placed on the outer wall of the nozzle.

In practice, these modifications proved more difficult than envisioned. It was found that this simulated core airflow exiting from the back of the nozzle would sandblast not only the air tube but the wall of the fluidized bed as well. Thus, it was necessary to capture the air and direct it out of the fluidized bed; this was done with a concentric tube around the air supply tube. Also, when a heat shield was present, it was necessary to seal any gaps to prevent sand from getting under it; these gaps were filled with a putty-like material that transformed into a ceramic upon curing.

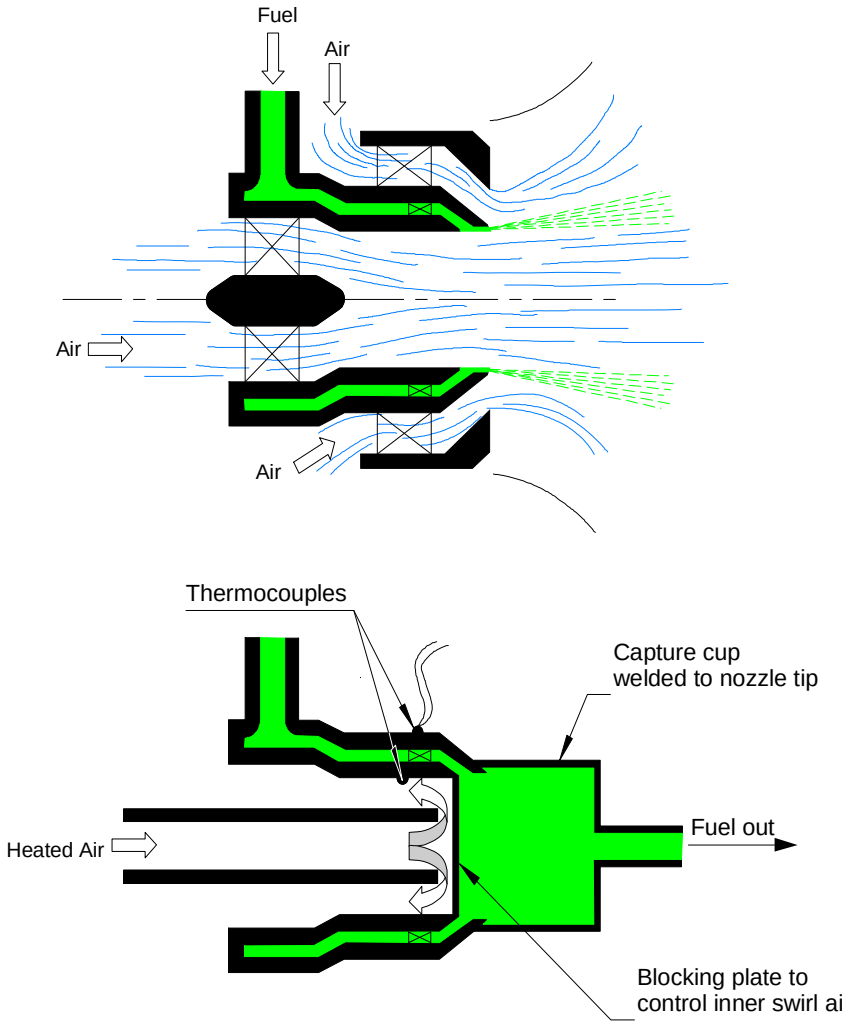

Figure 20. Prefilming Airblast Atomizer Test

Figure 21 shows the reality of a modification to a prefilming airblast atomizer.

Figure 22 shows the design concept of a hybrid airblast atomizer. These were the most difficult to modify due to the presence of the small pressure atomizer in the center of the core, and because the internal swirl air enters the nozzle through a number of holes, typically six, around the periphery. The inner swirl air then flows out through the narrow annulus between the central pressure atomizer and the filming surface. It was more difficult to engineer an effective block across the narrow annulus than the larger central core of prefilming airblast atomizer simply because the size is so much smaller and less accessible. Silver-soldering a washer into the air swirl annulus successfully blocked the airflow.

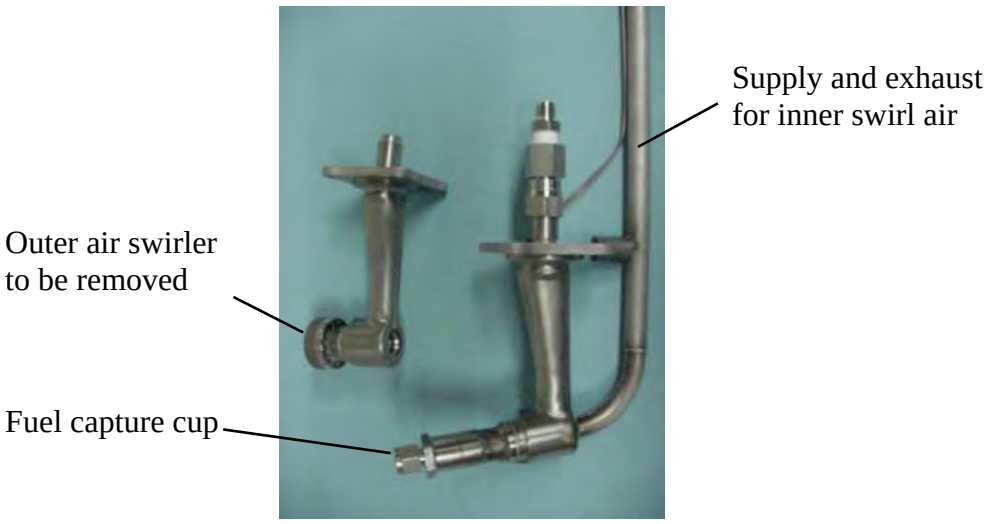

Figure 21. Prefilming Airblast Atomizer With Modifications to Remove Fuel and Inner Swirl Air

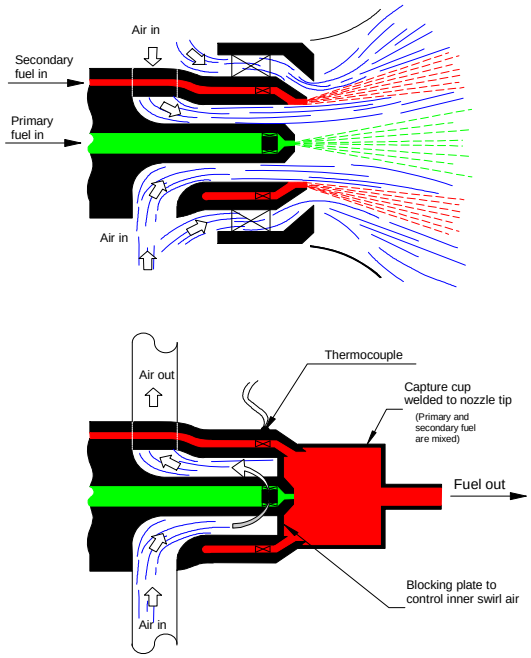

Figure 22. Hybrid Airblast Atomizer Test

Here, too, reality was more difficult than concept. Small-diameter tubing was welded to each of the six holes to provide both inlet and exhaust for the swirl air. The air was brought in through alternate holes and exited out of the other holes. Again, it was not possible to instrument the inside wall temperature; the best that could be done was to flow heated air through the system at the temperature and flow rate prescribed by the manufacturer. In the initial test before the exhaust was ducted away, the air sand-blasted a hole in the nozzle sheath. Figure 23 is a picture of a hybrid airblast atomizer showing the modifications.

The inner air was heated with one or more commercially available 1-inch-diameter electric duct heaters.

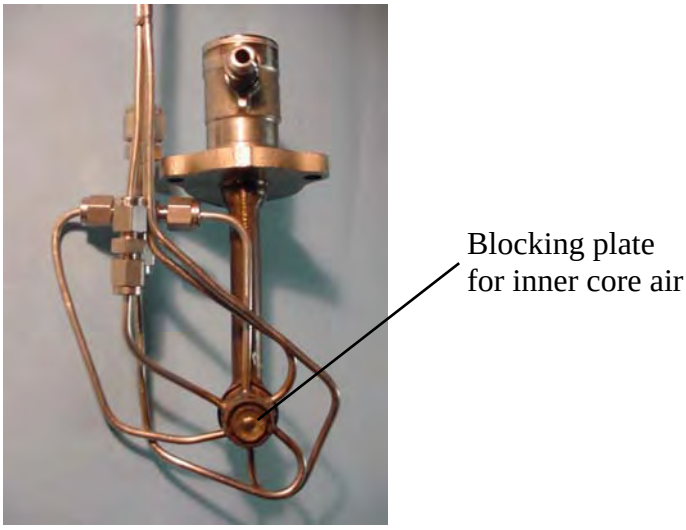

Figure 23. Hybrid Airblast Atomizer Showing Blocking Plate and Modifications to Remove Inner Swirl Air

5.3.4 Test Description.

In addition to the basic operating temperature conditions, the primary data recorded were the fuel flow rate and the pressure drop across the fuel nozzle. With the airblast atomizers, the airflow and air temperature were also recorded. Each fuel nozzle test was conducted until a significant measure of performance degradation was achieved, e.g., a 5-percent decrease in flow number.

Generally, new nozzles were used for each test to assure similarity of test conditions. If a test had to be stopped prematurely for some reason and the nozzle had experienced only a small degradation of flow number, the nozzle was sometimes reused to save time and expense. This was especially true with the airblast atomizers, which required extensive modification for testing, as discussed in the previous section.

The test fuel was always fresh; spent fuel was discarded and not reused in these tests. Before testing, the fuel nozzles were flushed with a solvent to purge any preservatives from the flow passages, which otherwise might affect the deposit test. When possible, the nozzle-fouling tests were conducted on a 24-hour per day basis to minimize start-up/shutdown concerns.

To accelerate the fouling, the fuel inlet temperature was increased to higher than normal. It was desirable to have test times on the order of 25 hours to allow for reasonable test times without testing at temperatures where the kinetics of deposition may change. Typical fuel temperatures were in the range of 150° to 205°C (300° to 400°F). For a given nozzle and fuel combination, the temperature variation was 17° to 22°C (30° to 40°F); this was usually sufficient to cause a 5- to 10-fold variation in fouling rate.

The fuel was heated by flowing it through a narrow annulus, created by a 1.6-cm- (0.625-inch-) diameter electric cartridge heater inserted into a length of 1.9-cm- (0.75-inch-) diameter tubing; the annulus height was 0.13 mm (0.005 inch), and the heated length was 81 cm (32 inches). This heater design minimized the skin temperature of the heater so as not to overheat the fuel; the typical temperature difference between the heater wall and the fuel was about 10°C (18°F).

Process controllers were used on critical test parameters to maintain stable conditions over the test duration. The most important of these were the fuel flow rate and the fuel temperature. It was also necessary to maintain a constant temperature of the nozzle tip. It was not practical to place this temperature under direct control because of the time delay between the air heaters on the fluidized bed and the test article due to the thermal inertia of the sand. Instead, the air temperature of the fluidized bed was controlled as the means of maintaining constant wall temperature.

The fuel flow rate and pressure drop across the test nozzle were monitored continuously so that the instantaneous flow number (FN) of the nozzle could be determined. The rate of degradation of flow number is called the fouling rate (FR) and is the metric used for quantifying nozzle fouling and evaluating the effect of contamination.

$$FR = \frac{d(FN)}{dt}$$

where

$$FN = \frac{m_f}{\sqrt{\Delta P}}$$

and

mf = fuel flow rate
ΔP = pressure drop across the nozzle

Figure 24 presents one experiment's typical temperature-time history for the fluidized bed, the tip of the nozzle, and the fuel at the nozzle inlet to illustrate the stability of the test conditions over many hours. Figure 25 presents the corresponding time history of fuel flow, pressure drop, and flow number. At this scale, the change in flow number is not apparent. Figure 26 shows the history of the flow number on a larger scale. The slope or fouling rate is also shown.

Graphical presentations of the fouling results are presented in appendices A through I to this report. The results are separated according to nozzle type, the test fuel, and the fuel temperature of the test. The test data for the operating conditions of the individual tests were not included with this report simply because of the large amount of data collected and the proprietary nature of some of the tests results.

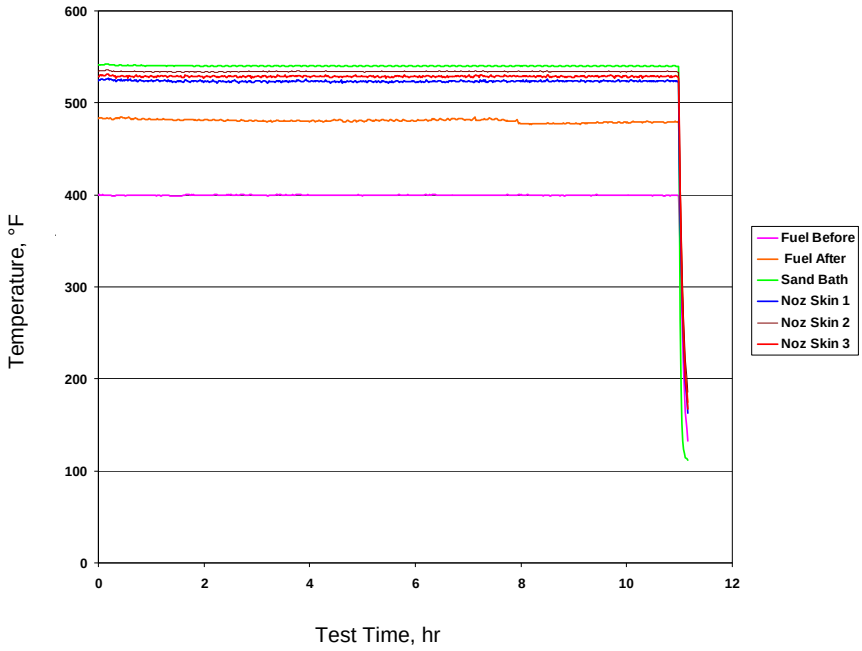

Figure 24. Temperature History for a Nozzle Fouling Test

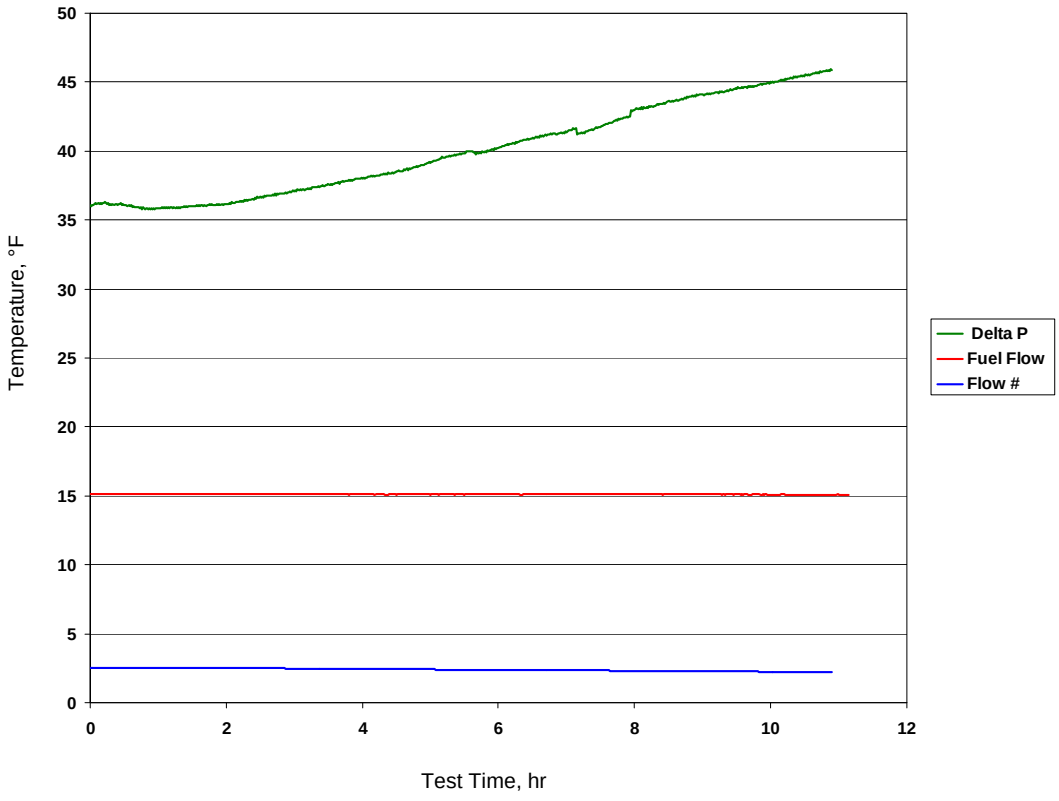

Figure 25. Time History of Flow Parameters

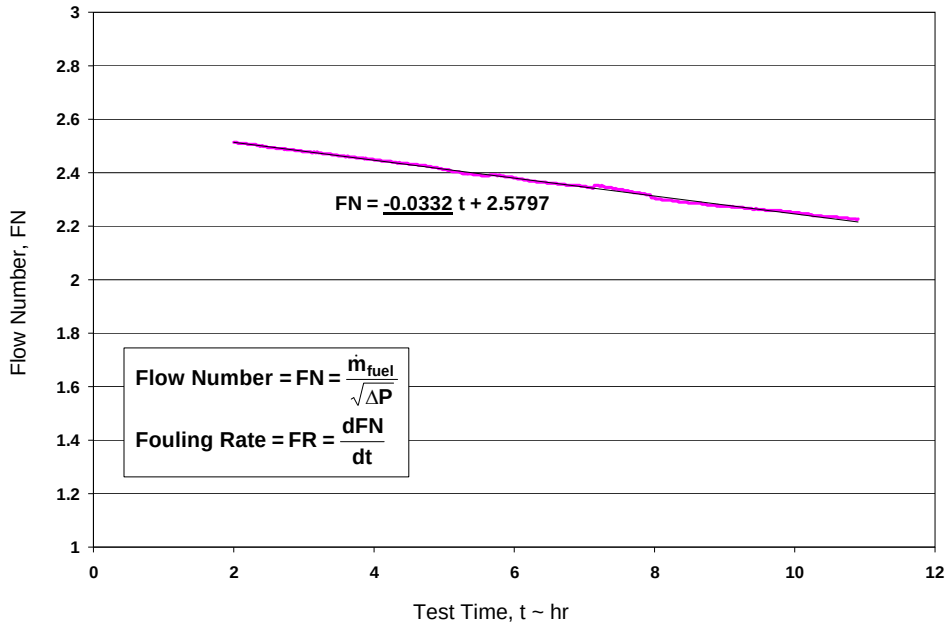

Figure 26. Time History of Flow Number During a Nozzle Fouling Test

5.3.5 Analysis of Nozzle Fouling Tests.

Fouling tests were first conducted on the following three fuels, nominally at three temperatures each:

1. Reference fuel, JFTOT breakpoint temperature = 265°C (509°F)

2. Base fuel, JFTOT breakpoint temperature = 285°-90°C (545°-194°F)

3. Base fuel + 0.55 mg/L of red dye, JFTOT breakpoint temperature = 280°-285°C (536°-545°F)

If the tests with red dye resulted in an increase in fouling rate, another set of tests were conducted at a dye concentration of 0.275 mg/L. A few of the nozzles did not show sensitivity to red dye, and tests at lower concentrations were not conducted. Tests at higher concentrations were not attempted because 0.55 mg/L represents the dye that would be present if the jet fuel were contaminated with 5% fully dyed diesel fuel, considering that most would escape other quality control tests at the airport.

Fouling characteristics for each fuel nozzle design were developed by graphing the fouling rate against the fuel temperature of the individual test. As fuel temperature is increased, the fouling rate increases exponentially. When fuels are changed, if the thermal stability is higher, i.e., a higher JFTOT breakpoint temperature, the fouling rate is lower.

Figure 27 shows the results for test nozzle TN-G. The fouling rate characteristics of the reference fuel are much higher than the base fuel, i.e., at a given fuel temperature, the fouling rate for the reference fuel is much higher than the base fuel. This is consistent with the higher

JFTOT breakpoint temperature of the base fuel. Only one concentration of red dye was tested on this nozzle because the presence of 0.55 mg/L had no apparent effect.

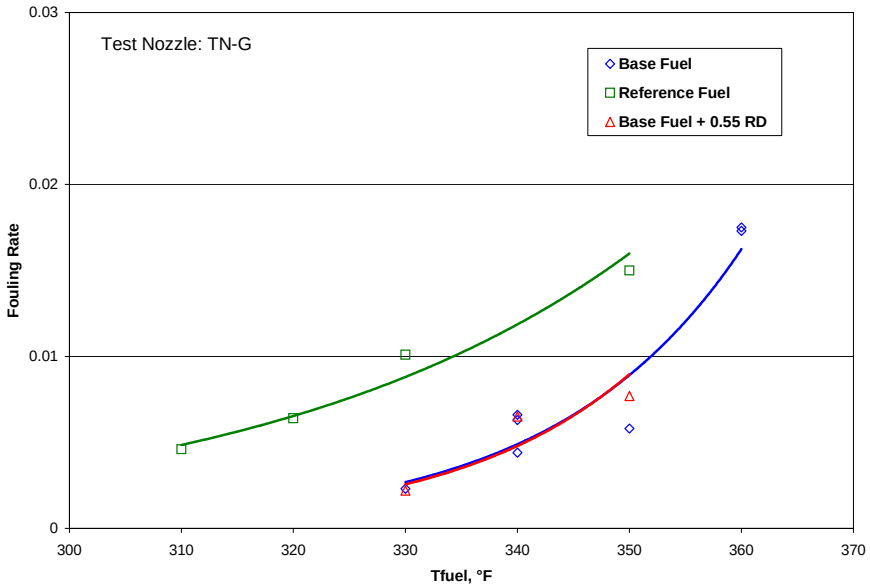

Figure 27. Summary of Fouling Rates for a Test Nozzle Not Sensitive to Red Dye (TN-G)

Figure 28 shows a case where red dye did increase the fouling characteristics of the nozzle. The presence of 0.55 mg/L of red dye resulted in a doubling of the fouling rate. When the concentration was reduced to 0.275 mg/L, the results fell in between 0.0 and 0.55 mg/L.

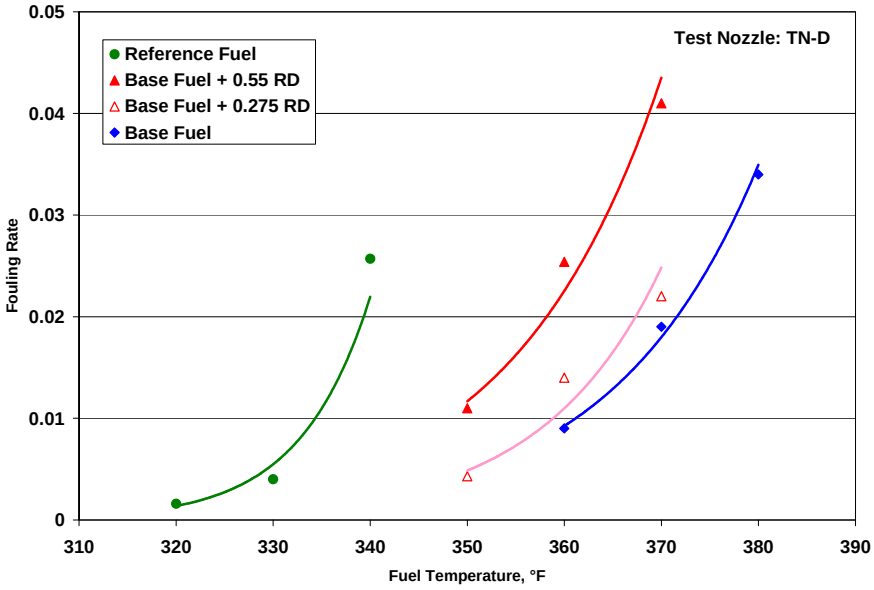

Figure 28. Summary of Fouling Rates for a Test Nozzle Sensitive to Red Dye (TN-D)

Note that while the general shapes of the curves in figure 28 are similar to figure 27, it was necessary to conduct the tests at higher fuel temperatures to get the same fouling rates; this was the case for each nozzle type.

In this presentation of the fouling characteristics, it is difficult to relate the general increase in fouling rate as a function of red-dye concentration. Arrhenius plots of the log of the fouling rate against $1/T_{fuel}$ were more useful. Figure 29 shows the data replotted for the red-dye effect in figure 28. In this presentation, the exponential curve fits become straight lines that are almost parallel for the three fuels; the fact that they are not parallel is thought to be due to experimental variations.

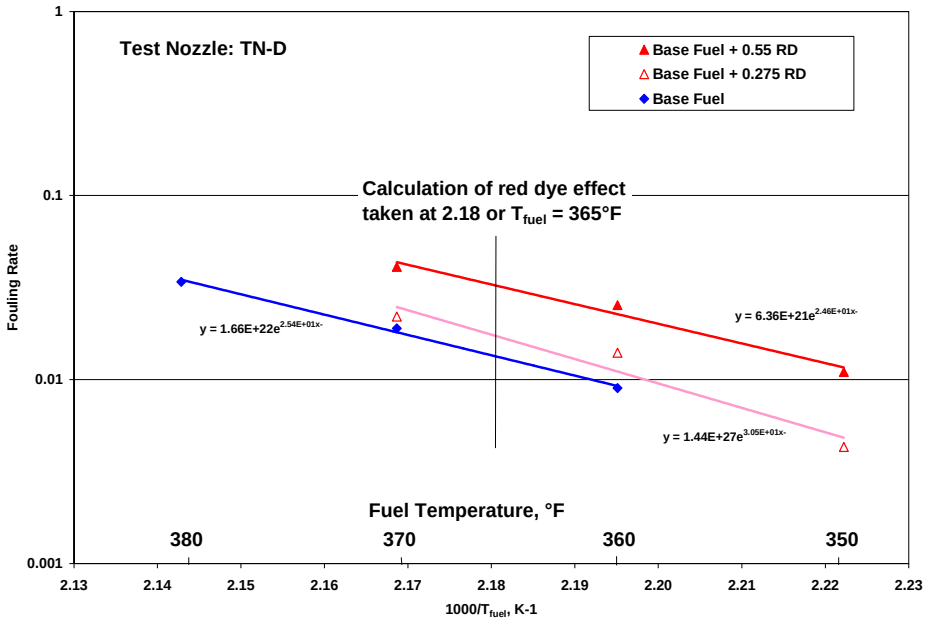

Figure 29. Arrhenius Plot of Fouling Rates for a Test Nozzle Sensitive to Red Dye (TN-D)

Arrhenius plots are commonly used to present results from chemical reaction rates because such processes are exponential with temperature and, in this type of presentation, the slope related to the activation energy of the reaction. Here, the fact that the data are well correlated with an exponential curve fit shows that chemical mechanism controlling deposition is not changing over the temperature range of the experiments. This means that increasing the fuel temperature to accelerate the tests has not changed the chemistry, and the results are considered valid for lower temperatures as well.

The fact that these correlations are more or less parallel makes it possible to relate the increase in fouling rate to dye concentration. A comparison of the fouling rates is made at an average temperature over the range of the tests, in this case, 185°C (365°F). The value of the respective correlation equations is determined at the common temperature and compared. Figure 30 shows the effect of red-dye contamination on the fouling rate of test nozzle TN-D. The actual values are summarized in table 6 along with three other comparisons that will be discussed.

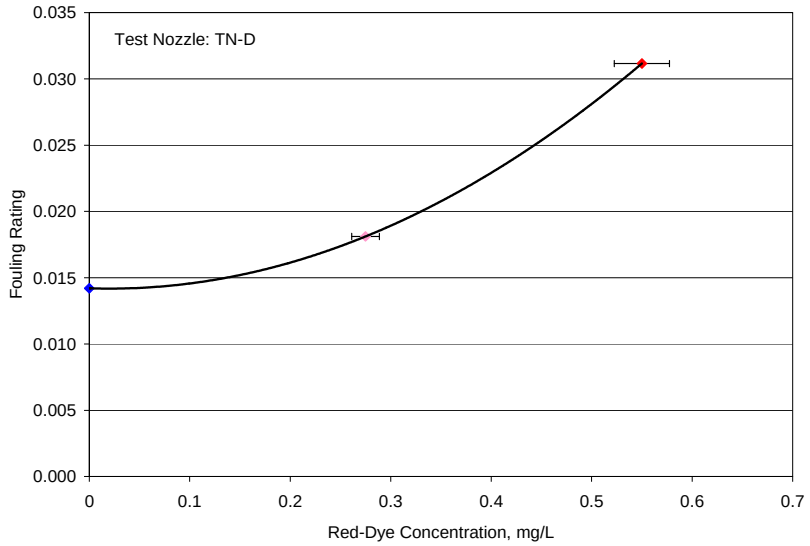

Figure 30. Effect of Red-Dye Contamination on Fouling Rate of Test Nozzle TN-D

Table 6. Analysis of Effect of Red Dye on Fouling Characteristics of Test Nozzle TN-D

Red-Dye Concentration (mg/L)	Correlation Equation	Fouling Rate	Relative Fouling Rate	Fouling Life Ratio	Equivalent Flights Lost
0.0	$1.659E+22 \times \exp(-25{,}440/T_{fuel})$	0.0142	1.0	1.0	0.0
0.275	$1.438E+27 \times \exp(-30{,}540/T_{fuel})$	0.0181	1.3	0.78	0.3
0.55	$1.659E+22 \times \exp(-24{,}600/T_{fuel})$	0.0312	2.2	0.46	1.2

The relative fouling rate is considered to be more important than the actual fouling rate. Relative fouling rate allows all fuel nozzles to be compared on the same basis. Also, due to the parallel nature of the correlation lines in figure 29, these relative rates are expected to be roughly the same at lower fuel temperatures more typical of actual flight operation.

The fouling life ratio is the inverse of the relative fouling rate and represents the effect of red dye on the fouling life of fuel nozzles if they were to experience a steady diet of contaminated fuel. In this case, the fouling life on a steady diet of 0.55 mg/L of red dye would be a little less than half, a very significant effect for a seemingly small amount of contaminant.

Another consideration is the effect of fouling life of an occasional, emergency flight on contaminated fuel. This scenario is one in which the contamination is not caught in the bulk storage tank and makes it into the airport hydrant system and/or onboard an aircraft. If the aircraft were allowed to fly, it is apparent that fouling would not be catastrophic, but would result in a little more deposit than if the fuel were not contaminated. In this case, the amount of deposit on one flight with 0.55 mg/L of red-dye contamination would be the same as that laid down in 2.2 flights of uncontaminated fuel. Thus, the fouling life of the fuel nozzles would be reduced by 1.2 flights.

5.3.6 Results of Nozzle Fouling Tests.

Of the nine fuel nozzle designs that were evaluated, five were found to be sensitive to red dye, i.e., the fouling rates were measurably increased by red-dye contamination. Three nozzles did not show a measurable sensitivity to red dye. The tests on the last fuel nozzle were inconclusive because the test results were inconsistent. In some cases, the fouling rate was found to increase in a test at a lower temperature. Likewise, some tests with red-dye contamination had lower fouling rates than tests without red dye.

Companion summary graphs like figures 28 and 29 are included in the respective appendix (A through I) for each nozzle design. Table 7 lists the effect of red-dye contamination for each of the nozzle designs following the methodology described in the previous section.

Table 7. Summary of Effects of 0.55 mg/L of Red-Dye Contamination on Fouling Rates of Test Nozzles

Test Nozzle	Relative Fouling Rate			Fouling Life Ratio			Equivalent Flights Lost		
	0.0	0.275	0.55	0.0	0.275	0.55	0.0	0.275	0.55
TN-A	1.0	–	1.16	1.0	–	0.86	0	–	0.2
TN-B	1.0	–	1.0	1.0	–	1.0	0	–	0
TN-C	1.0	2.50	3.96	1.0	0.40	0.25	0	1.5	3.0
TN-D	1.0	1.28	2.19	1.0	0.78	0.46	0	0.3	1.2
TN-E	1.0	–	1.0	1.0	–	1.0	0	–	0
TN-F	1.0	–	3.02	1.0	–	0.33	0	–	2.0
TN-G	1.0	–	1.0	1.0	–	1.0	0	–	0
TN-H	1.0	INC	INC	1.0	INC	INC	0	INC	INC
TN-I	1.0	2.52	3.20	1.0	0.40	0.31	0	1.5	2.5

INC = inconclusive

Figures 31 and 32 compare the results of the effects of red-dye contamination on relative fouling rate and equivalent flights lost for the five nozzles that were sensitive to red dye. It is important to note that, in general, the concentration effect increases steadily rather than either rising rapidly and then leveling off or staying low and then increasing rapidly.

Tests at the second concentration of 0.275 mg/L were not conducted on nozzle TN-A because the effect at 0.55 mg/L was relatively low. It was intended to conduct tests on the second concentration for nozzle TN-F, but the tests were delayed due to some technical difficulties with the fuel and then the program ran out of time and short on funds so the tests could not be conducted. This deficiency does not detract from the overall results since the concentration effect appears to be relatively linear.

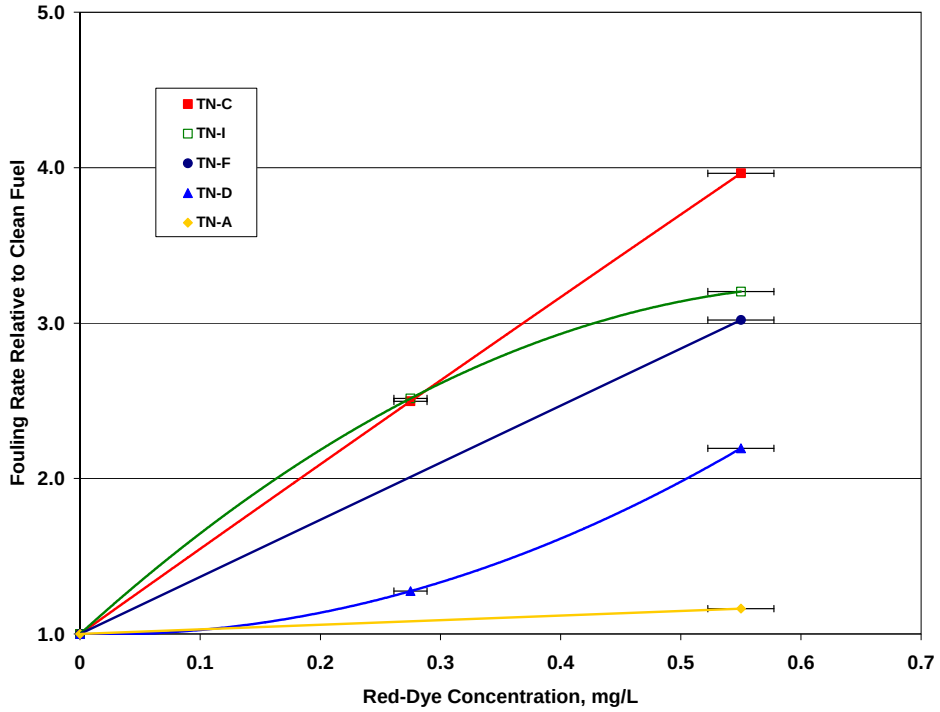

Figure 31. Summary of Effects of Red-Dye Contamination on Nozzle Fouling Rates Relative to Uncontaminated Fuel

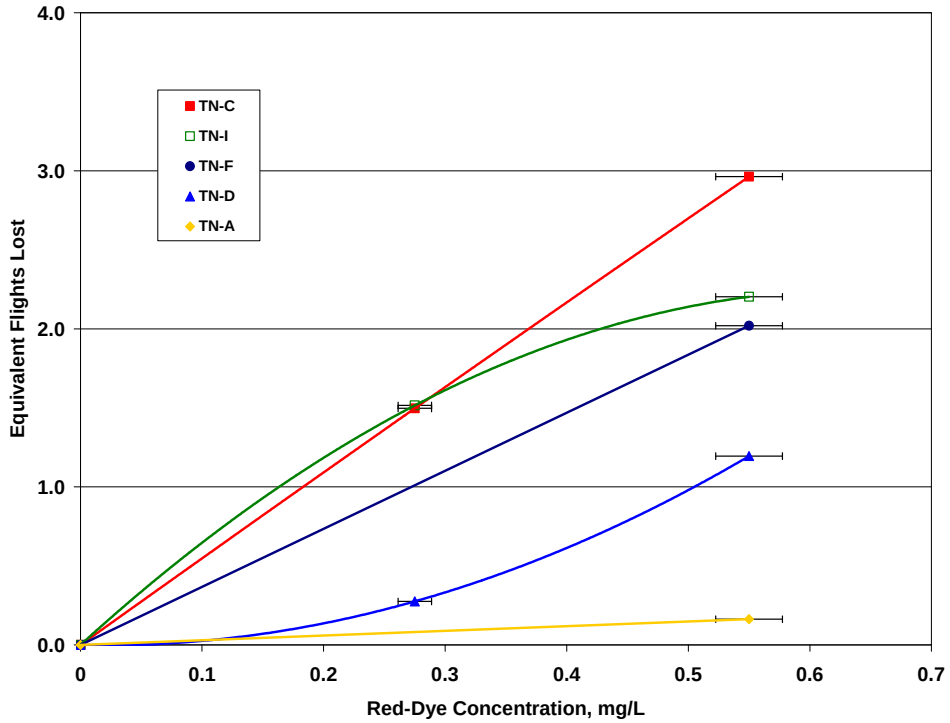

Figure 32. Summary of Effect of Red-Dye Contamination on Equivalent Flights Lost

5.4 TORQUE MOTOR FILTER FOULING TESTS.

5.4.1 Overview.

The torque motor filter fouling test was very similar to the nozzle fouling tests. Heated fuel was flowed through the test filter and the pressure drop monitored as a function of time. The filter screen was selected by Honeywell as typical of torque motor filter screens used in fuel control systems. The test conditions were provided by Honeywell also. The selection had the concurrence of the engine manufacturers. The tests were conducted at three fuel temperatures.

5.4.2 Test Article and Fixture.

Figure 33 shows the torque motor filter screen. The overall length is approximately 4.1 cm (1.625 inches). The active screen is approximately 2.8 cm (1.125 inches) in length and 0.5 cm (0.2 inch) in diameter.

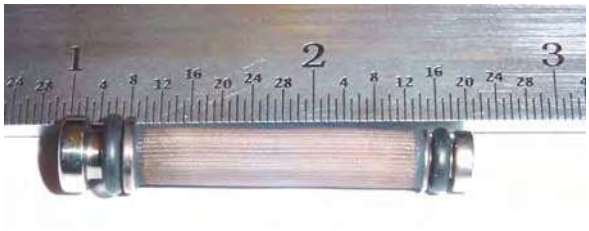

Figure 33. Torque Motor Filter Screen

A special fixture was fabricated following a design supplied by Honeywell. This is illustrated in figure 34. The flow through the filter is from the outside in. The means of securing the filter in place after it is inserted from the left into the fixture is not shown in this drawing.

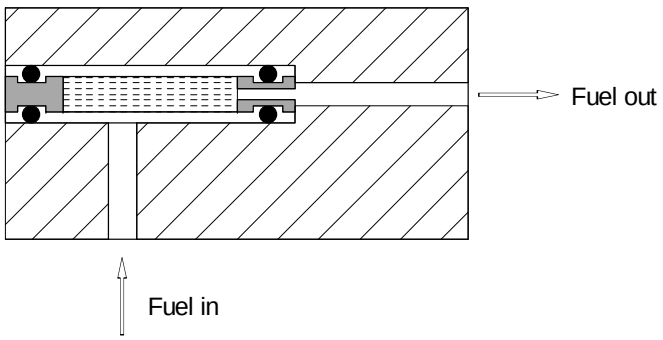

Figure 34. Schematic of Fixture for Torque Motor Filter Screen Tests

The fuel flow system for the filter tests was essentially the same as that used for the nozzle fouling tests shown in figure 15. One exception was a pressure relief valve installed to limit the pressure drop across the filter to 34 kPa (5 psid). The fuel heater was a smaller version of the fuel heater used with the nozzle fouling tests described in section 5.3.4. The fixture was insulated and heated by the fuel flowing through it; no external heat source was used. Typically, the block temperature was less than 3°C (5°F) lower than the fuel inlet temperature.

In addition to the fuel flow rate and pressure drop, the inlet and outlet temperatures of the fuel were monitored as was the temperature of the fixture.

5.4.3 Test Conditions.

The filter fouling tests were conducted at three fuel temperatures: 154°, 165°, and 177°C (310°, 330°, and 350°F). The nominal fuel flow rate was 16.1 kg/hr (35.5 lbm/hr), as suggested by Honeywell. The reference fuel was not tested because the thermal stability of the reference fuel had deteriorated by the time these tests were conducted.

5.4.4 Test Results.

The results of the filter tests were analyzed in the same manner as the nozzle fouling tests. Figure 35 is an Arrhenius plot of the fouling rates for the base fuel and two concentrations of red dye at each of the three test temperatures. It is evident that the fouling rates are much less sensitive to fuel temperature than the fouling rates of the fuel nozzles. An increase in fuel temperature of 4.4°C (40°F) resulted in increases in fouling rates on the order of 30% to 50%, whereas typically, nozzle fouling rates were found to increase on the order of 100% for only a 10° increase in fuel temperature. Similarly, the sensitivity to the level of red-dye concentration is lower than all but one of the fuel nozzles. This is shown in the insert on figure 35.

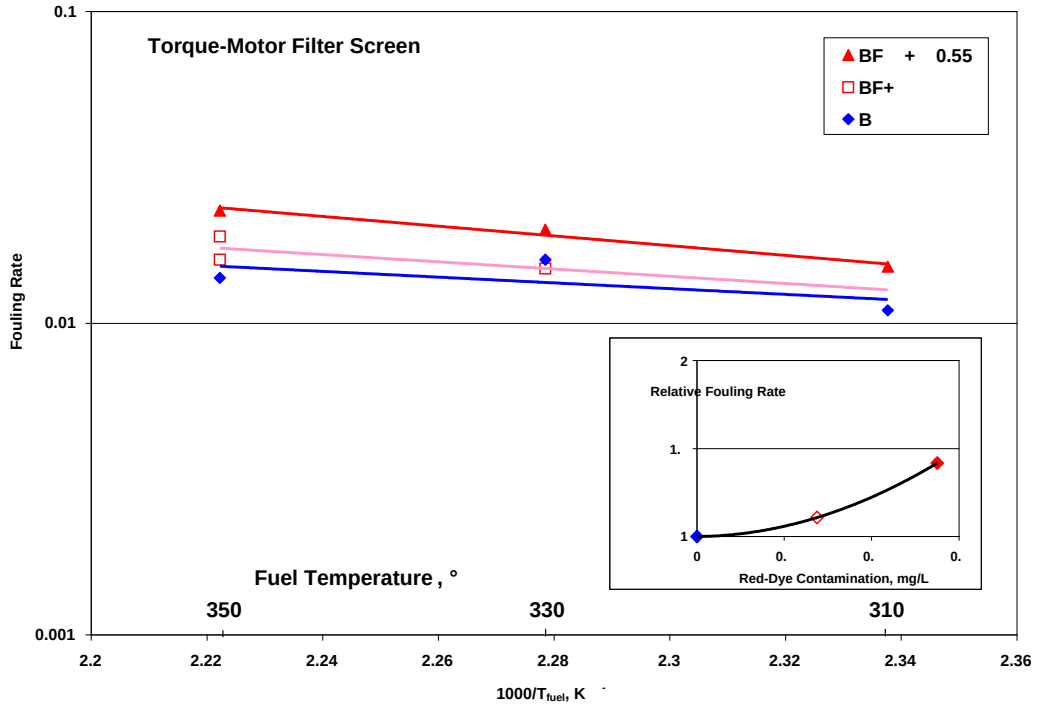

Figure 35. Effect of Red-Dye Contamination on the Fouling of Torque Motor Filter Screens

5.4.5 Conclusions on Fouling Tests of Torque Motor Filter Screens.

It is concluded that torque motor filter screens do not suffer any catastrophic fouling problems as the result of occasional use of fuel contaminated with red dye. Furthermore, the performance of the fuel nozzles is likely to deteriorate at a faster rate than the filters.

5.5 SPOOL VALVE TEST RESULTS.

5.5.1 Overview.

The objective of these tests was to evaluate the effects of fuel thermal stability, whether natural or due to contamination, on the operation of spool valves that may be used in fuel controllers or possibly other types of hydromechanical control devices that come into contact with fuel. Spool valves are used to control the flow of fuel to other devices. The spool valve slides in a sleeve with very tight clearance. A control pressure is applied at one end to move the valve against a spring. Any formation of deposit on the sliding surface will increase the resistance for valve motion and increase the required pressure to move the valve, making the valve slow to respond. In the extreme, the valve could stick, causing loss of control.

No particular test standard exists for determining long-term effects of fuel additives and contaminants on close tolerance flow components. Special test rigs were fabricated by Honeywell. The three engine manufacturers agreed that this one test would be representative of the spool valves used in the fuel systems of their engines. The test rig consisted of a stainless steel block bored to accept a sleeve and spool valve and to provide control ports in addition to the inlet and outlet ports for fuel flow. The spool and sleeve were production items fabricated from standard materials with appropriate dimensions and tolerances.

The test procedures along with the flow rates and environmental conditions were provided by the Honeywell engineering staff with the concurrence of the engine manufacturers.

5.5.2 Test Environment.

The fuel flow system for the spool valve tests was very similar to that used for the nozzle fouling tests shown in figure 15, with the major exception of a high-pressure fuel line that was added to control pressure. The fuel heater was a smaller version of the fuel heater used in the nozzle fouling tests described in section 5.3.4. The fixture was insulated and heated by the fuel flowing through it; no external heat source was used. Typically, the block temperature was less than 3°C (5°F) lower than the fuel inlet temperature.

5.5.3 Test Procedure.

Steady-state flow was established through the spool valve at 15 lb/hr; every 2 hours, the flow was pulsed twice to 35 lb/hr to simulate control changes, such as throttle moment. The flow was pulsed twice because the first cycle cleaned any deposit off the sliding surface before starting the second cycle. Waiting a long time between movements simulates a cruise condition, where there is very little control change for an extended period of time. This is considered a worst-case

situation in which there is no valve motion to clean off thin deposits as they form, thus preventing any significant buildup.

During each test, the following parameters were monitored with data being acquired at a rate of once per minute.

- Spool valve inlet fuel pressure (pressure at the supply port)
- Spool valve inlet fuel temperature
- Pressure drop across the spool valve (supply port to control port)
- Control pressure (ΔP across the actuator supply port to return port)
- Spool valve outlet fuel temperature (measured at the control port)
- Temperature of fuel to the actuator supply port
- Spool valve block temperature
- Fuel flow rate exiting the control port

At the beginning and end of each test, hysteresis tests were conducted as a means of evaluating the possible formation of deposits on the sliding surface. These tests were conducted by exercising the valve over the full stroke and documenting the flow performance parameter (flow coefficient), Cv, as a function of control pressure. Cv is a parameter similar to the flow number, FN, used in the nozzle fouling tests, except that it is based on volume flow rate rather than mass flow rate. These tests were conducted at a constant temperature of 40°C (120°F) rather than at the test fuel temperature to ensure constant fuel properties for the flow test. (This was not necessary for the fuel nozzle tests because the reduction in performance was being measured in real time during the test rather than just at the beginning and end.)

To obtain hysteresis curves, the spool valve was brought to flow shutoff by increasing the control pressure (defined as the differential pressure between the supply actuator port and the return port). The control pressure was then steadily decreased and the corresponding increase in-flow through the spool valve was recorded. When the spool valve reached its physical stop and the maximum flow through the valve was reached, the control pressure was gradually increased until the fuel flow was shutoff. This constituted one flow cycle (zero flow to maximum flow, back to zero flow). This process was repeated so that two hysteresis cycles were obtained. Conducting two hysteresis tests was recommended by Honeywell: The first stroke acts to clean any loose deposits from the surface, as would happen in real life with throttle movement during a flight; the second stroke determines if there is a permanent stiction problem caused by fuel deposits. It is normal for a new and clean spool valve to exhibit hysteresis. This is generally caused by relaxation of the spring in relation to the initial set of the internal sliding spool within the carriage spool. As deposits buildup in the valve or if other physical changes occur, the hysteresis loop becomes more distorted.

5.5.4 Test Matrix.

Seven 100-hour tests were conducted using the reference fuel, the base fuel, and one concentration of red-dye contamination in the base fuel. Table 8 summarizes the test matrix for the spool valve evaluations.

Table 8. Matrix of Test Conditions for Spool Valve Tests

Test No.	Test Fuel	Temperature (°F/°C)	Valve Block	Spool Set
1	Base fuel	325/163	009	X033
2	Base fuel	350/177	008	X031
3	Base fuel + 0.55 mg/L of red dye	325/163	008	X032
4	Base fuel + 0.55 mg/L of red dye	350/177	008	X031
5	Reference fuel	325/163	008	X032
6	Reference fuel	300/149	008	X031
7	Reference fuel	275/135	008	X030

5.5.5 Results of Spool Valve Hysteresis Tests.

The results of the hysteresis tests for the matrix identified in table 6 are presented in graphical form. Each graph consists of two parts designated “a” and “b”; the a graph compares the hysteresis loops of the first cycle, i.e., the cleaning cycle, and the b graph compares the hysteresis of the second cycle. Comparing a and b graphs indicates whether there was any cleaning action during the first stroke. The following discussion focuses primarily on the temperature and fuel effects.

Figures 36a and 37b present the results of spool valve Tests 1 and 2, comparing the temperature effect on the base fuel, which had a higher thermal stability than the reference fuel. The tests were conducted at 163°C (325°F) and 177°C (350°F), respectively. The hysteresis curves developed at the beginning and end of the 100-hour tests show no significant differences for the 163°C (325°F) case. However, when tests were conducted at 177°C (350°F), the posttest hysteresis curves generally shifted to the left. In other words, for a constant flow coefficient, less control pressure was required after the test than during the initial calibration. This was the only test where this apparent behavior occurred and might be explained if the spring within the spool valve had relaxed (lower apparent spring constant).

Figures 38a through 39b present the results of spool valve Tests 3 and 4, comparing the effect of fuel temperature on the performance of the spool valve with the base fuel contaminated with red dye. These tests were also conducted at 163° and 177°C (325° and 350°F), respectively. Figures 38a and 38b show that the pretest and posttest curves for Test 3 nearly fall on top of each other, indicating that the red-dye contamination did not affect performance at 163°C (325°F). However, the posttest hysteresis curves for Test 4 are somewhat wider than the pretest hysteresis curves, indicating some stiction within the valve. Also, Test 4, with red-dye contaminated fuel at 177°C (350°F), was the only test situation where the internal spool froze in place when the temperature was lowered at the conclusion of the test. The valve body had to be heated somewhat above 177°C (350°F) before the spool broke loose and the posttest hysteresis could be conducted. Once loosened, however, the valve moved with little difficulty. The posttest hysteresis curves for Test 3 show a reduction in the flow coefficient at the high end of the hysteresis curve; this might be due to a slight blockage of a spool orifice hole.

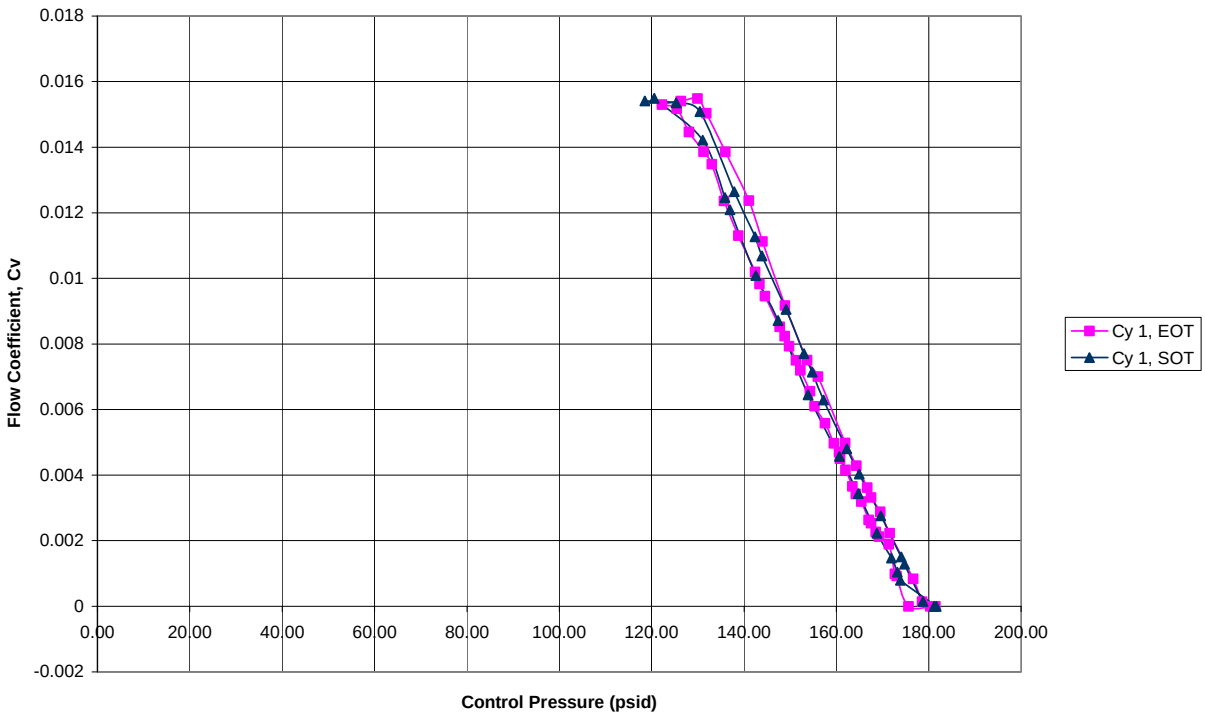

Figure 36a. Hysteresis Cycle 1 Curves for Test 1, Baseline Fuel at 163°C (325°F)

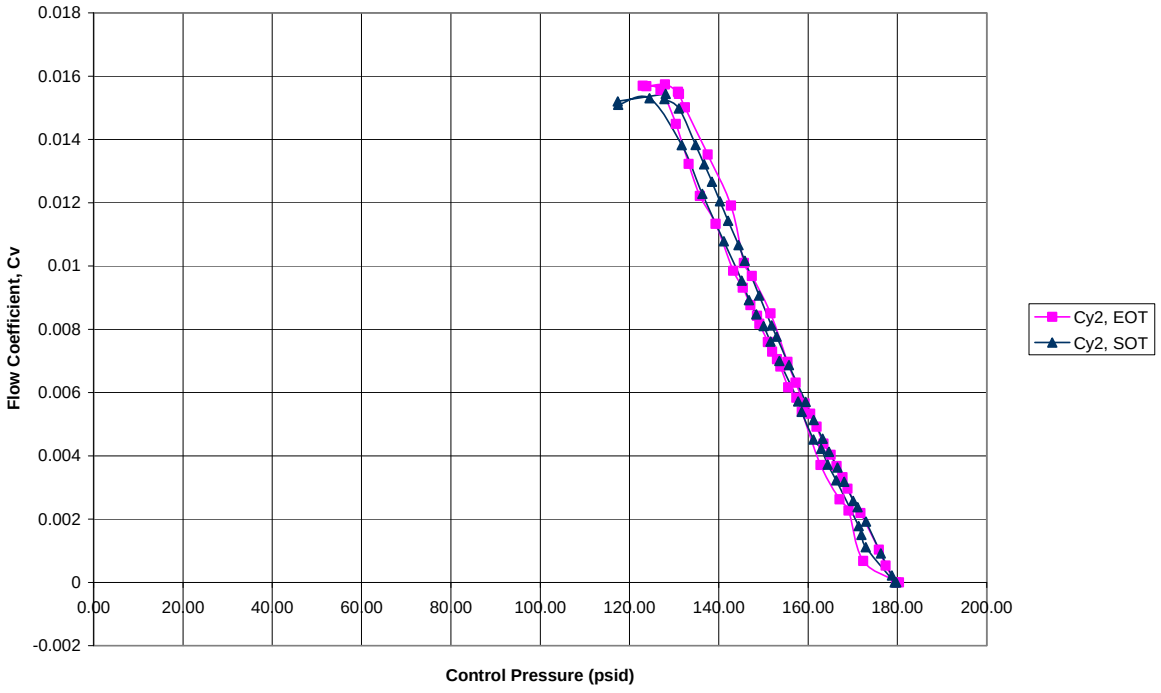

Figure 36b. Hysteresis Cycle 2 Curves for Test 1, Baseline Fuel at 177°C (325°F)

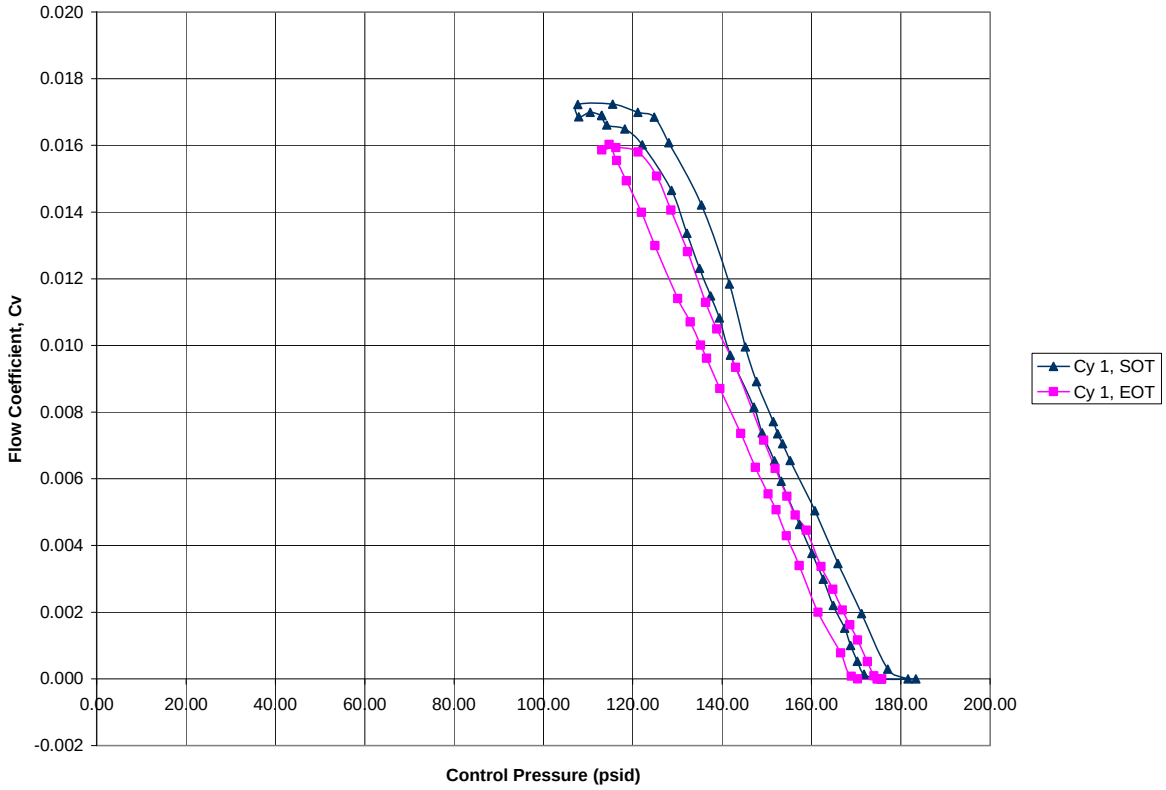

Figure 37a. Hysteresis Cycle 1 Curves for Test 2, Baseline Fuel at 177°C (350°F)

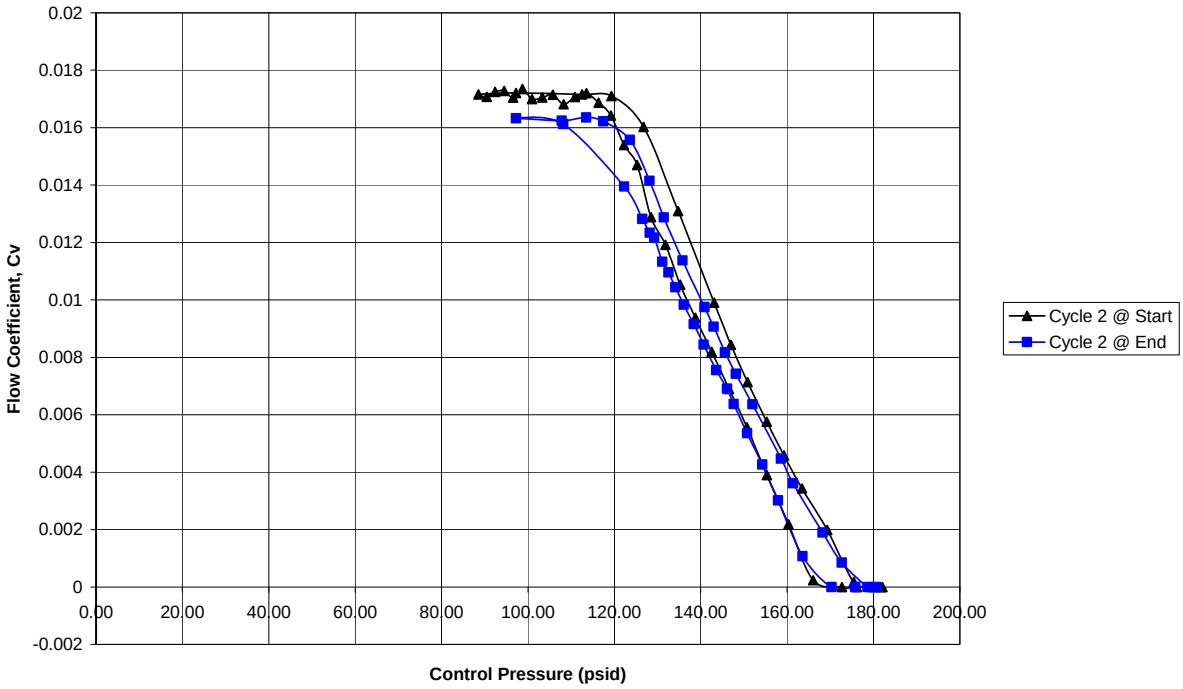

Figure 37b. Hysteresis Cycle 2 Curves for Test 2, Baseline Fuel at 177°C (350°F)

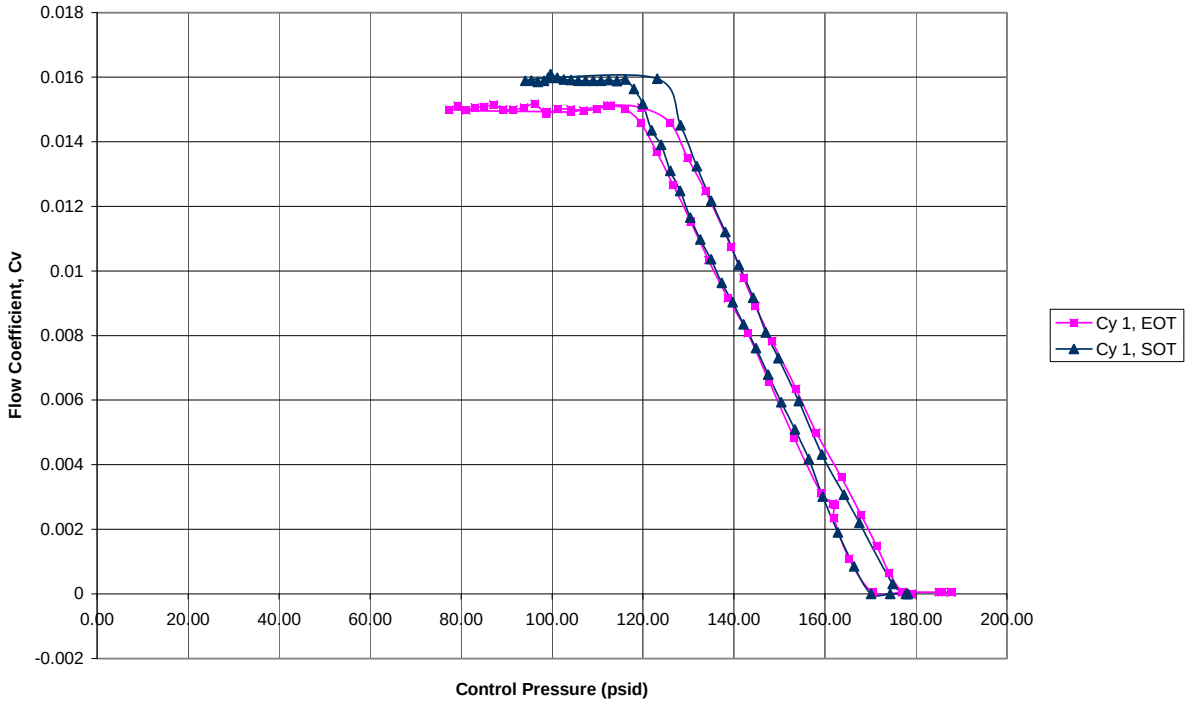

Figure 38a. Hysteresis Cycle 1 Curves for Test 3, Baseline Fuel + Red Dye at 163°C (325°F)

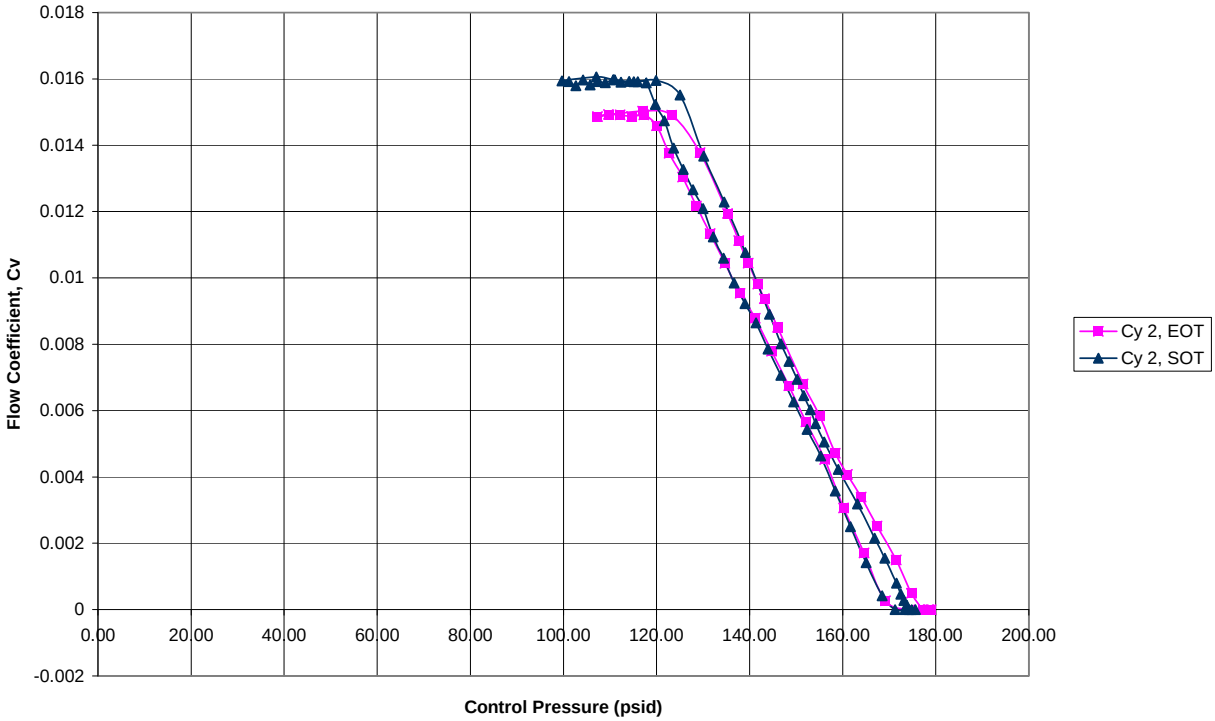

Figure 38b. Hysteresis Cycle 2 Curves for Test 3, Baseline Fuel + Red Dye at 163°C (325°F)

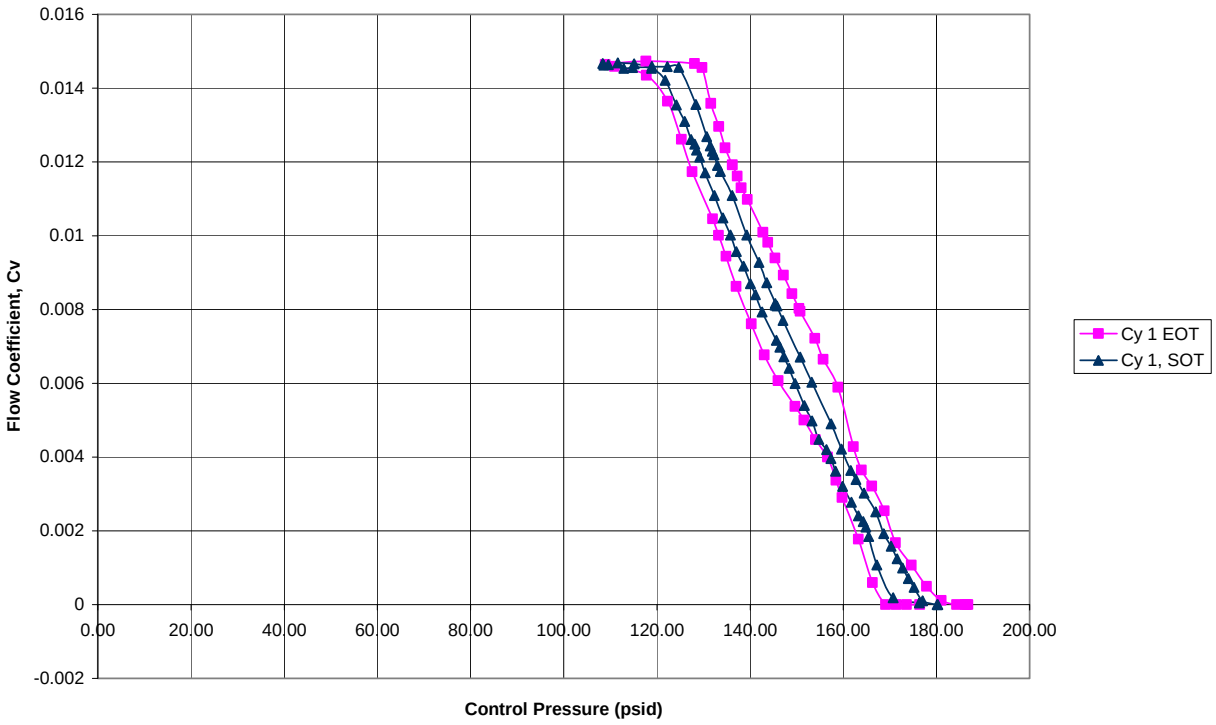

Figure 39a. Hysteresis Cycle 1 Curves for Test 4, Baseline Fuel + Red Dye at 177°C (350°F)

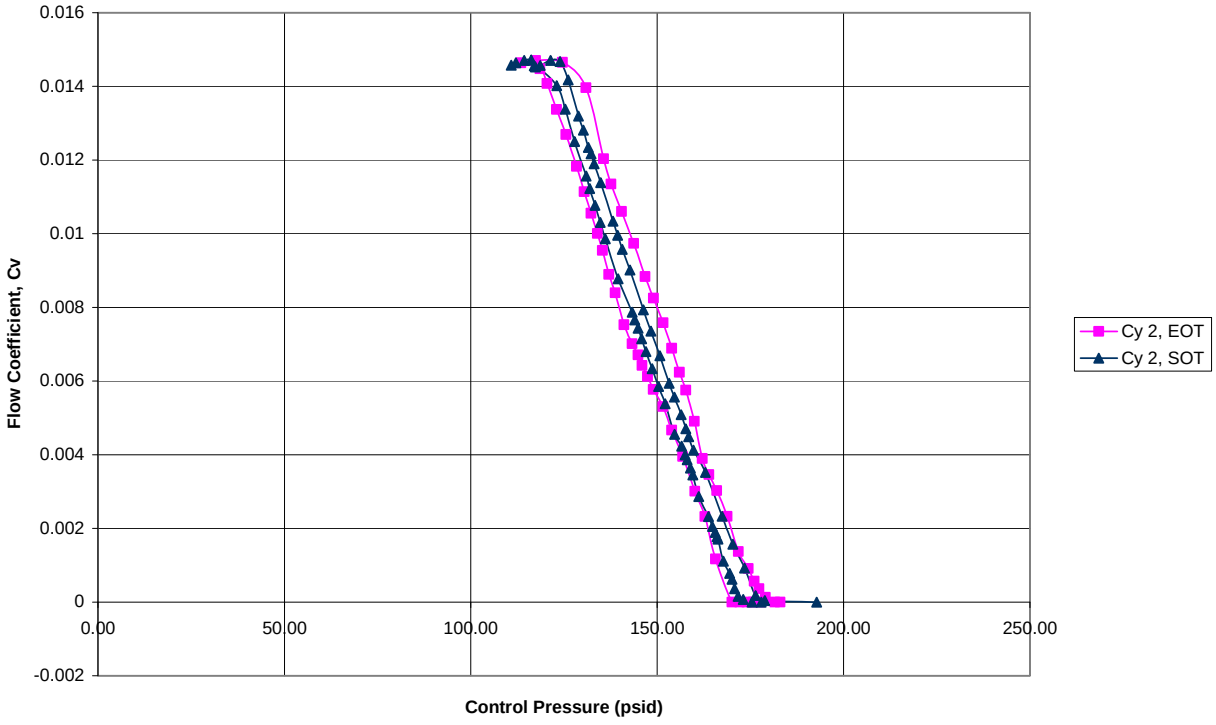

Figure 39b. Hysteresis Cycle 2 Curves for Test 4, Baseline Fuel + Red Dye at 177°C (350°F)

Figures 40a through 42b present the results of spool valve Tests 5, 6, and 7, respectively, comparing the effect of temperature on spool valve performance with the reference fuel. Figures 40a and 40b show a very significant increase in hysteresis, indicating that at 163°C (325°F), the reference fuel caused significant deposition on the sliding surface, much more so than either the neat base fuel or contaminated base fuel caused at 177°C (350°F). Figures 41a and 41b show the hysteresis to be reduced at 149°C (300°F), but it is still significantly greater than the other fuels at 177°C (350°F). Figures 42a and 42b show that at 135°C (275°F), the hysteresis became comparable to the other two fuels at 177°C (350°F).

It is apparent from the results of the spool valve tests that the thermal stability of the fuel, as measured by the JFTOT breakpoint temperature, is directly relatable to an increase in hysteresis. However, a method for quantifying the change in hysteresis so as to relate it to the red-dye contamination was not developed, as most of the effort was placed on finishing the nozzle fouling tests within the available funds. The presence of red dye in the base fuel appeared to cause a noticeable increase in hysteresis at the very high fuel temperature of 177°C (350°F); but even there, it was very small compared to the increase caused by a fuel that was within specification but had a lower thermal stability. At 163°C (325°F), the red-dye contamination had no apparent effect on hysteresis.

There is an open question as to why the valve was initially stuck at 177°C (350°F) on the contaminated fuel, but it seems likely that at fuel temperatures more typical of actual fuel control operation, the effect of 0.55 mg/L of red dye might be negligible.

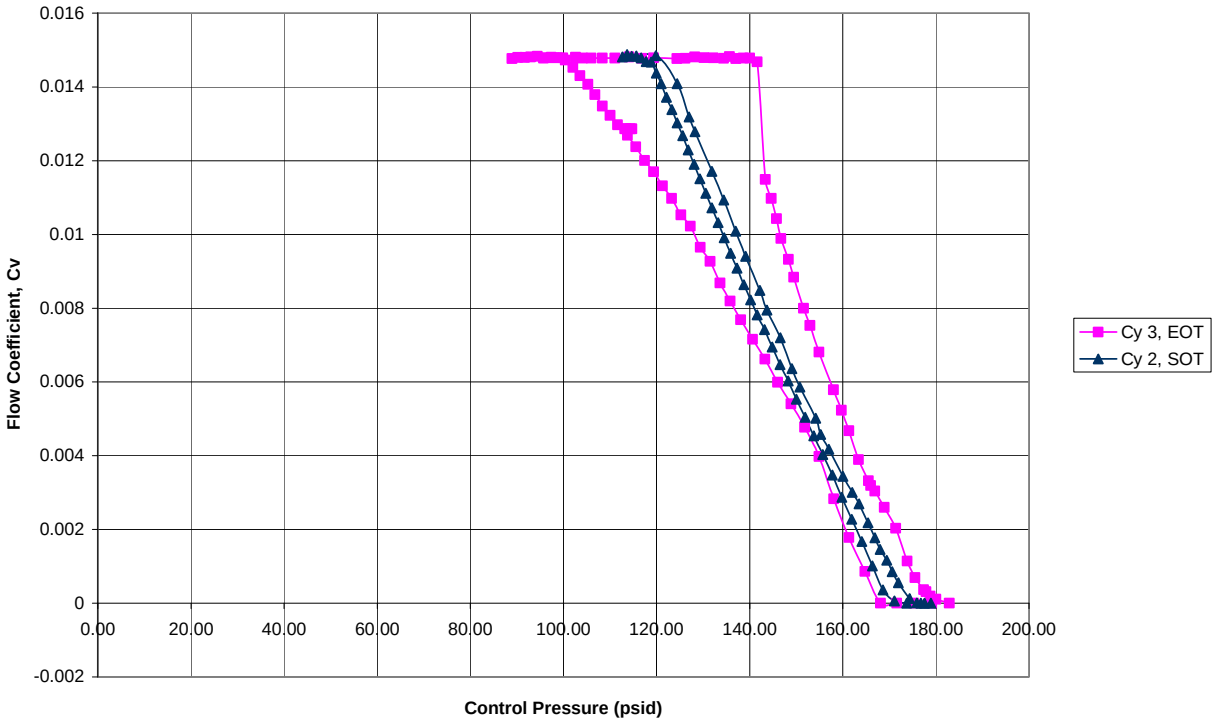

Figure 40a. Hysteresis Cycle 1 Curves for Test 5, Reference Fuel at 163°C (325°F)

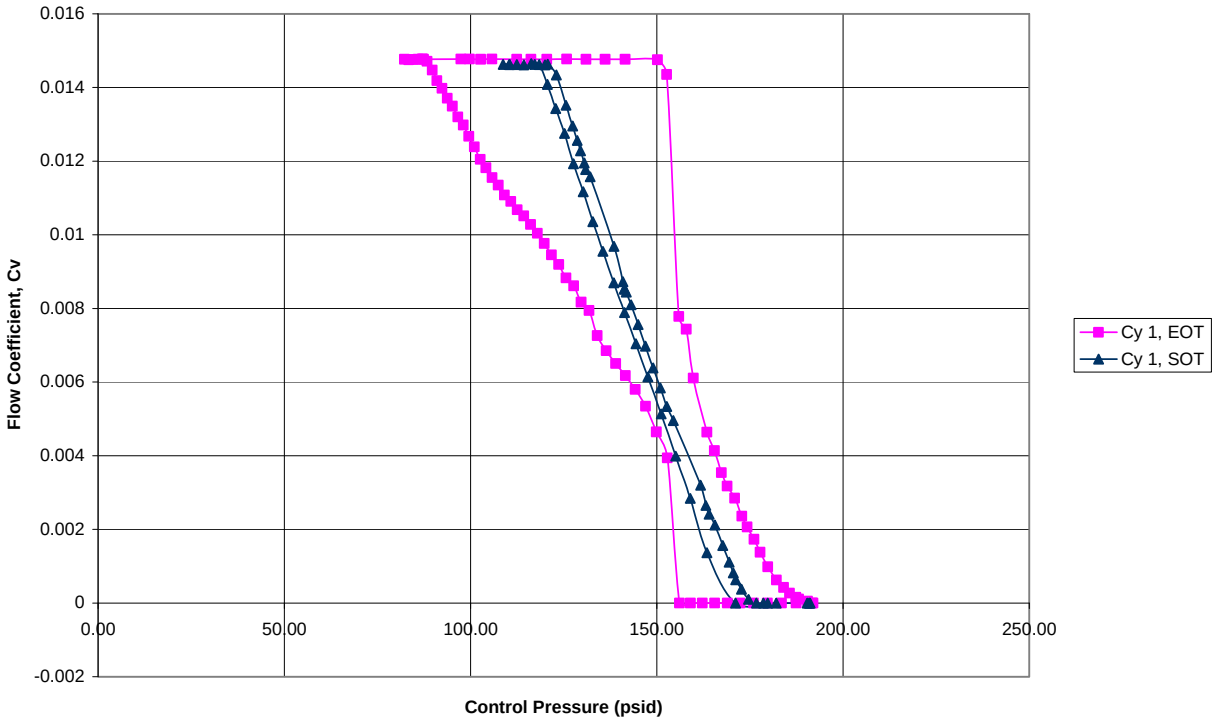

Figure 40b. Hysteresis Cycle 2 Curves for Test 5, Reference Fuel at 163°C (325°F)

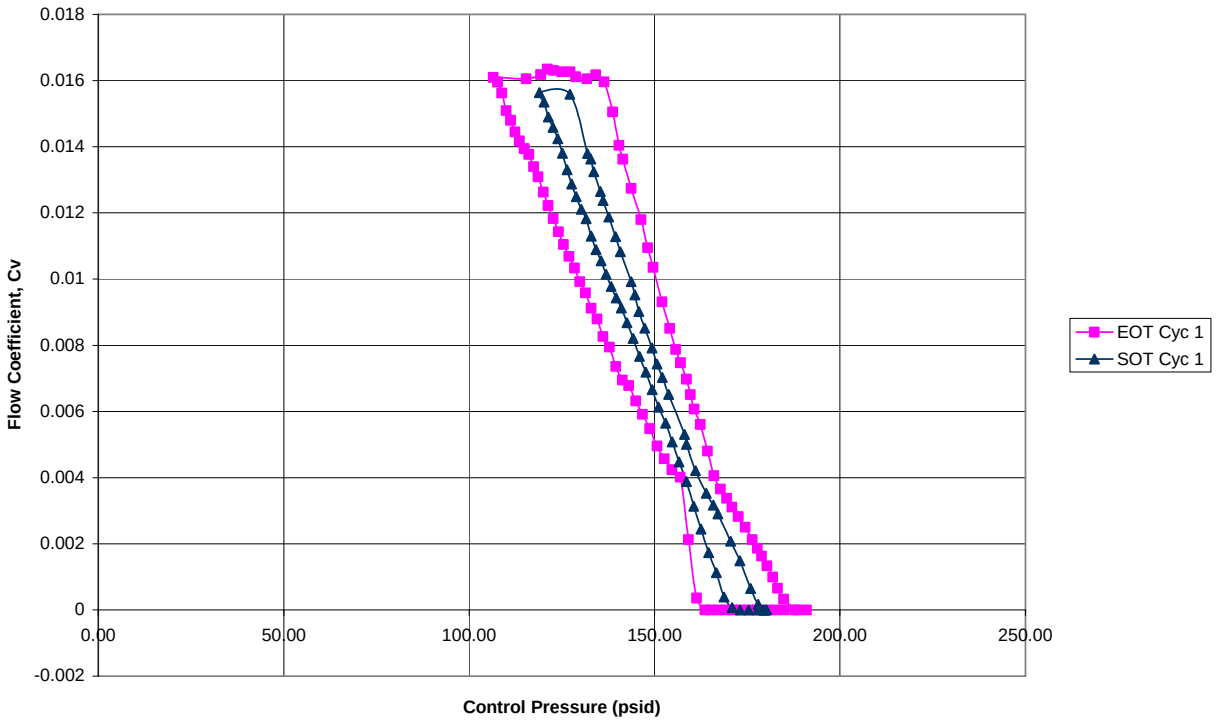

Figure 41a. Hysteresis Cycle 1 Curves for Test 5, Reference Fuel at 149°C (300°F)

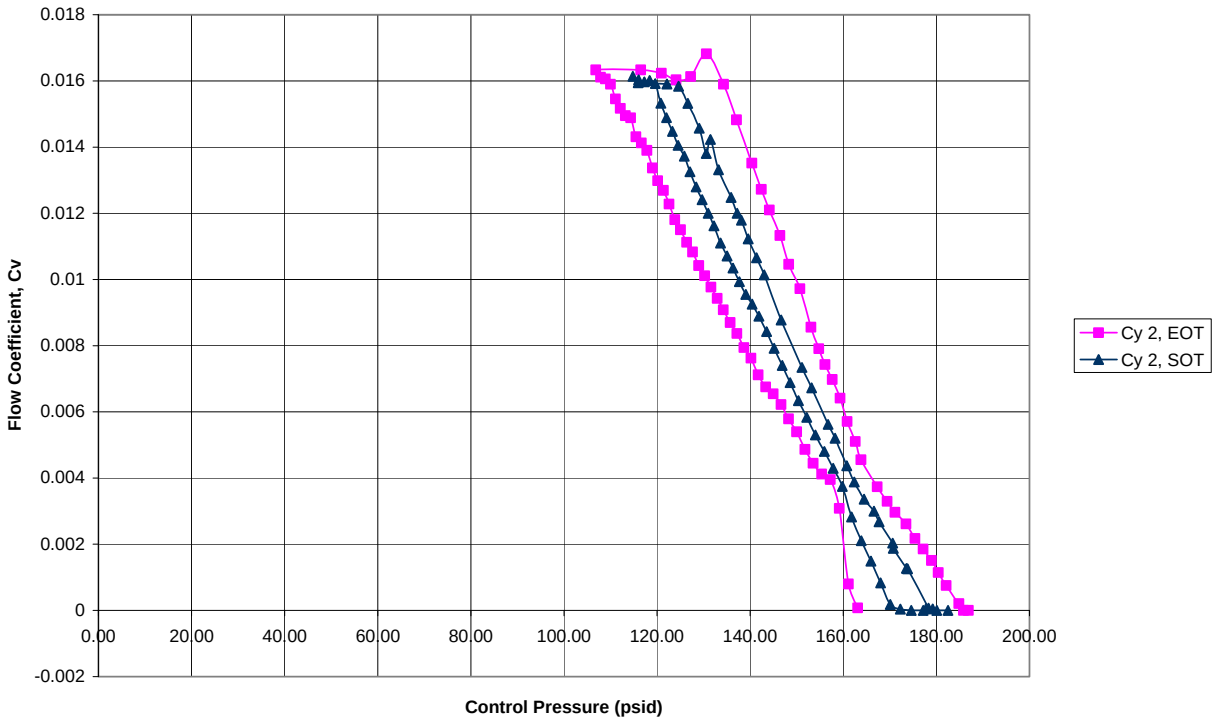

Figure 41b. Hysteresis Cycle 2 Curves for Test 5, Reference Fuel at 149°C (300°F)

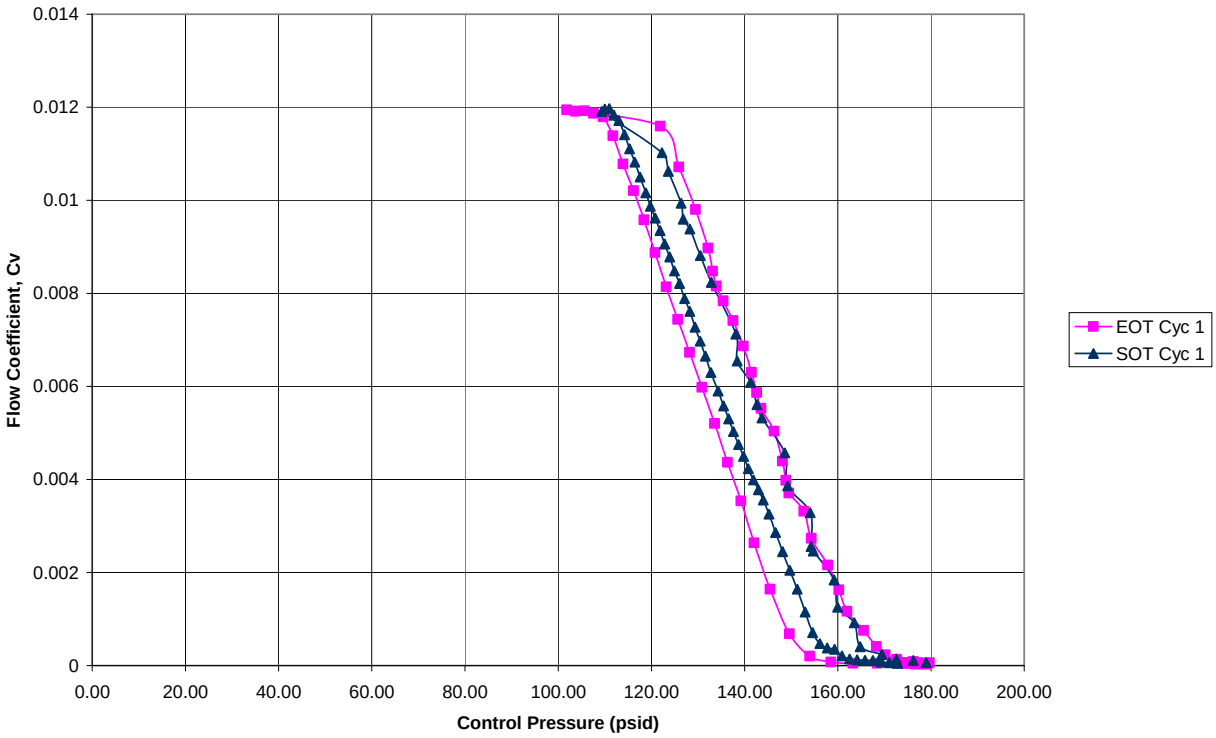

Figure 42a. Hysteresis Cycle 1 Curves for Test 5, Reference Fuel at 135°C (275°F)

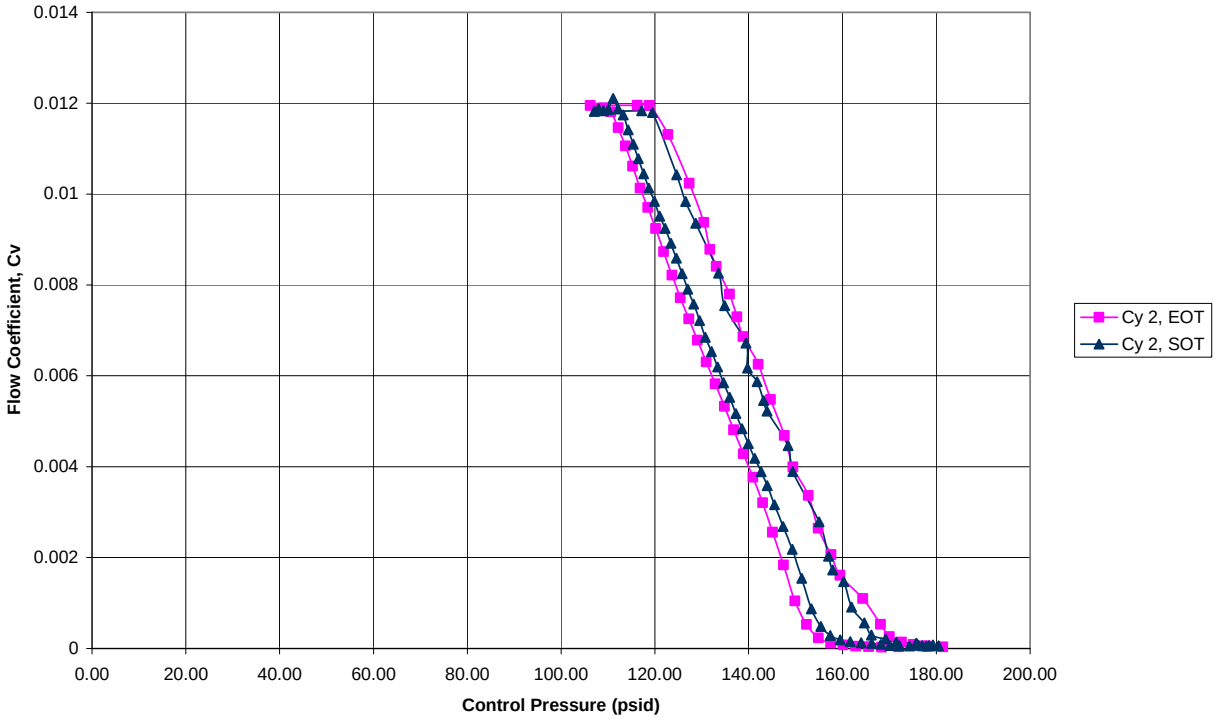

Figure 42b. Hysteresis Cycle 2 Curves for Test 5, Reference Fuel at 135°C (275°F)

6. SUMMARY AND CONCLUSIONS.

6.1 EFFECT OF RED-DYE CONTAMINATION ON JET FUEL THERMAL OXIDATION TESTER.

Based on the results of the fuel screening in Phase 1 of this project, 0.55 mg/L of red dye in jet fuel, as measured by the Petrospec JT-100, can cause a measurable reduction in the thermal stability of some jet fuels. It was found that the presence of red dye can increase the thickness of the deposit on the Jet Fuel Thermal Oxidation Tester (JFTOT) tube, even though the breakpoint temperature is not changed.

This degradation of thermal stability is independent of any impact of the diesel fuel or fuel oil that the presence of the red dye potentially represents. Since the thermal stability of diesel fuel and fuel oil is uncontrolled, the presence of these fuels is likely to have an even more serious impact than the red dye.

Fuel thermal stability and sensitivity to red dye were apparently due to trace chemistry since no correlations could be found with major components, such as aromatics, olefins, or sulfur. Additionally, neither thermal stability nor sensitivity to red-dye contamination appeared to be related to crude type or refining process.

The Ellipsometric Tube Analysis technique appears to be a valuable tool for quantifying JFTOT deposits. It provides additional information on the deposition rate under the conditions of the JFTOT test. The increase in the deposit thickness on the JFTOT tubes caused by the red-dye contamination was of the same order of magnitude as the increase in nozzle fouling rate.

6.2 EFFECT OF RED-DYE CONTAMINATION ON PERFORMANCE OF FUEL SYSTEM HARDWARE.

In the hardware tests of this project, the fouling rates of fuel nozzles and filter screens can be quantified and correlated with the thermal stability of the jet fuel. This provides a basis for evaluating the effect of red-dye contamination on the fouling rate of the hardware. A method for quantifying the degradation of hysteresis in spool valves was not developed due to a shortage of funds, although such a method seems possible.

Generally speaking, the fouling characteristics of the torque motor filter screens were found to be less sensitive to both fuel thermal stability and fuel temperature than the fouling characteristics of fuel nozzles.

Based upon the component fouling tests conducted in this program, the presence of red dye in jet fuel can measurably increase the fouling rates of engine fuel nozzles and, to a lesser extent, the filters. The effect is design-specific, as not all nozzles were found to be affected at the 0.55-mg/L contamination level. At 177°C (350°F), the presence of red dye was found to cause a small but noticeable increase in the hysteresis of spool valves; this increase was considered very small compared to the increase caused by a specification fuel of minimal thermal stability. It is

thought that at system fuel temperatures more typical of actual engine operation, that 0.55 mg/L of red dye would not increase the hysteresis of spool valves.

It was intended to also evaluate the effect of the diesel fuel contamination that the presence of red dye represents. Delays in securing the test hardware, as well as technical problems with the base fuel during the fouling tests, increased the program costs and precluded completing these tests. The results obtained justify the need to complete this testing and demonstrate a high likelihood of success.

These results have been forwarded to the engineering staffs of the aircraft engine manufacturers for their use in determining an industry consensus on the minimum acceptable level of red-dye contamination in jet fuel.

7. BIBLIOGRAPHY.

David, P., et al., 1997, "Development of an Ellipsometric JFTOT Tube Analyser (ETA)," *Proceedings of the 6th International Conference on Stability and Handling of Liquid Fuels,* Vancouver, British Columbia, October.

DESC, 2000, Petroleum Quality Information System Aviation Fuels Data (1998), Defense Energy Support Center, Ft. Belvoir, Virginia, April.

Moses, et al., 1984, "An Alternate Test Procedure to Qualify Fuels for Navy Aircraft," U.S. Naval Air Propulsion Center Report NAPC-PE-145C, August.

Strauss, K.H., 1997, "Jet Fuel Contamination by Diesel Fuel Dye," *Proceedings of the 6th International Conference on Stability and Handling of Liquid Fuels,* Vancouver, British Columbia, October.

APPENDIX A—EXPERIMENTAL RESULTS FOR TEST NOZZLE TN-A

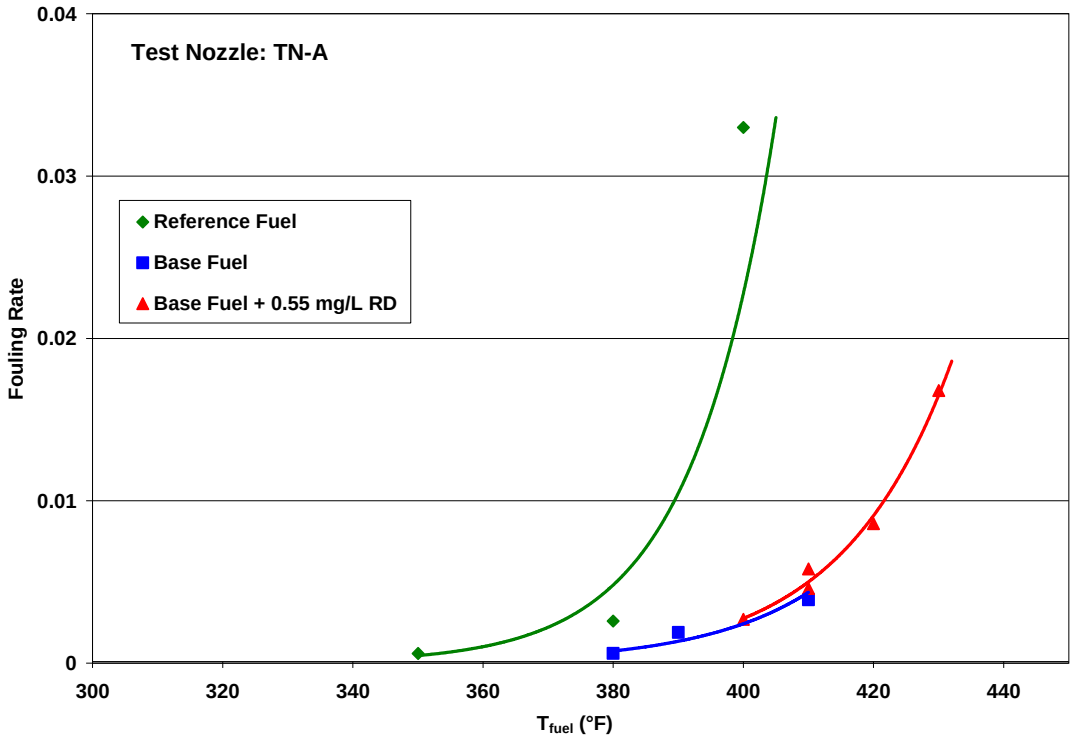

Figure A-1. Fouling Rate Summary

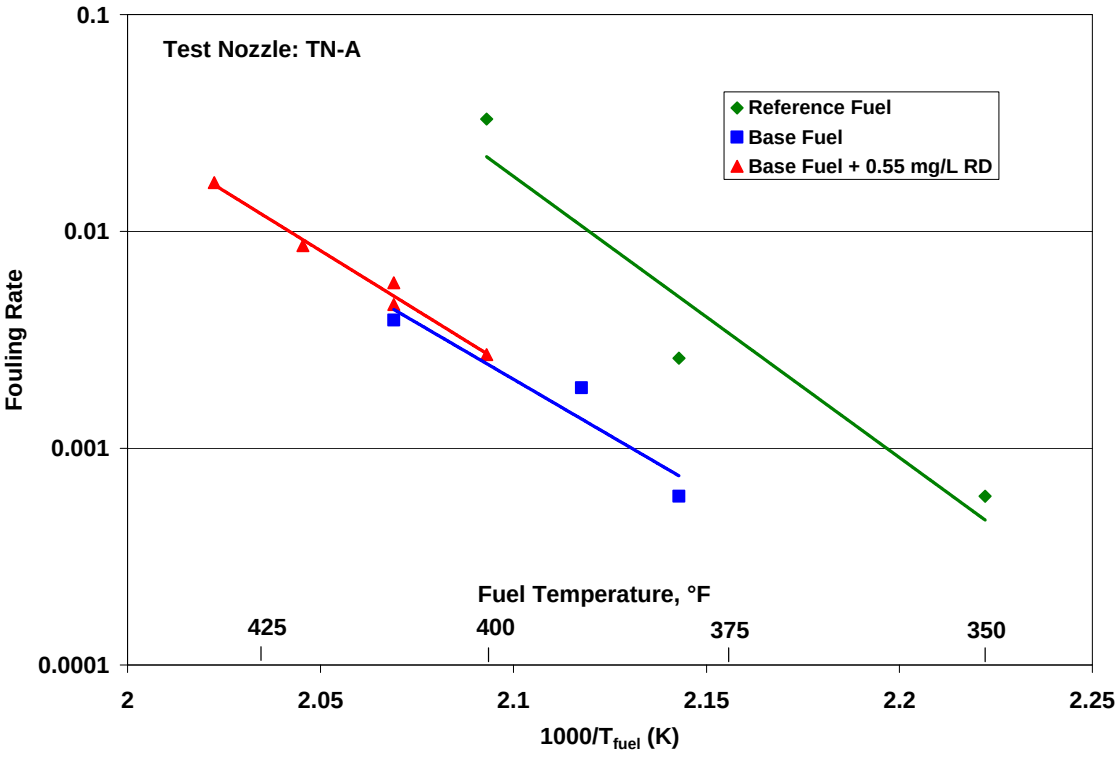

Figure A-2. Arrhenius Fouling Rate Summary

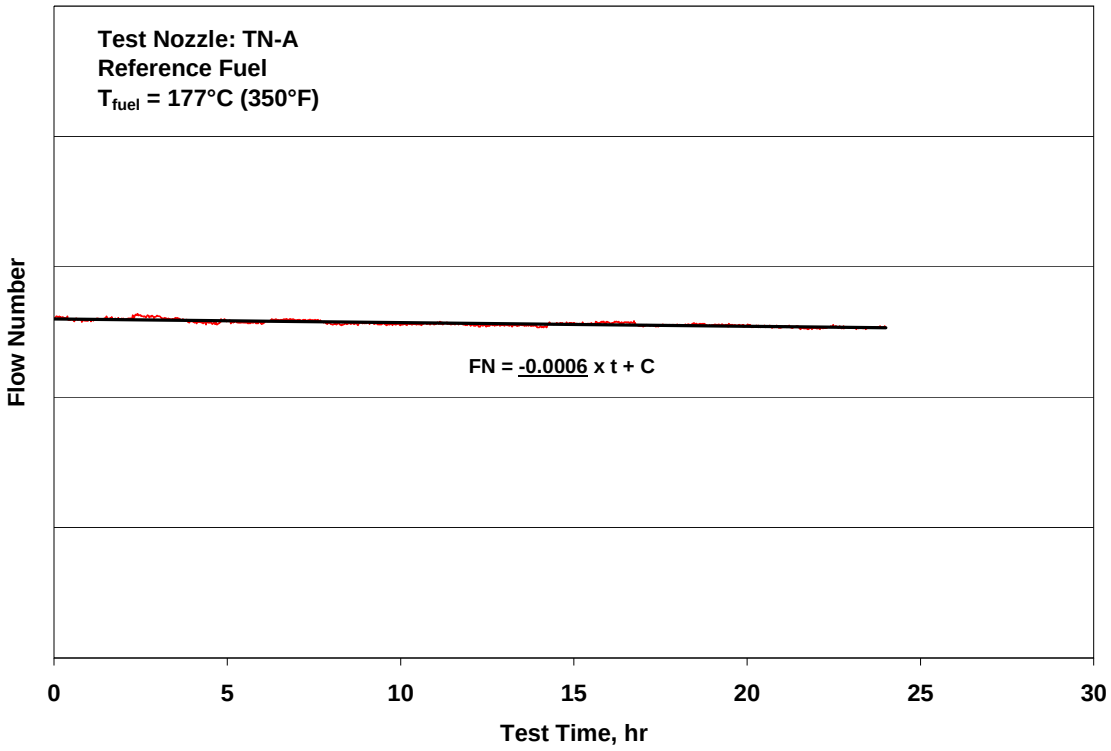

Figure A-3. Fouling Rate on Reference Fuel at T_{fuel} = 177°C (350°F)

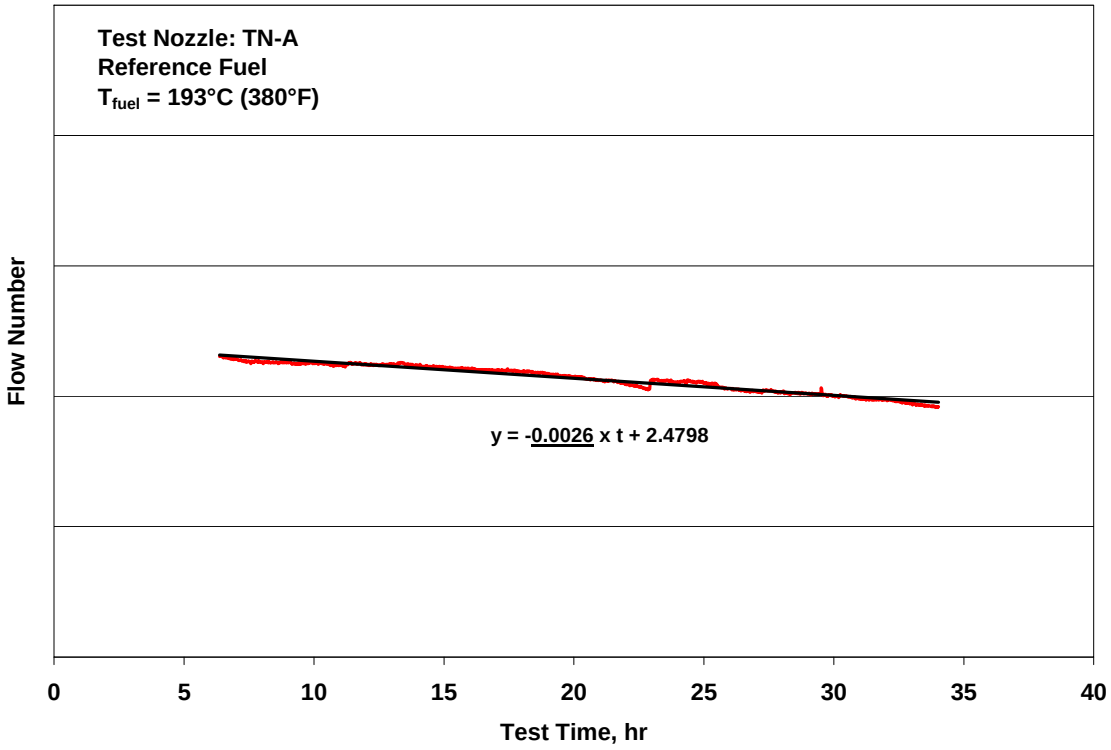

Figure A-4. Fouling Rate on Reference Fuel at T_{fuel} = 193°C (380°F)

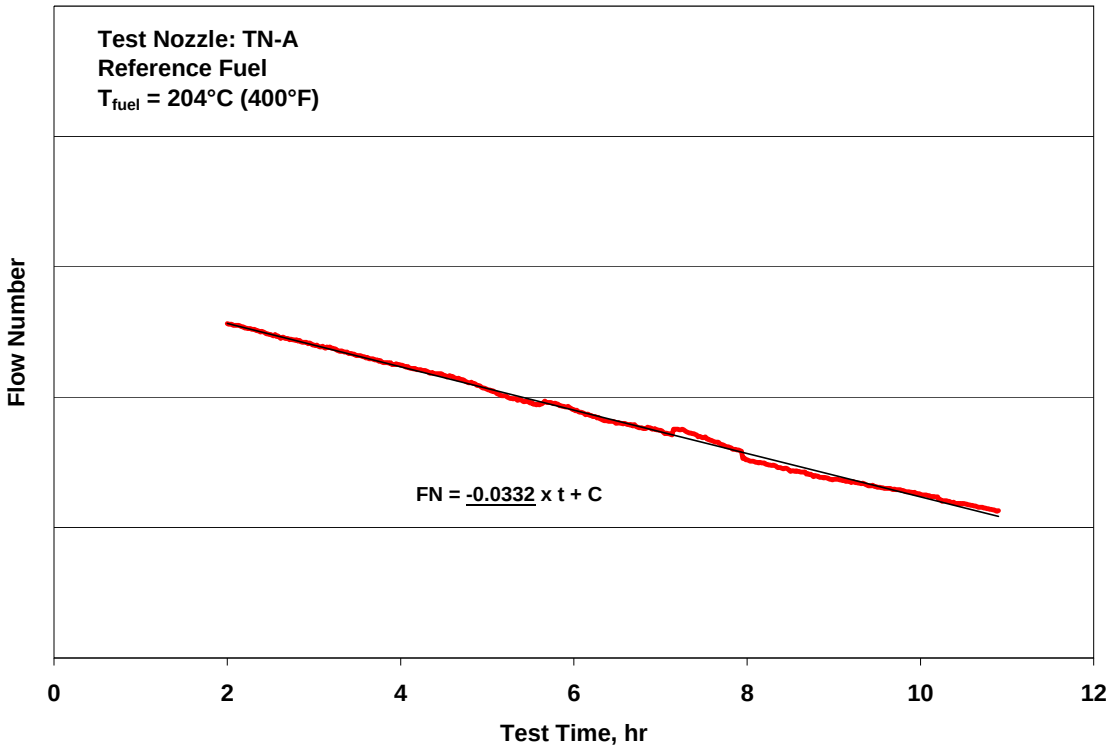

Figure A-5. Fouling Rate on Reference Fuel at T_{fuel} = 204°C (400°F)

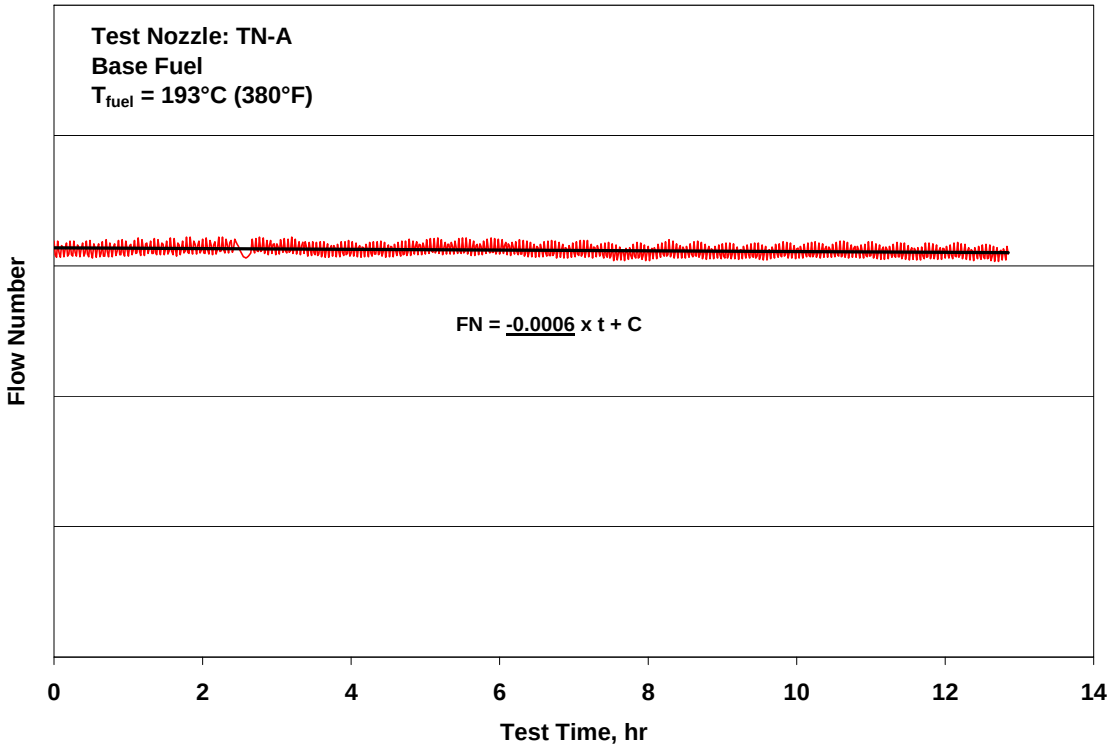

Figure A-6. Fouling Rate on Base Fuel at T_{fuel} = 193°C (380°F)

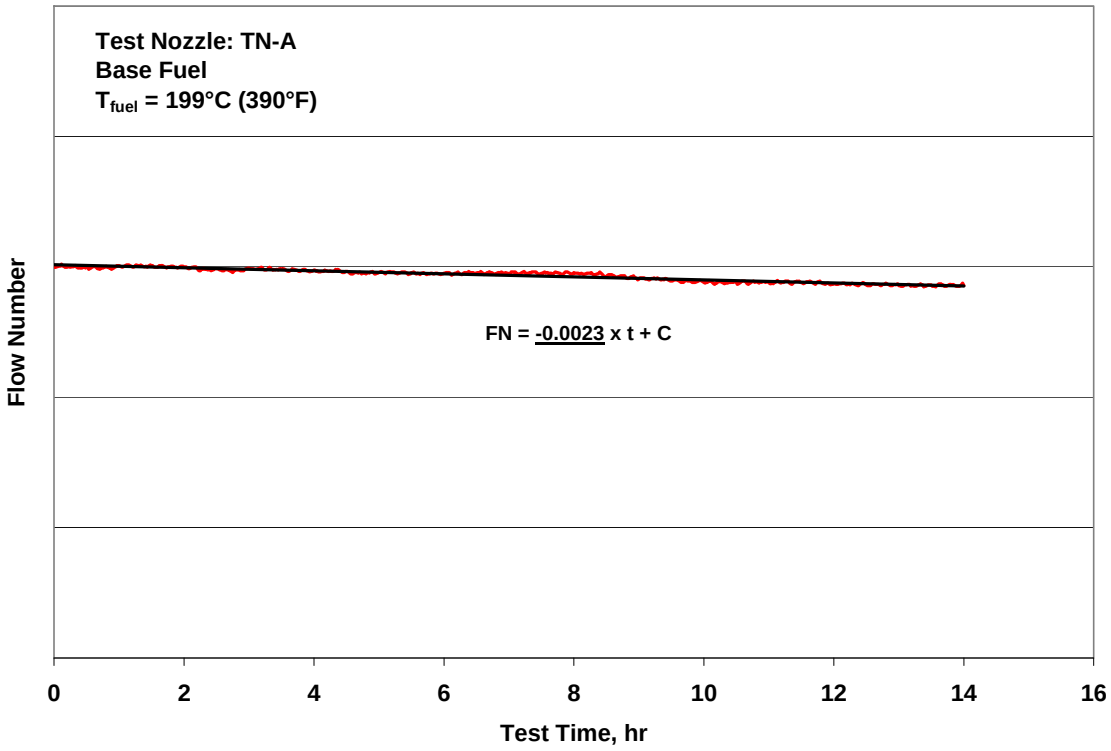

Figure A-7. Fouling Rate on Base Fuel at T_{fuel} = 199°C (390°F)

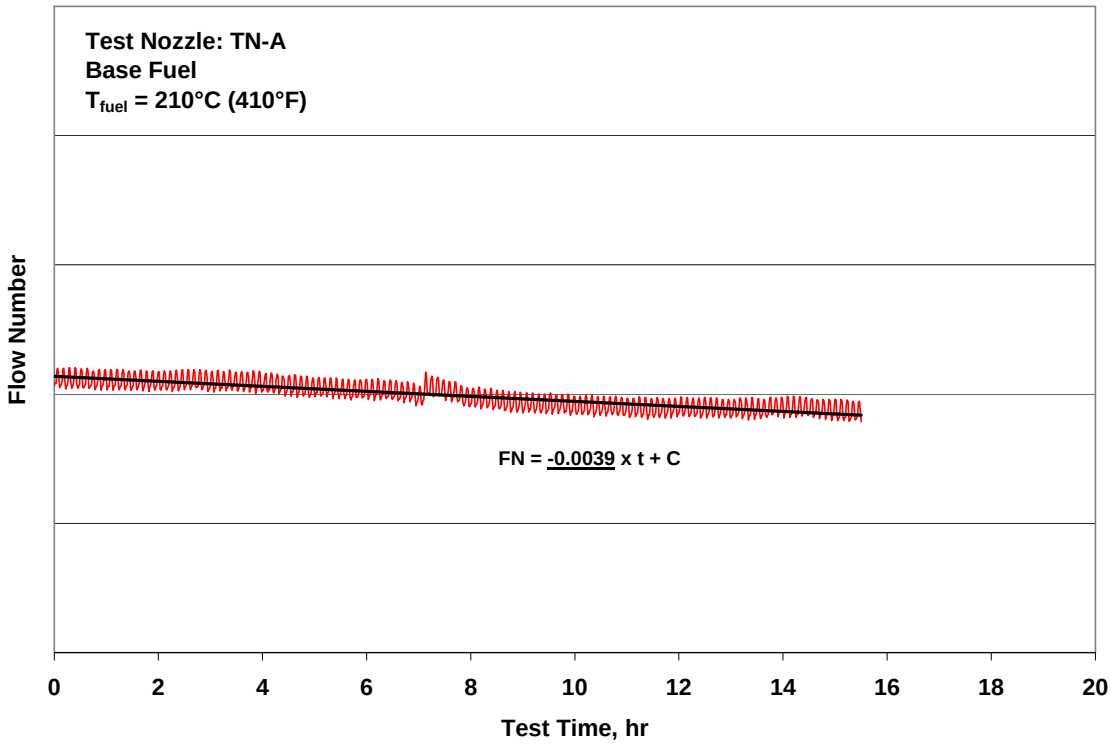

Figure A-8. Fouling Rate on Base Fuel at T_{fuel} = 210°C (410°F)

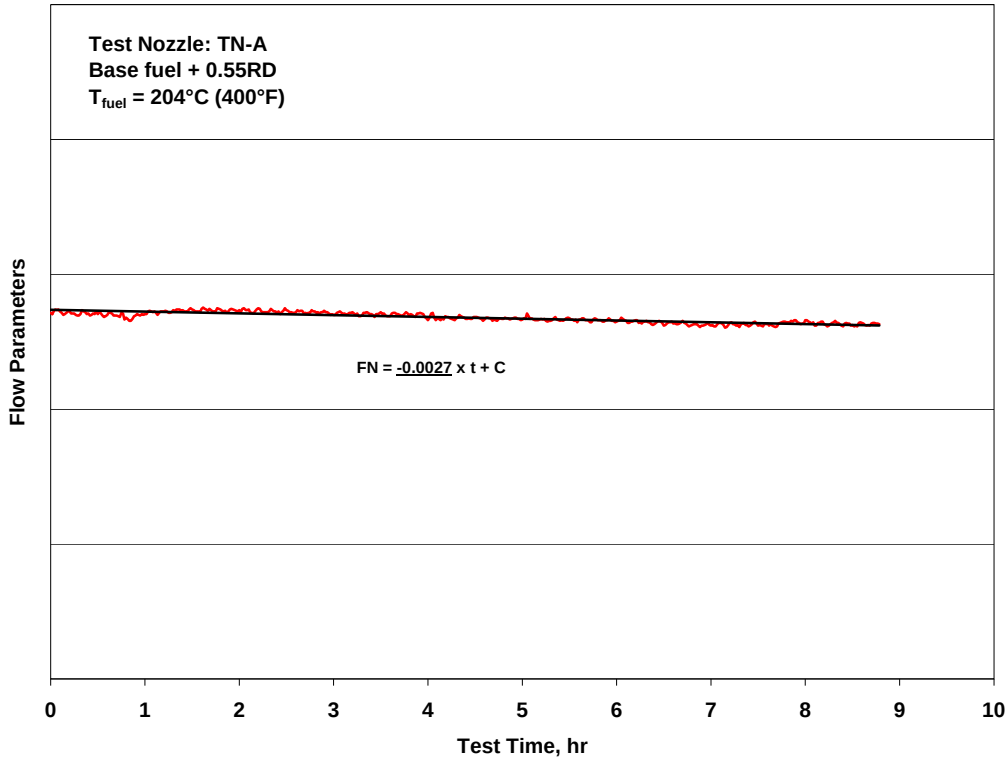

Figure A-9. Fouling Rate on Base Fuel + 0.55 mg/L of Red Dye at T_{fuel} = 204°C (400°F)

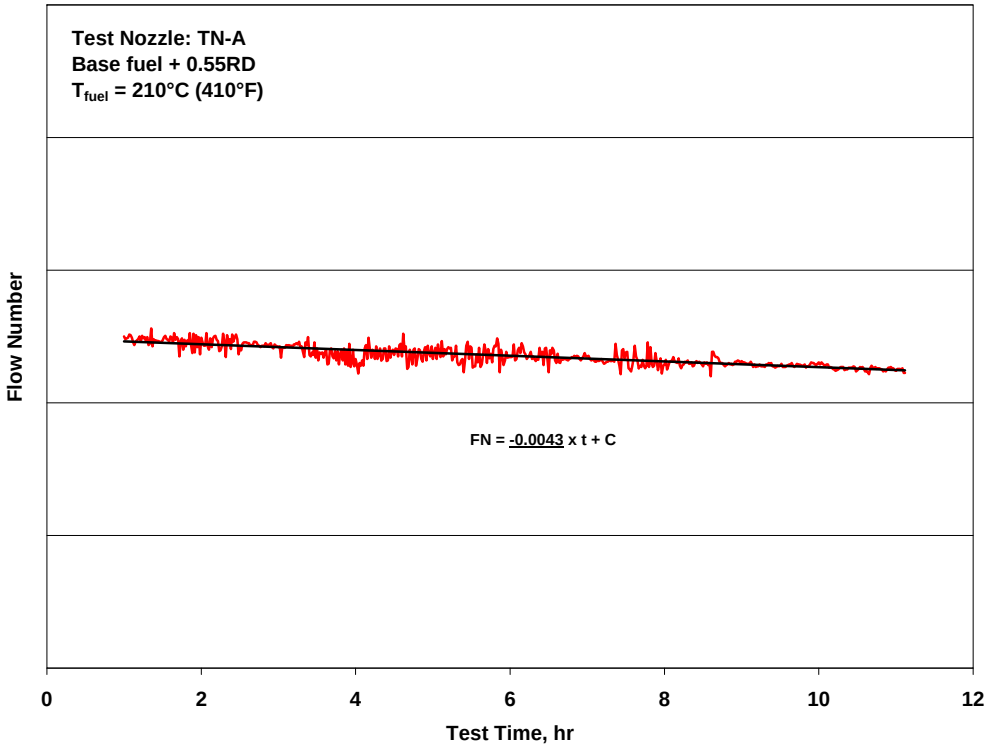

Figure A-10. Fouling Rate on Base Fuel + 0.55 mg/L of Red Dye at T_{fuel} = 210°C (410°F)

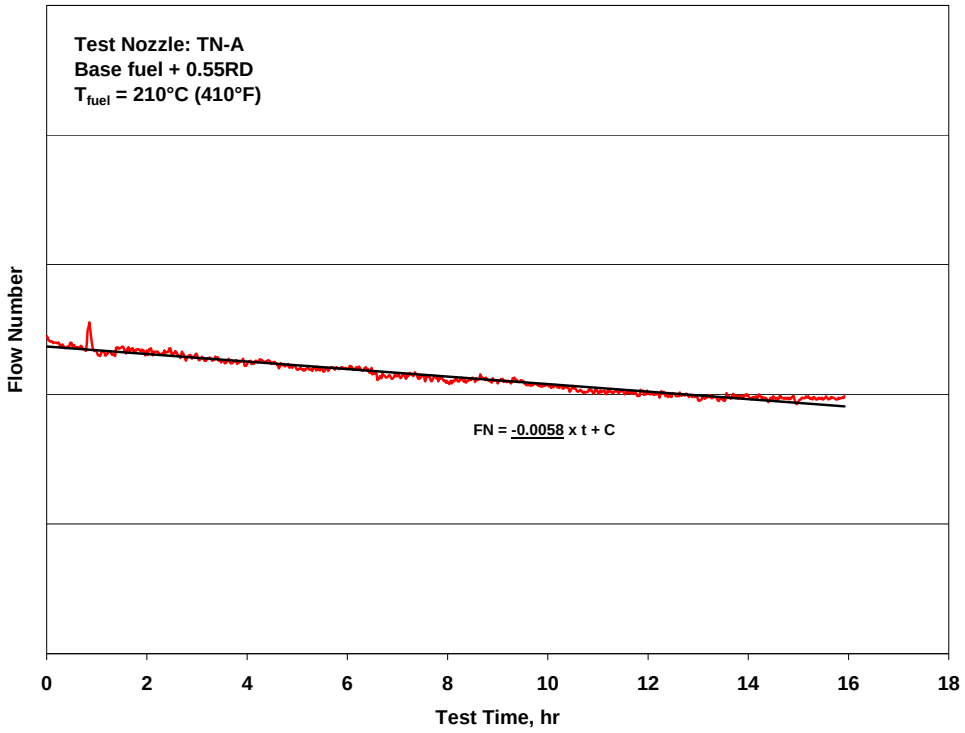

Figure A-11. Fouling Rate on Base Fuel + 0.55 mg/L of Red Dye at T_{fuel} = 210°C (410°F) (repeat)

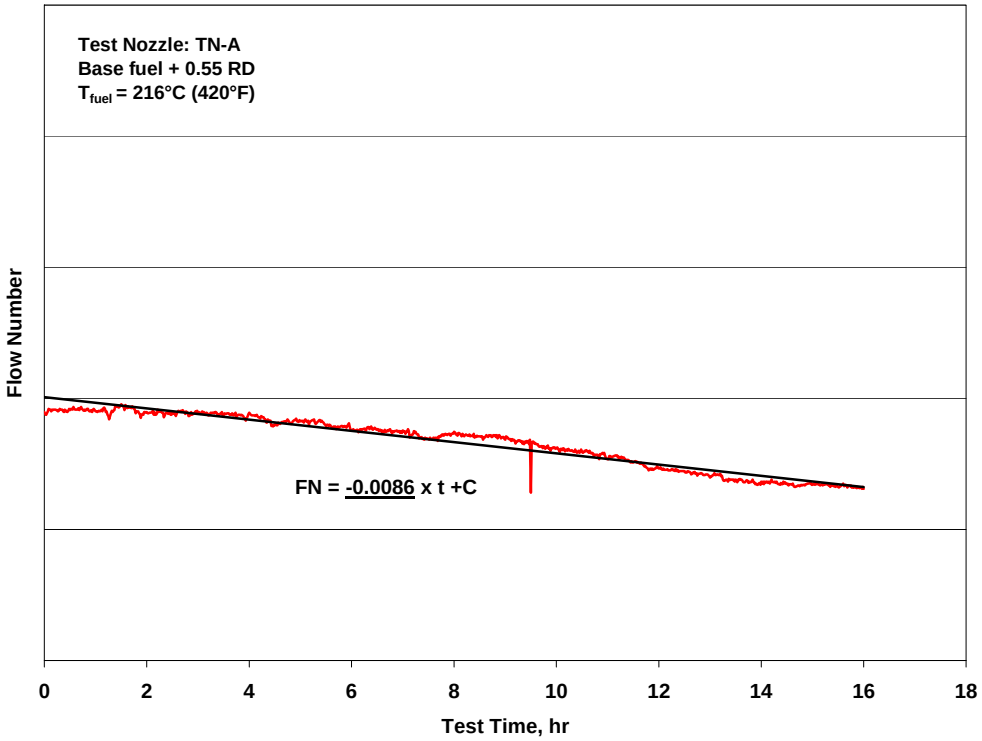

Figure A-12. Fouling Rate on Base Fuel + 0.55 mg/L of Red Dye at T_{fuel} = 216°C (420°F)

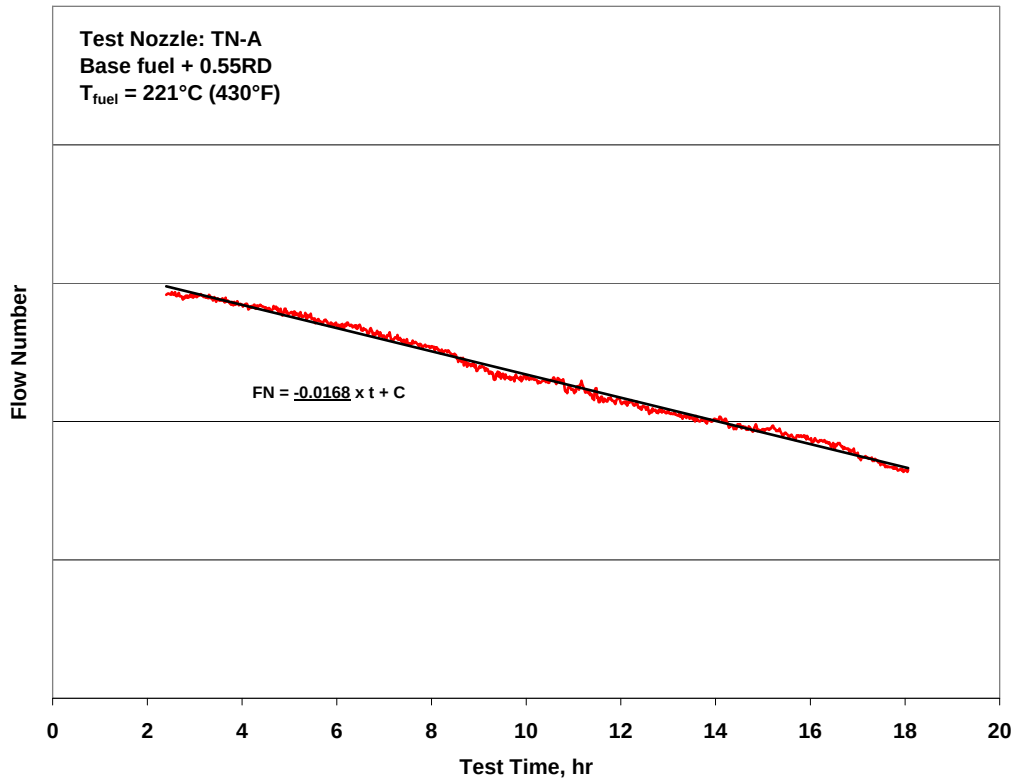

Figure A-13. Fouling Rate on Base Fuel + 0.55 mg/L of Red Dye at T_{fuel} = 221°C (430°F)

APPENDIX B—EXPERIMENTAL RESULTS FOR TEST NOZZLE TN-B

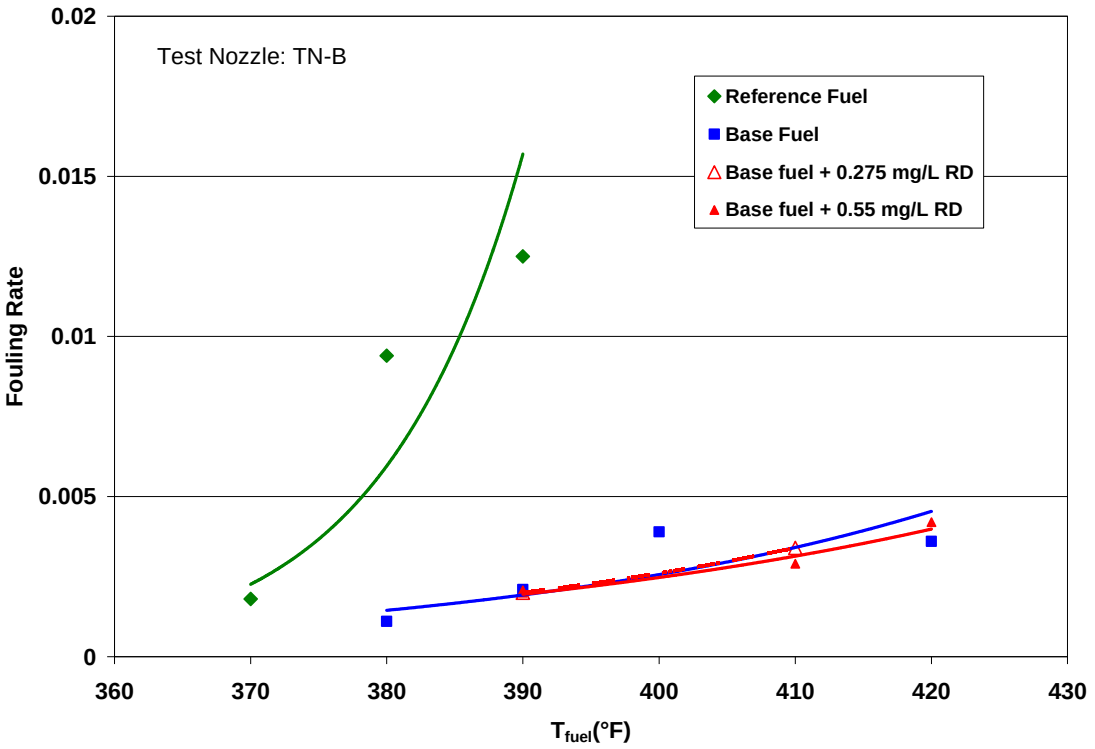

Figure B-1. Fouling Rate Summary

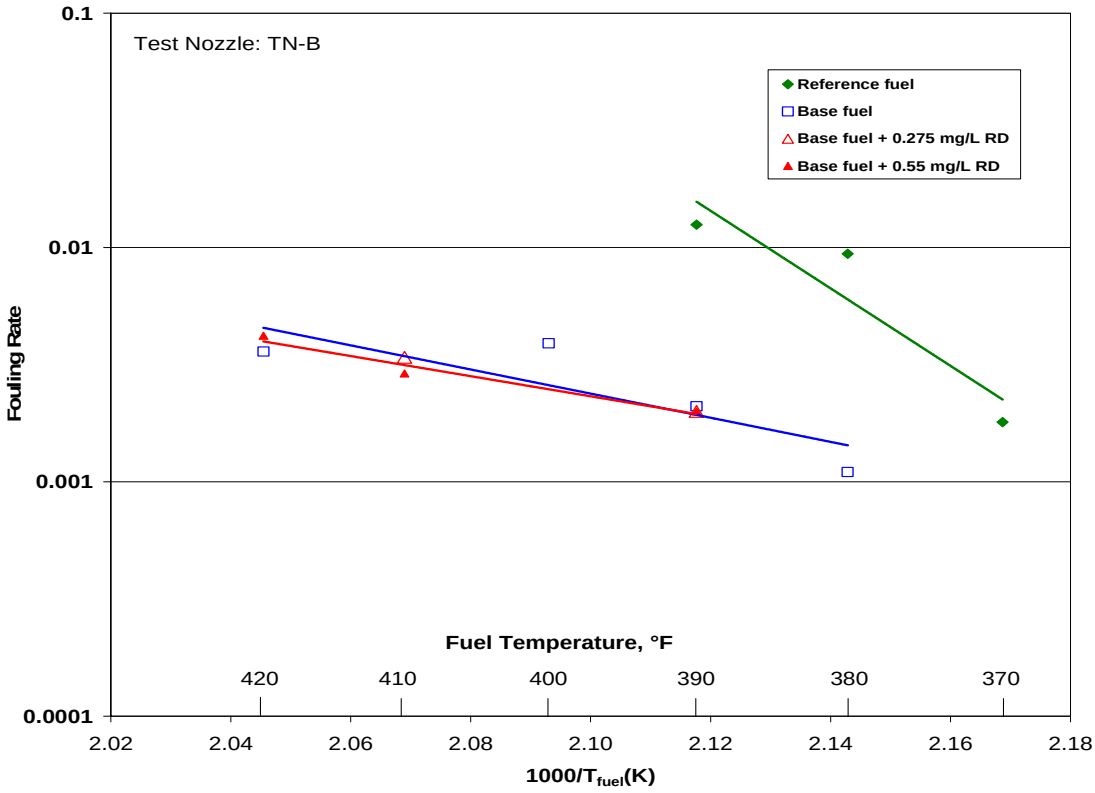

Figure B-2. Arrhenius Fouling Rate Summary

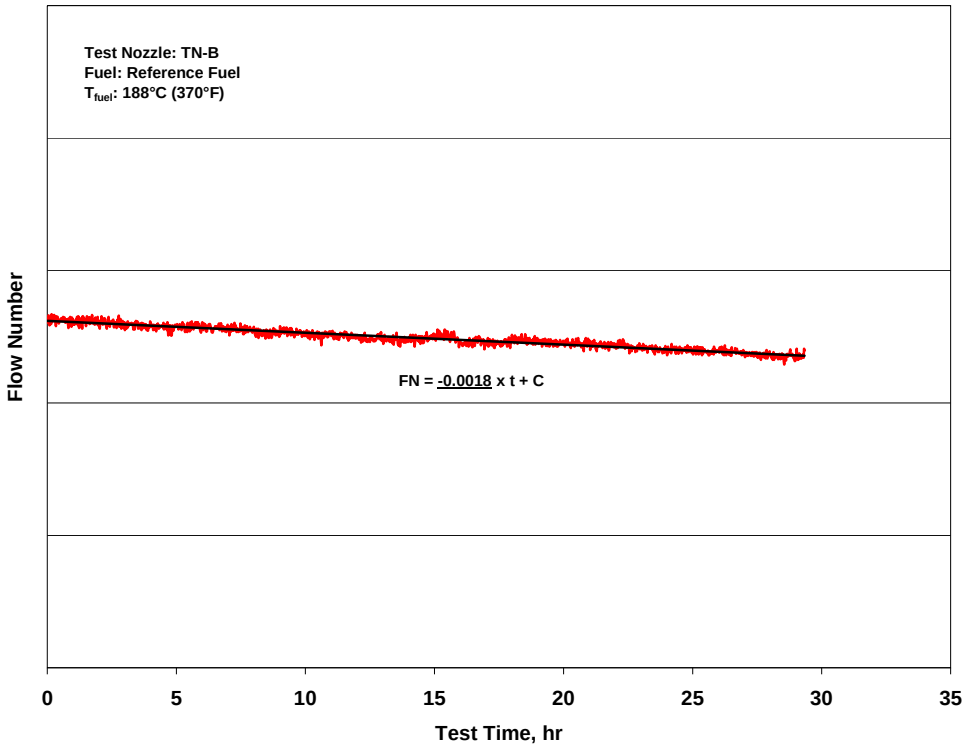

Figure B-3. Fouling Rate on Reference Fuel at T_{fuel} = 188°C (370°F)

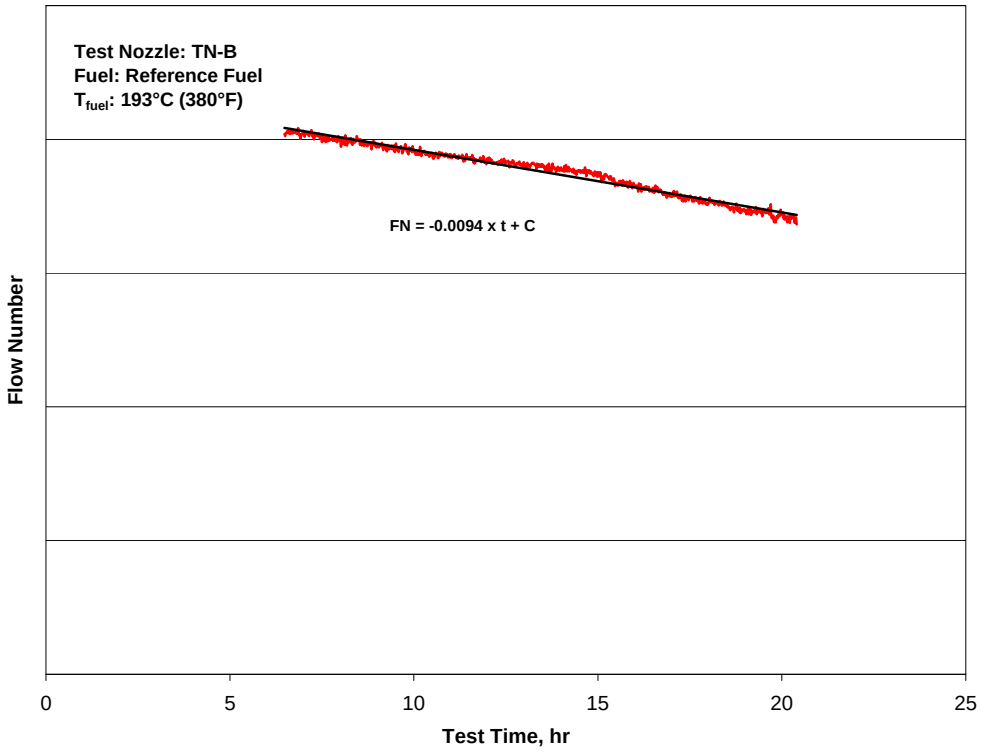

Figure B-4. Fouling Rate on Reference Fuel at T_{fuel} = 193°C (380°F)

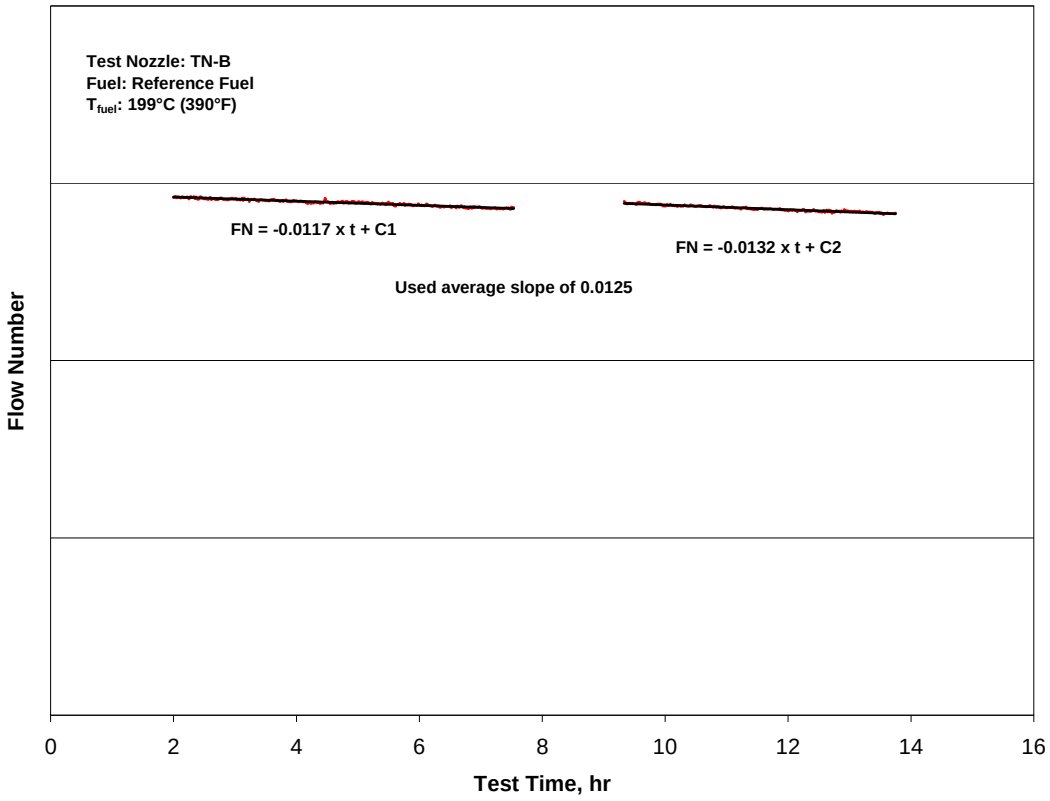

Figure B-5. Fouling Rate on Reference Fuel at T_{fuel} = 199°C (390°F)

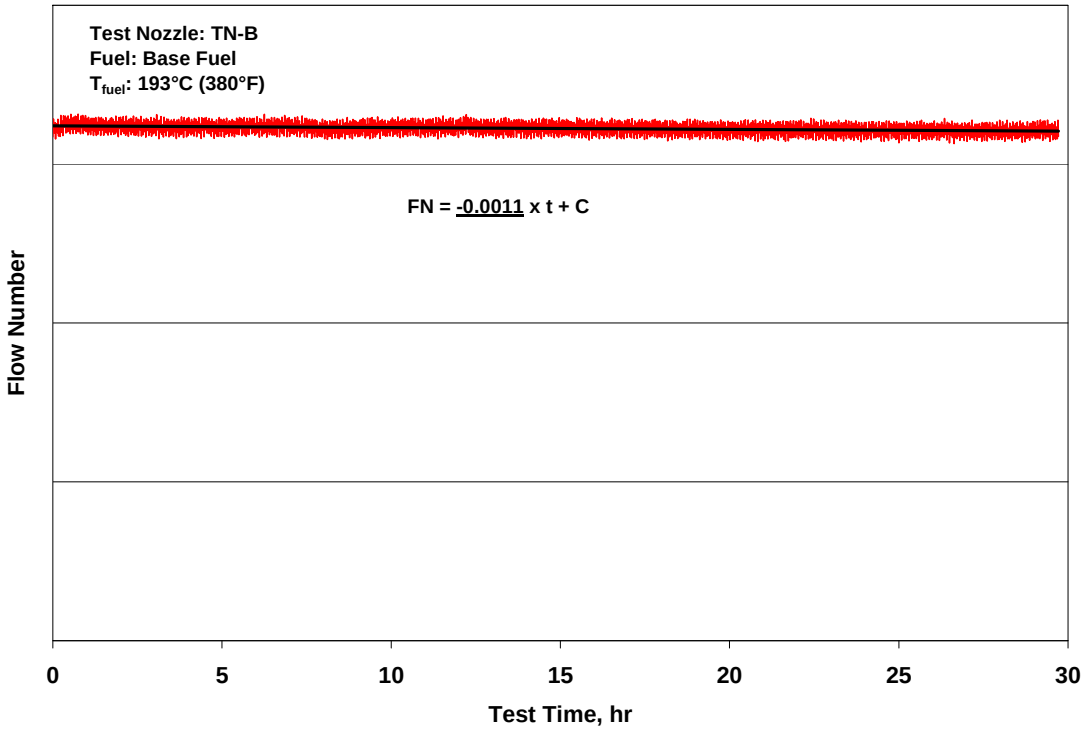

Figure B-6. Fouling Rate on Base Fuel at T_{fuel} = 193°C (380°F)

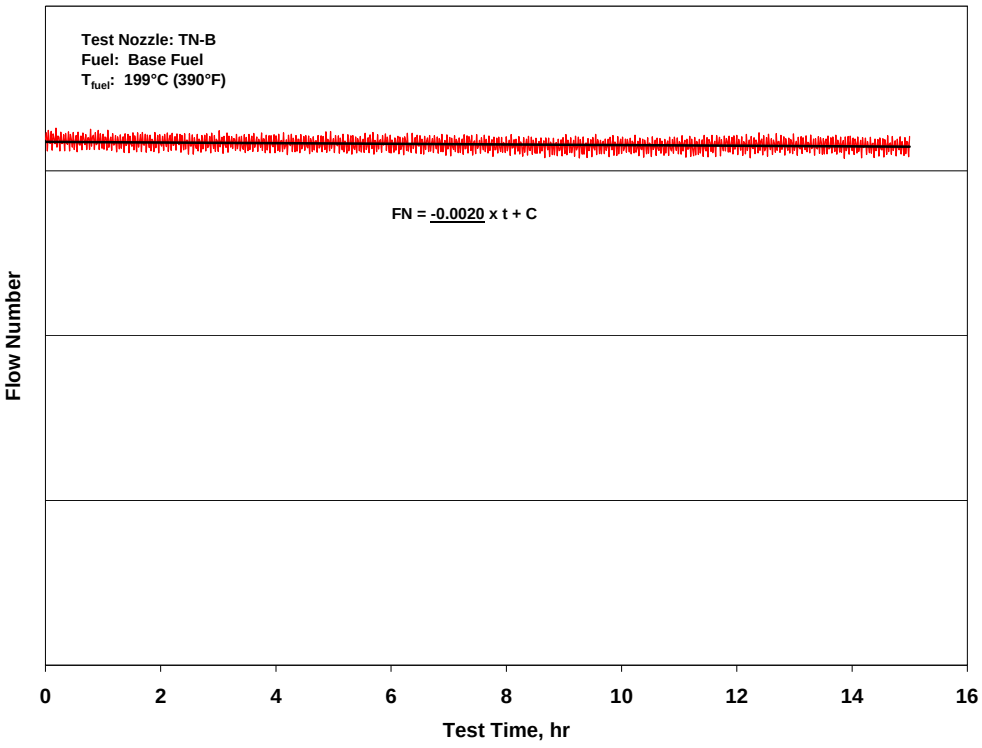

Figure B-7. Fouling Rate on Base Fuel at T_{fuel} = 199°C (390°F)

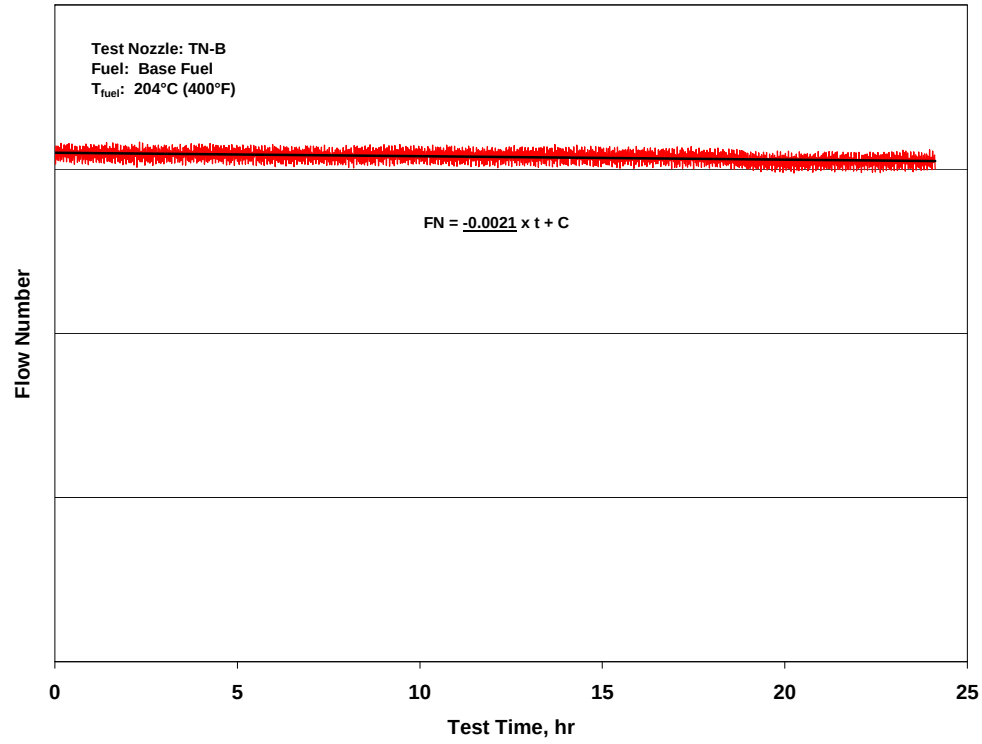

Figure B-8. Fouling Rate on Base Fuel at T_{fuel} = 204°C (400°F)

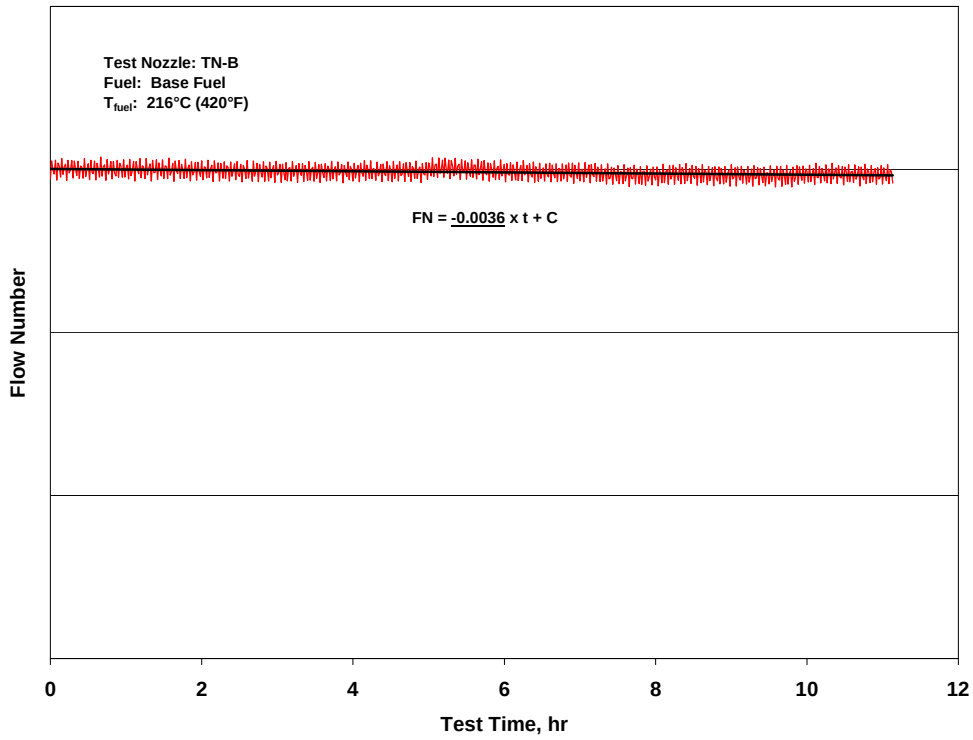

Figure B-9. Fouling Rate on Base Fuel at T_{fuel} = 216°C (420°F)

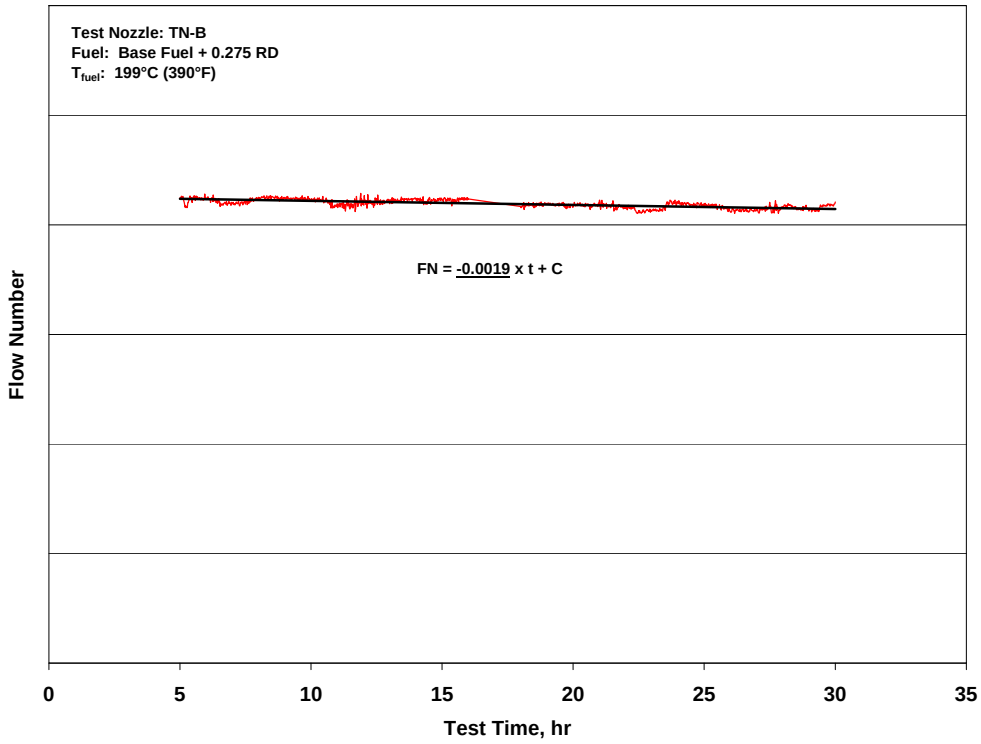

Figure B-10. Fouling Rate on Base Fuel + 0.275 mg/L of Red Dye at T_{fuel} = 199°C (390°F)

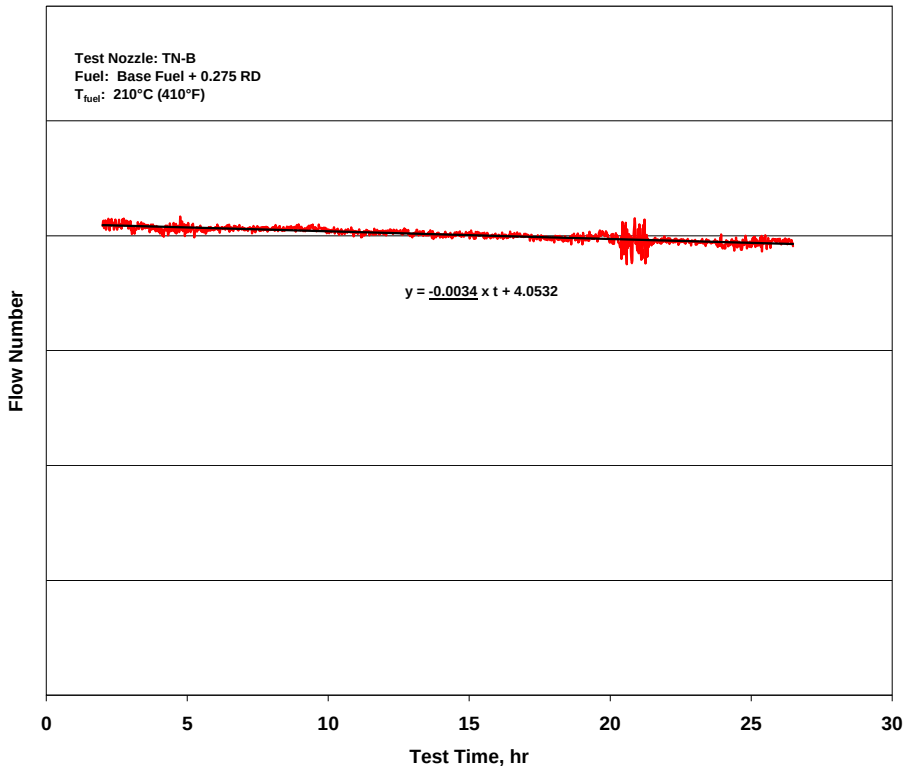

Figure B-11. Fouling Rate on Base Fuel + 0.275 mg/L of Red Dye at T_{fuel} = 210°C (410°F)

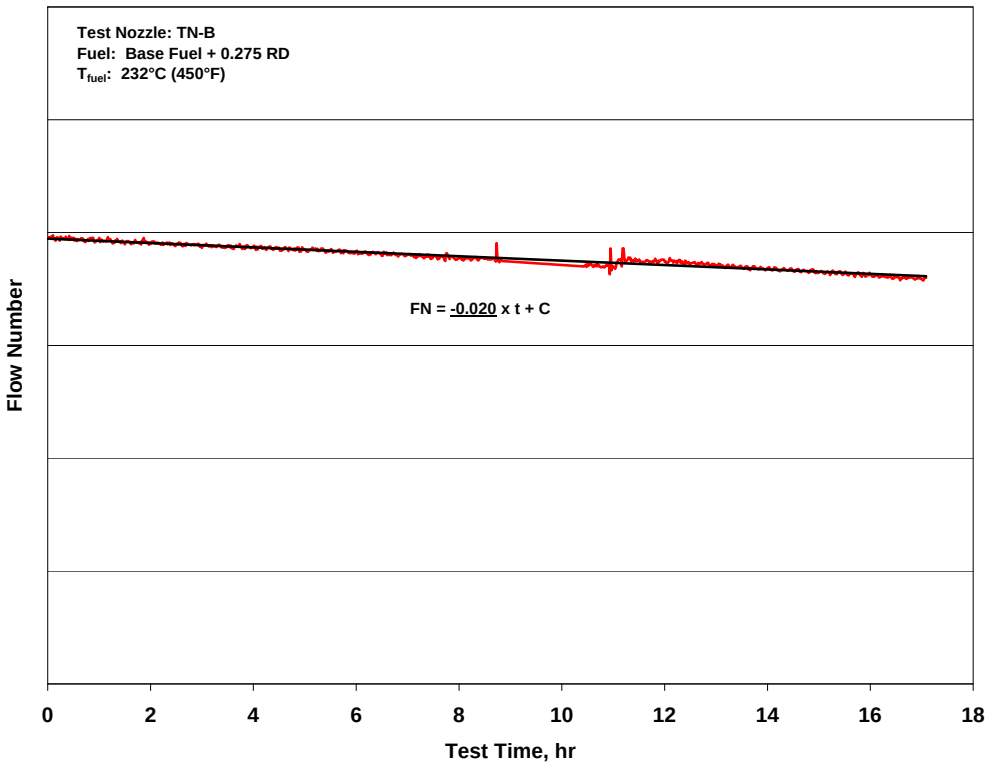

Figure B-12. Fouling Rate on Base Fuel + 0.275 mg/L of Red Dye at T_{fuel} = 232°C (450°F)

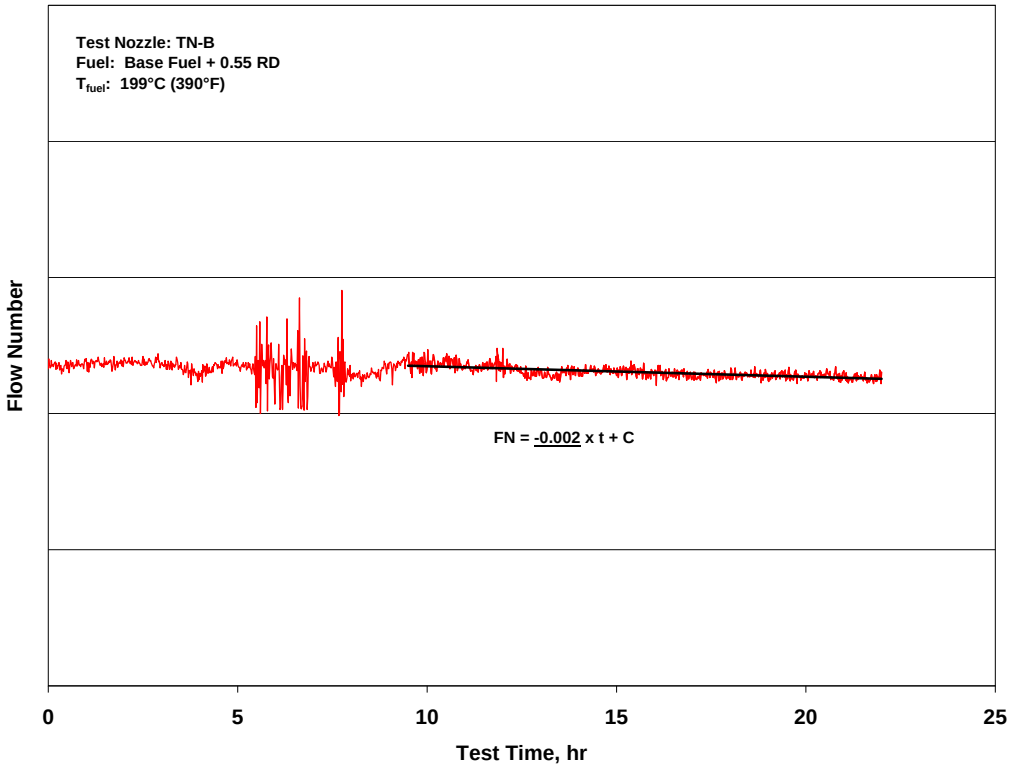

Figure B-13. Fouling Rate on Base Fuel + 0.55 mg/L of Red Dye at T_{fuel} = 199°C (390°F)

APPENDIX C—EXPERIMENTAL RESULTS FOR TEST NOZZLE TN-C

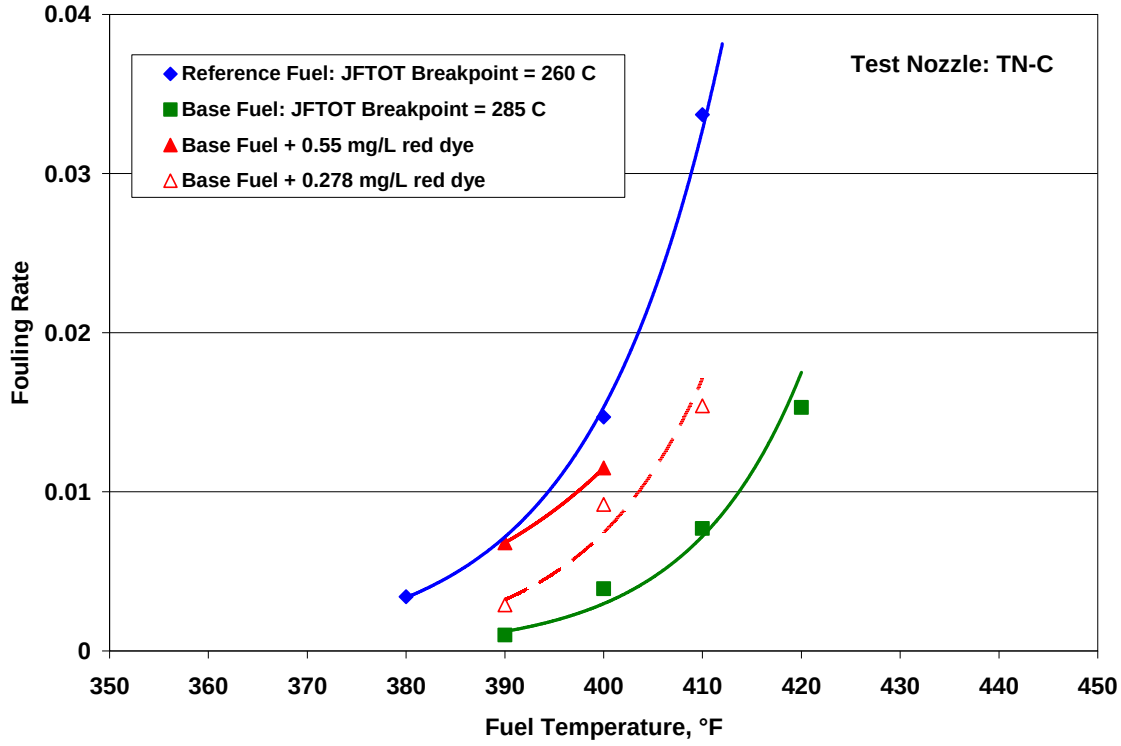

Figure C-1. Fouling Rate Summary

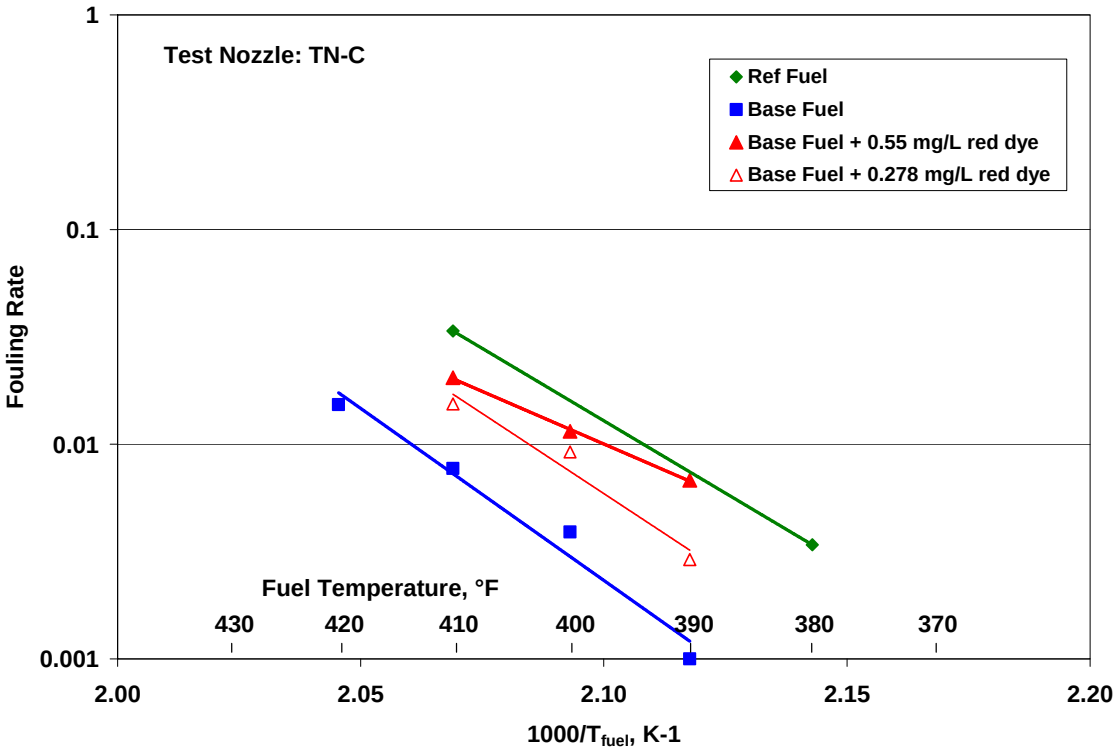

Figure C-2. Arrhenius Fouling Rate Summary

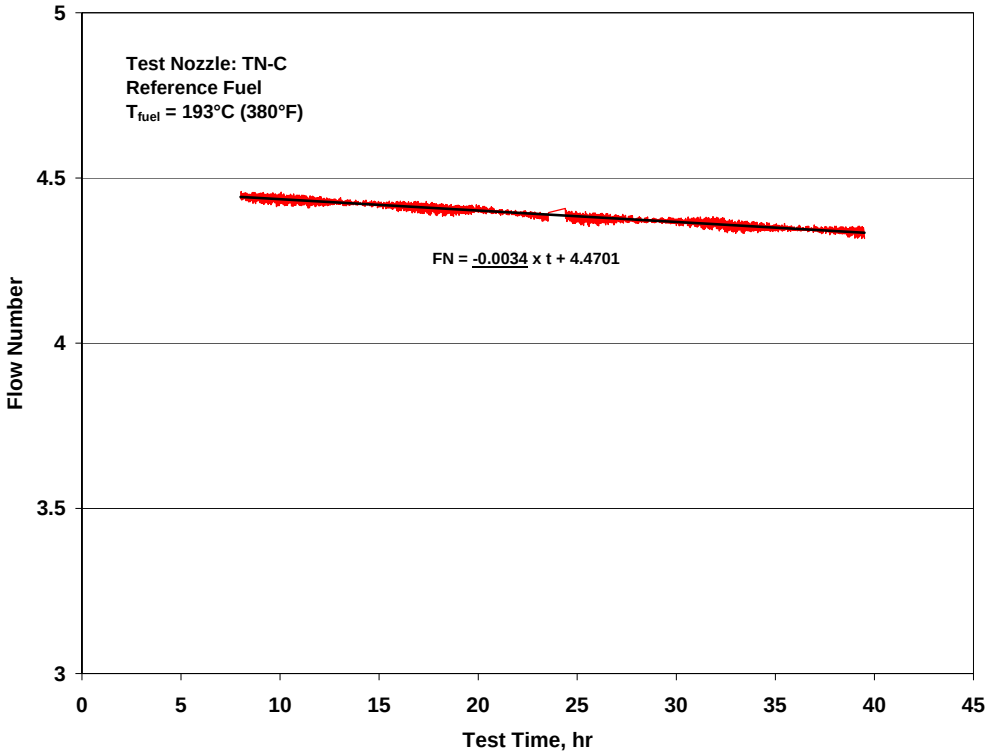

Figure C-3. Fouling Rate on Reference Fuel at T_{fuel} = 193°C (380°F)

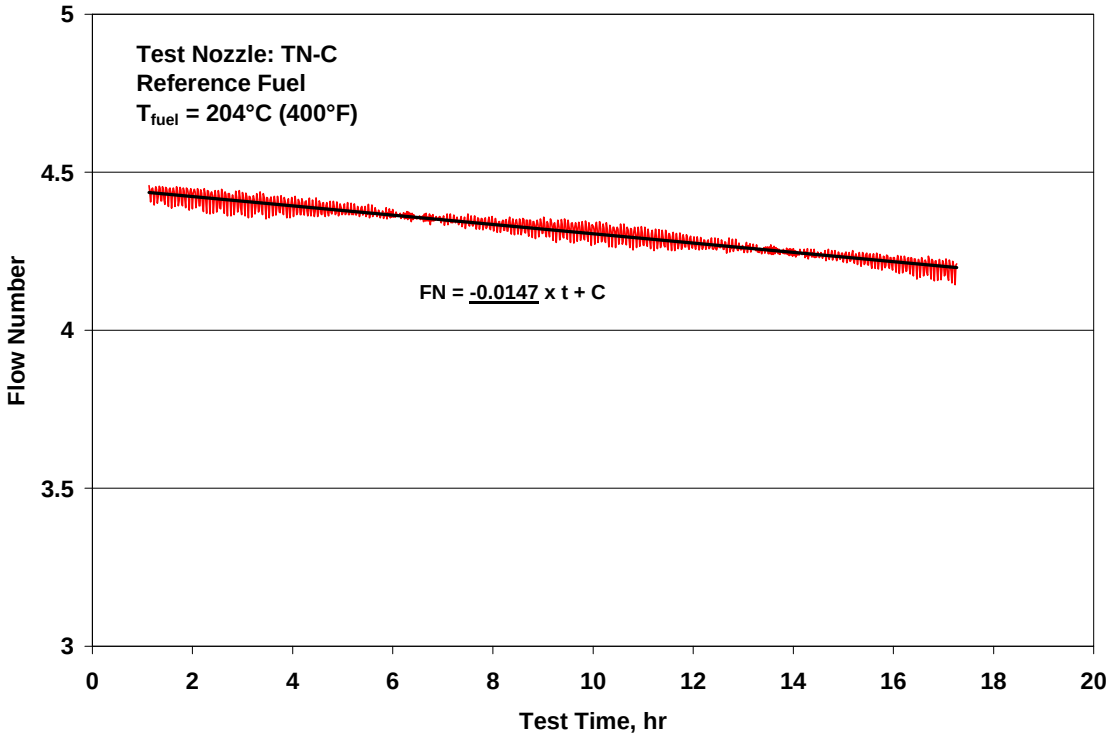

Figure C-4. Fouling Rate on Reference Fuel at T_{fuel} = 204°C (400°F)

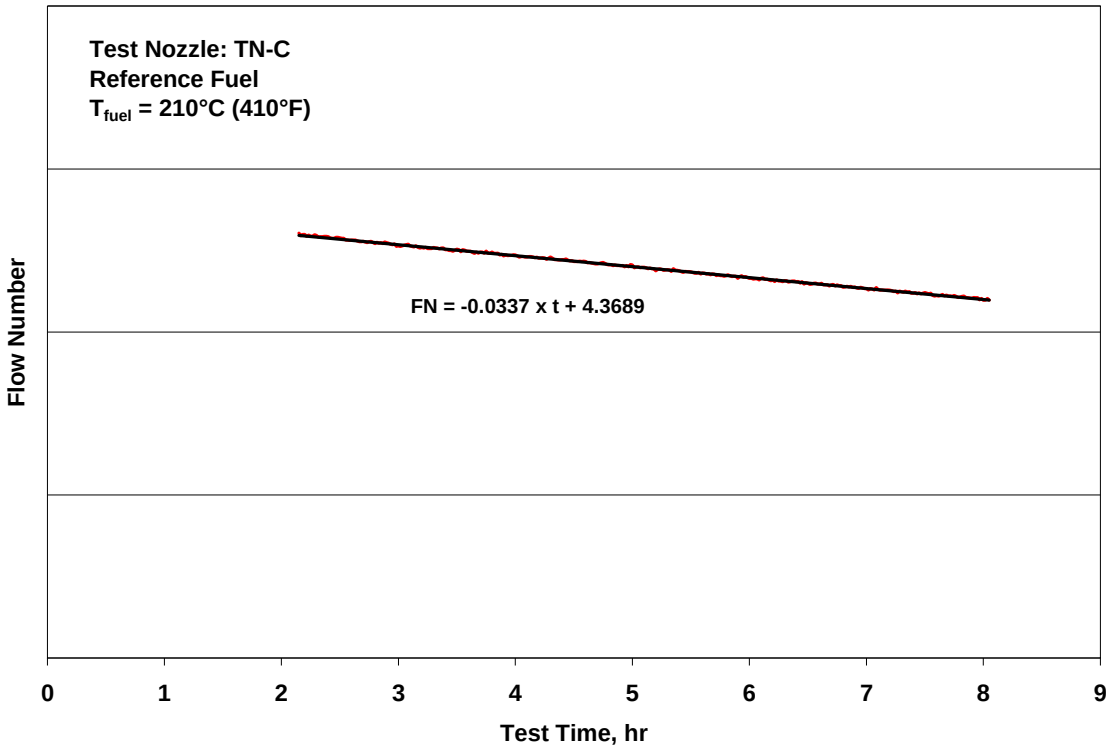

Figure C-5. Fouling Rate on Reference Fuel at T_{fuel} = 210°C (410°F)

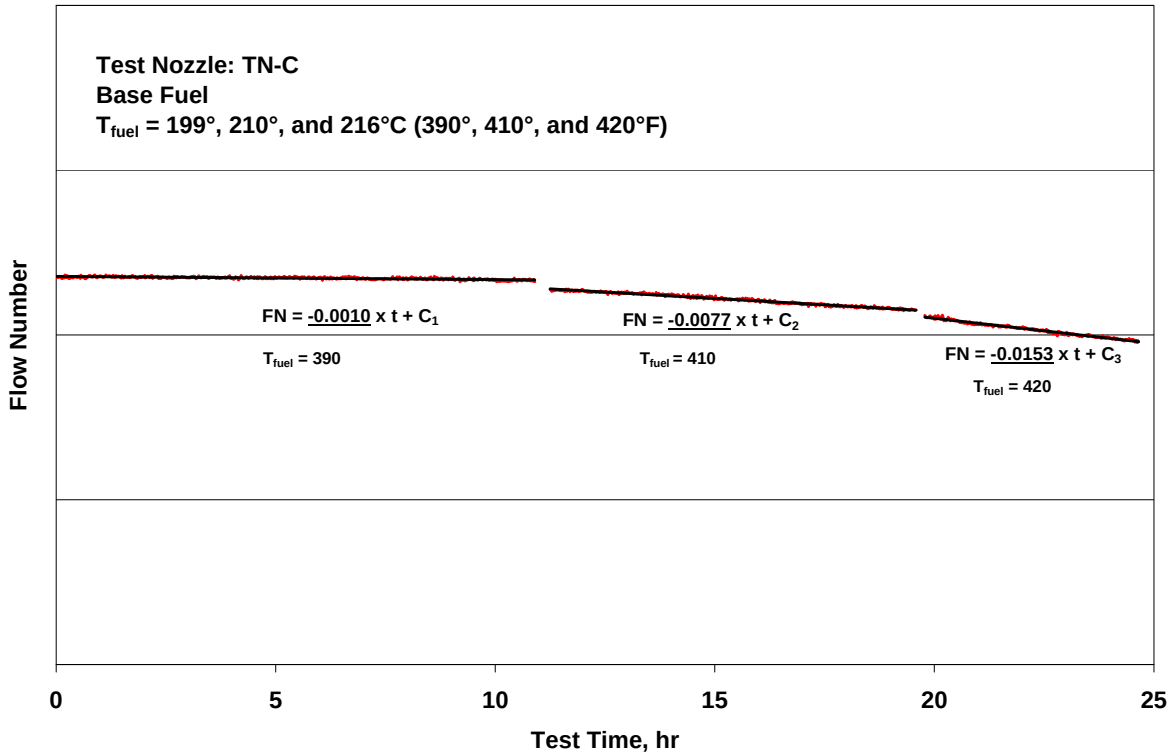

Figure C-6. Fouling Rate on Base Fuel at T_{fuel} = 199°, 210°, and 216°C (390°, 410°, and 420°F)

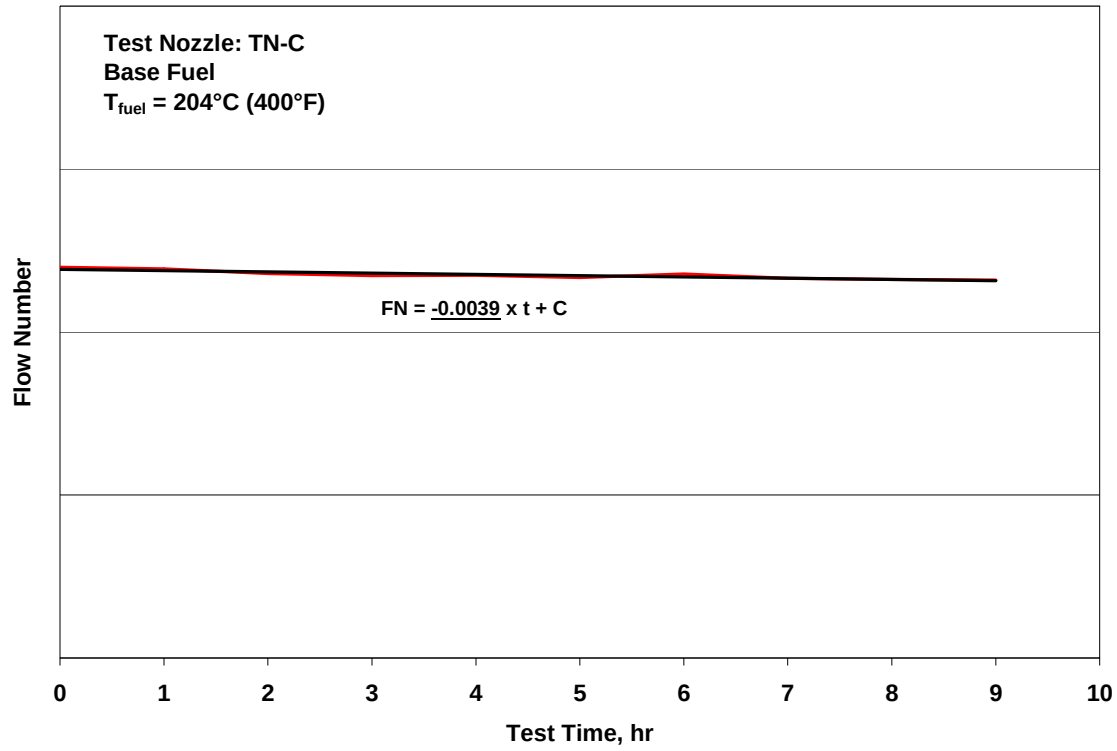

Figure C-7. Fouling Rate on Base Fuel at T_{fuel} = 204°C (400°F)

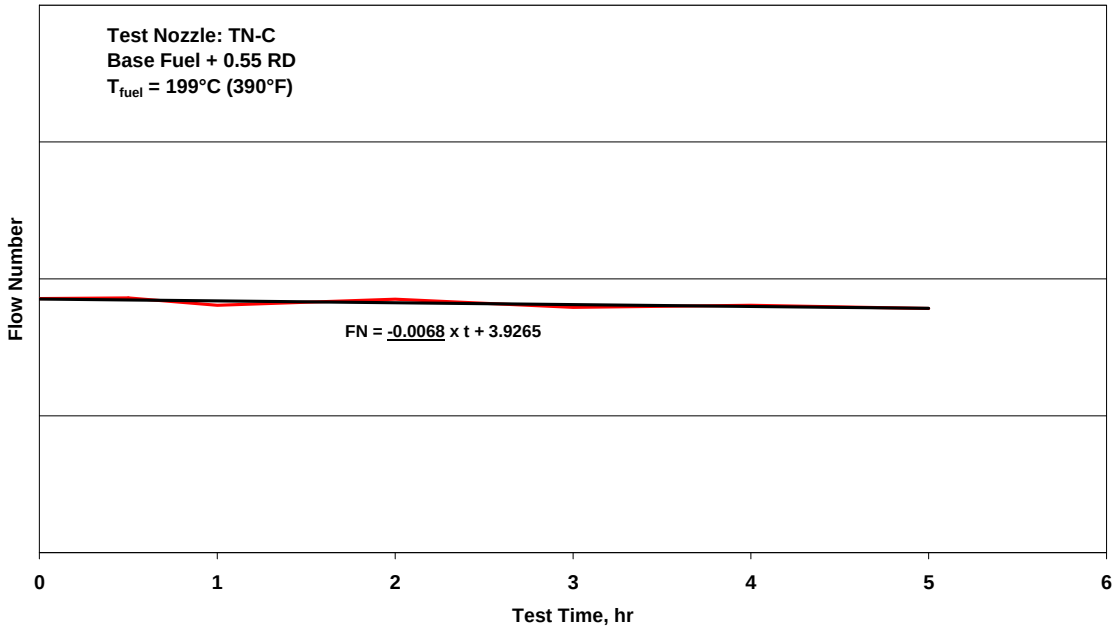

Figure C-8. Fouling Rate on Base Fuel + 0.55 mg/L of Red Dye at T_{fuel} = 199°C (390°F)

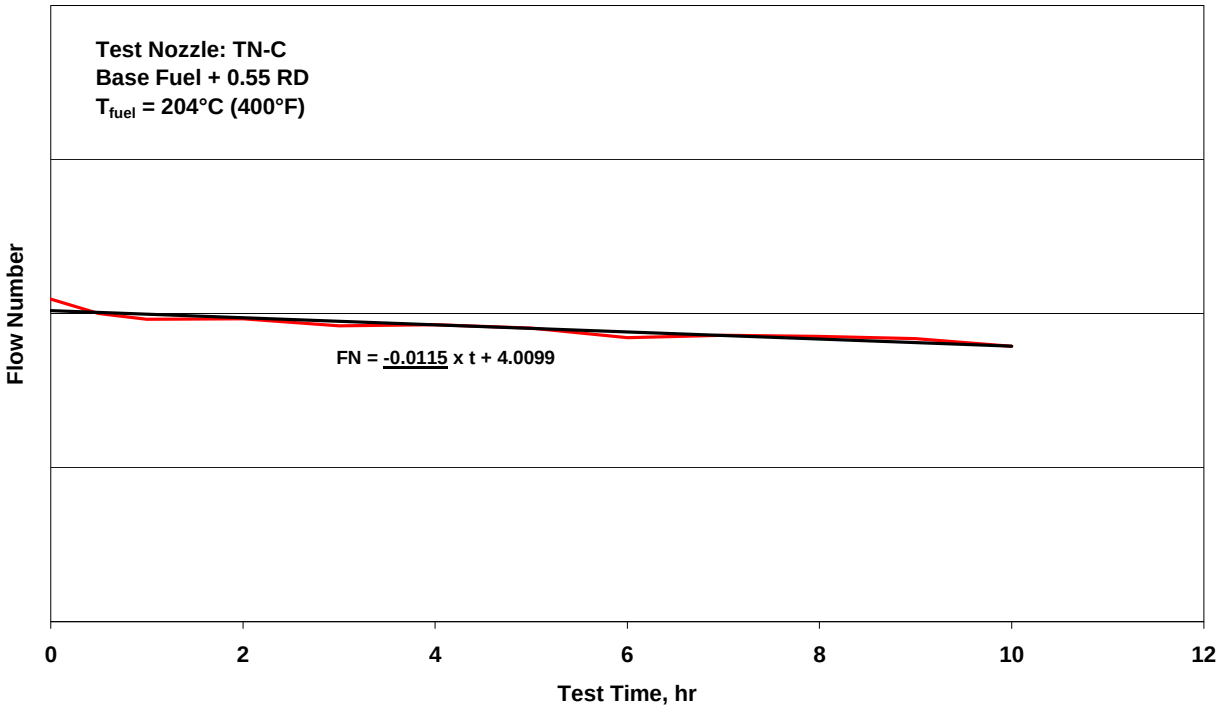

Figure C-9. Fouling Rate on Base Fuel + 0.55 mg/L of Red Dye at T_{fuel} = 204°C (400°F)

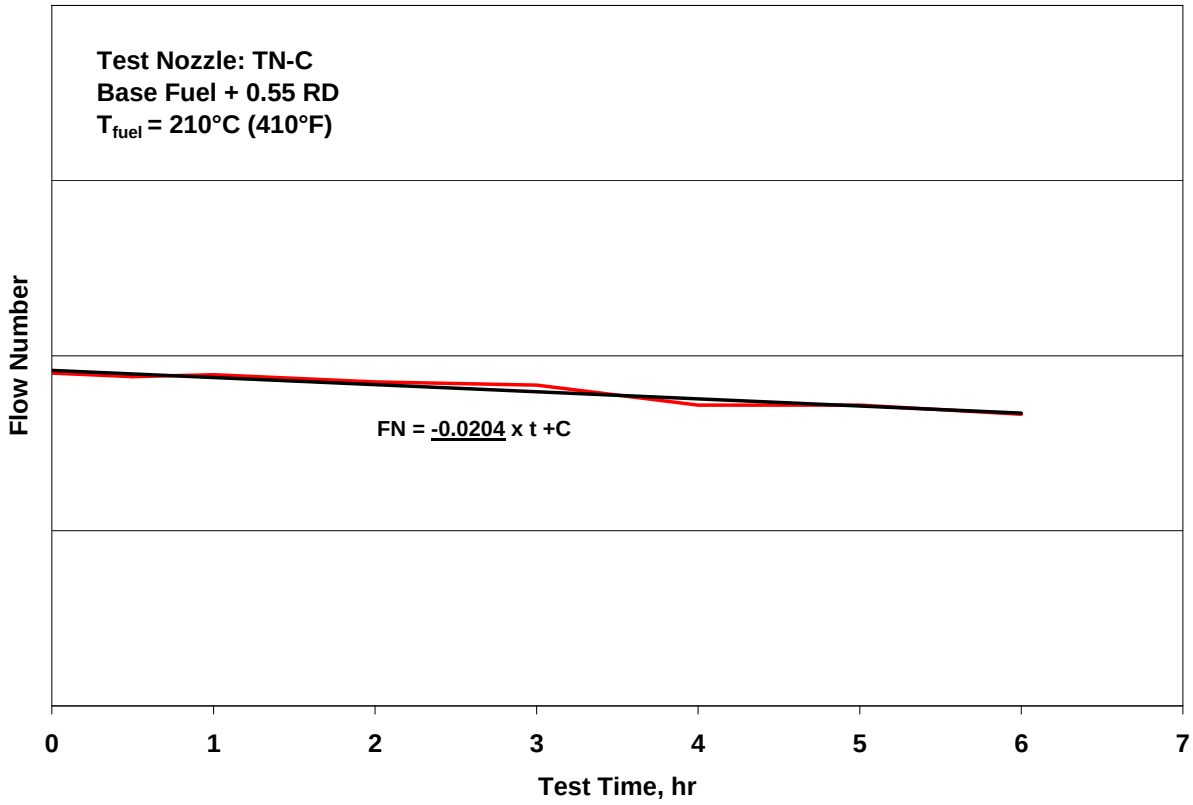

Figure C-10. Fouling Rate on Base Fuel + 0.55 mg/L of Red Dye at T_{fuel} = 210°C (410°F)

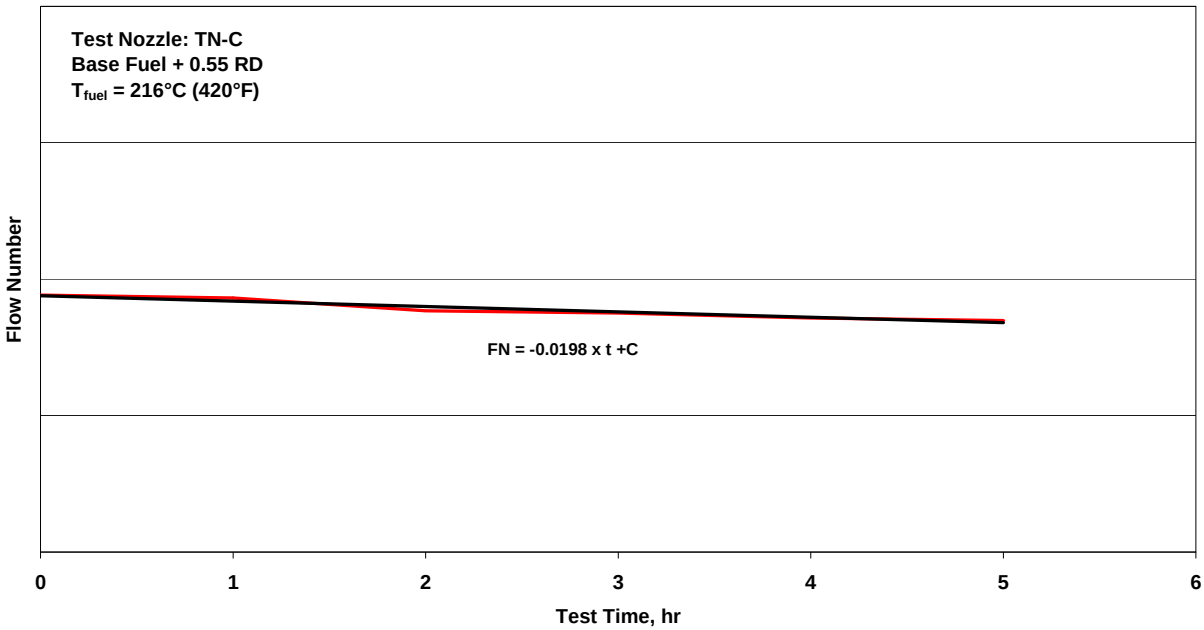

Figure C-11. Fouling Rate on Base Fuel + 0.55 mg/L of Red Dye at T_{fuel} = 216°C (420°F)

APPENDIX D—EXPERIMENTAL RESULTS FOR TEST NOZZLE TN-D

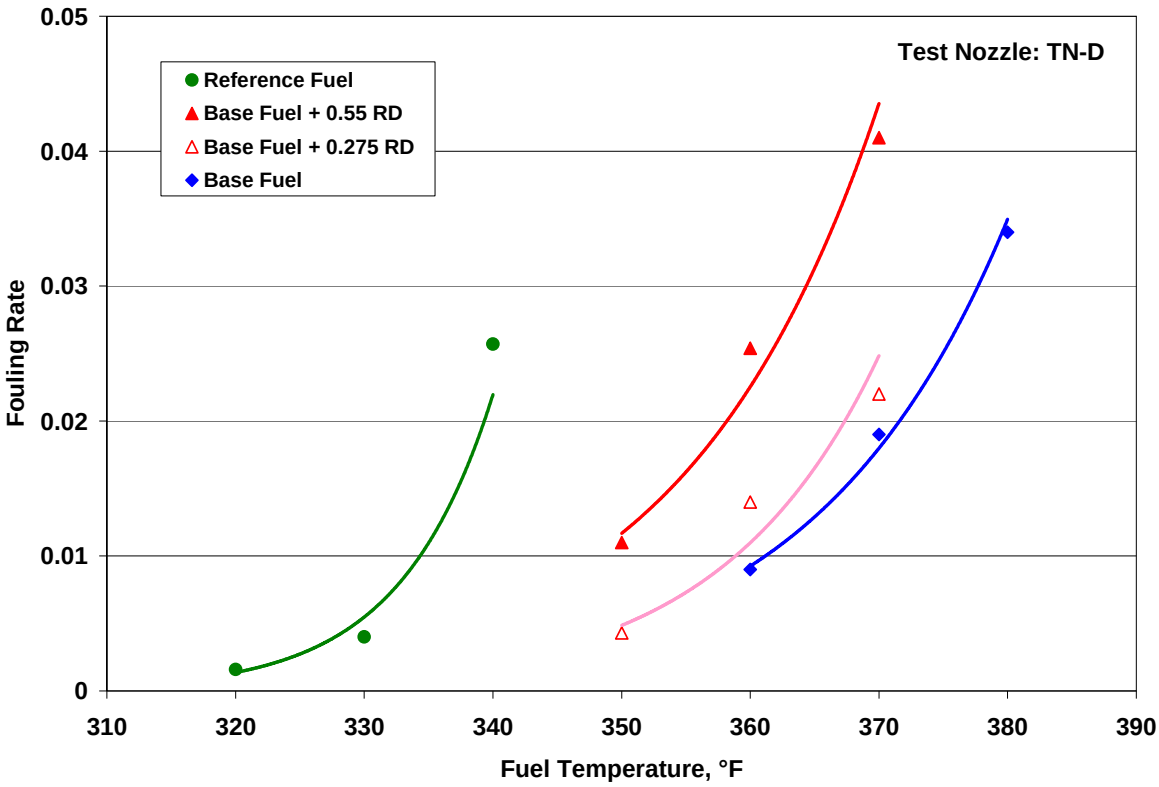

Figure D-1. Fouling Rate Summary

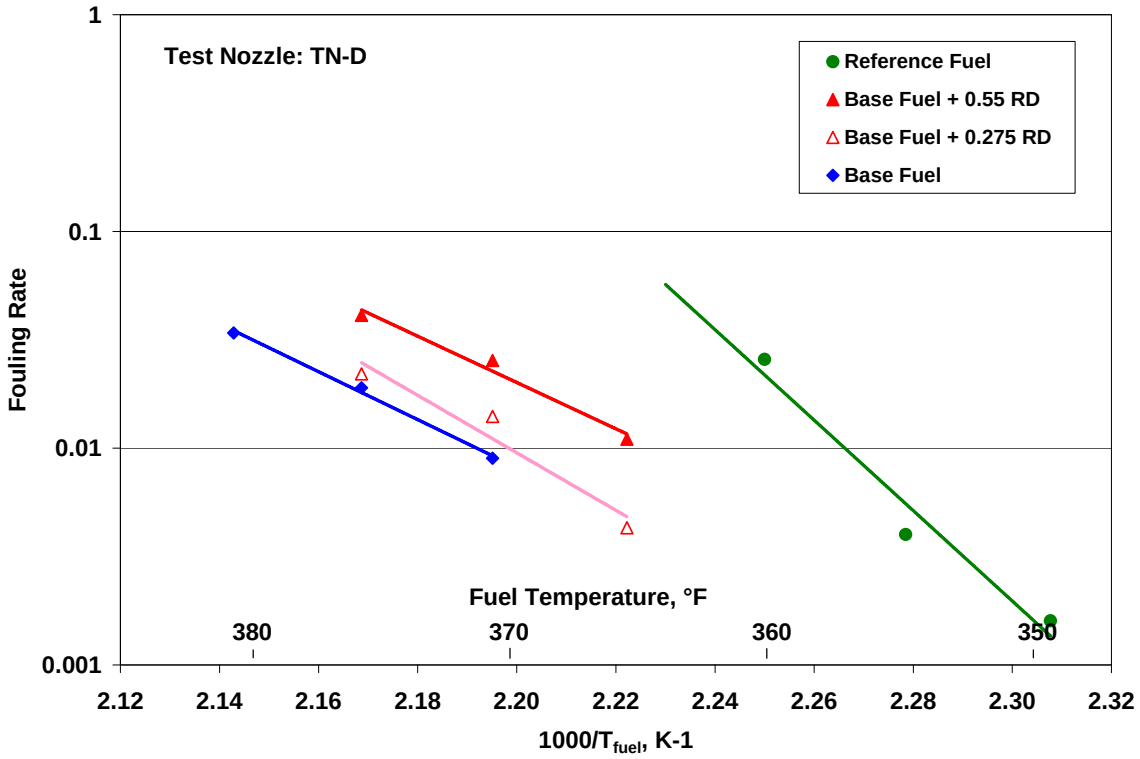

Figure D-2. Arrhenius Fouling Rate Summary

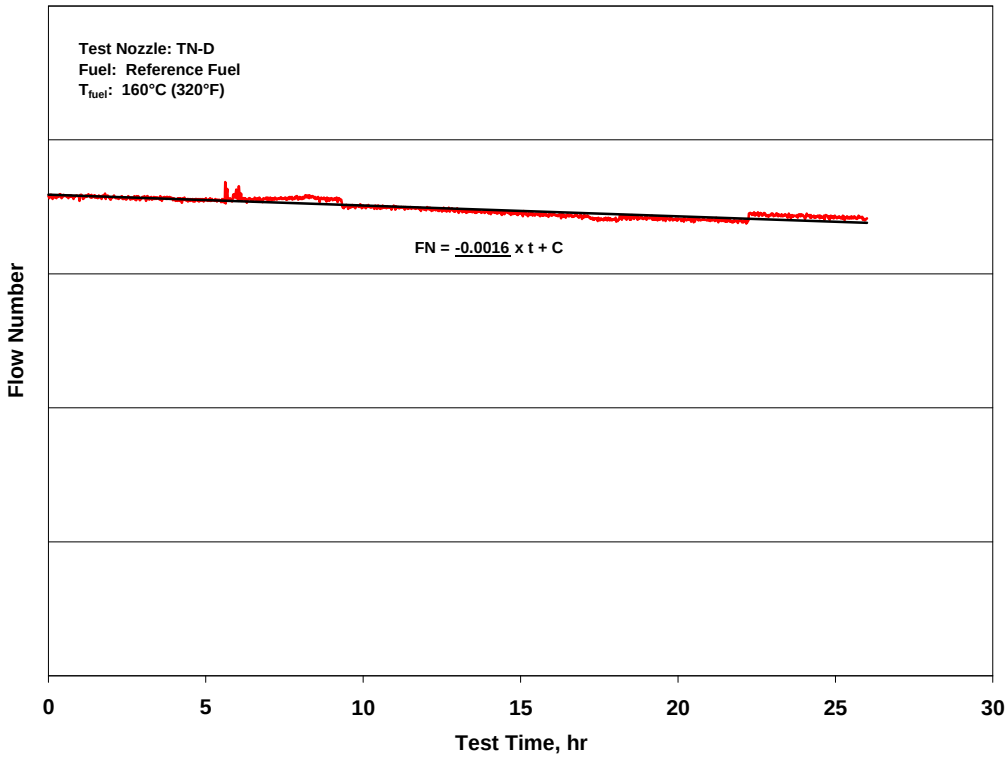

Figure D-3. Fouling Rate on Reference Fuel at T_{fuel} = 160°C (320°F)

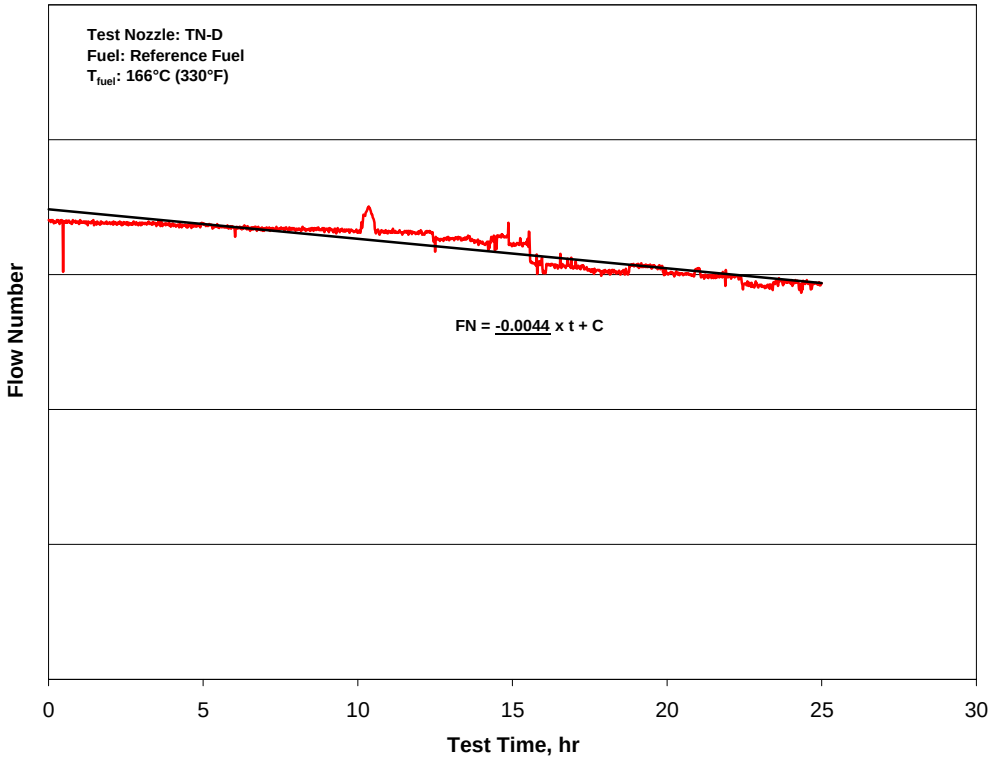

Figure D-4. Fouling Rate on Reference Fuel at T_{fuel} = 166°C (330°F)

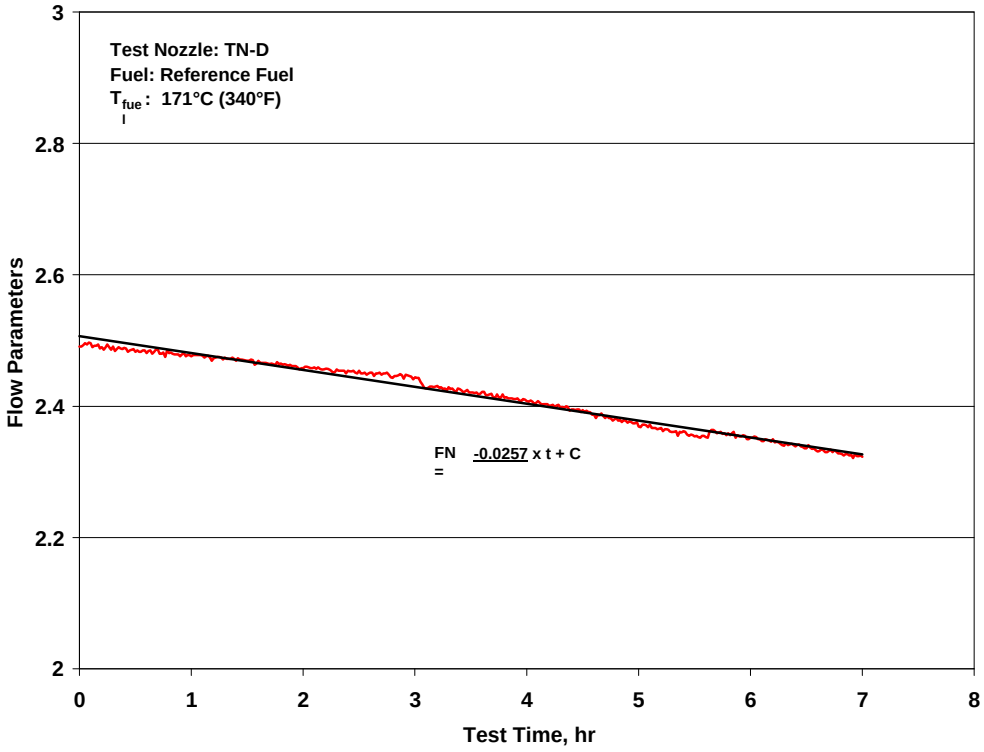

Figure D-5. Fouling Rate on Reference Fuel at T_{fuel} = 171°C (340°F)

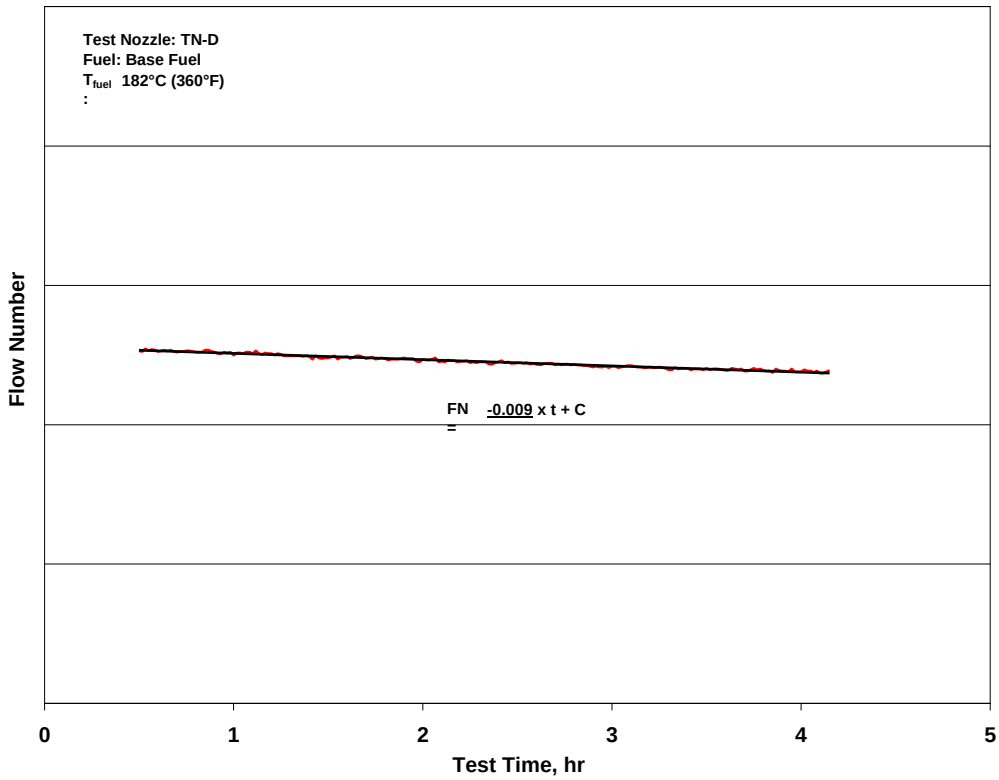

Figure D-6. Fouling Rate on Base Fuel at T_{fuel} = 182°C (360°F)

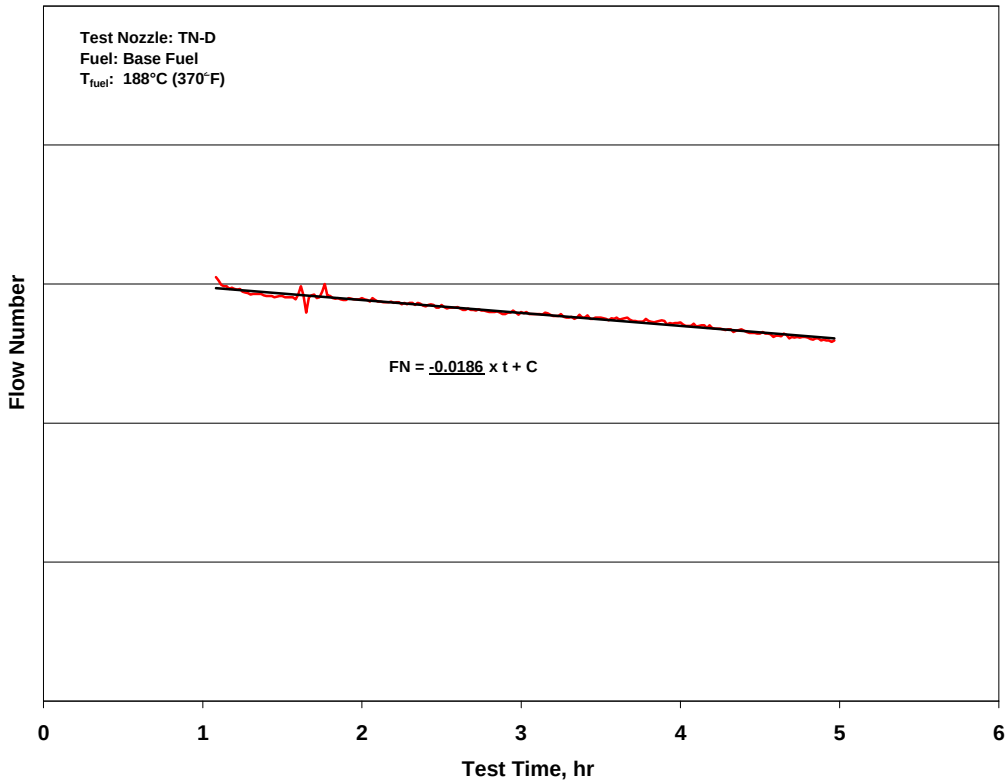

Figure D-7. Fouling Rate on Base Fuel at T_{fuel} = 188°C (370°F)

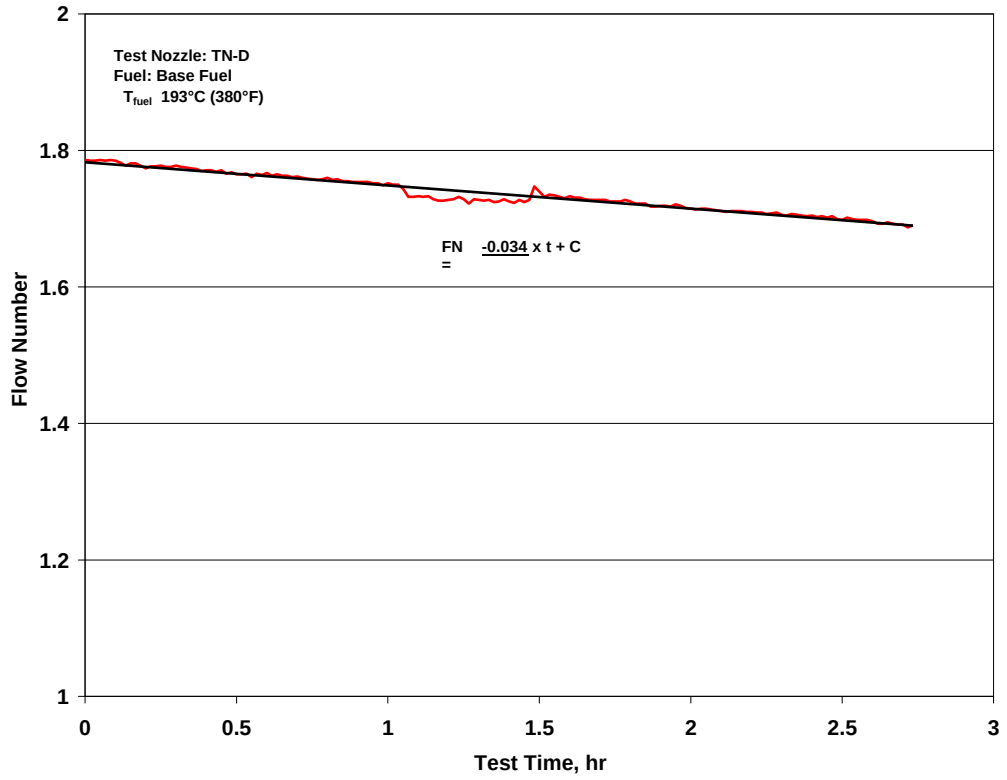

Figure D-8. Fouling Rate on Base Fuel at T_{fuel} = 193°C (380°F)

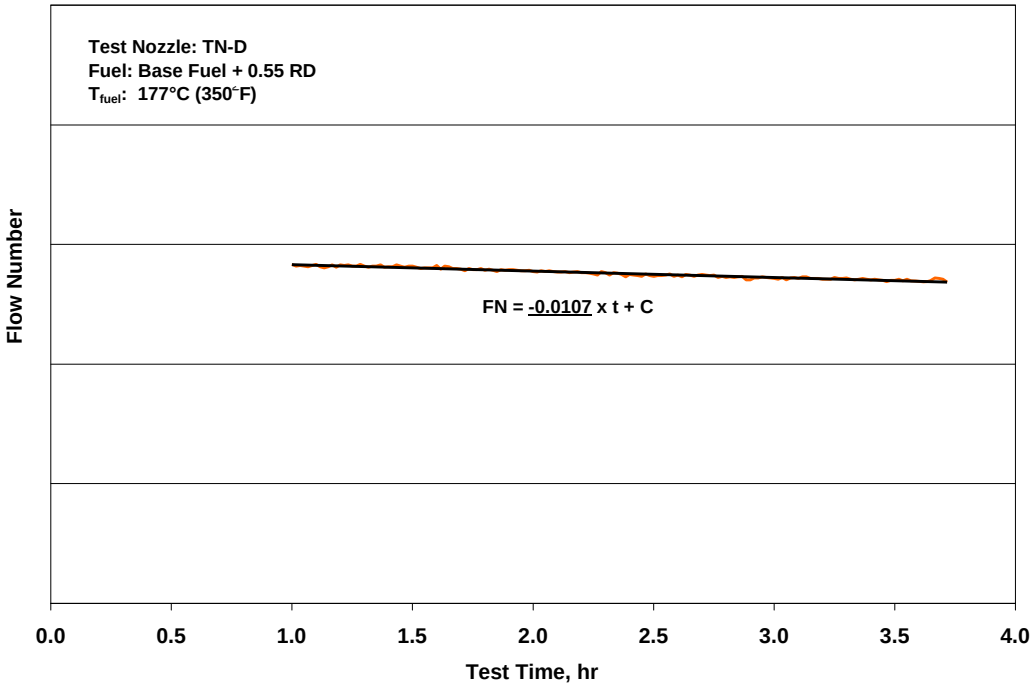

Figure D-9. Fouling Rate on Base Fuel + 0.55 mg/L of Red Dye at T_{fuel} = 177°C (350°F)

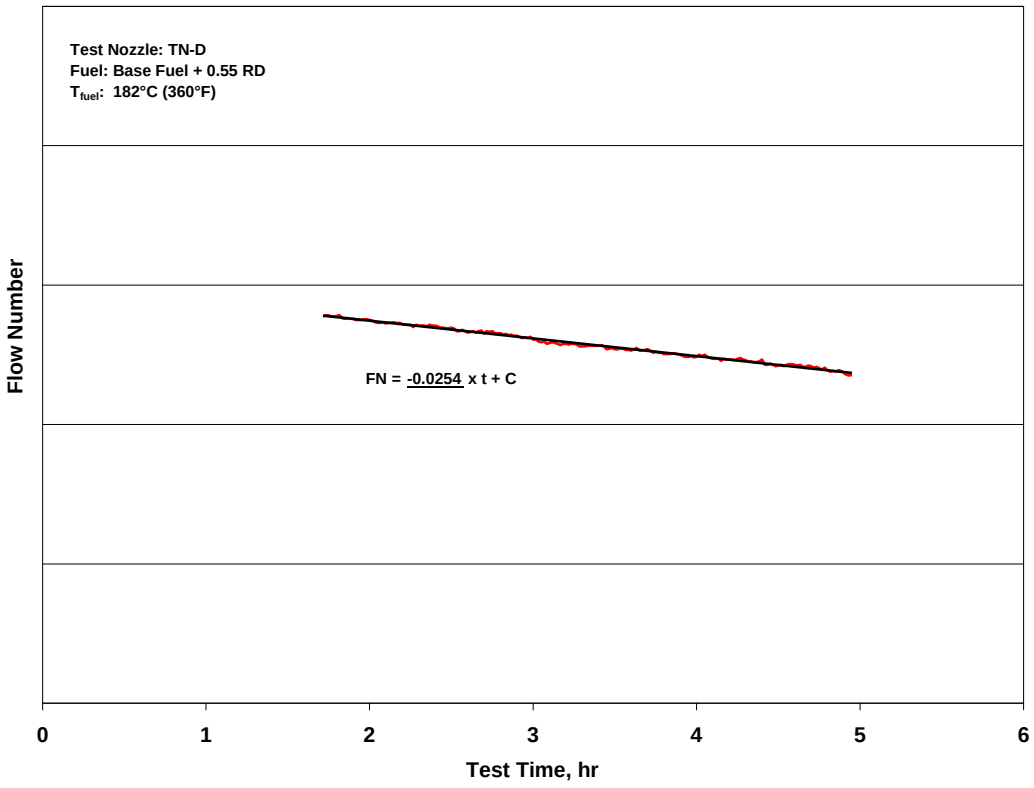

Figure D-10. Fouling Rate on Base Fuel + 0.55 mg/L of Red Dye at T_{fuel} = 182°C (360°F)

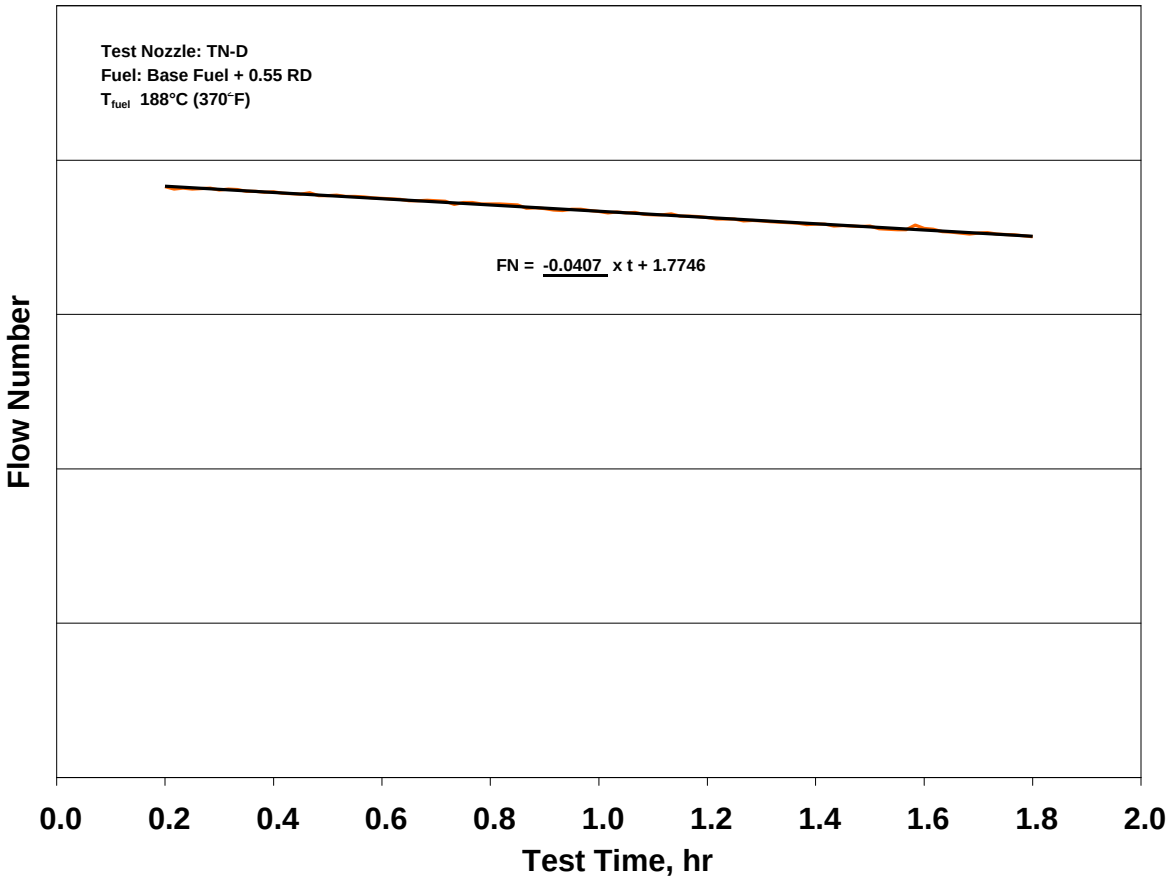

Figure D-11. Fouling Rate on Base Fuel + 0.55 mg/L of Red Dye at T_{fuel} = 188°C (370°F)

APPENDIX E—EXPERIMENTAL RESULTS FOR TEST NOZZLE TN-E

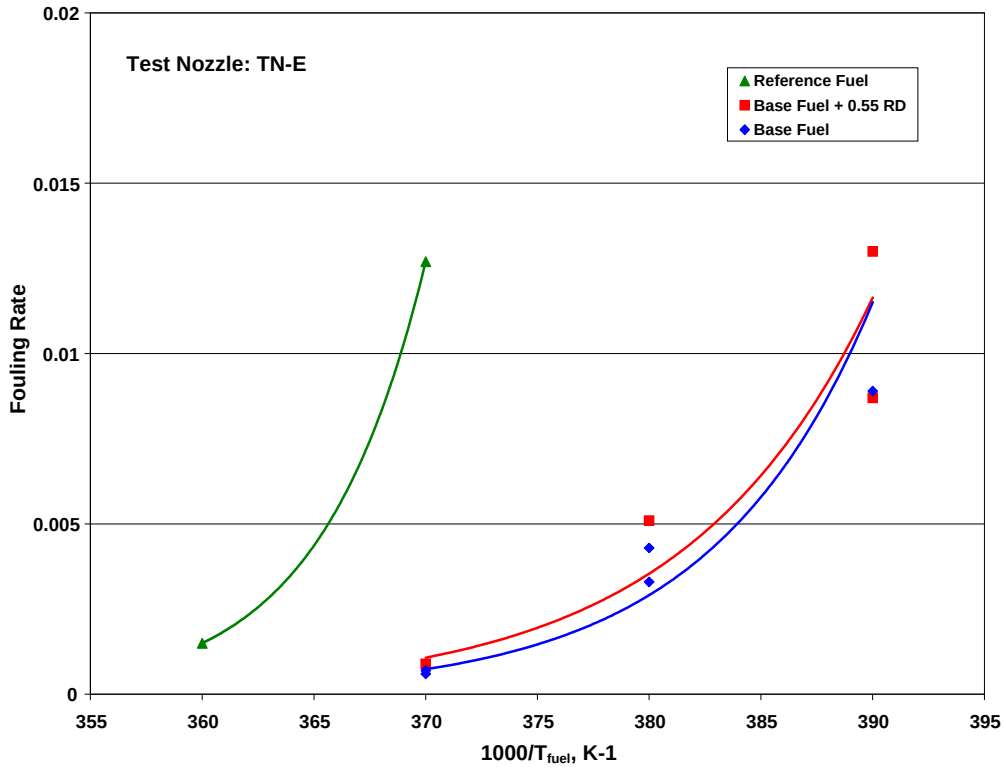

Figure E-1. Fouling Rate Summary

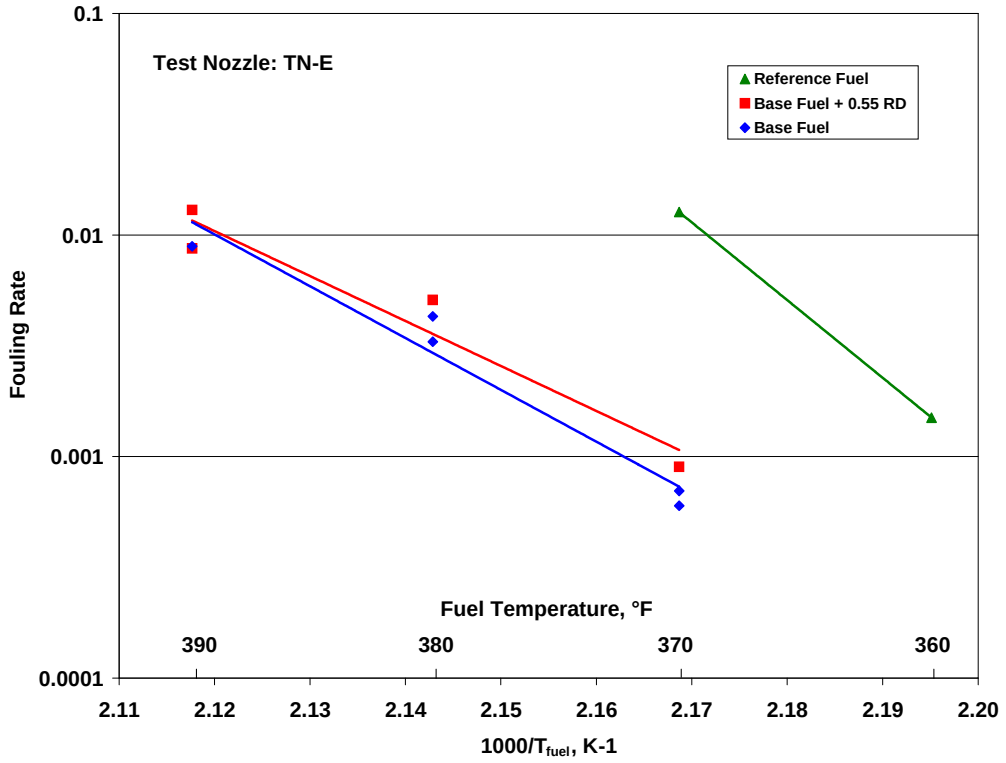

Figure E-2. Arrhenius Fouling Rate Summary for Test Nozzle TN-E

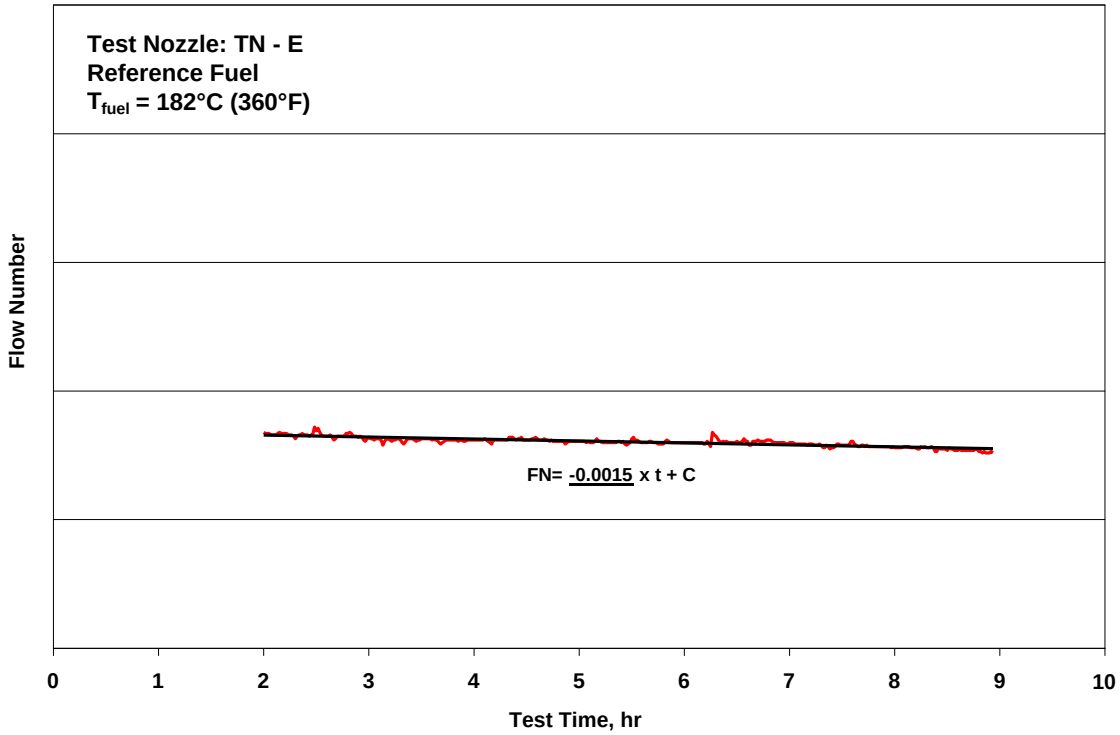

Figure E-3. Fouling Rate on Reference Fuel at T_{fuel} = 182°C (360°F)

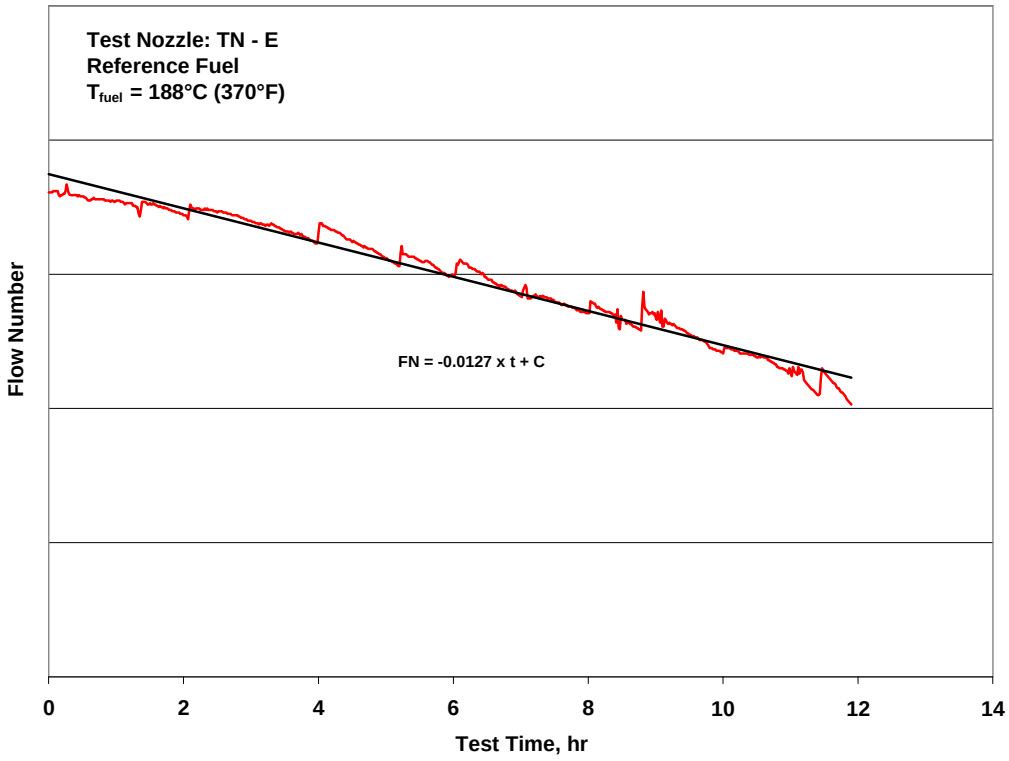

Figure E-4. Fouling Rate on Reference Fuel at T_{fuel} = 188°C (370°F)

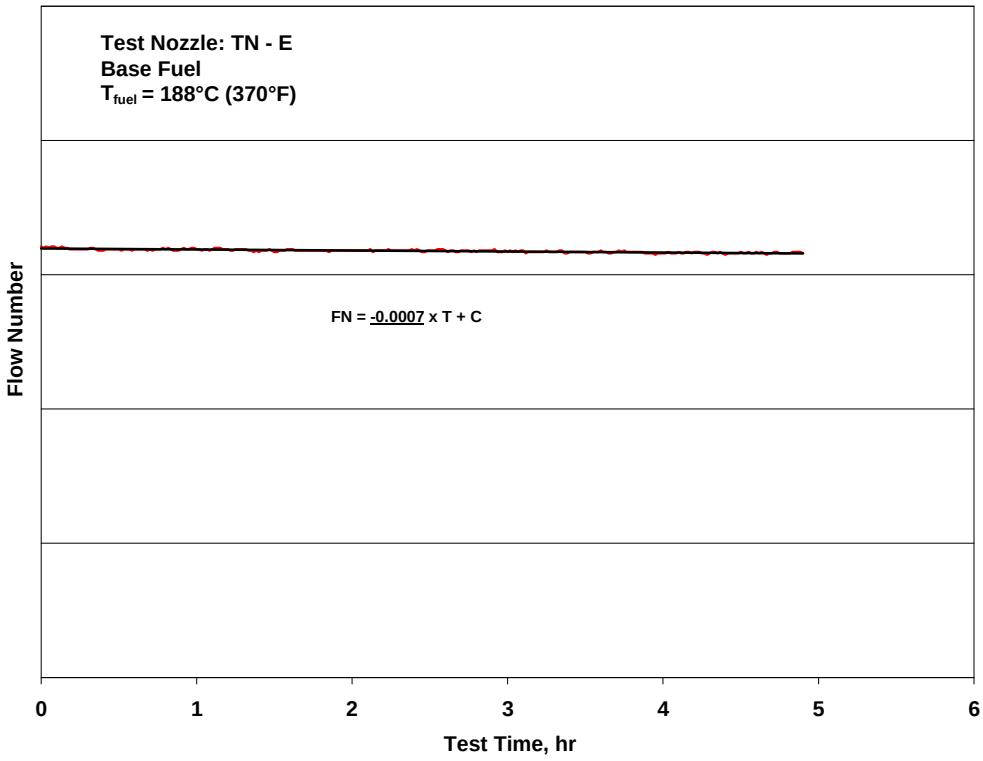

Figure E-5. Fouling Rate on Base Fuel at T_{fuel} = 188°C (370°F)

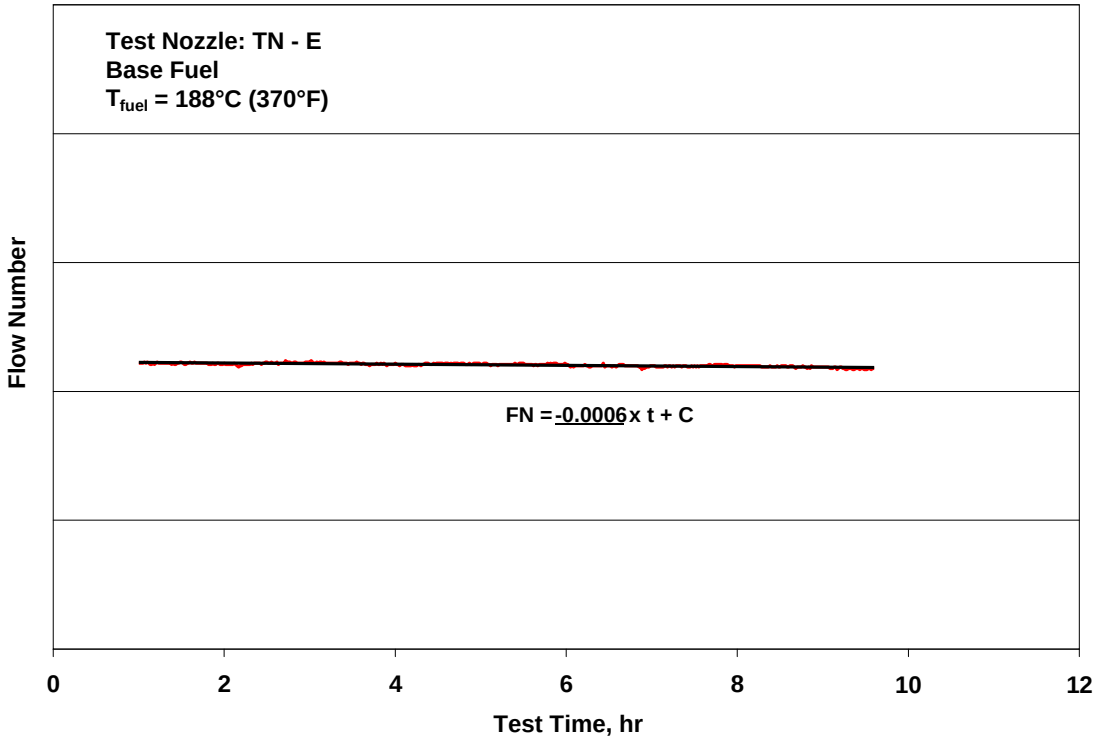

Figure E-6. Fouling Rate on Base Fuel at T_{fuel} = 188°C (370°F) (repeat)

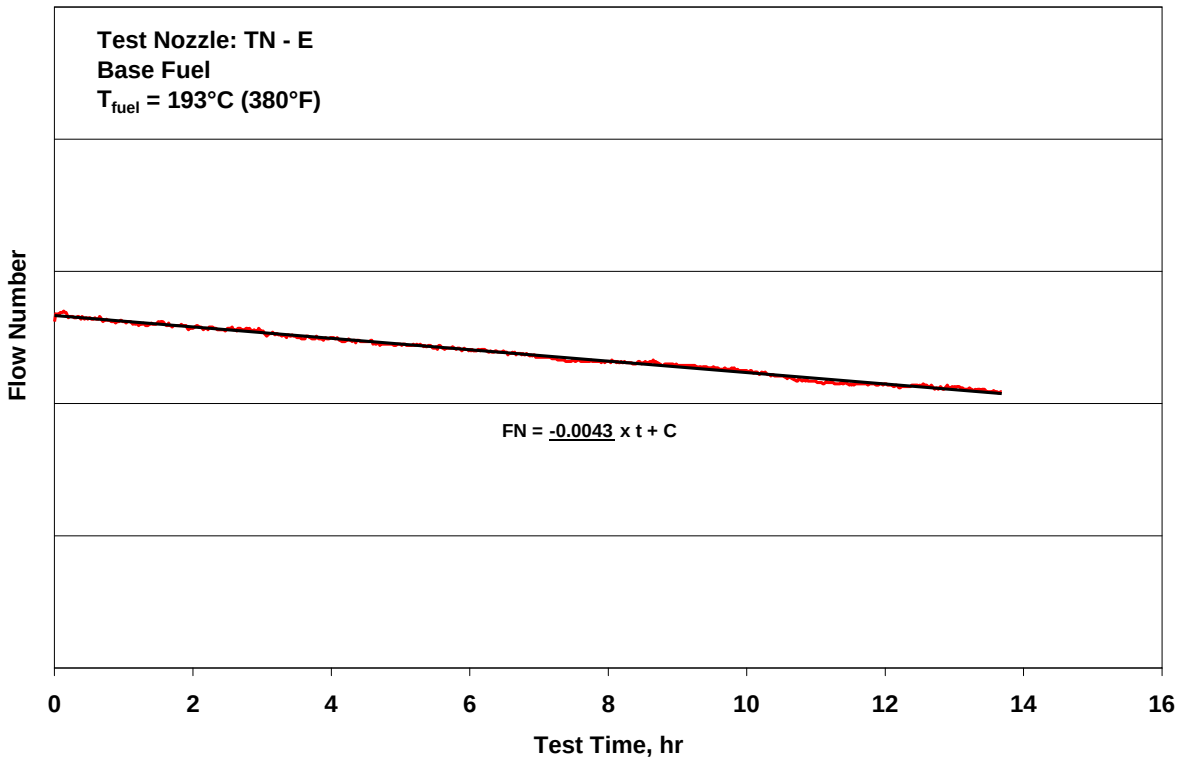

Figure E-7. Fouling Rate on Base Fuel at T_{fuel} = 193°C (380°F)

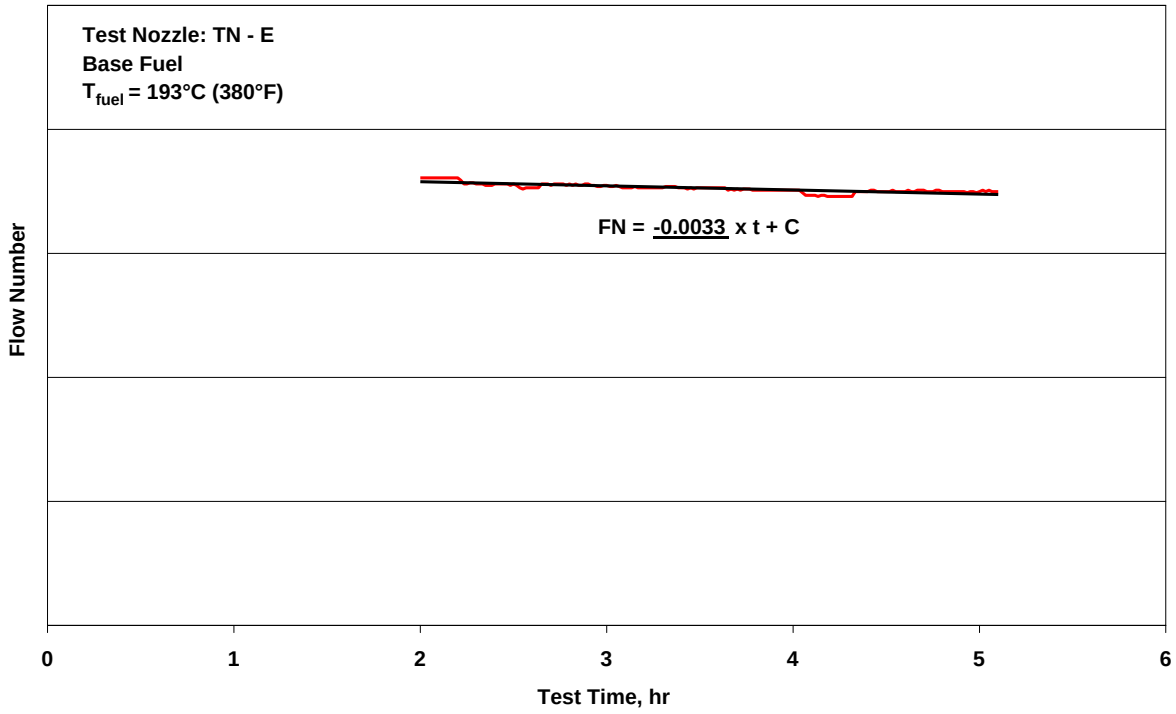

Figure E-8. Fouling Rate on Base Fuel at T_{fuel} = 183°C (380°F) (repeat)

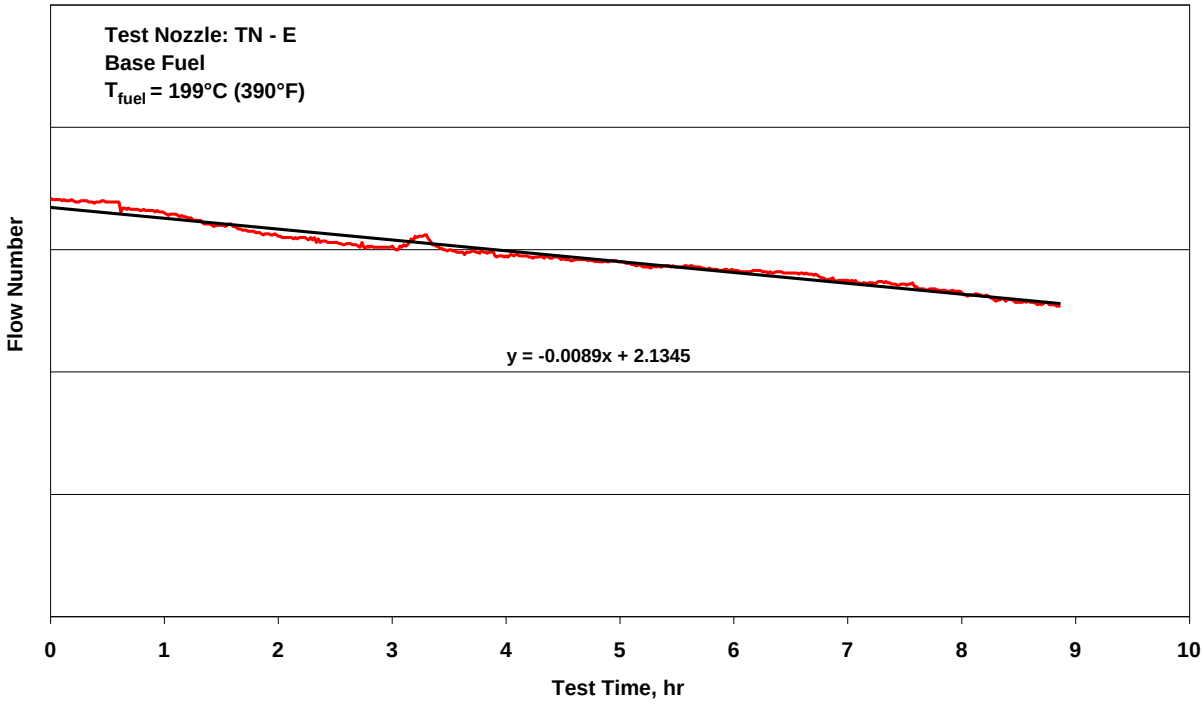

Figure E-9. Fouling Rate on Base Fuel at T_{fuel} = 199°C (390°F)

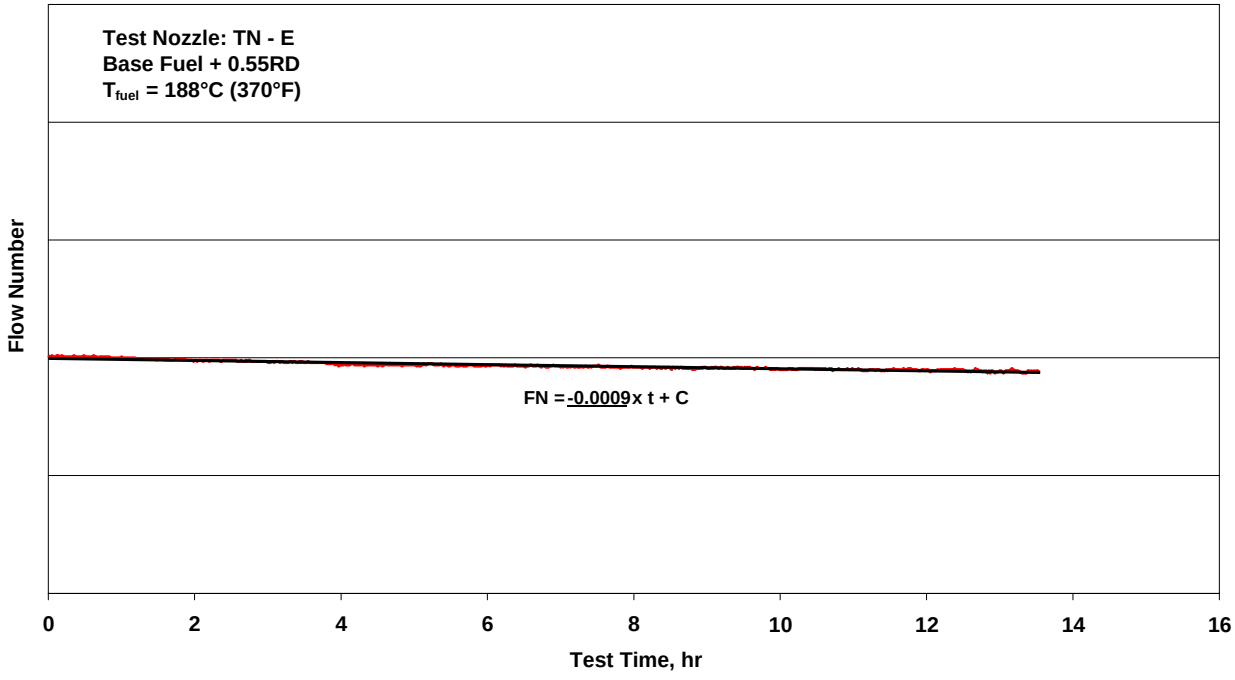

Figure E-10. Fouling Rate on Base Fuel + 0.55 mg/L of Red Dye at T_{fuel} = 188°C (370°F)

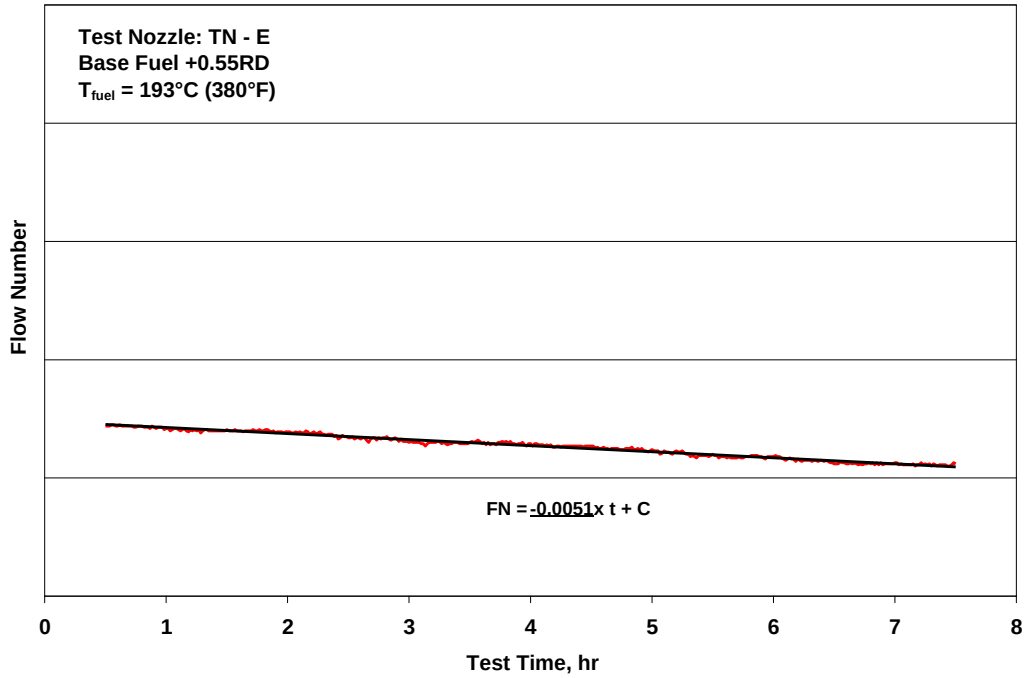

Figure E-11. Fouling Rate on Base Fuel + 0.55 mg/L of Red Dye at T_{fuel} = 193°C (380°F)

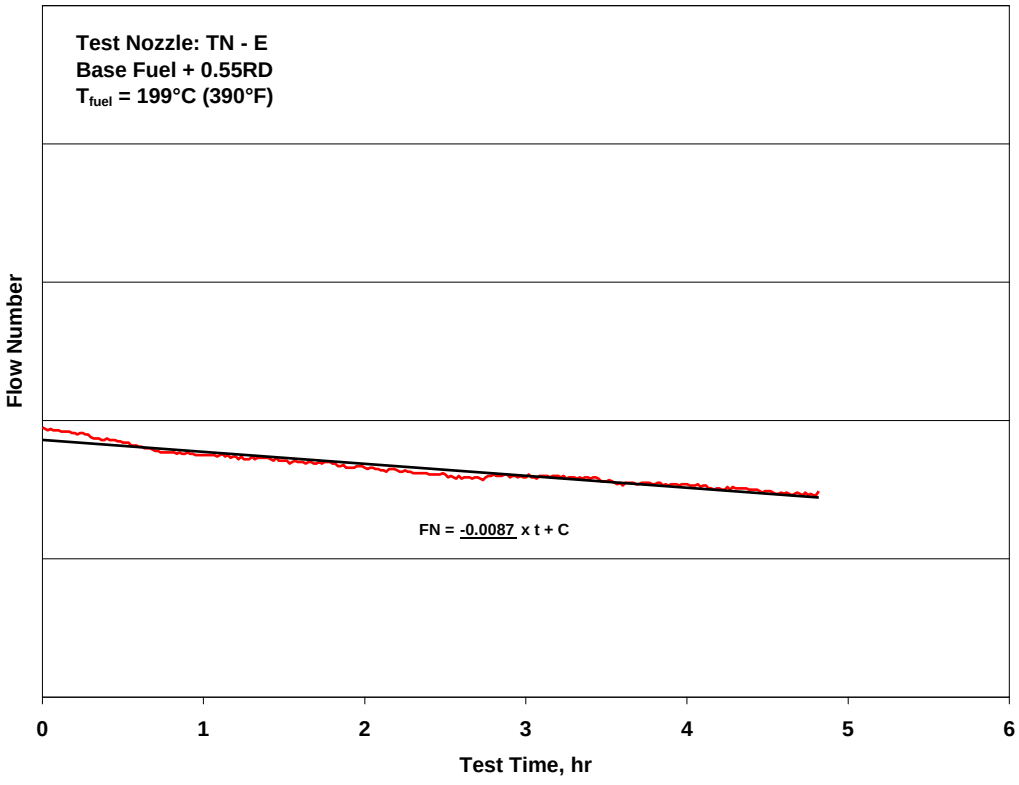

Figure E-12. Fouling Rate on Base Fuel + 0.55 mg/L of Red Dye at T_{fuel} = 199°C (390°F)

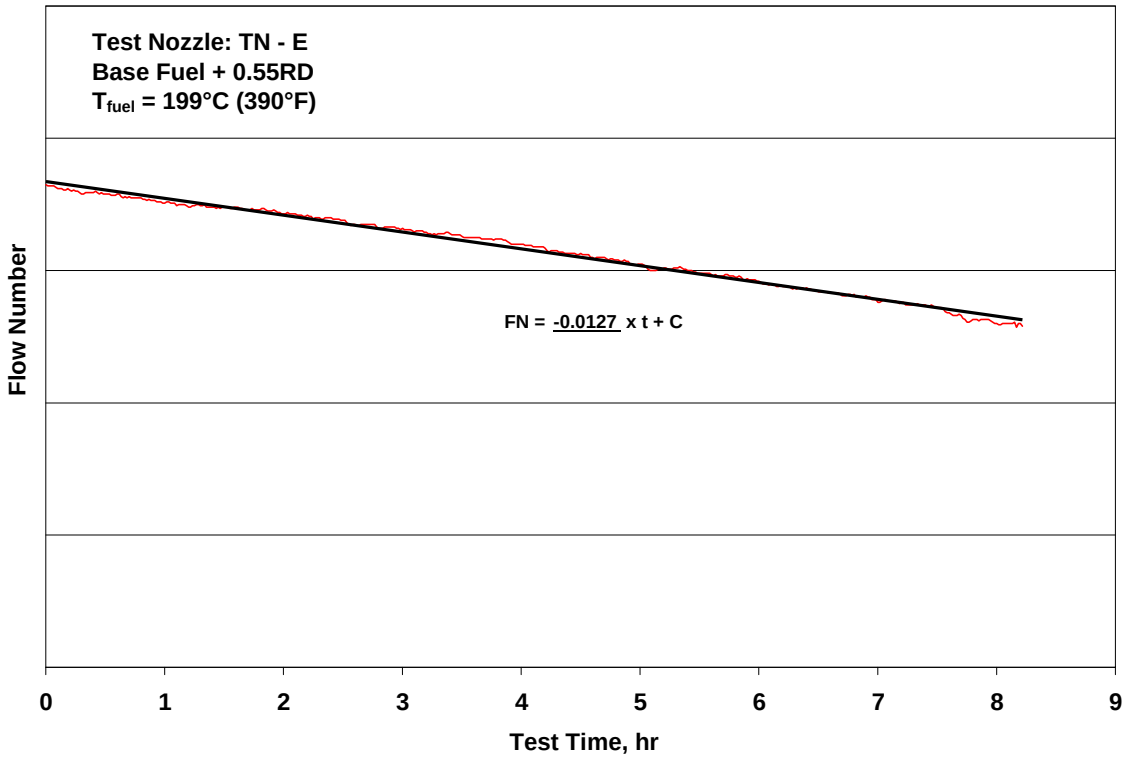

Figure E-13. Fouling Rate on Base Fuel + 0.55 mg/L of Red Dye at T_{fuel} = 199°C (390°F)

APPENDIX F—EXPERIMENTAL RESULTS FOR TEST NOZZLE TN-F

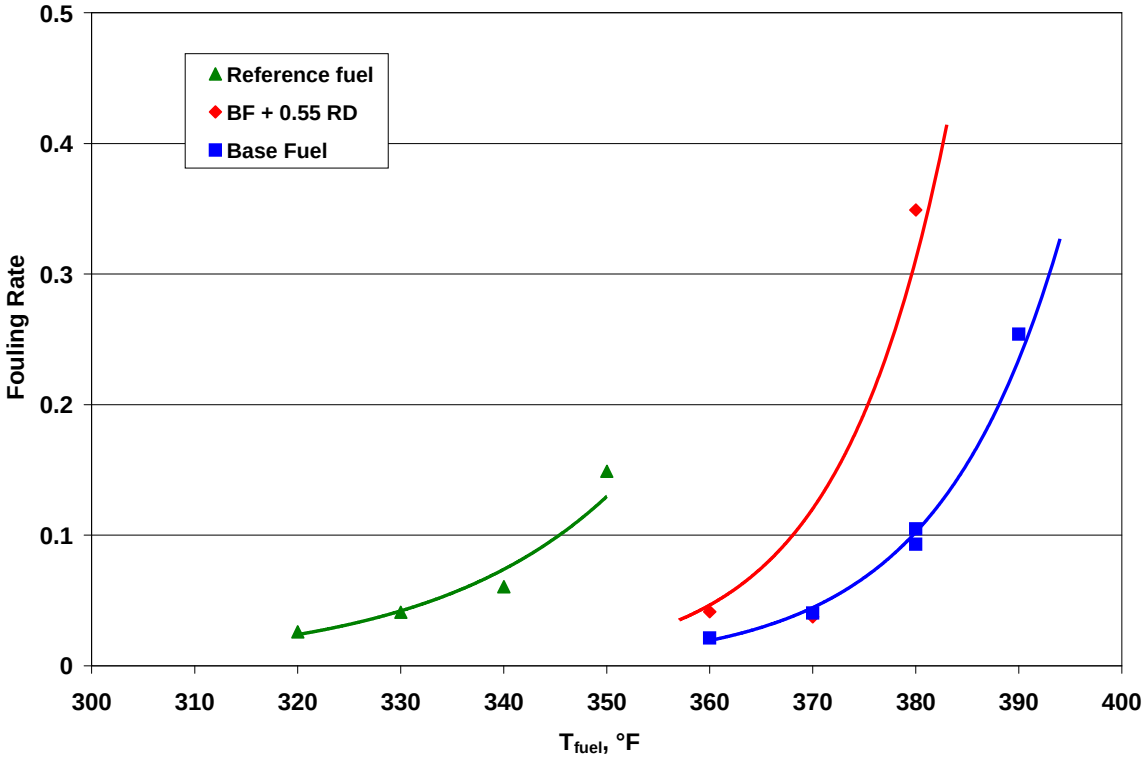

Figure F-1. Fouling Rate Summary

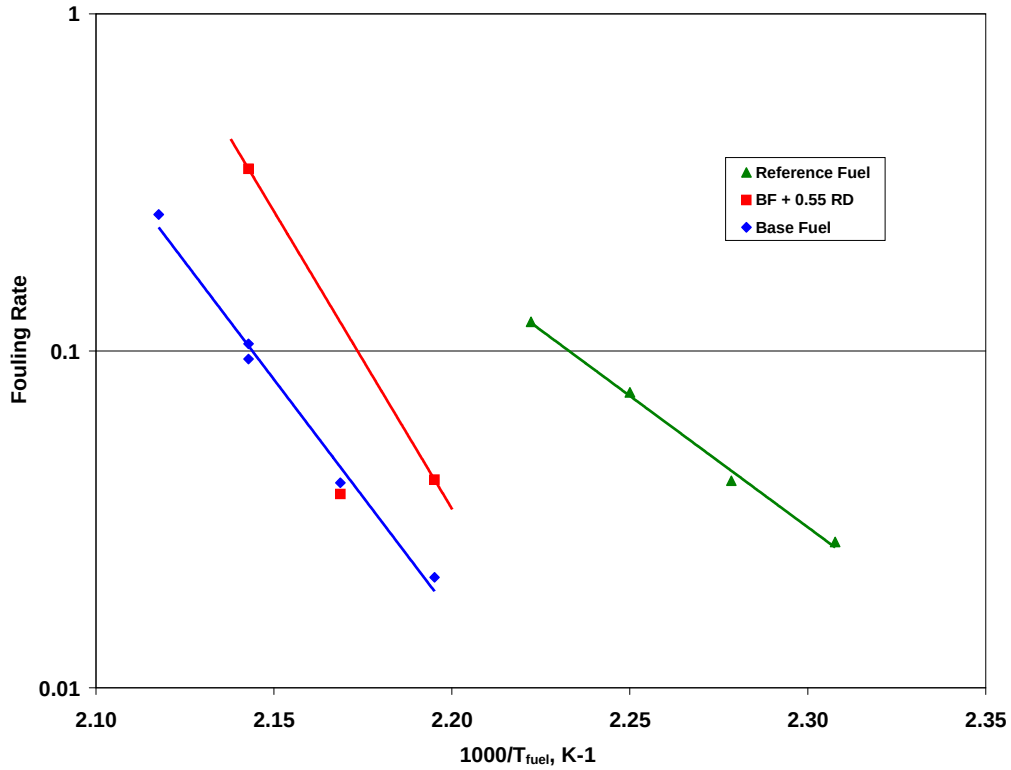

Figure F-2. Arrhenius Fouling Rate Summary

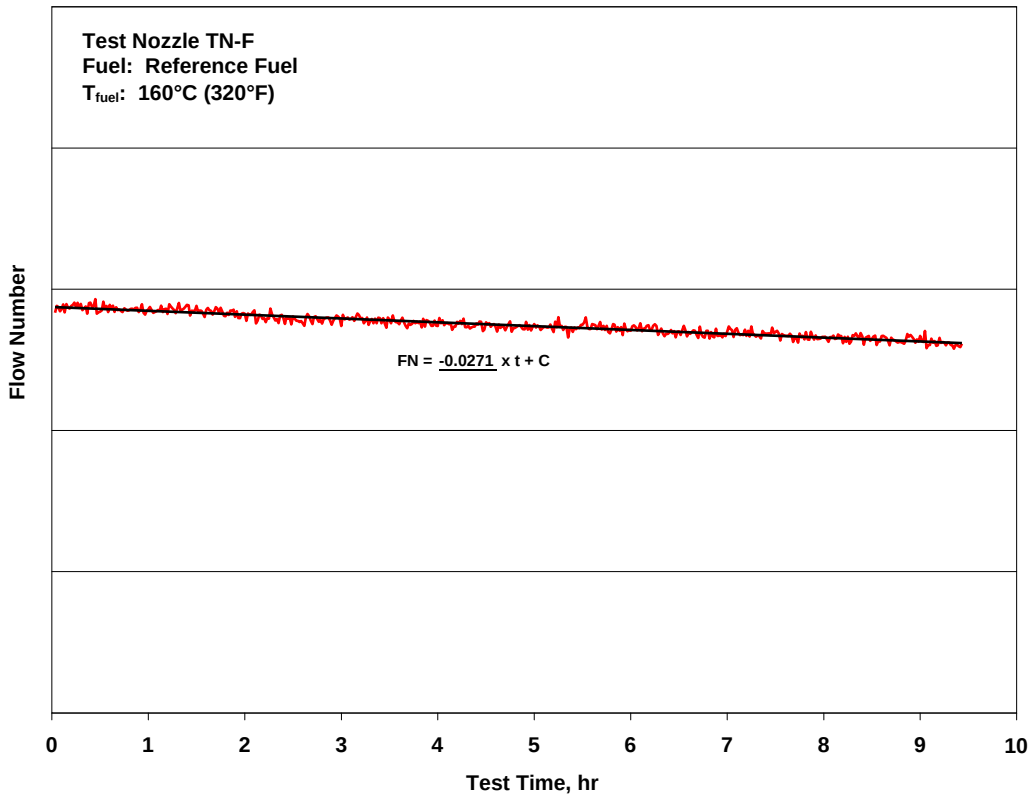

Figure F-3. Fouling Rate on Reference Fuel at T_{fuel} = 160°C (320°F)

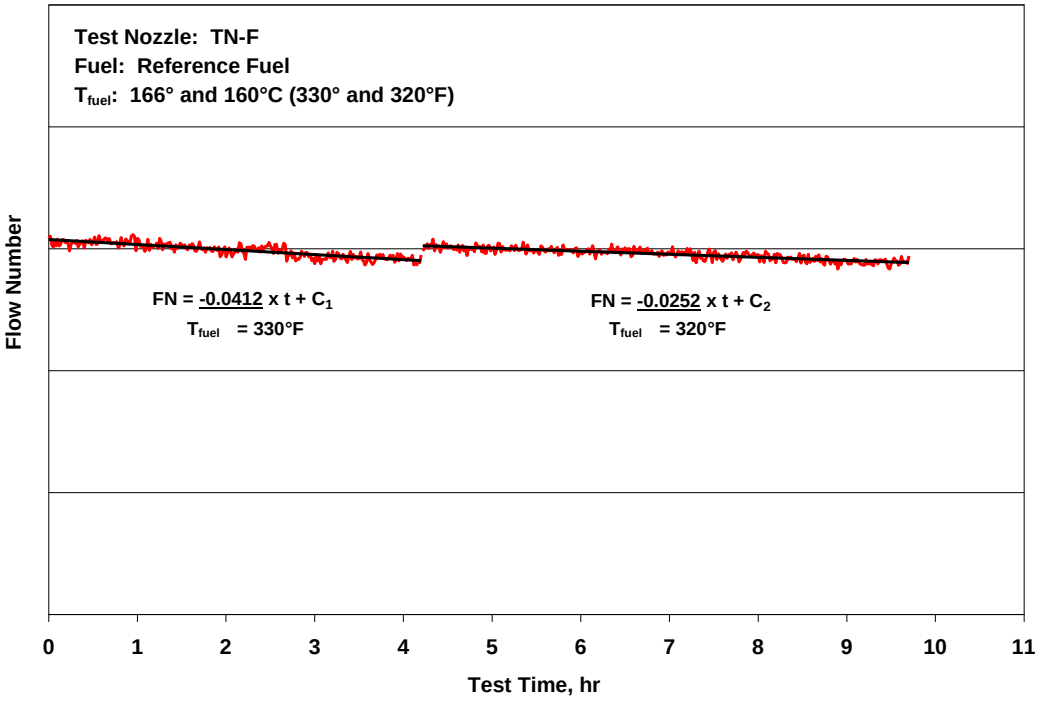

Figure F-4. Fouling Rate on Reference Fuel at T_{fuel} = 166° and 160°C (330° and 320°F)

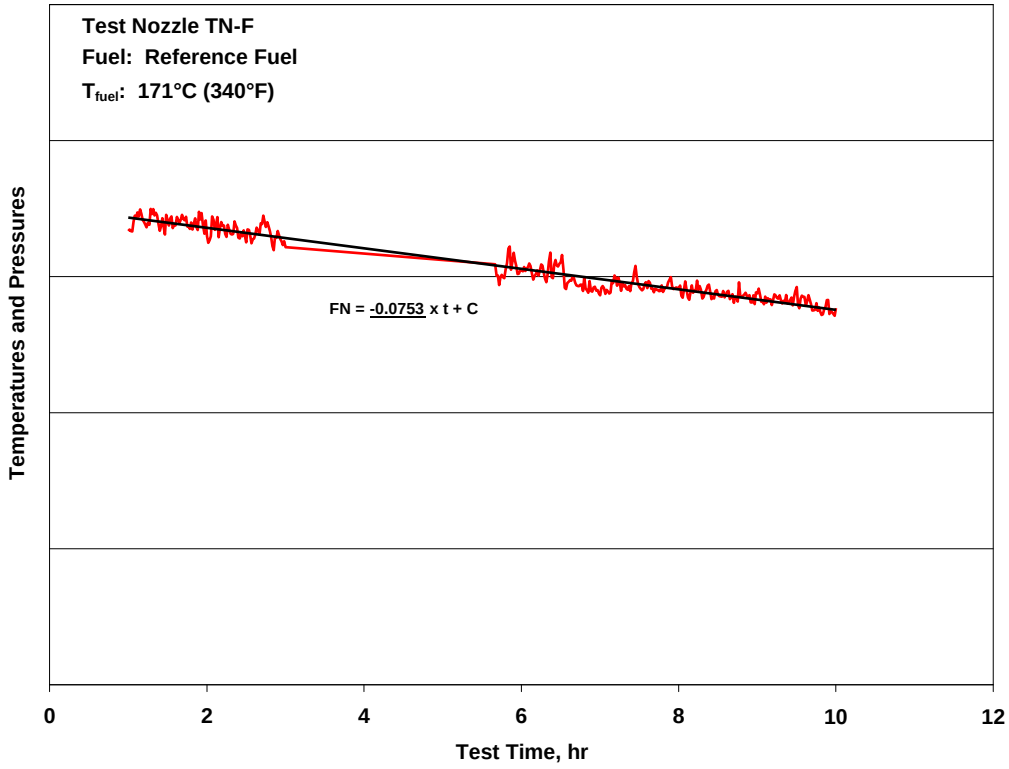

Figure F-5. Fouling Rate on Reference Fuel at T_{fuel} = 171°C (340°F)

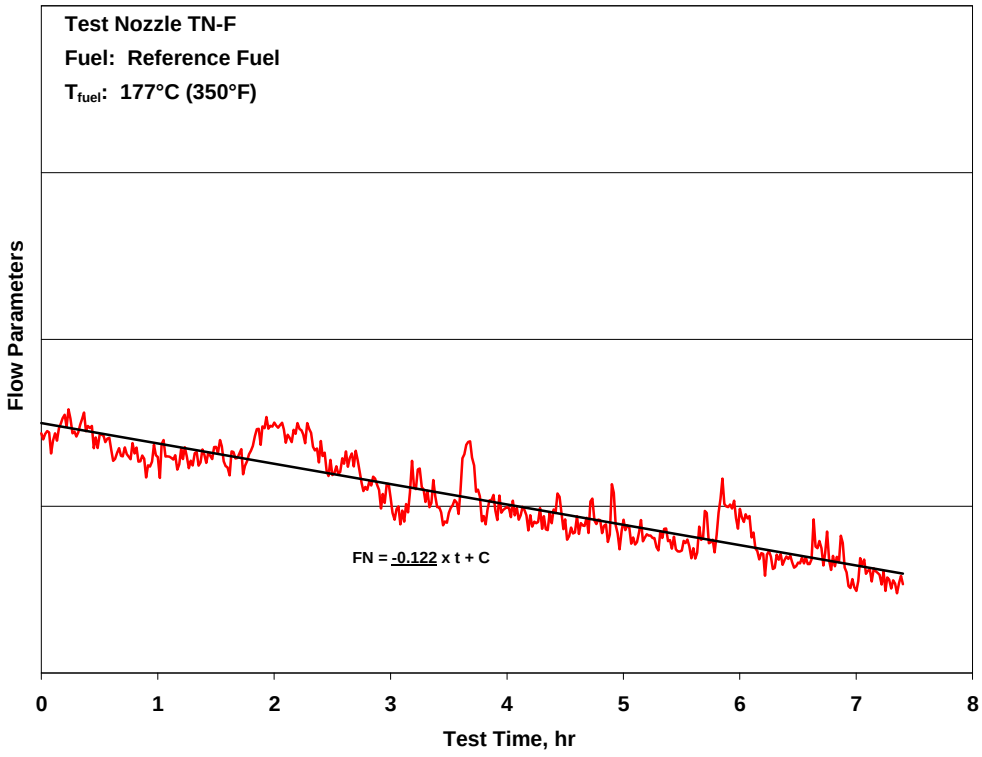

Figure F-6. Fouling Rate on Reference Fuel at T_{fuel} = 177°C (350°F)

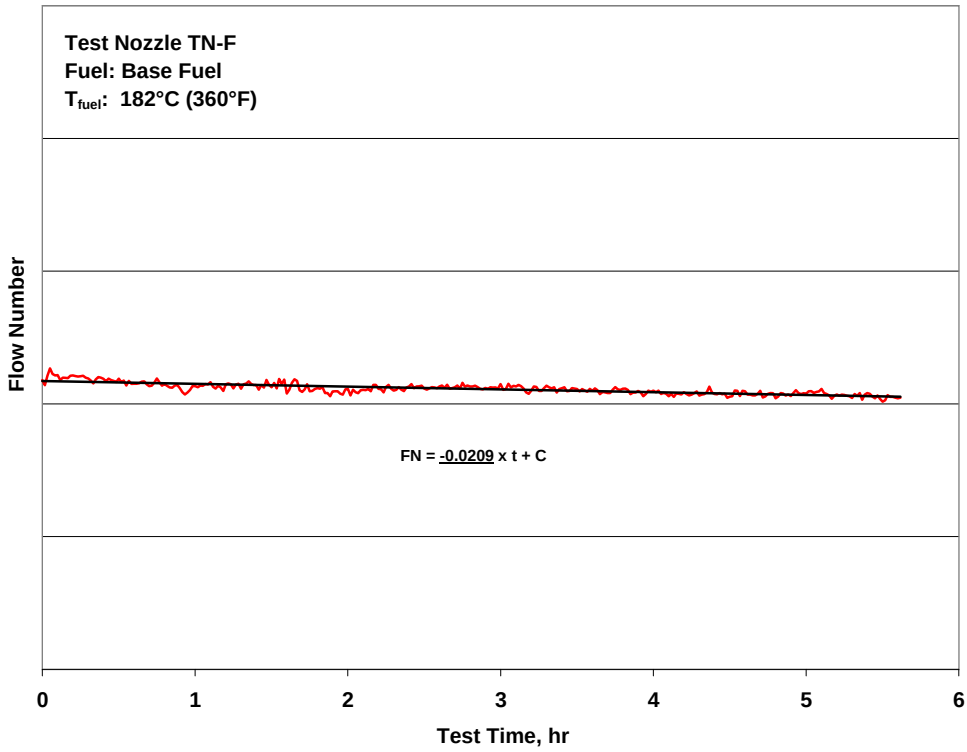

Figure F-7. Fouling Rate on Base Fuel at T_{fuel} = 182°C (360°F)

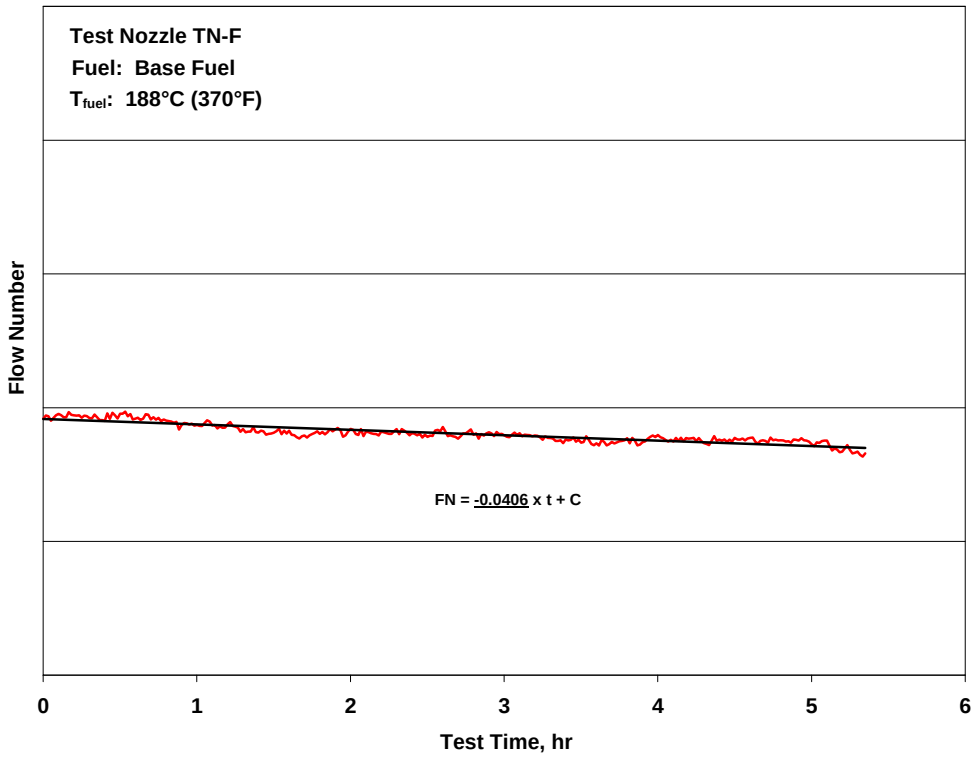

Figure F-8. Fouling Rate on Base Fuel at T_{fuel} = 188°C (370°F)

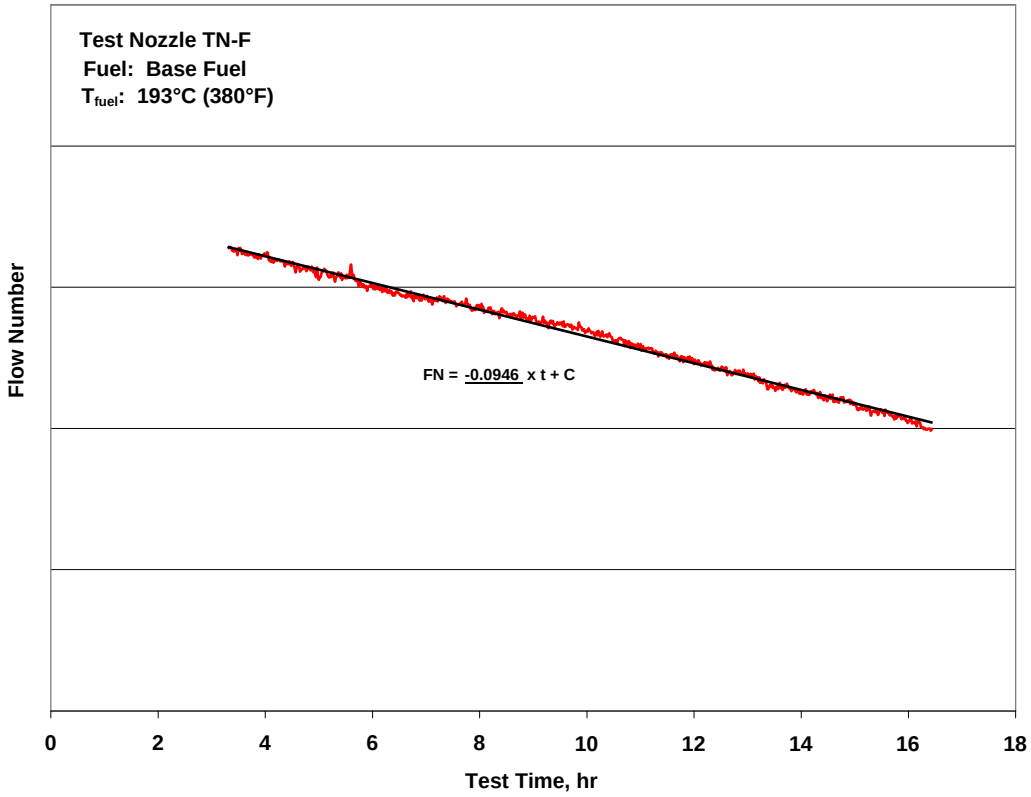

Figure F-9. Fouling Rate on Base Fuel at T_{fuel} = 193°C (380°F)

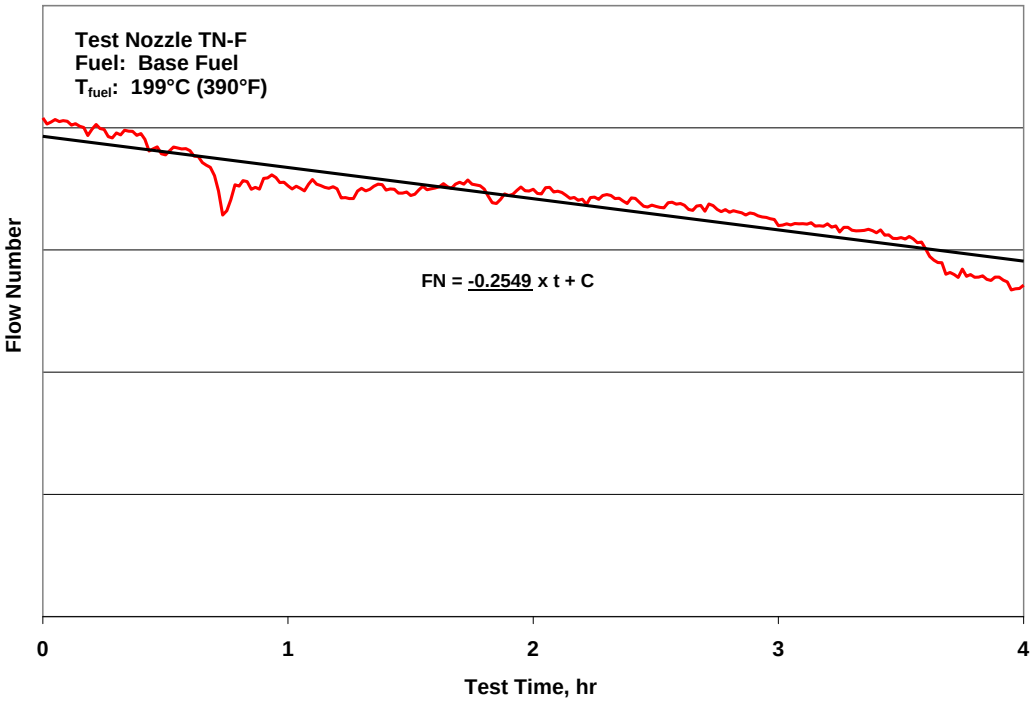

Figure F-10. Fouling Rate on Base Fuel at T_{fuel} = 199°C (390°F)

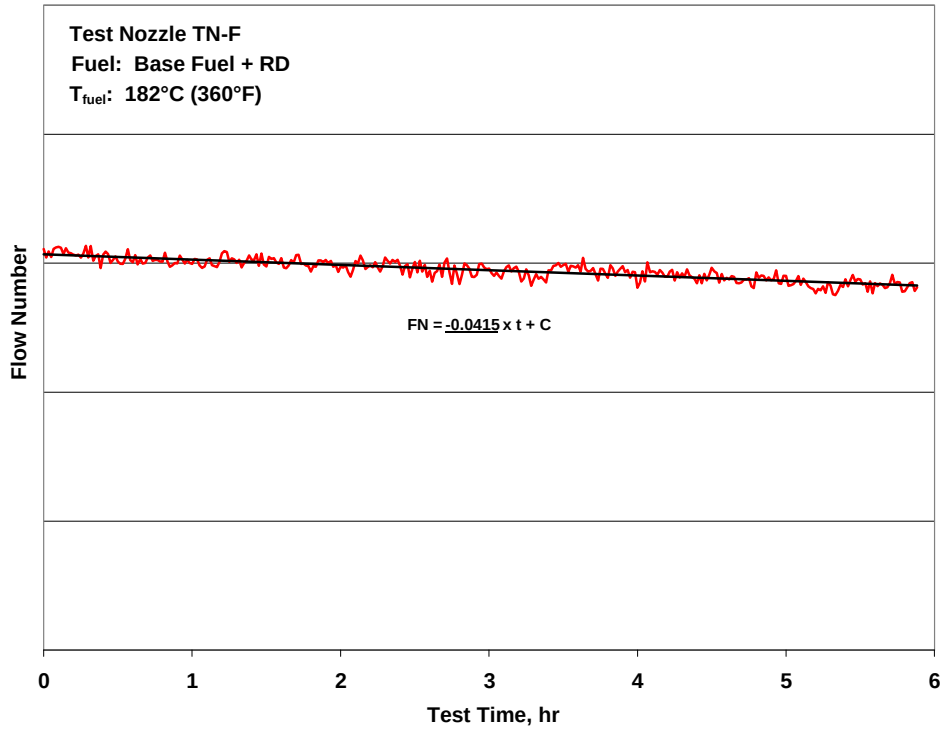

Figure F-11. Fouling Rate on Base Fuel + 0.55 mg/L of Red Dye at T_{fuel} = 182°C (360°F)

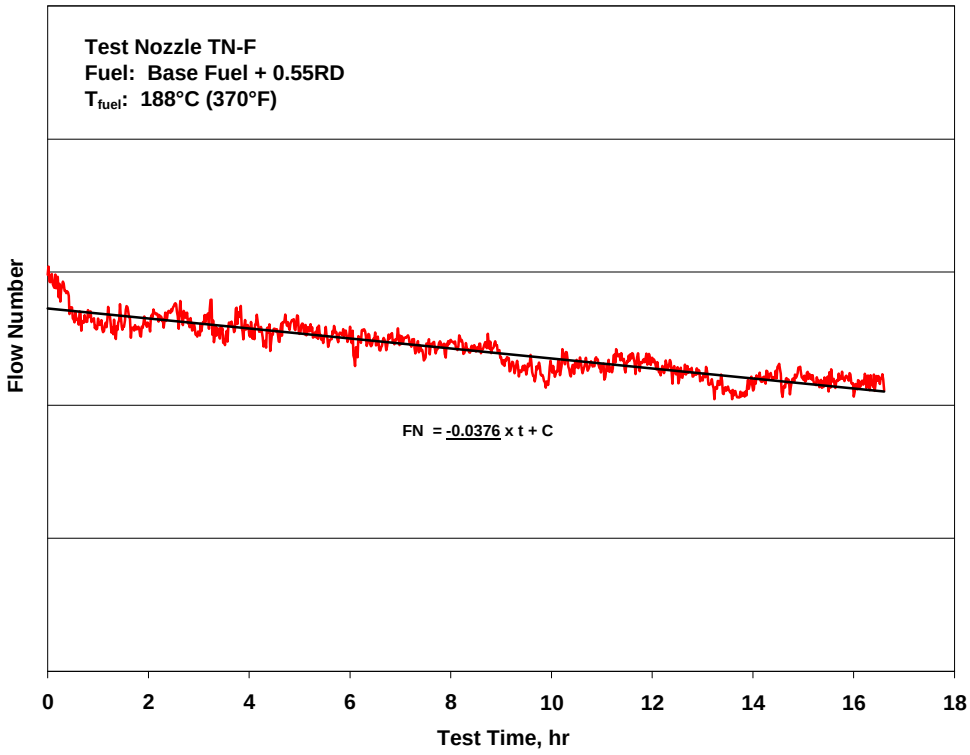

Figure F-12. Fouling Rate on Base Fuel + 0.55 mg/L of Red Dye at T_{fuel} = 188°C (370°F)

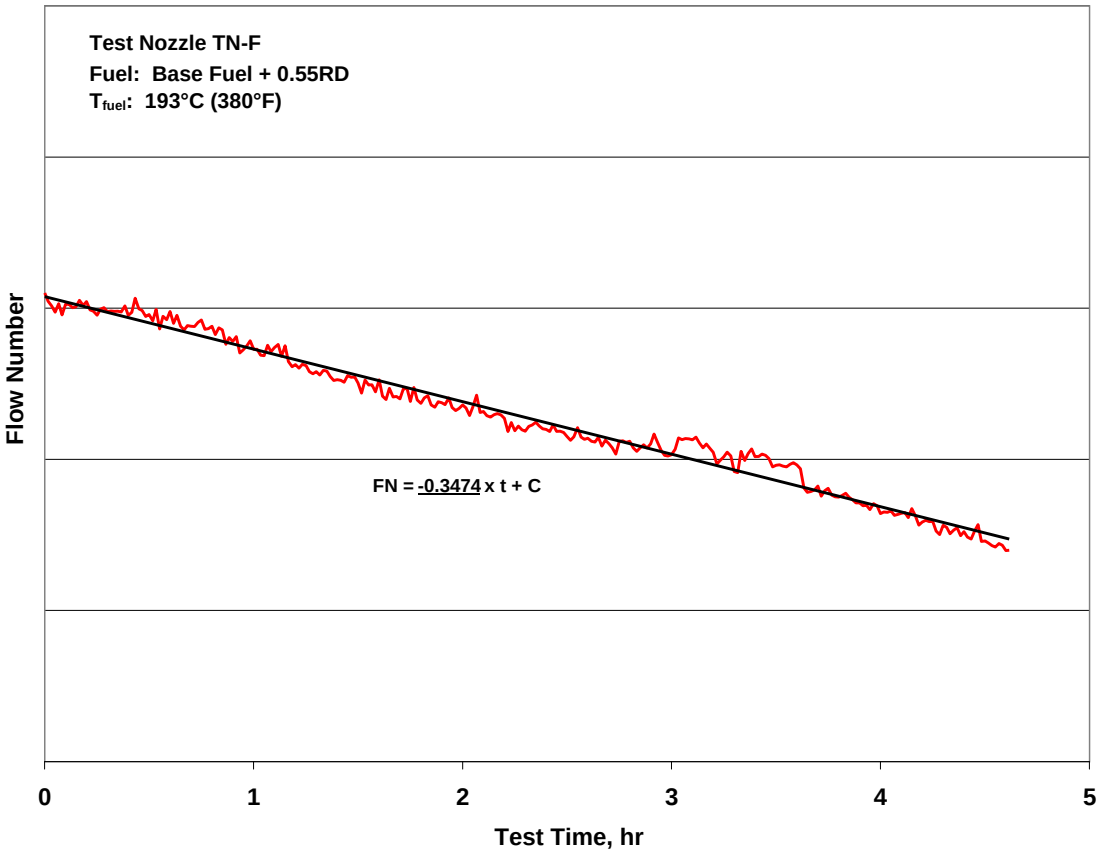

Figure F-13. Fouling Rate on Base Fuel + 0.55 mg/L of Red Dye at T_{fuel} = 193°C (380°F)

APPENDIX G—EXPERIMENTAL RESULTS FOR TEST NOZZLE TN-G

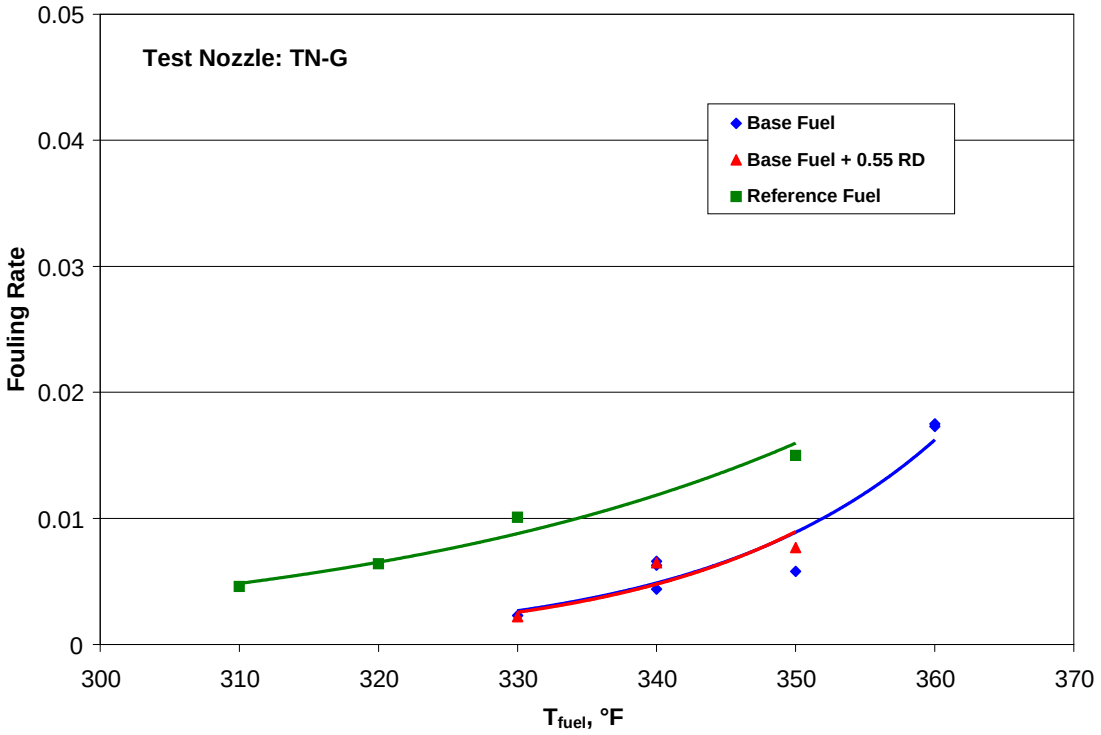

Figure G-1. Fouling Rate Summary

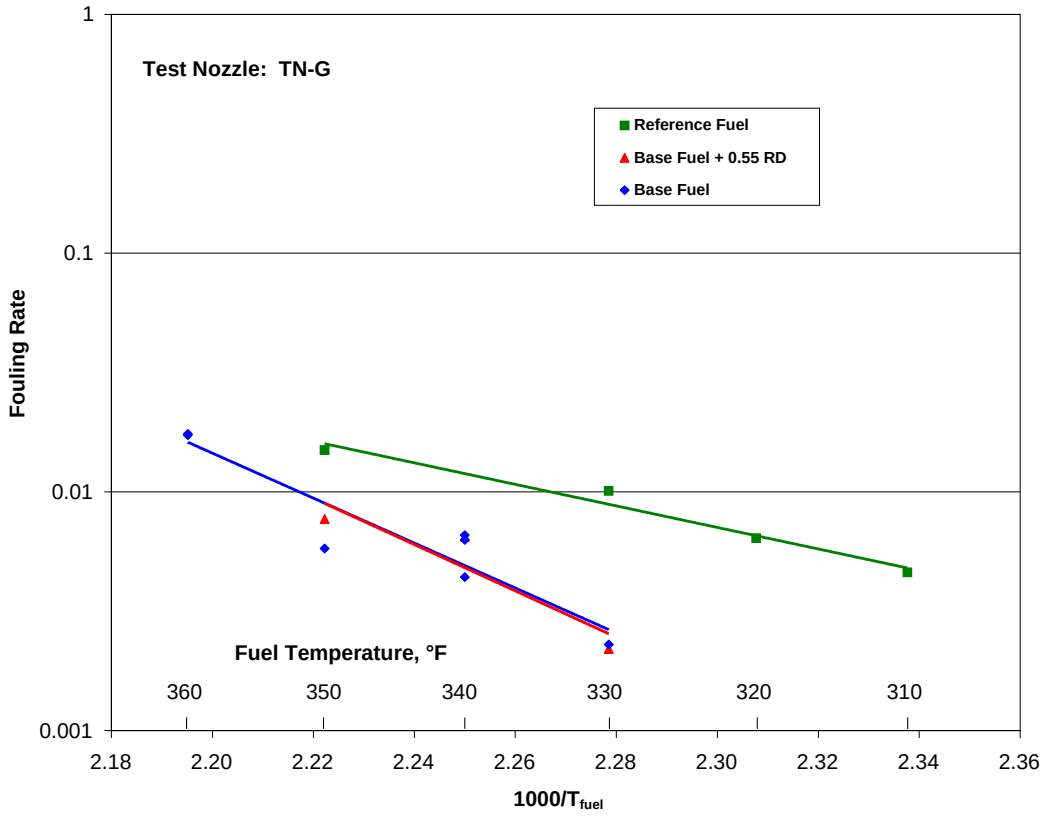

Figure G-2. Arrhenius Fouling Rate Summary

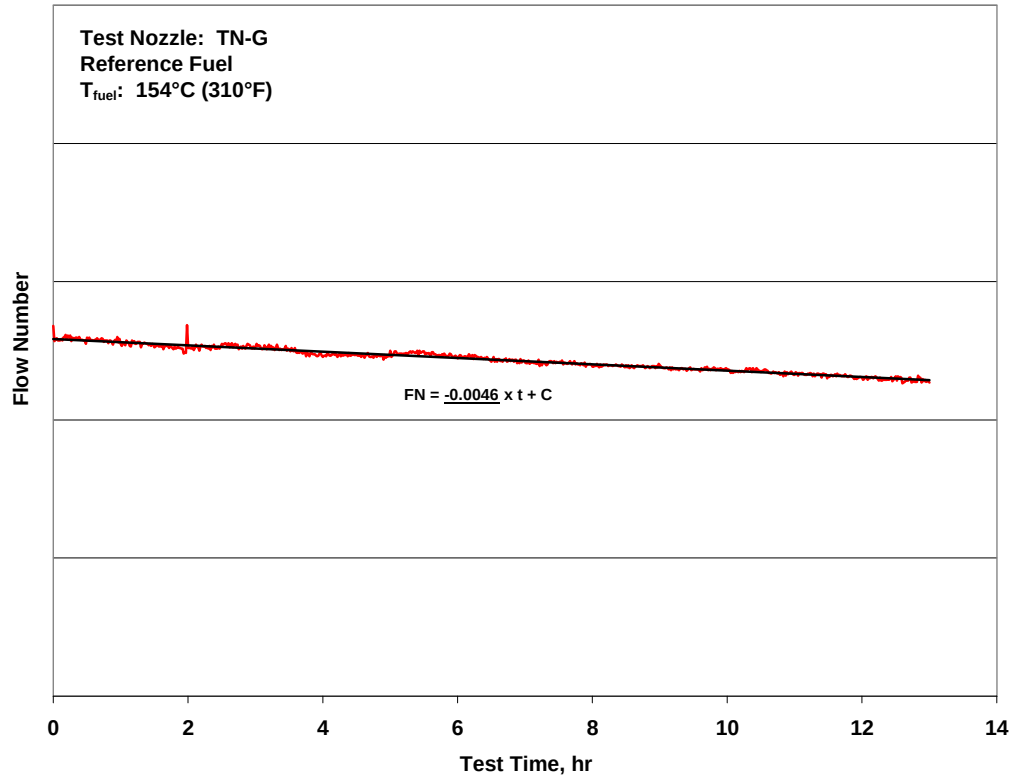

Figure G-3. Fouling Rate on Reference Fuel at T_{fuel} = 154°C (310°F)

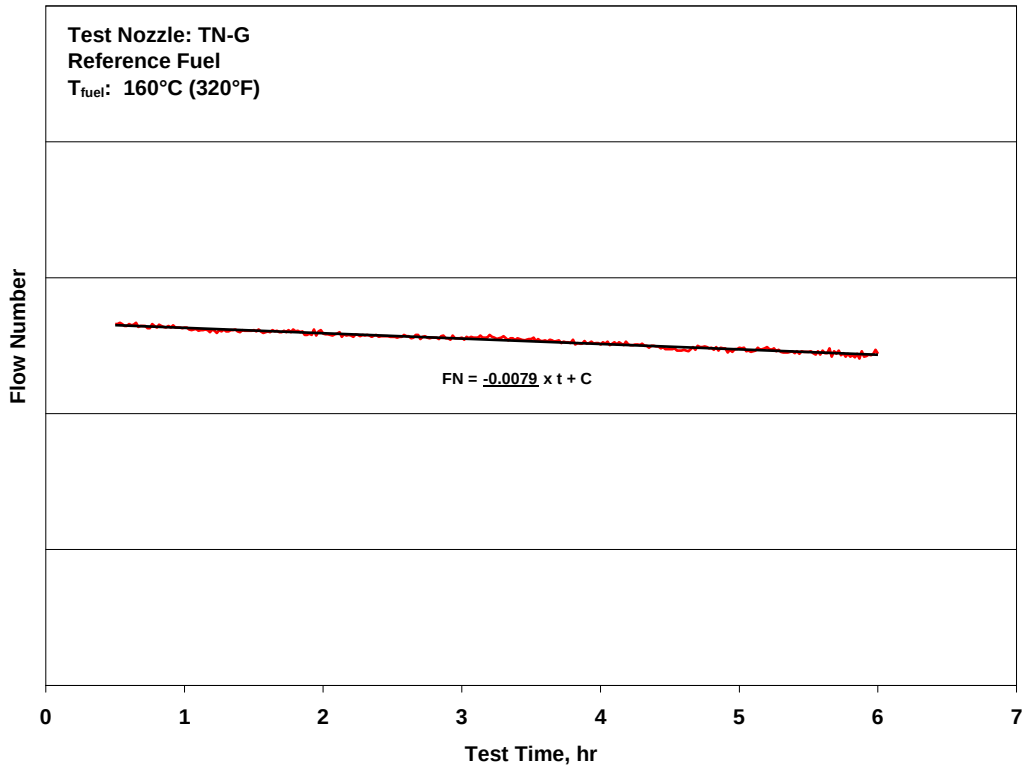

Figure G-4. Fouling Rate on Reference Fuel at T_{fuel} = 160°C (320°F)

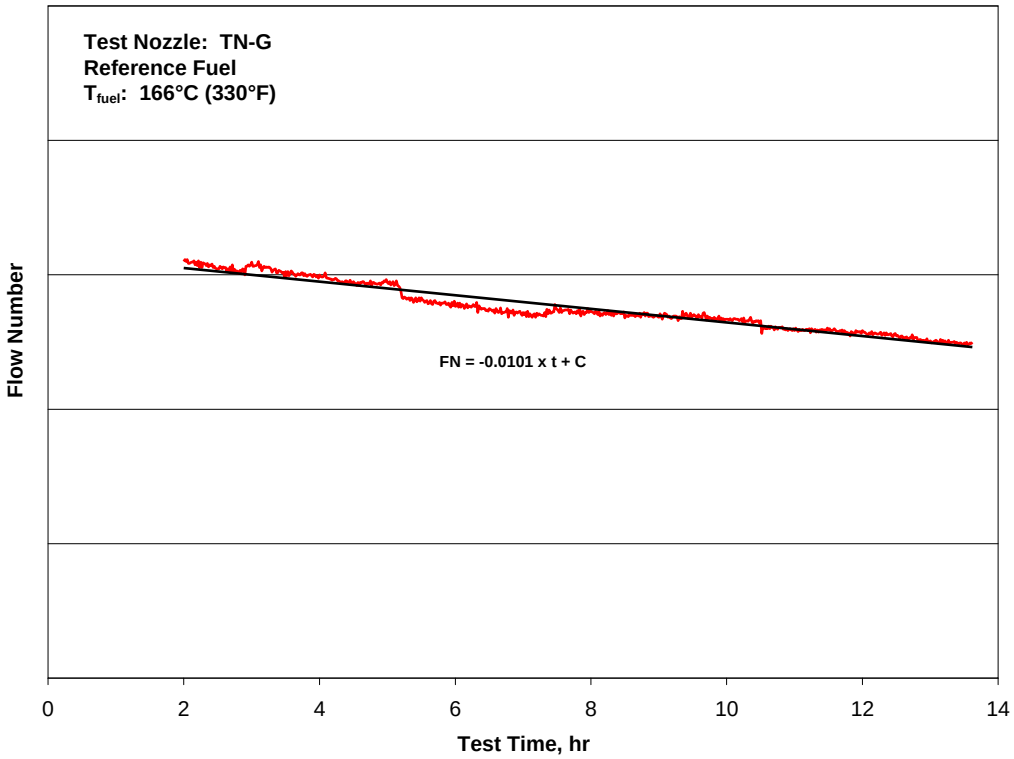

Figure G-5. Fouling Rate on Reference Fuel at T_{fuel} = 166°C (330°F)

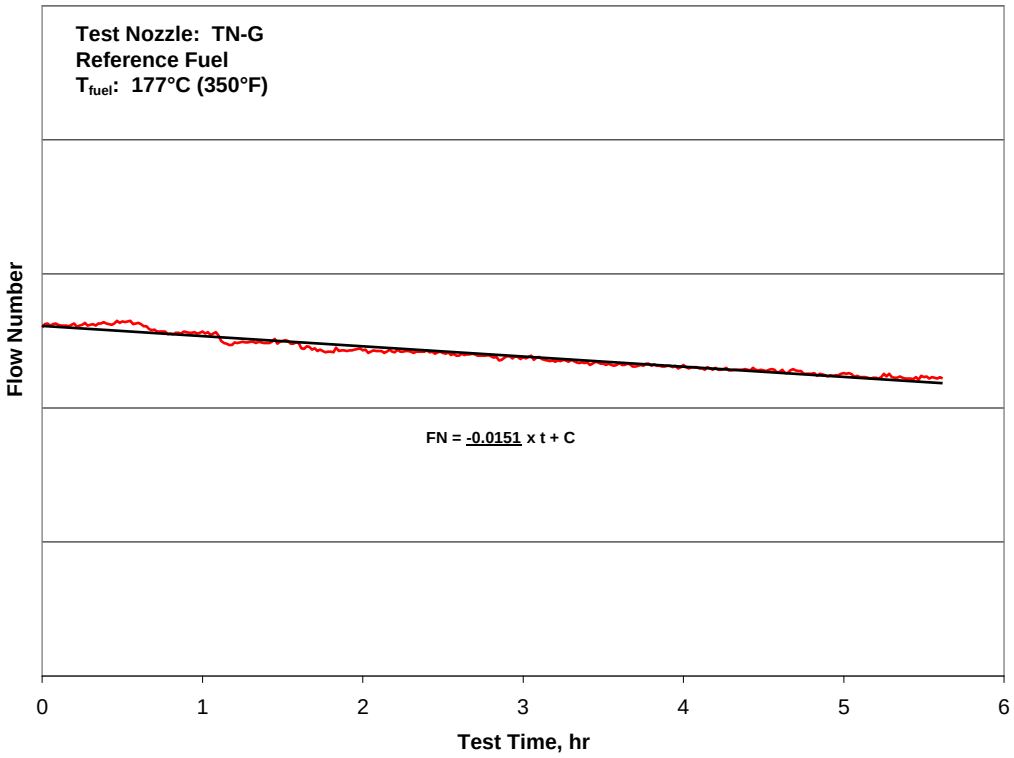

Figure G-6. Fouling Rate on Reference Fuel at T_{fuel} = 177°C (350°F)

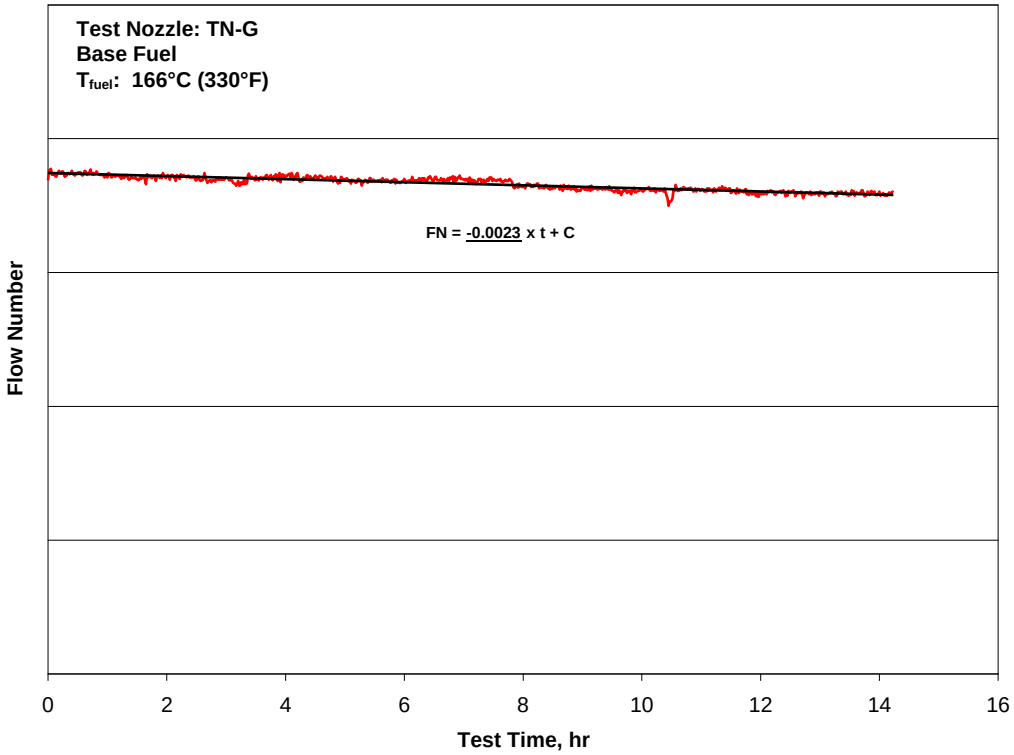

Figure G-7. Fouling Rate on Base Fuel at T_{fuel} = 166°C (330°F)

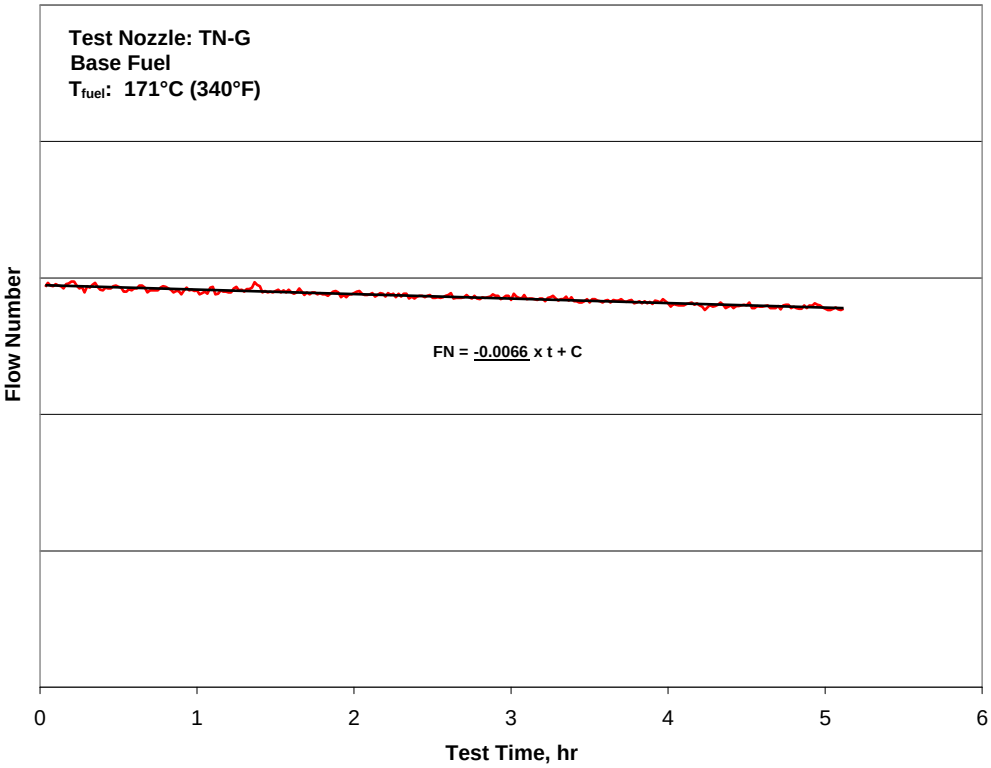

Figure G-8. Fouling Rate on Base Fuel at T_{fuel} = 171°C (340°F)

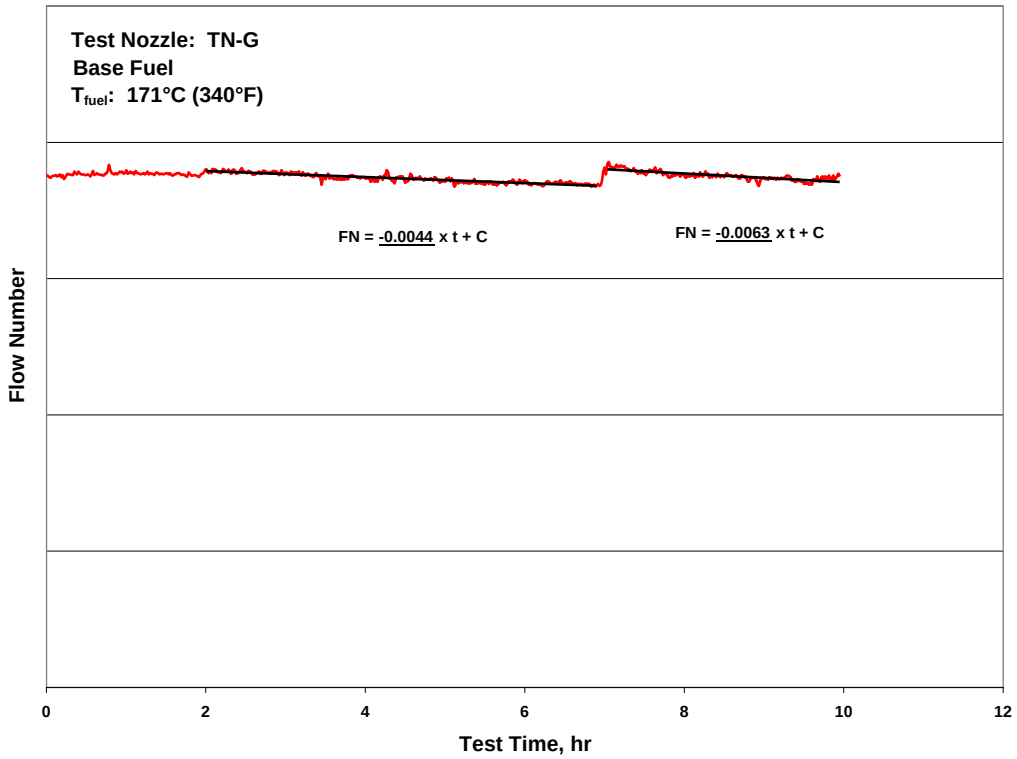

Figure G-9. Fouling Rate on Base Fuel at T_{fuel} = 171°C (340°F) (repeat)

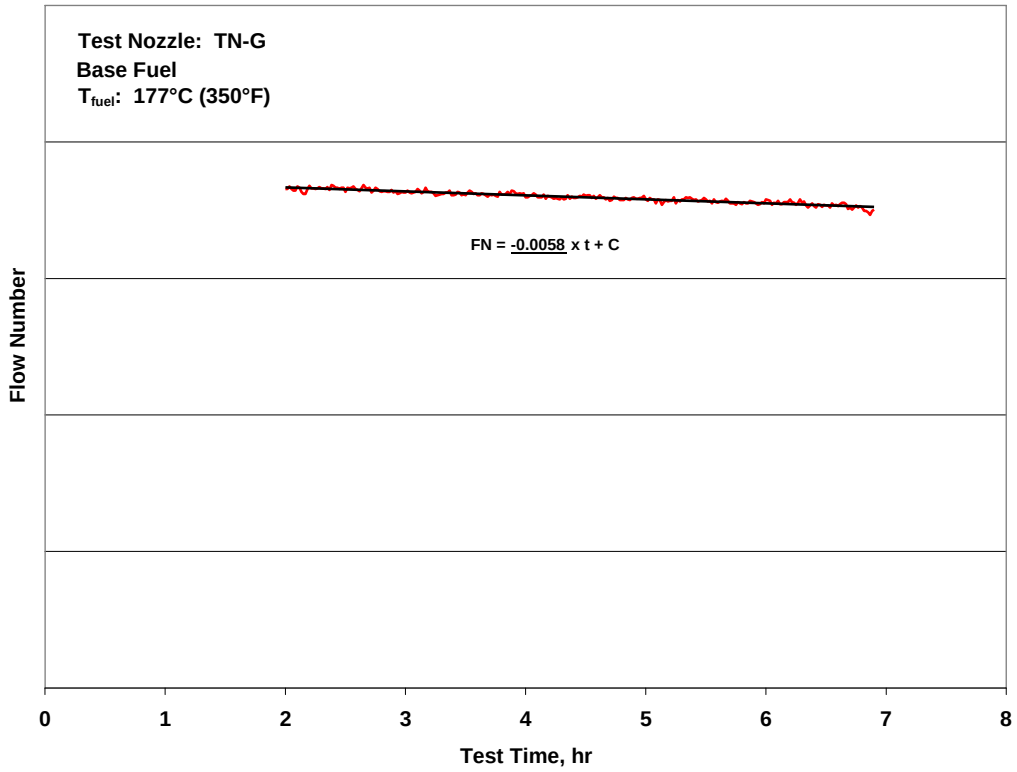

Figure G-10. Fouling Rate on Base Fuel at T_{fuel} = 177°C (350°F)

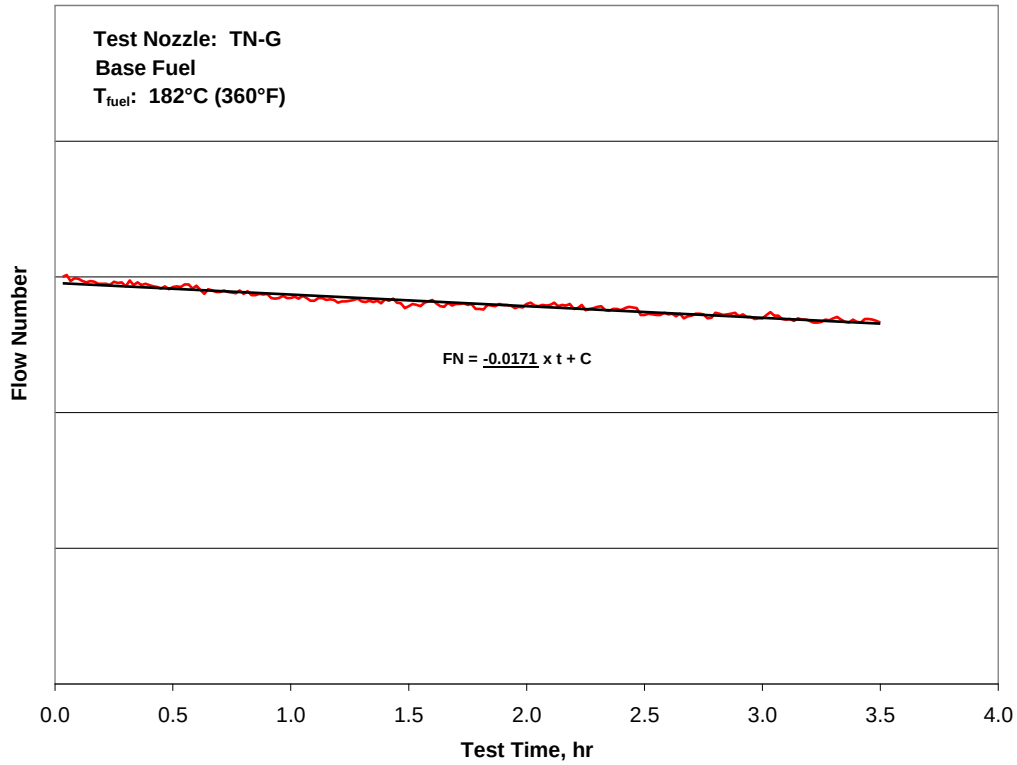

Figure G-11. Fouling Rate on Base Fuel at T_{fuel} = 182°C (360°F)

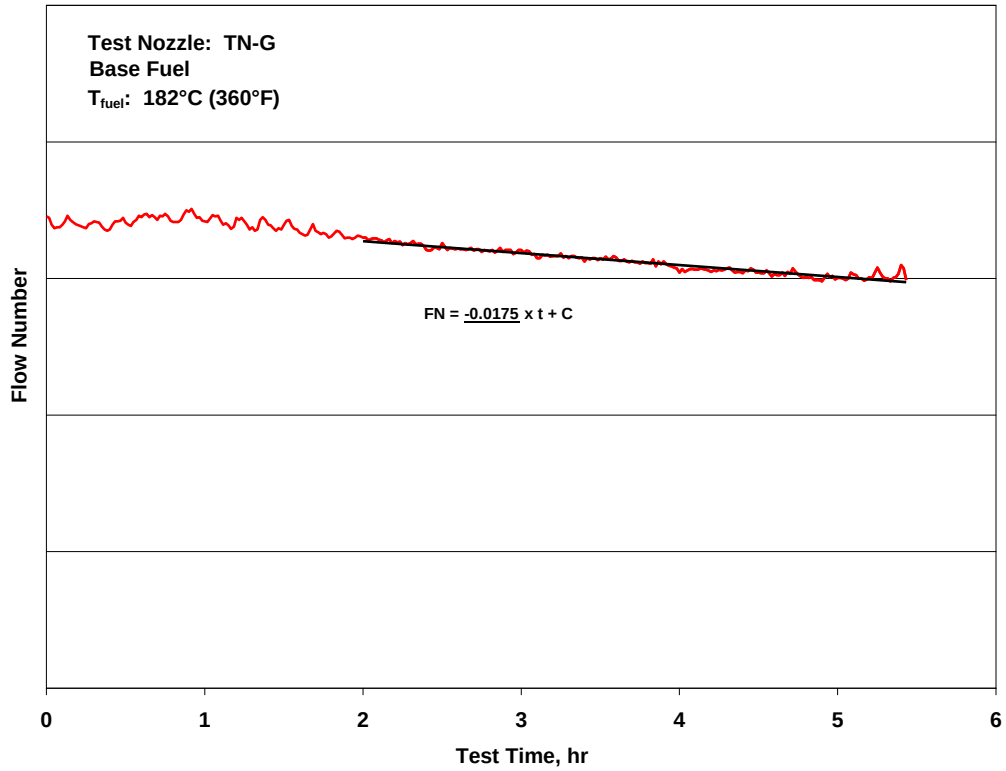

Figure G-12. Fouling Rate on Base Fuel at T_{fuel} = 182°C (360°F) (repeat)

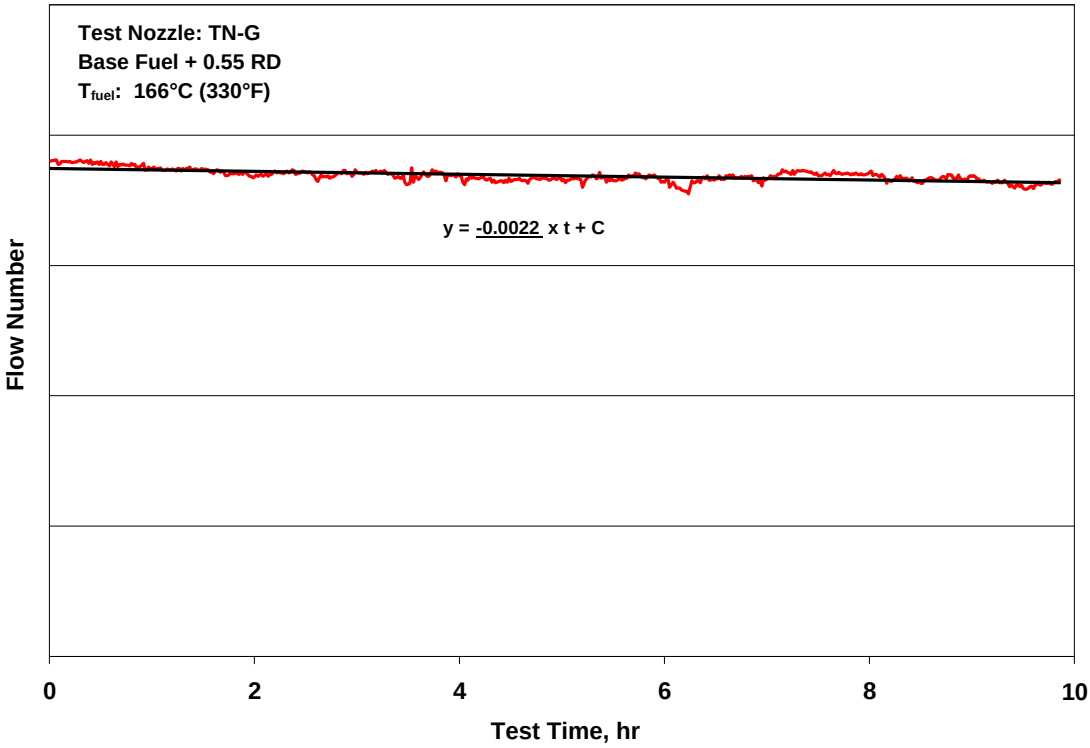

Figure G-13. Fouling Rate on Base Fuel + 0.55 mg/L of Red Dye at T_{fuel} = 166°C (330°F)

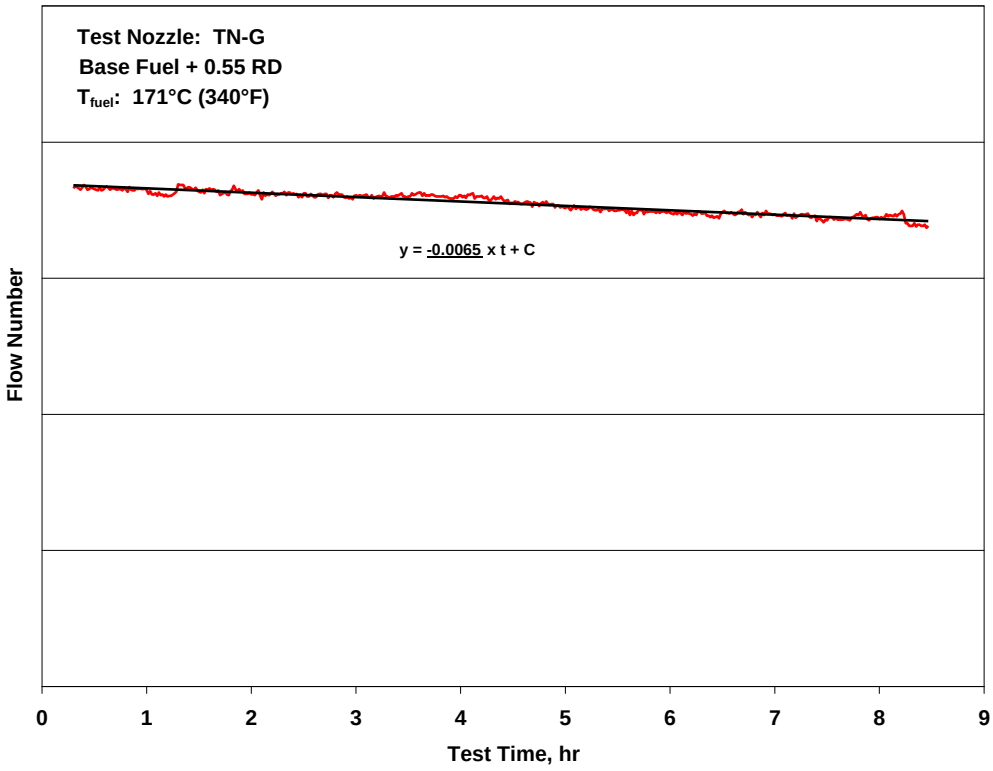

Figure G-14. Fouling Rate on Base Fuel + 0.55 mg/L of Red Dye at T_{fuel} = 171°C (340°F)

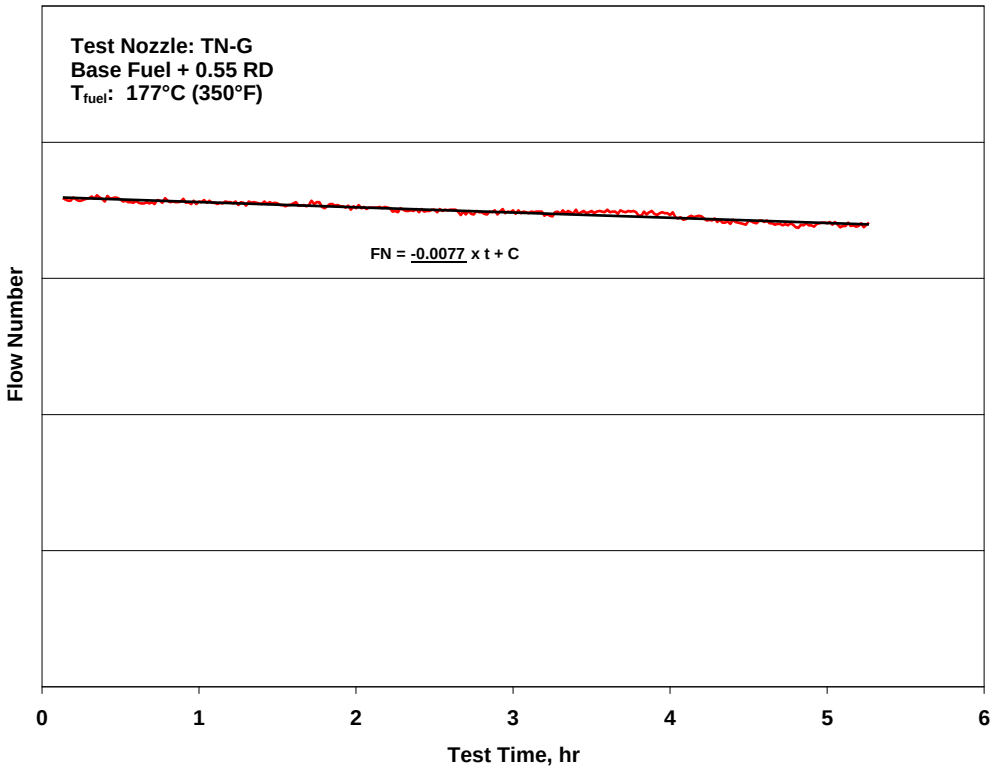

Figure G-15. Fouling Rate on Base Fuel + 0.55 mg/L of Red Dye at T_{fuel} = 177°C (350°F)

APPENDIX H—EXPERIMENTAL RESULTS FOR TEST NOZZLE TN-H

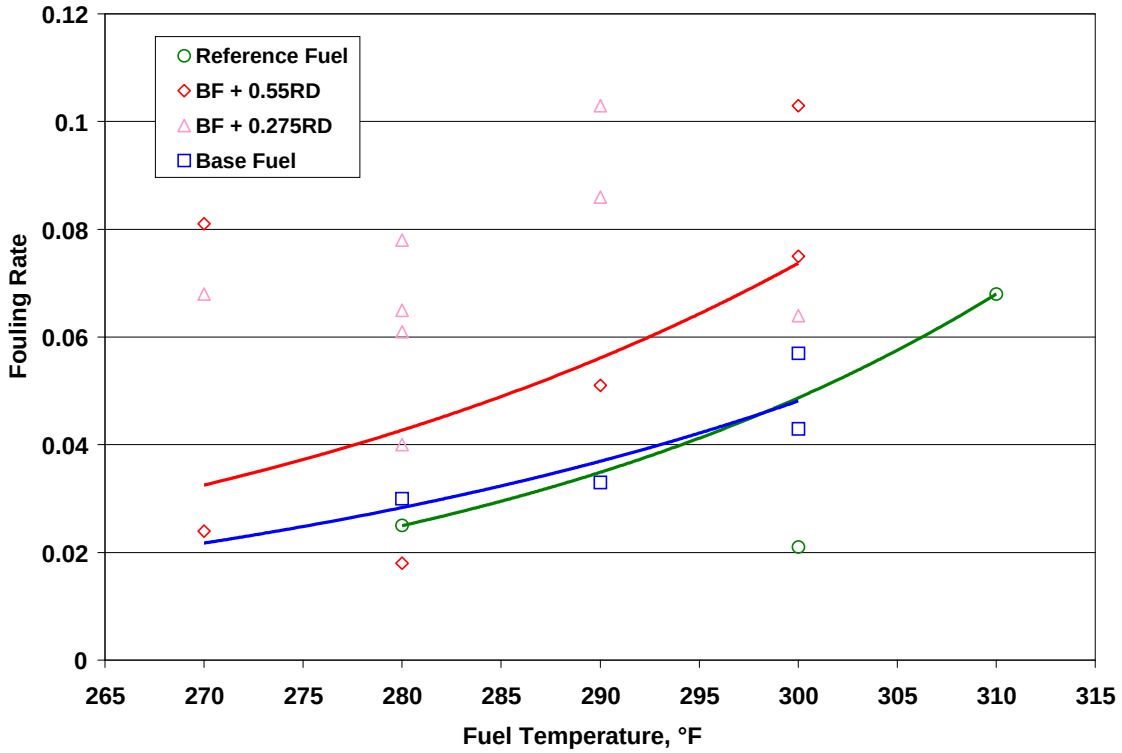

Figure H-1. Fouling Rate Summary

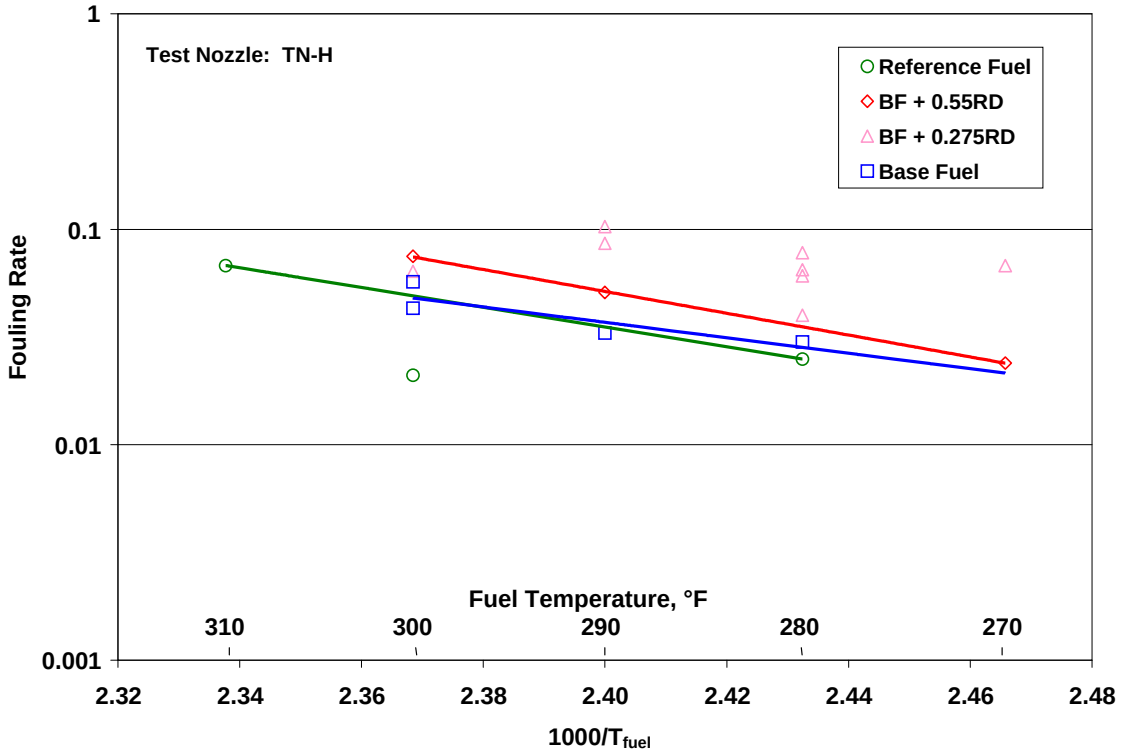

Figure H-2. Arrhenius Fouling Rate Summary

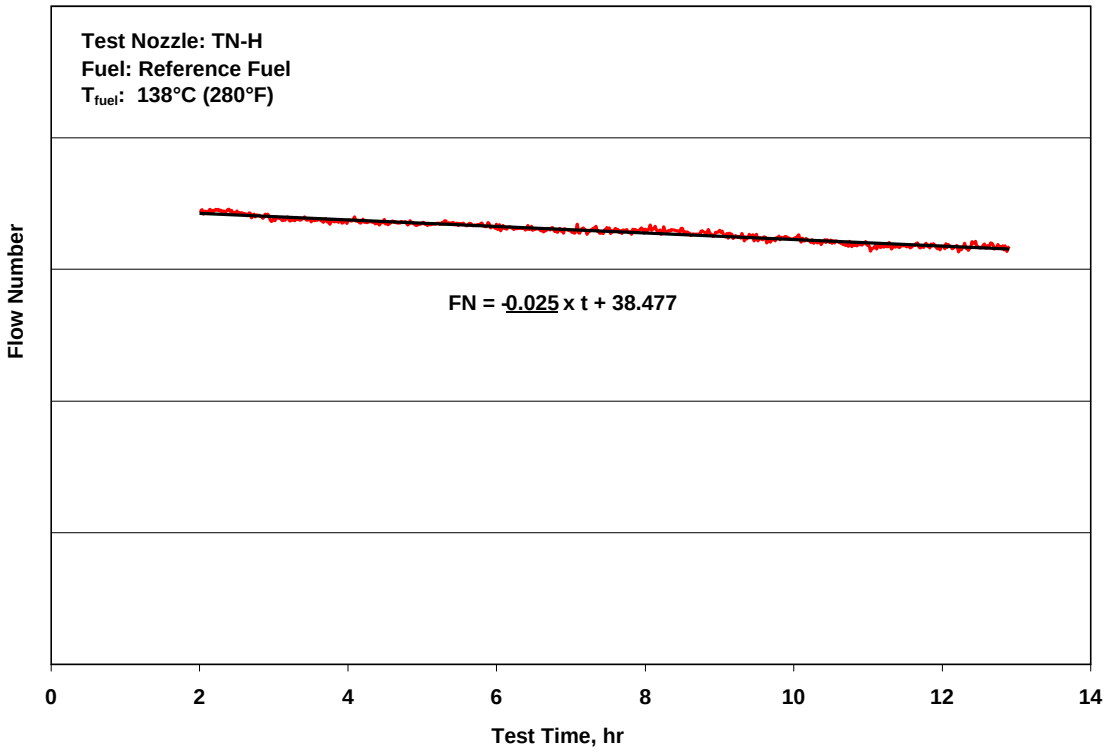

Figure H-3. Fouling Rate on Reference Fuel at T_{fuel} = 138°C (280°F)

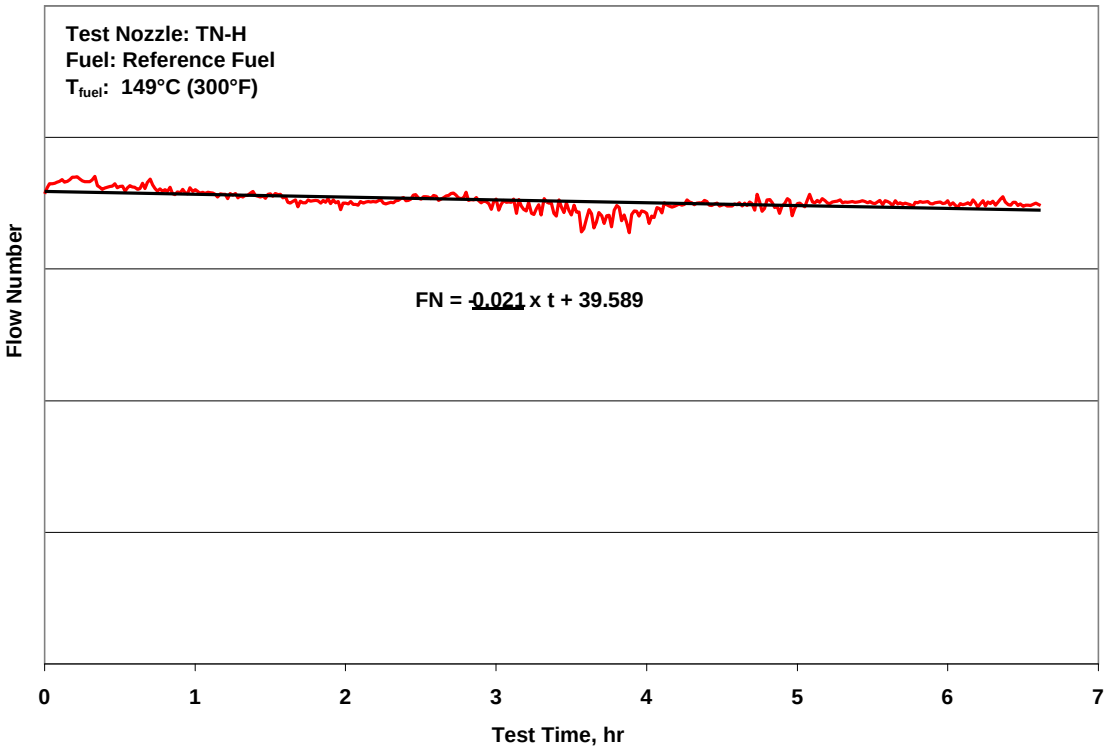

Figure H-4. Fouling Rate on Reference Fuel at T_{fuel} = 149°C (300°F)

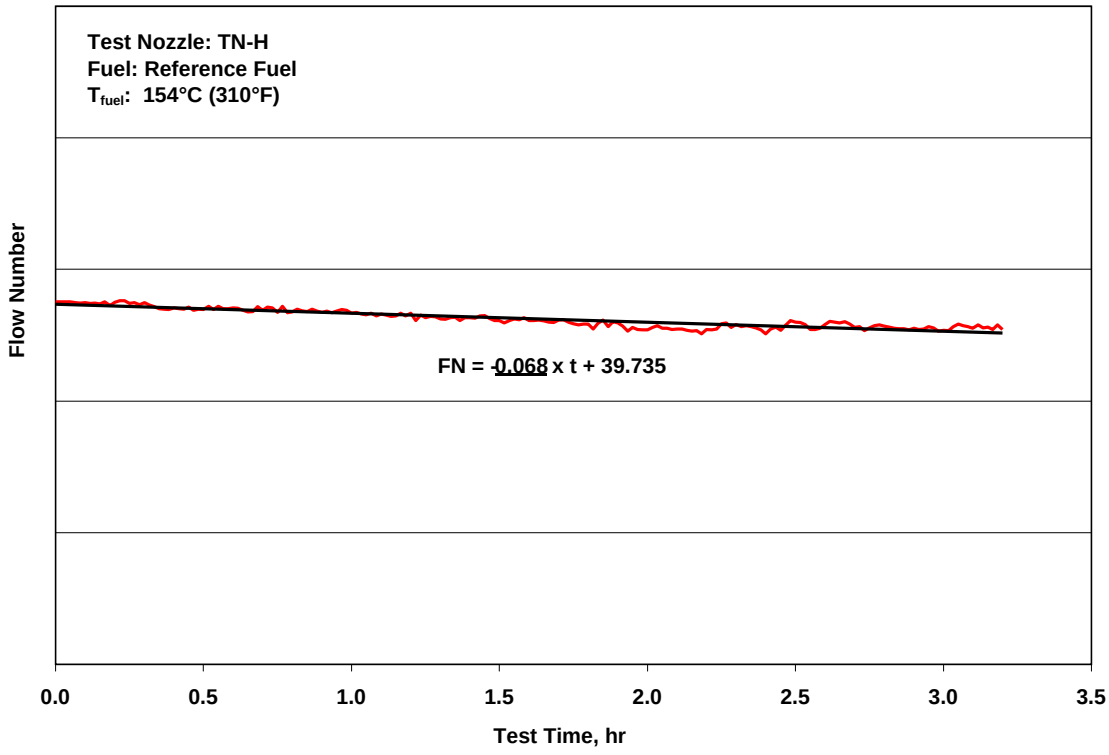

Figure H-5. Fouling Rate on Reference Fuel at T_{fuel} = 154°C (310°F)

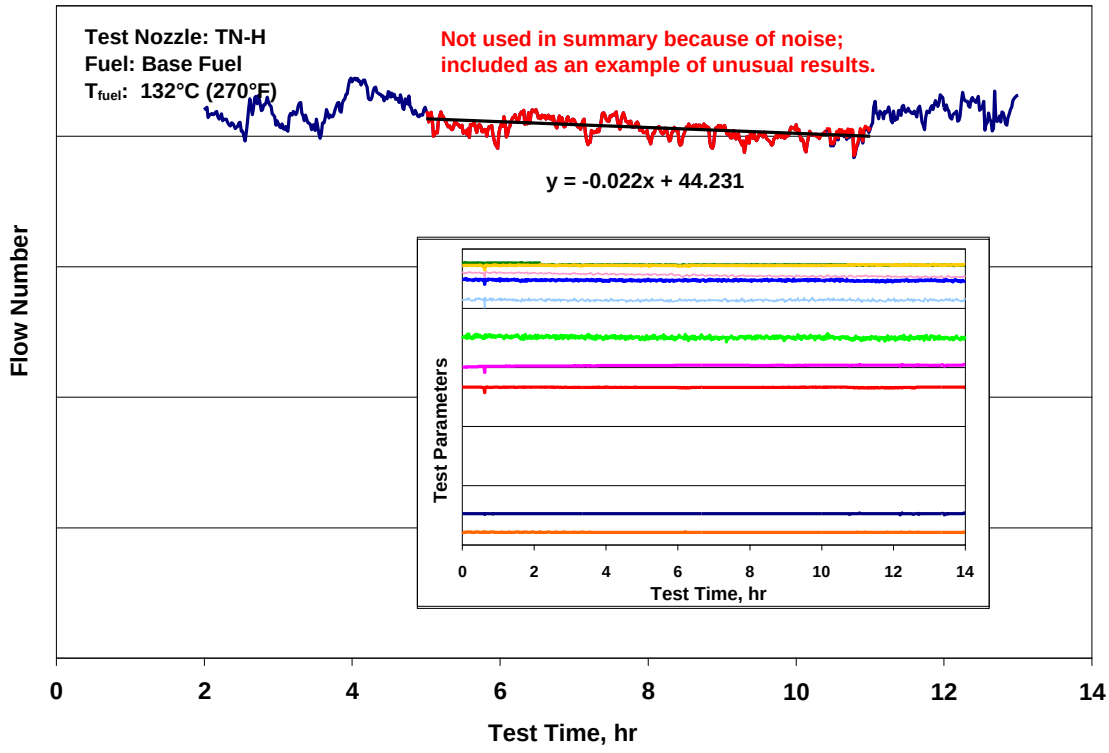

Figure H-6. Fouling Rate on Base Fuel at T_{fuel} = 132°C (270°F)

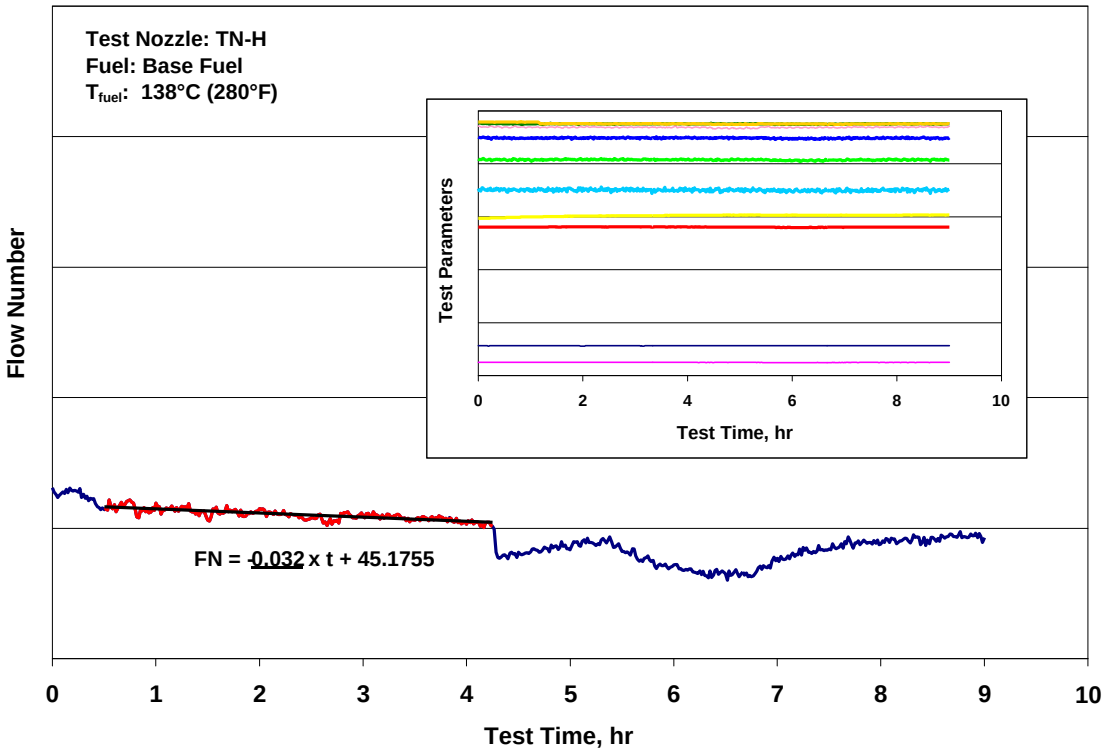

Figure H-7. Fouling Rate on Base Fuel at T_{fuel} = 138°C (280°F)

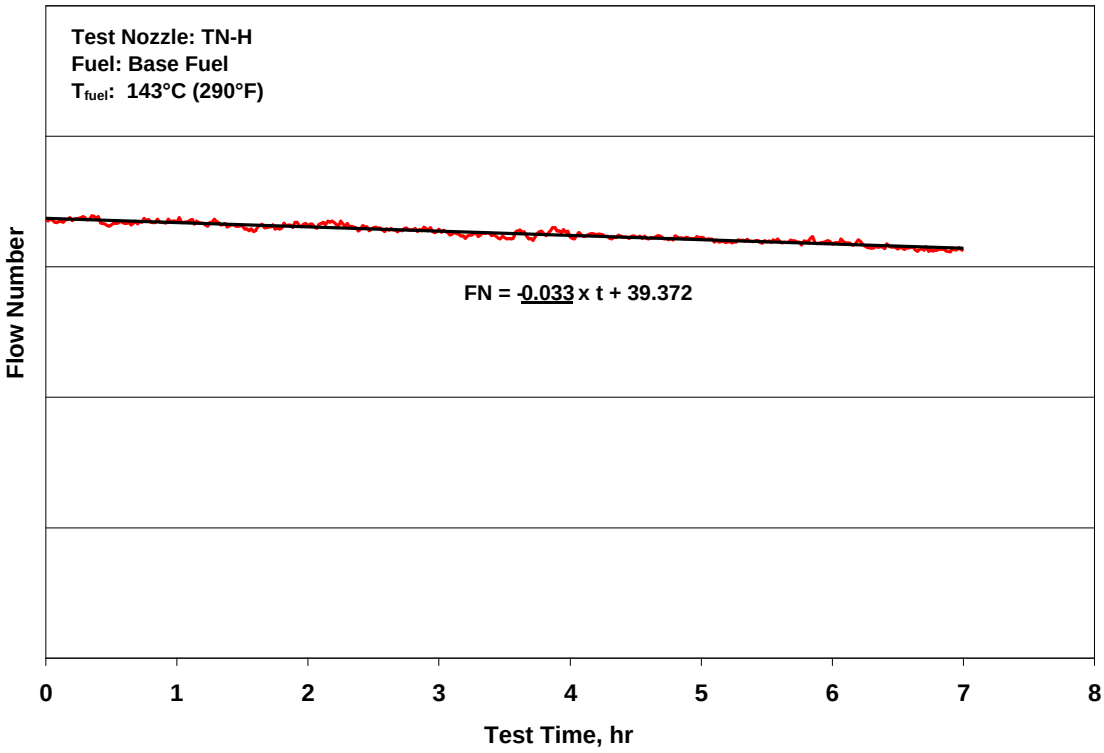

Figure H-8. Fouling Rate on Base Fuel at T_{fuel} = 143°C (290°F)

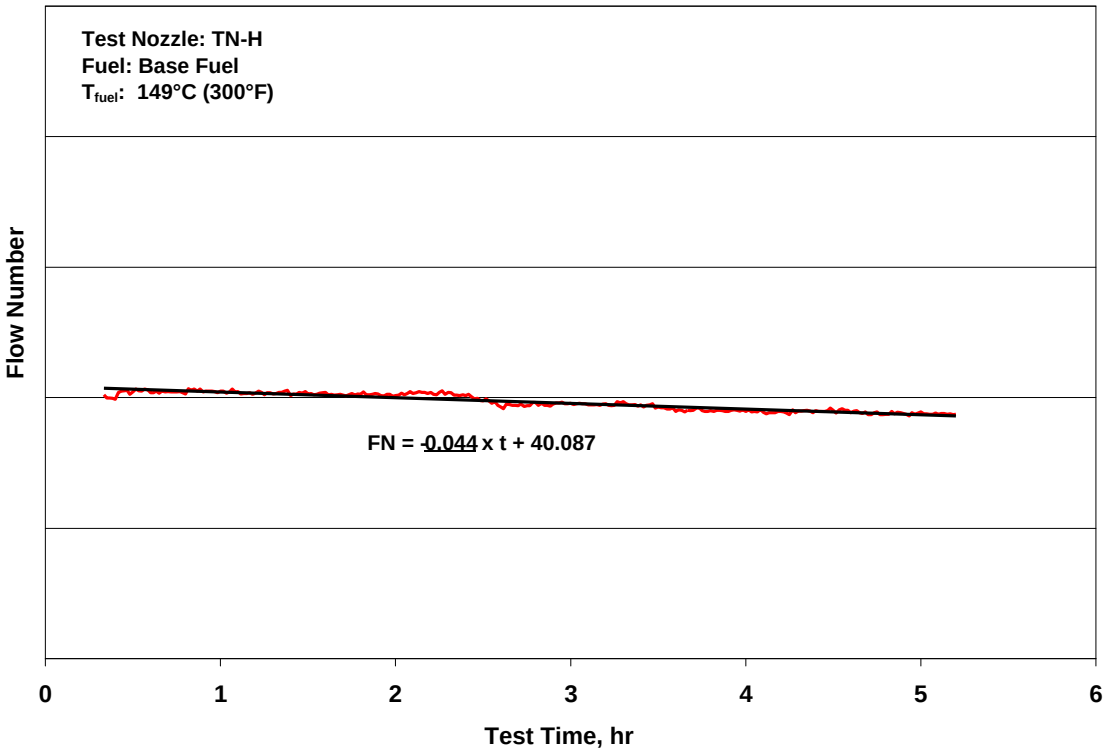

Figure H-9. Fouling Rate on Base Fuel at T_{fuel} = 149°C (300°F)

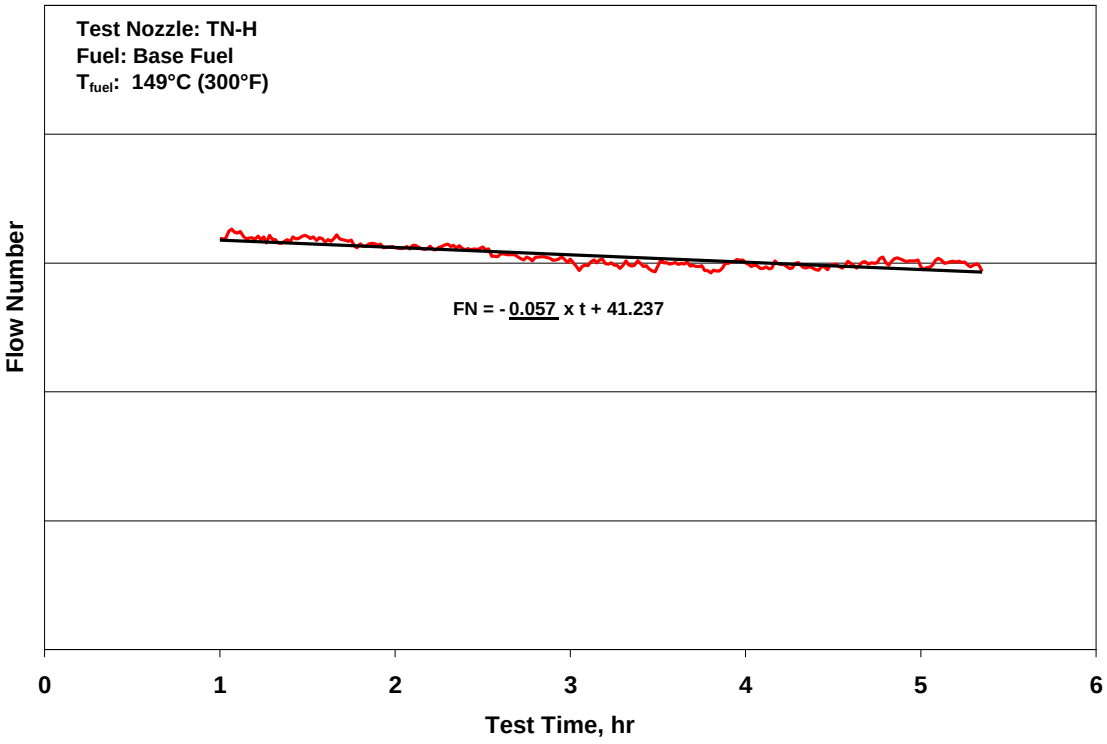

H-10. Fouling Rate on Base Fuel at T_{fuel} = 149°C (300°F) (repeat)

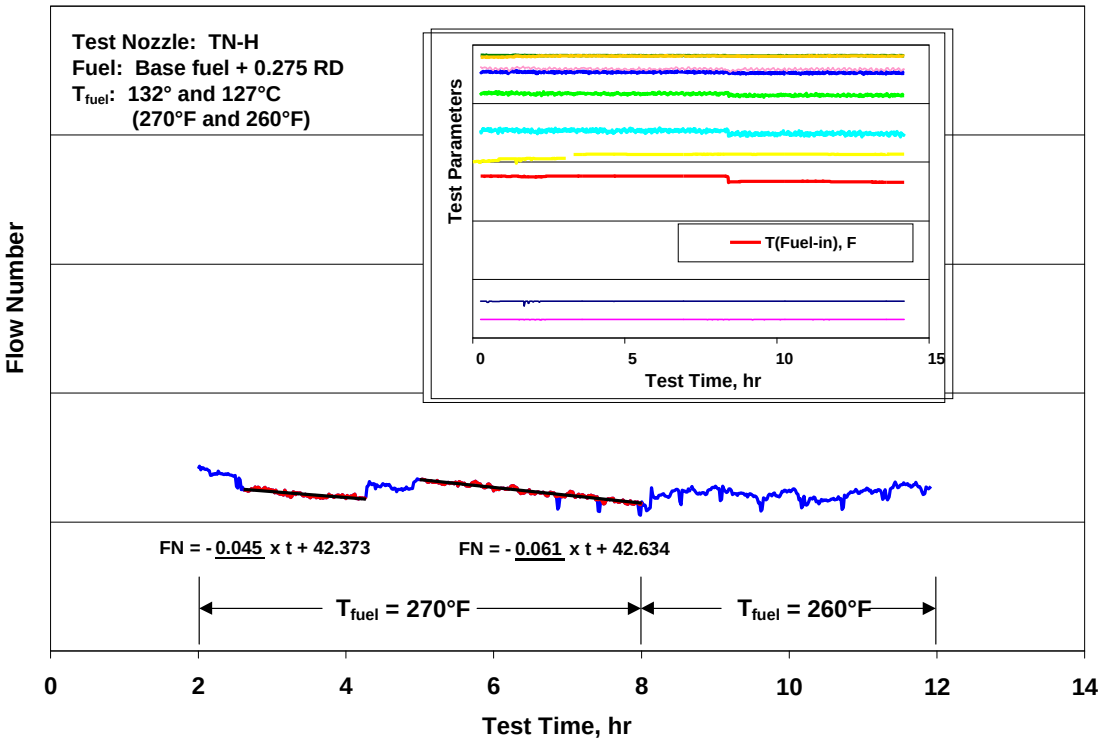

Figure H-11. Fouling Rate on Base Fuel + 0.275 mg/L of Red Dye at T_{fuel} = 132° and 127°C (270° and 260°F)

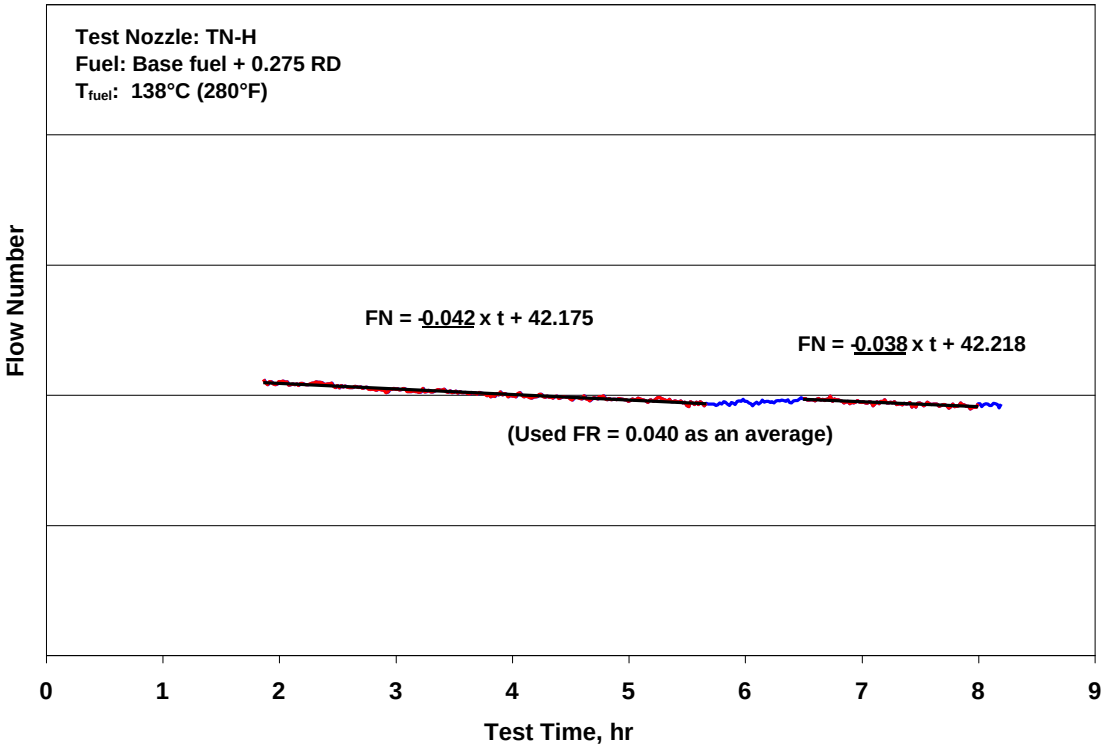

Figure H-12. Fouling Rate on Base Fuel + 0.275 mg/L of Red Dye at T_{fuel} = 138°C (280°F)

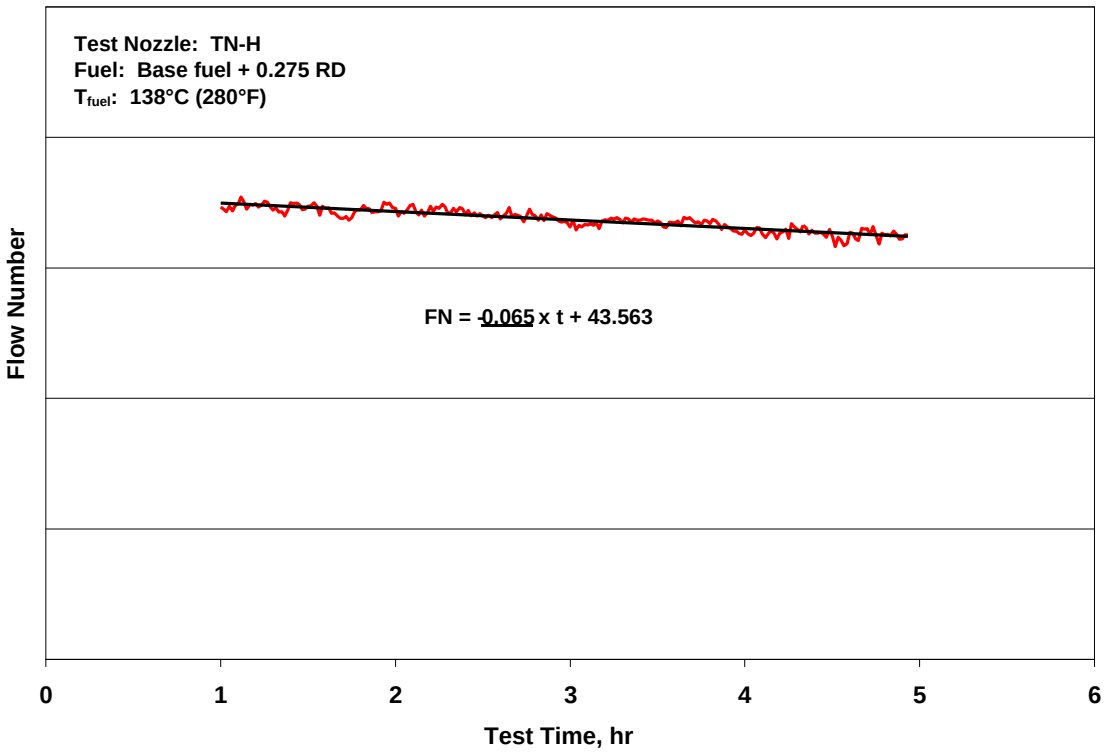

Figure H-13. Fouling Rate on Base Fuel + 0.275 mg/L of Red Dye at T_{fuel} = 138°C (280°F) (repeat)

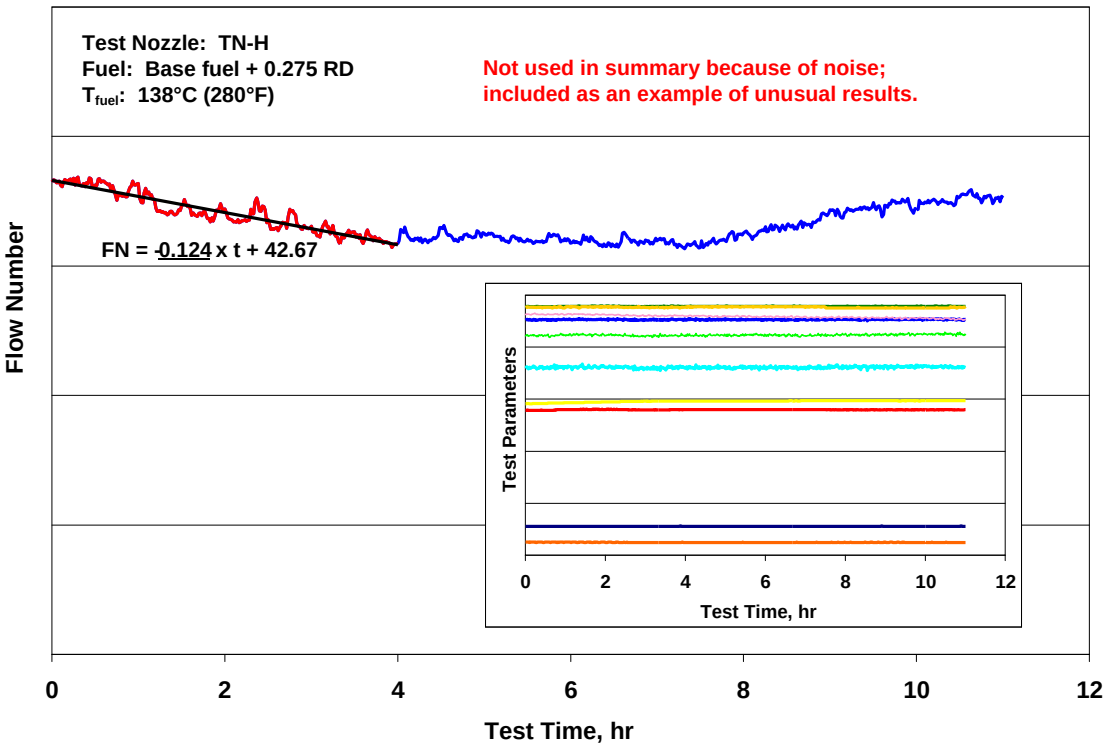

Figure H-14. Fouling Rate on Base Fuel + 0.275 mg/L of Red Dye at T_{fuel} = 138°C (280°F) (Not used)

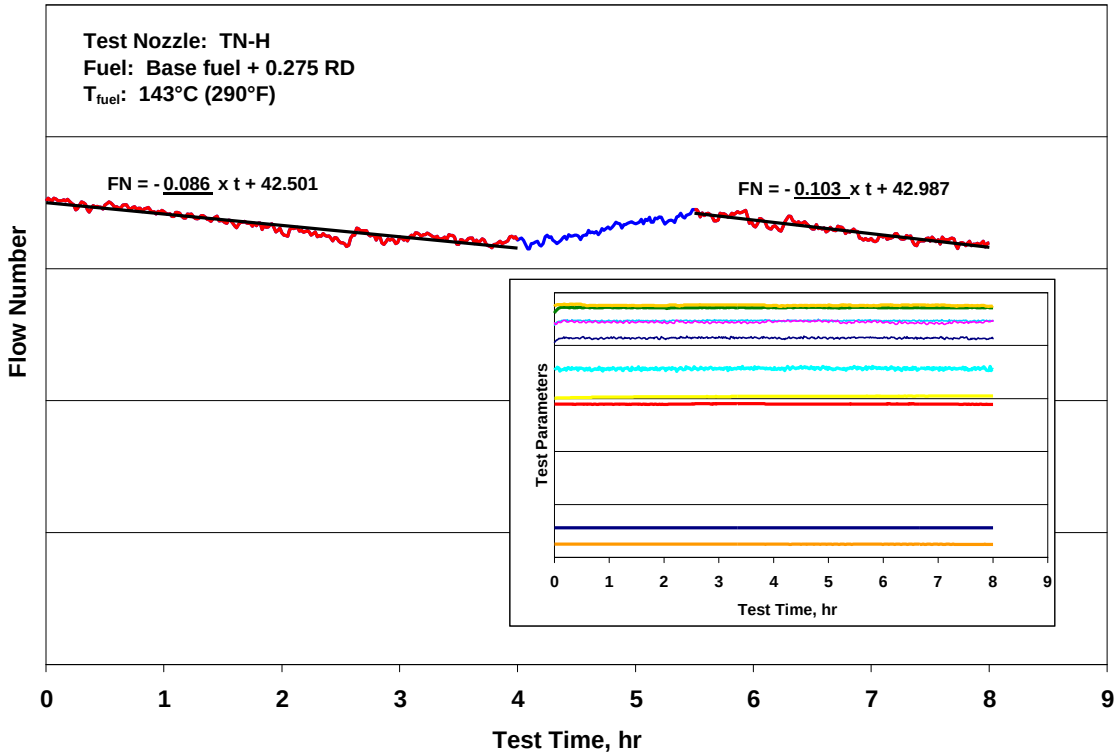

Figure H-15. Fouling Rate on Base Fuel + 0.275 mg/L of Red Dye at T_{fuel} = 143°C (290°F)

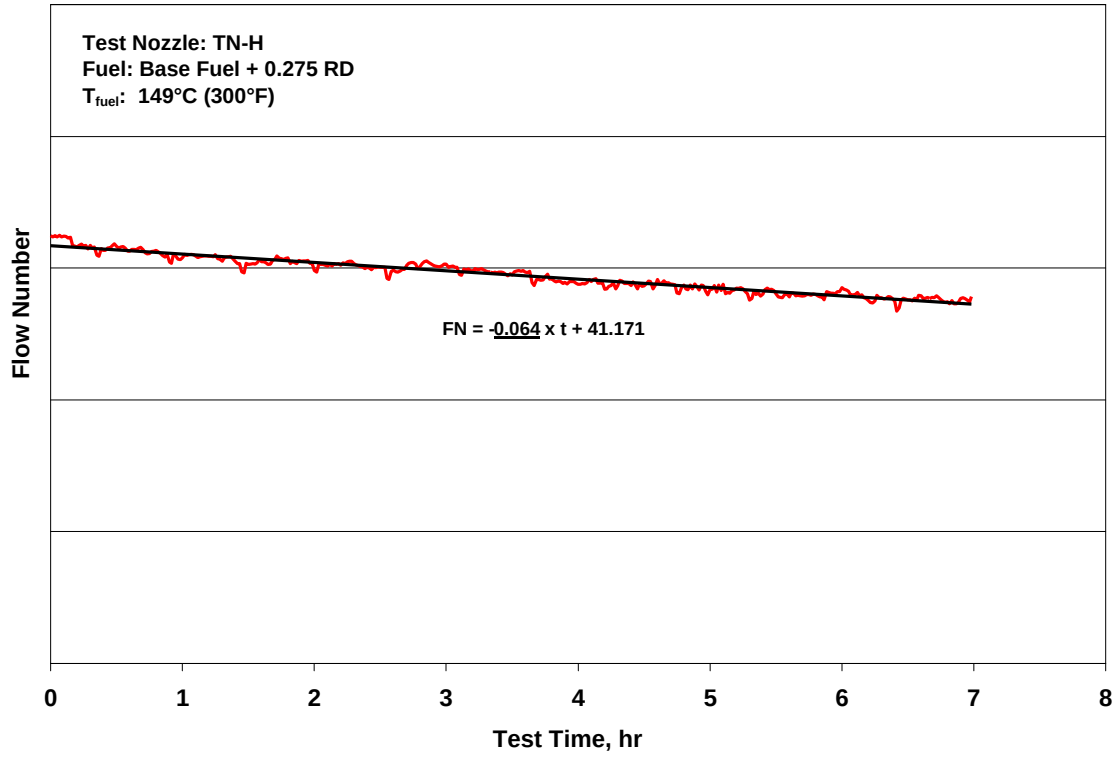

Figure H-16. Fouling Rate on Base Fuel + 0.275 mg/L of Red Dye at T_{fuel} = 149°C (300°F)

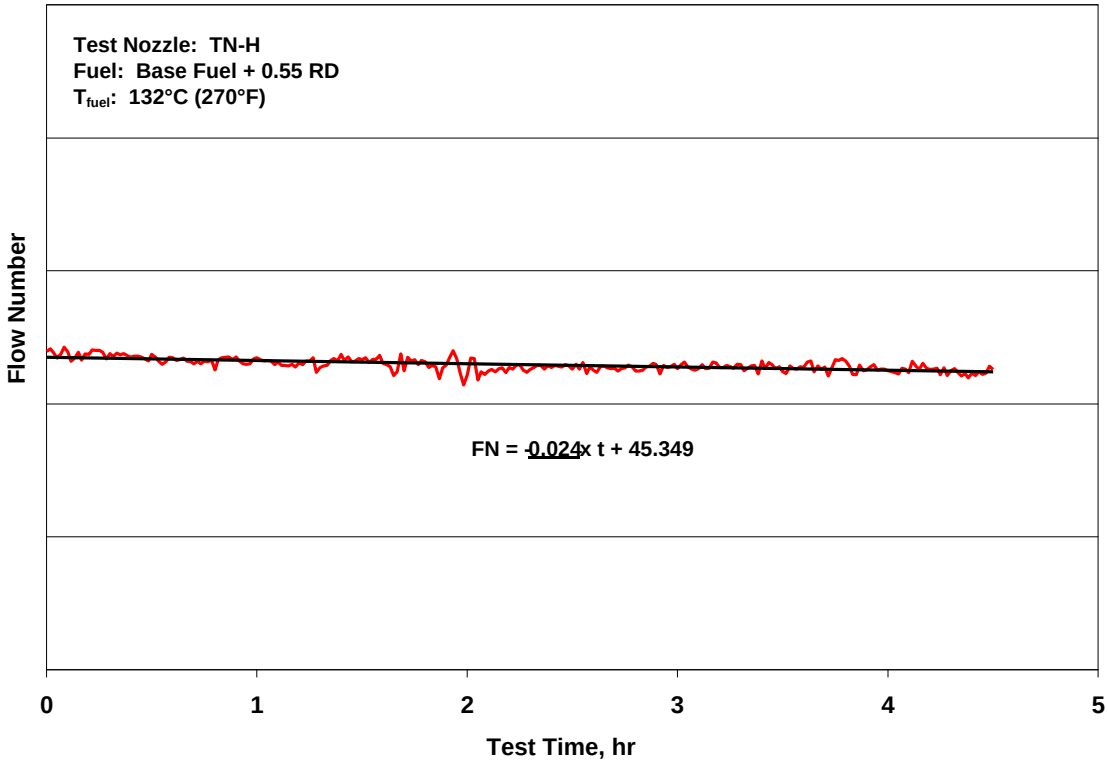

Figure H-17. Fouling Rate on Base Fuel + 0.55 mg/L of Red Dye at T_{fuel} = 132°C (270°F)

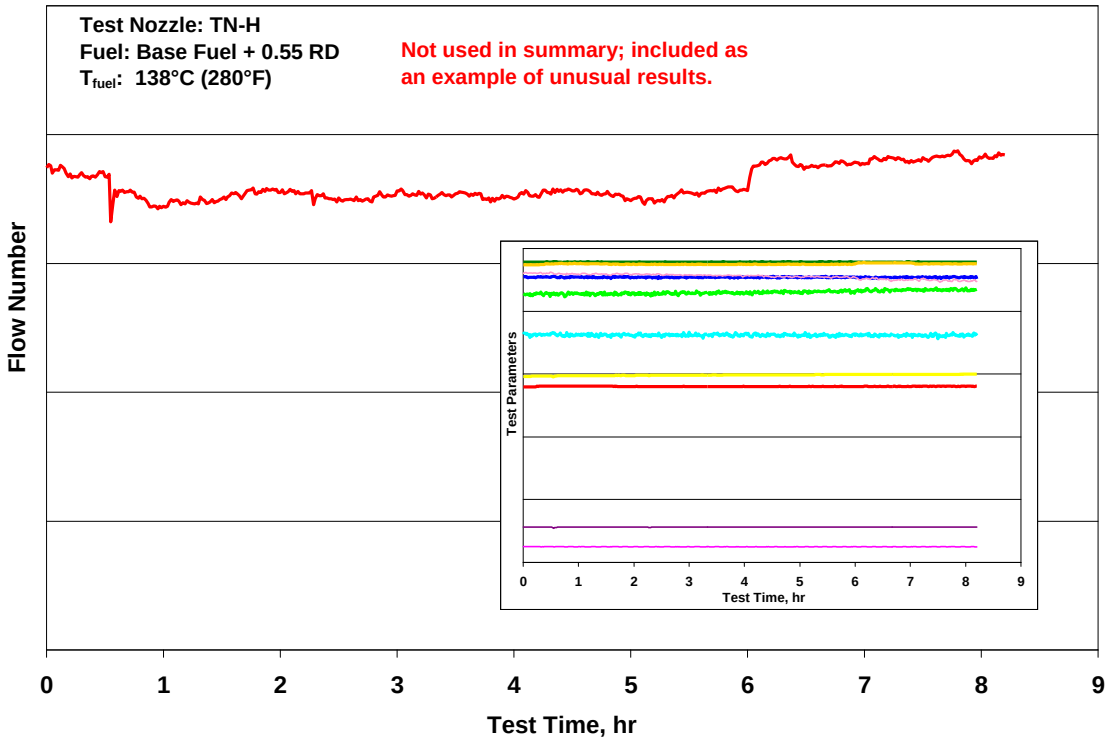

Figure H-18. Fouling Rate on Base Fuel + 0.55 mg/L of Red Dye at T_{fuel} = 138°C (280°F)

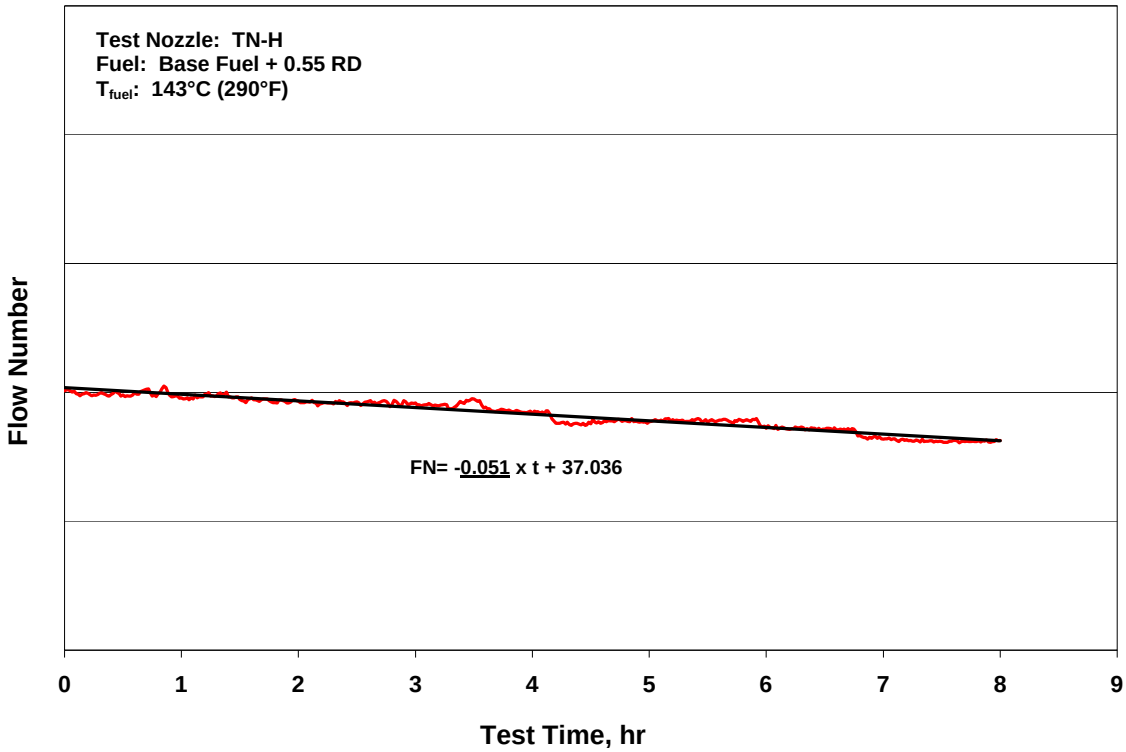

Figure H-19. Fouling Rate on Base Fuel + 0.55 mg/L of Red Dye at T_{fuel} = 143°C (290°F)

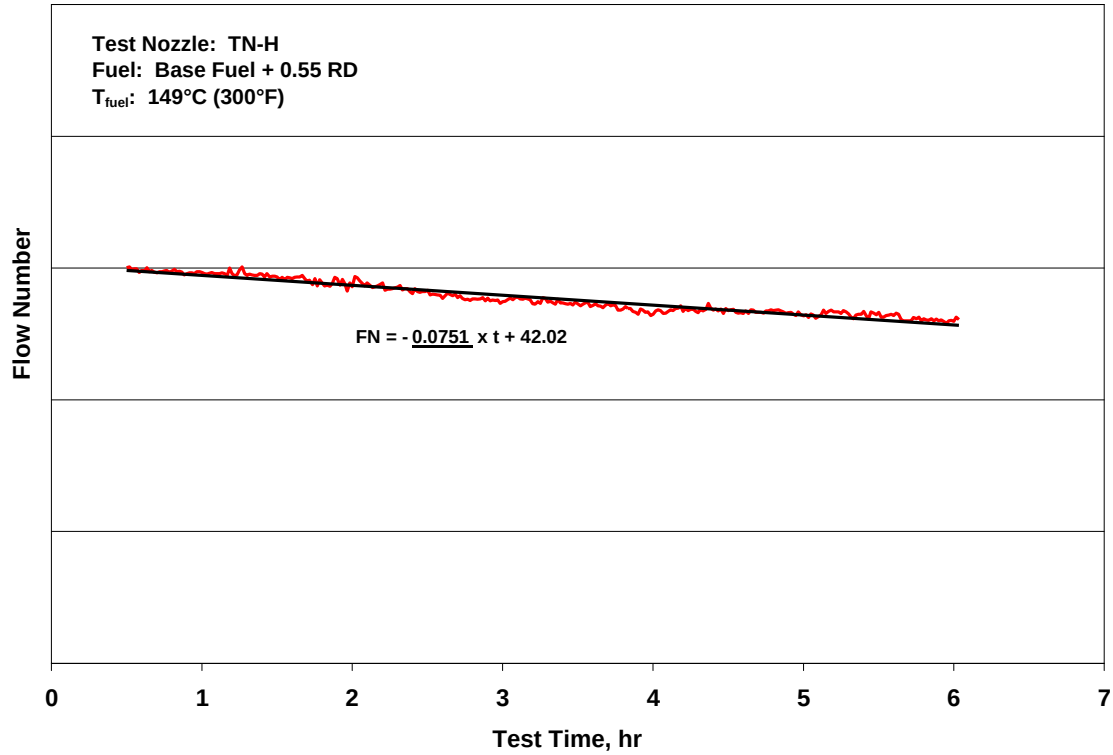

Figure H-20. Fouling Rate on Base Fuel + 0.55 mg/L of Red Dye at T_{fuel} = 149°C (300°F)

APPENDIX I—EXPERIMENTAL RESULTS FOR TEST NOZZLE TN-I

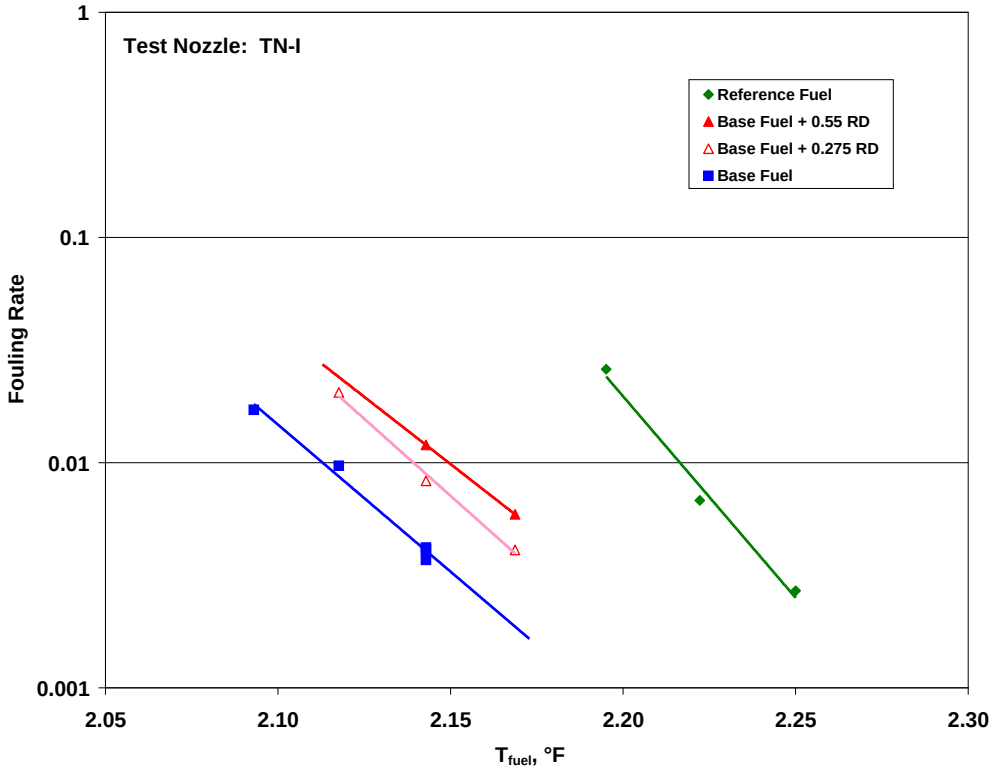

Figure I-1. Fouling Rate Summary for Test Nozzle TN-I

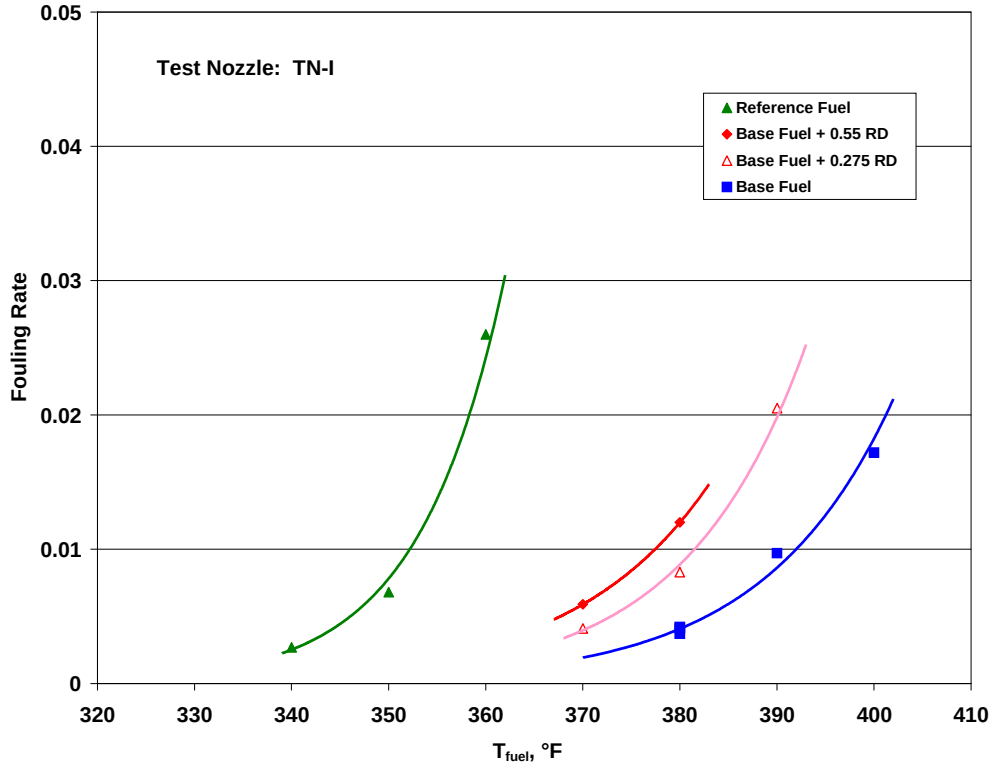

Figure I-2. Arrhenius Fouling Rate Summary for Test Nozzle TN-I

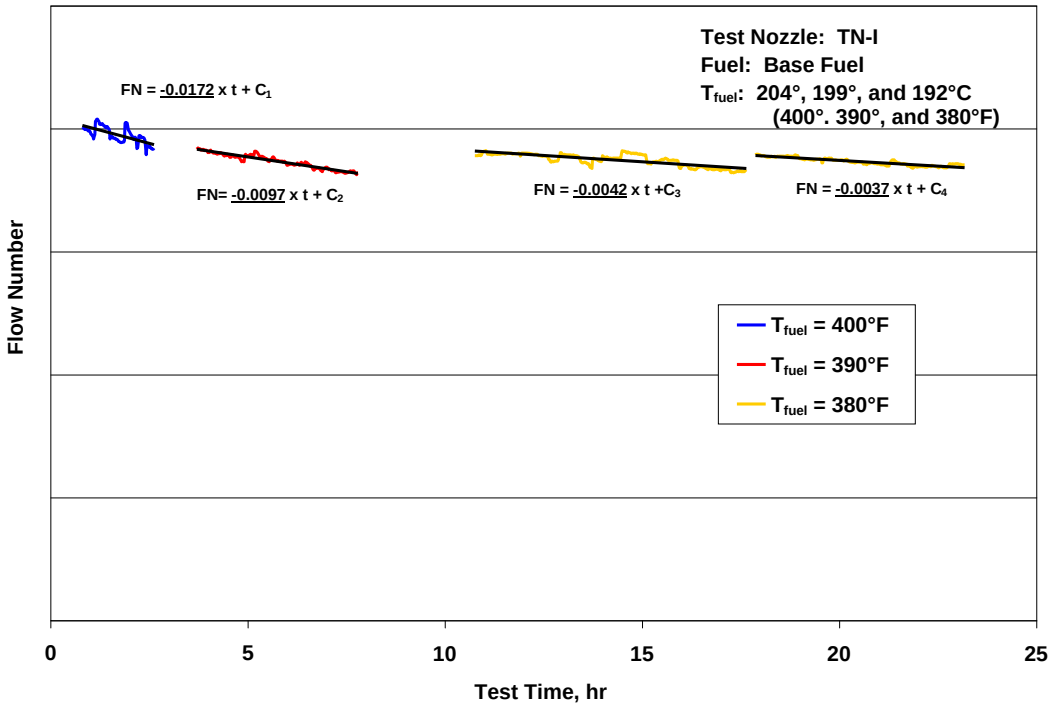

Figure I-3. Fouling Rate on Base Fuel at T_{fuel} = 204°, 199°, and 193°C (400°, 390°, and 380°F)

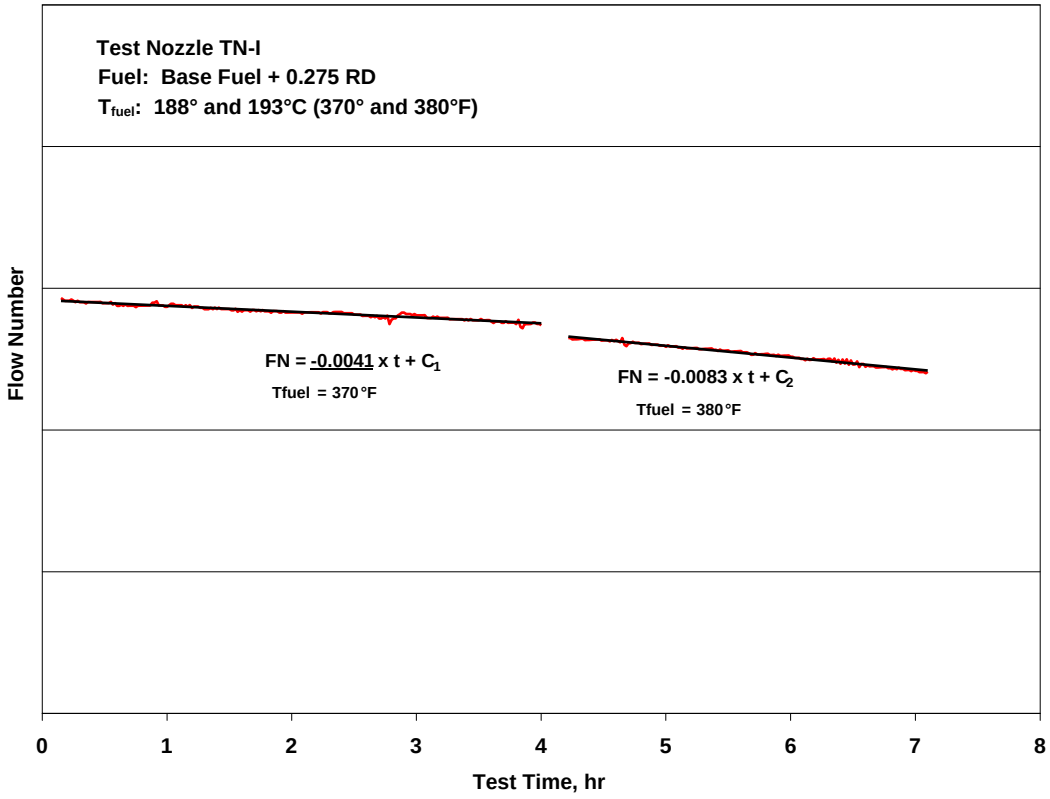

Figure I-4. Fouling Rate on Base Fuel + 0.275 mg/L of Red Dye at T_{fuel} = 188° and 193°C (370° and 380°F)

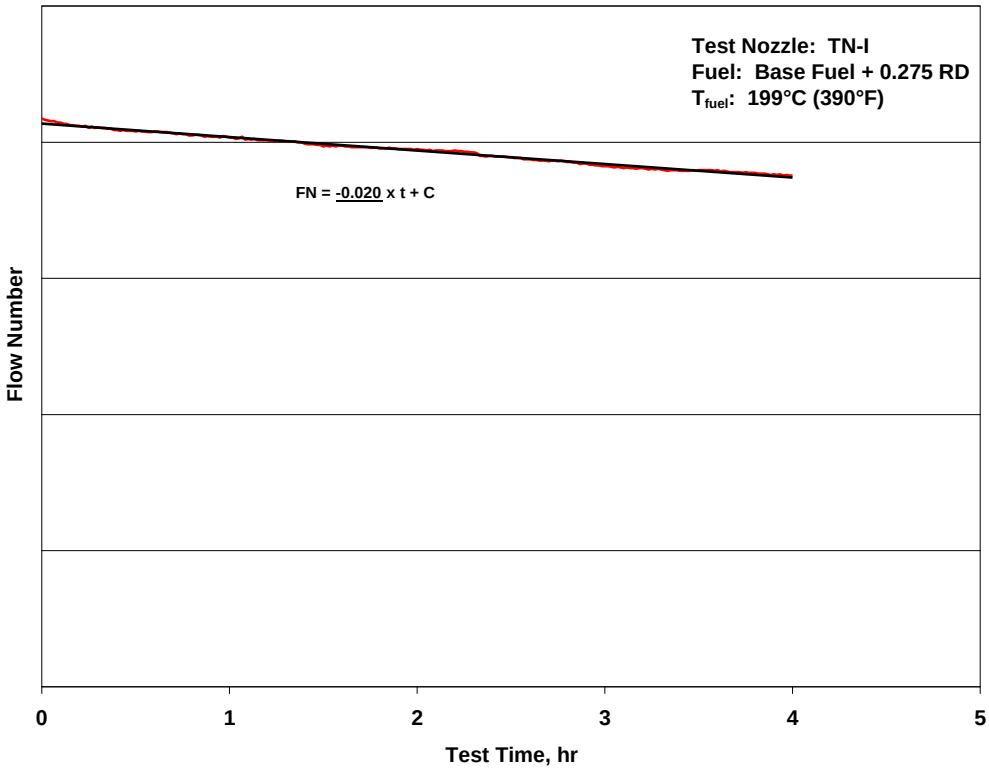

Figure I-5. Fouling Rate on Base Fuel + 0.275 mg/L of Red Dye at T_{fuel} = 199°C (390°F)

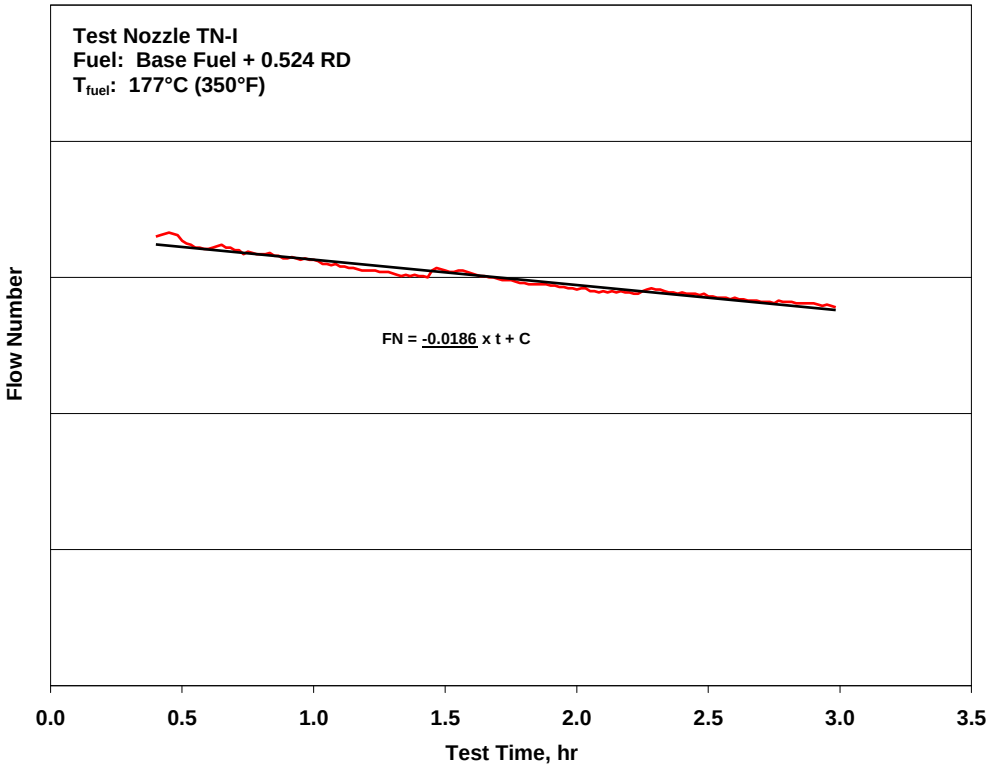

Figure I-6. Fouling Rate on Base Fuel + 0.524 mg/L of Red Dye at T_{fuel} = 177°C (350°F)

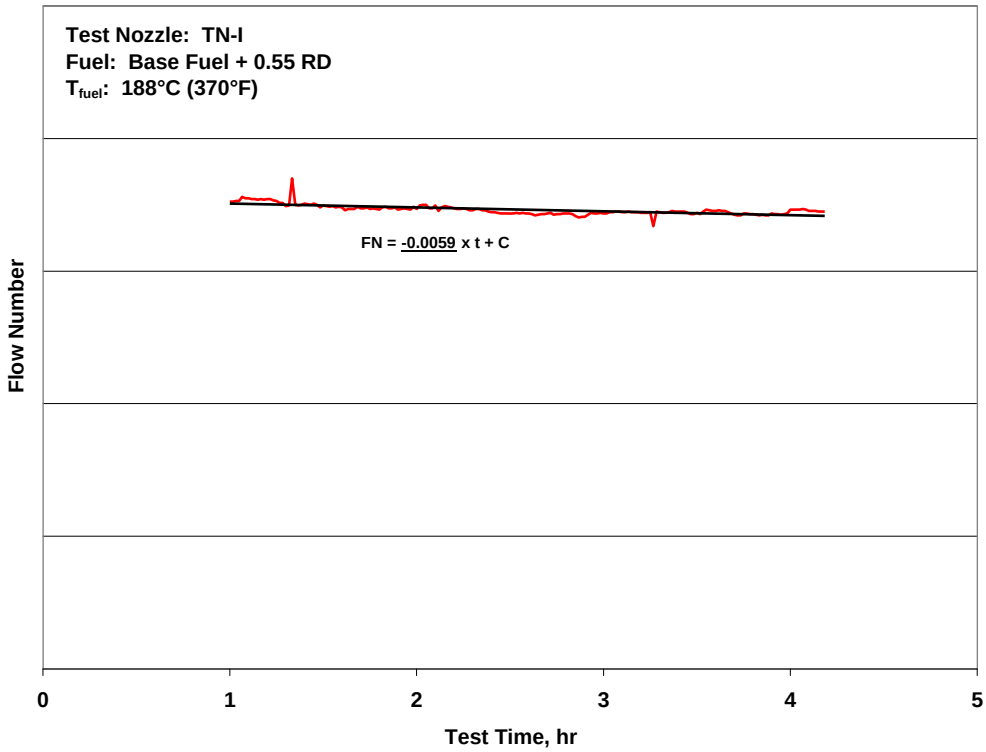

Figure I-7. Fouling Rate on Base Fuel + 0.55 mg/L of Red Dye at T_{fuel} = 188°C (370°F)

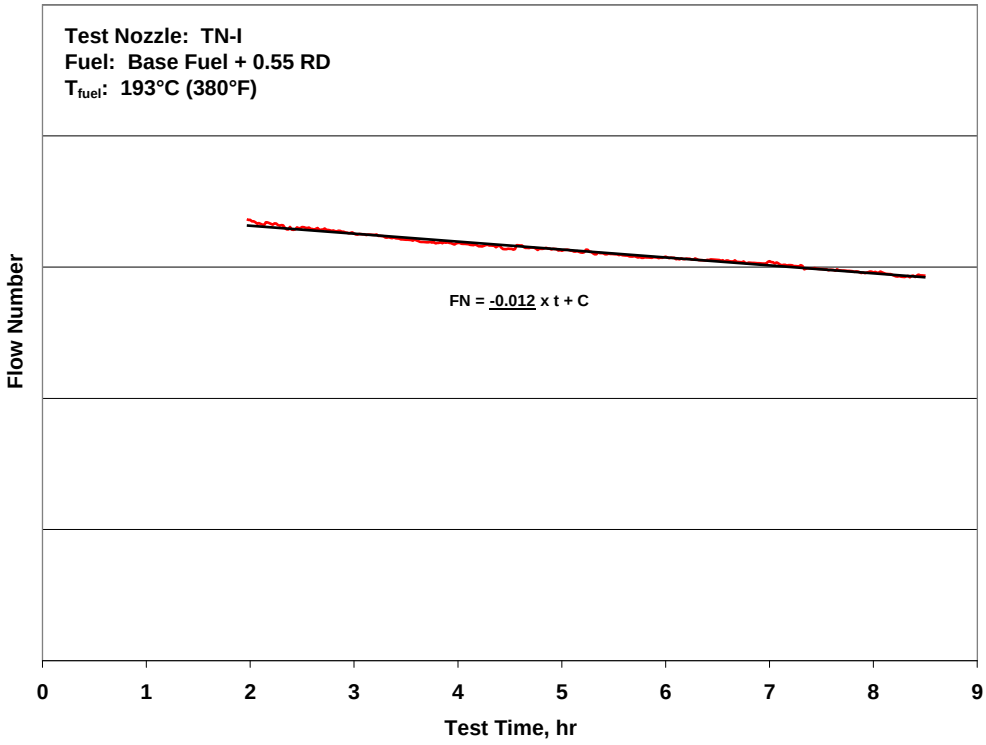

Figure I-8. Fouling Rate on Base Fuel + 0.55 mg/L of Red Dye at T_{fuel} = 193°C (380°F)

APPENDIX J—THERMAL STABILITY/RED-DYE PROGRAM PHASE 2: SUPPLEMENTAL TESTING

J.1 BACKGROUND.

Since 1994, the Internal Revenue Service of the United States has required that nontaxed diesel fuel, including home heating oil, be dyed with a strong red dye to clearly distinguish between taxable and nontaxable fuel to ensure that proper taxes are paid on diesel fuel used on the highways. Shortly thereafter, instances of pink jet fuel began to be reported at airports served by multiproduct pipelines in which the jet fuel had come in contact with the dyed diesel fuel, despite the great care that the pipeline companies take to prevent diesel fuel getting into the jet fuel from delivered to the airport.

Once the fuel was known to be contaminated, it was no longer acceptable as jet fuel and had to be downgraded. Because the pipelines only transport fuel in one direction, the fuel had to be transported via truck. Some of the known contaminations involved hundreds of thousands of gallons, e.g., one was on the order of 1.5 million gallons—very sizeable quantities to transport and downgrade.

A major concern was that contaminated fuel would somehow get into the hydrant system. If this were to happen, the airport would have to shutdown until the hydrant system was flushed. To avoid this, the airlines asked the engine and airframe companies for a level of contamination under which they would be allowed to fly unrestricted on the contaminated fuel. This would allow the airport to be "cleaned out" and avoid a shutdown. While offering some guidance, the airframe companies deferred to the engine companies for the technical solution.

A preliminary study conducted by the Aviation Fuels Committee of the Coordinating Research Council concluded that the primary effect of red-dye contamination was a reduction in the thermal stability of the fuel, as measured by the Jet Fuel Thermal Oxidation Tester (JFTOT). This was confirmed in an engine test conducted by General Electric. Unfortunately, it was not possible to actually quantify the effect of such a contamination on the fouling rates of hardware due to a lack of correlation between the JFTOT and other bench-scale deposition tests and actual fuel system hardware.

Southwest Research Institute® proposed an experimental study in which actual hardware would be placed in a thermal environment, simulating the conditions of engine installation. This approach was based on earlier work for the U.S. Navy to study fuel effects on fuel nozzle fouling rates.

As a result, an experimental study of the effect of diesel fuel red-dye contamination on the thermal stability of jet fuel was undertaken by the Federal Aviation Administration (FAA) with multiple sponsorship, including the U.S. Defense Energy Support Center, the Airline Transport

Association, the engine and airframe manufacturers, and the American Petroleum Institute. The program had two objectives:

- To quantify the effect of red-dye contamination on fuel thermal stability
- To identify and validate a methodology for evaluating thermal stability issues

Figure J-1 presents the final results of that study, showing that small concentrations of red dye can have a significant effect on the fouling rates of representative fuel nozzles from the various engine manufacturers. Also shown is that various fuel nozzles have different sensitivities to the presence of red dye.

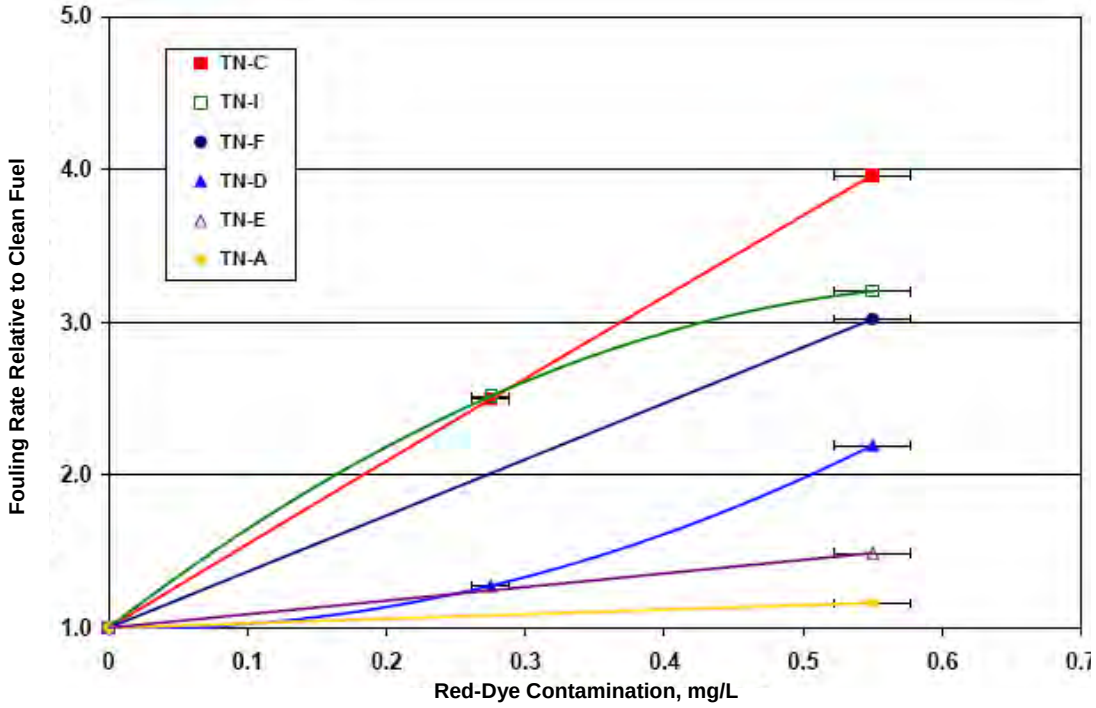

Figure J-1. Effect of Red-Dye Concentration on Fouling Rate of Fuel Nozzle TN-C

These results were well received by the original equipment manufacturers (OEM), but the increases in fouling rates were considered to be much higher than could be allowed. The OEMs were not sure whether the results could be extrapolated to lower concentrations, and they requested further testing to evaluate lower concentrations in hopes of finding a concentration below which there was no measurable effect.

In the meantime, two other potential fuel contaminants have become important to the airline industry through potential contact with diesel fuel:

- Diesel lubricity additives (DLA) are now required in ultra-low sulfur diesel fuel.

- Fatty-acid methyl esters (FAME) are being considered for use in biodiesel fuels under pressure by environmentalists.

This appendix summarizes the results of the fouling tests on a contamination of red dye that is just above the visible limit. In addition, the results of limited nozzle fouling tests with contaminations of two different DLAs and two different FAMEs are reported. Recommendations are provided based on the results of both series of tests.

J.2 OBJECTIVE.

The primary objective of this effort was to determine if the linear relationship between red-dye concentration and the increase in the fouling rate found in the earlier study of fuel nozzles remained valid at lower concentrations of red dye.

A second objective was to provide preliminary data on the effect of the presence of either a DLA or FAME from a biodiesel as a contaminant to jet fuel during pipeline operation.

J.3 EXPERIMENTAL PROGRAM.

J.3.1 EXPERIMENTAL.

All tests were conducted with a single fuel nozzle design at three fuel temperatures. These temperatures were the same temperatures used with this nozzle type in the earlier test program. The test protocol and the methodology of data analysis were exactly as described in the main body of this report.

J.3.2 TEST NOZZLE.

The test nozzle used in this study was TN-C, as described in the main body of this report. (The fuel nozzles were coded for proprietary reasons.) This fuel nozzle was chosen because it experienced the greatest increase in fouling rate due to red-dye contamination, as was shown in figure J-1.

J.3.3 TEST FUELS.

J.3.3.1 Base Fuel.

A new volume of base fuel was procured from the Defense Energy Support Center with the understanding that it came from the same refinery as the base fuel used in the original tests performed from 2001 to 2002. The primary concerns were that the fuel had the same thermal stability characteristics as the original fuel, and it was degraded by the presence of red dye.

The JFTOT breakpoint temperature of the new fuel was found to be 5°C higher than the original fuel. This was considered acceptable since the accuracy of the breakpoint temperature determination is considered to be no better than 5°C.

When red dye was added at the level of 0.55 mg/L, the breakpoint temperature was reduced by 5°C compared to the reduction of 10°C with the original fuel; again, this was within the stated accuracy of the determination of breakpoint temperature. Moreover, the visual pattern of the

deposit was the same for the new fuel when contaminated with red dye as with the original fuel when contaminated. A unique deposit streak was present with both fuels when contaminated with red dye that was not present with the uncontaminated fuel.

Since the new fuel had about the same JFTOT breakpoint temperature and appeared to respond to red-dye contamination in a similar manner, it was concluded that the new fuel was as close to the original as could be expected and would be suitable for use as the base fuel to complete the testing with red dye.

J.3.3.2 Red-Dye Contamination.

The red-dye contamination level was 0.055 mg/L. This level is just above the visible limit for red-dye contamination and was suggested by the Program Advisory Committee (PAC).

J.3.3.3 Contamination With Diesel Fuel Additives.

Four contaminants were selected with concurrence of the PAC. Two were DLAs and two were FAMEs. For proprietary reasons, these will be referred to by number:

- DLA-1 and -2
- FAME-1 and -2

In each case, the two were chosen from a number of candidate materials based on their impact on the results of the JFTOT thermal stability test as determined by deposit thickness on the JFTOT tube. In each case, one of the two was found to have little effect on the deposit thickness, while the other was considered to have a significant effect on the deposit thickness. It was thought that this would give the engine manufacturers (OEM) an understanding of the possible range of effects of these two classes of additives.

The concentrations of these additives were 100 ppm at the request of the engine manufacturers. This concentration was selected because the OEMs are under pressure to permit 100 ppm of DLA and/or FAME in jet fuel in Europe. Pressure for similar levels in the U.S. market could be possible in the future.

J.4 RESULTS.

J.4.1 COMPARISON OF NOZZLE FOULING RATES ON BASE FUELS.

Figure J-2 compares the fouling rate of the new base fuel with the base fuel of the previous test program. The fouling rates are both well correlated by an exponential function, as expected. While the fouling rate of the new base fuel is lower, corresponding to the higher thermal stability (i.e., breakpoint temperature), the slopes appear to be significantly different. The reason for this is not known.

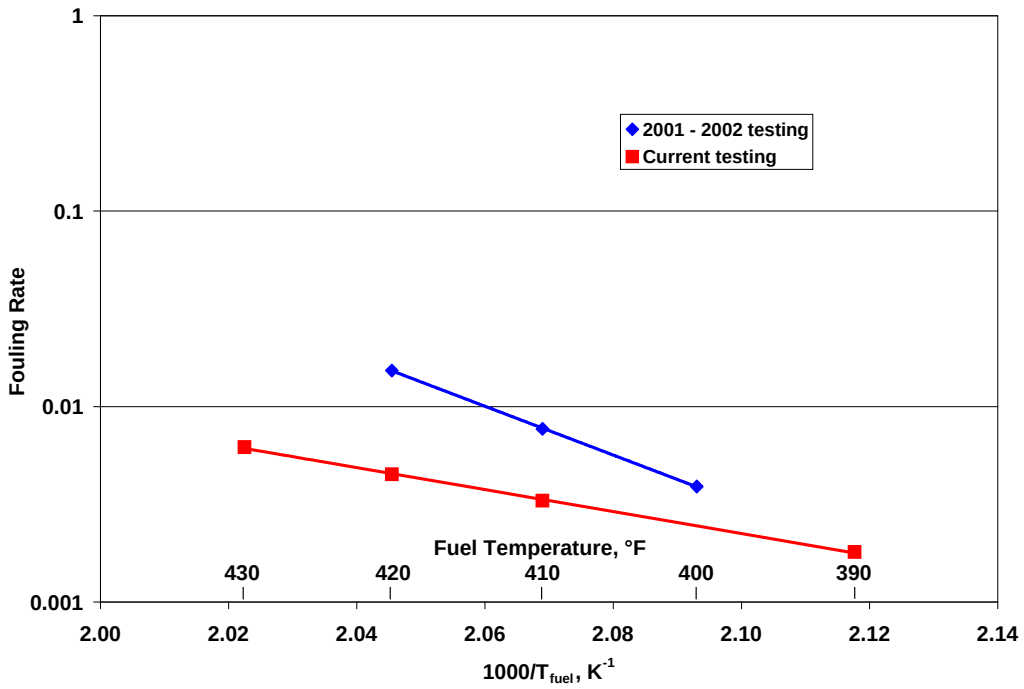

Figure J-2. Comparison of Fouling Characteristics of Base Fuels

This difference in the fouling characteristics of the two base fuels is not critical because the effect of red dye on the fouling rate is determined as a ratio of the fouling rate of the contaminated fuel to the fouling rate of the base fuel.

J.4.2 EFFECT OF RED-DYE CONTAMINATION.

Figure J-3 compares the fouling characteristics of the base fuel contaminated with 0.055 mg/L of red dye with that of the uncontaminated fuel. For comparison, figure J-4 is a similar graph from the original program showing the effect of the contamination level on fouling rate. The value for the concentration of 0.14 mg/L is taken from a supplementary test funded by one of the engine manufacturers with interest in getting preliminary data at a concentration lower than those of the original program.

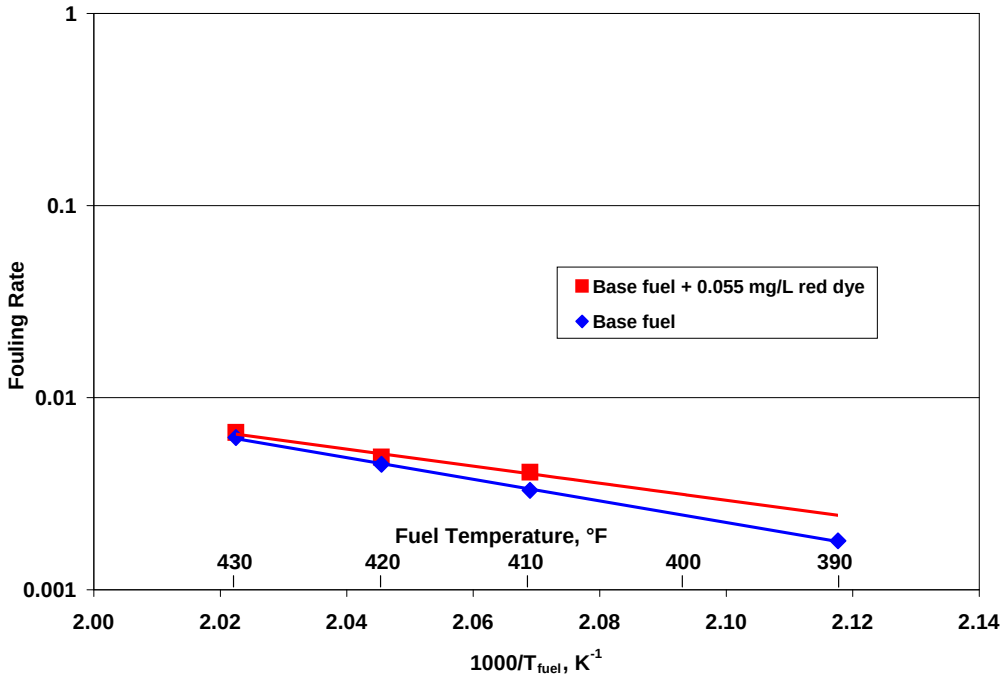

Figure J-3. Effect of 0.055 mg/L of Red Dye on Fouling Rate of TN-C Fuel Nozzle

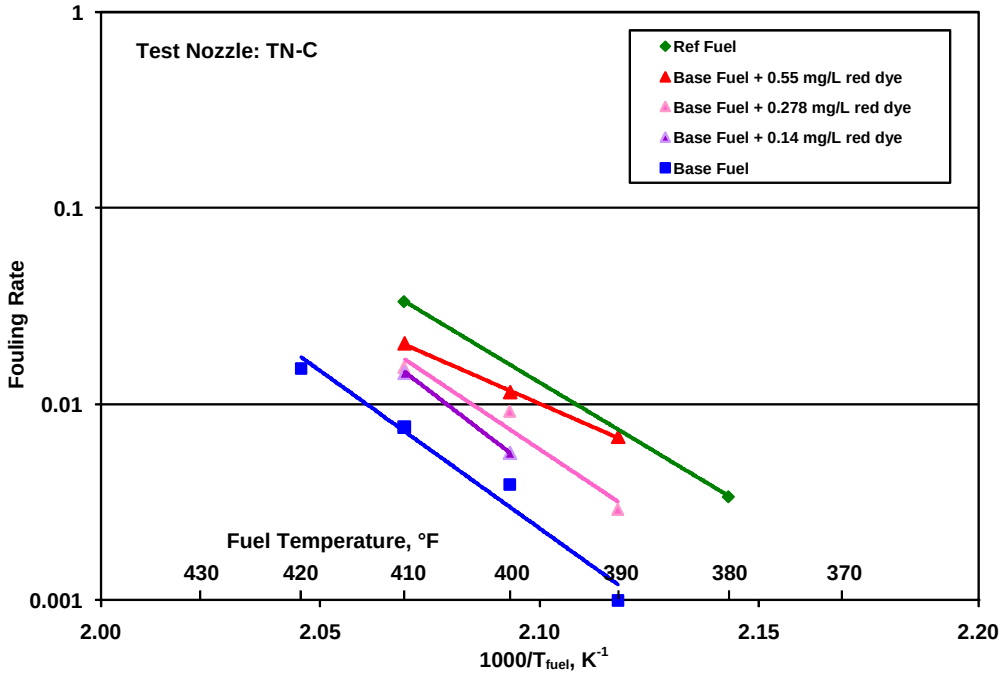

Figure J-4. Effect of Red-Dye Contamination on Fouling Rate of TN-C Fuel Nozzle

Figure J-5 summarizes the effect of red-dye concentration on relative fouling rate for the TN-C fuel nozzles at a fuel temperature of 400°F. The data for the concentrations of 0.55, 0.27, and 0.14 mg/L are taken from the data shown in figure J-4. The value at the concentration of

0.055 mg/L is from this research. In each case, the relative fouling rate is based on the base fuel used at that time.

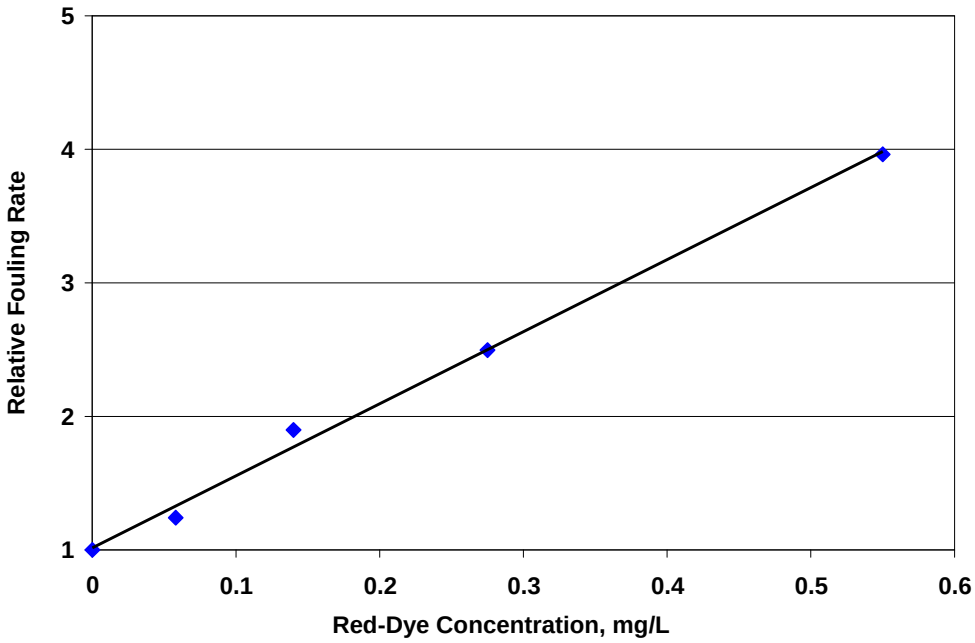

Figure J-5. Summary of Relative Effect of Red-Dye Contamination on TF-C Nozzles

Figure J-5 shows that the effect of red-dye contamination on fouling rate is linear over the range of concentrations tested, and that the current results follow the trend established by the earlier data.

J.4.3 EFFECT OF DLA AND FAME.

Figure J-6 summarizes the effects of the two DLAs on the fouling characteristics of the TN-C fuel nozzle. The fact that the slopes are different than the base fuel could indicate that a different chemical mechanism is controlling deposition, although it is not very different.

Figure J-7 presents a similar summary of the effect of the two FAME products on nozzle fouling. FAME-2 appears to have very little effect on the fouling rate of this nozzle over the range of temperatures tested. On the other hand, FAME-1 actually reduced the fouling rate over this temperature range.

Recalling that the concentration of DLA was 100 ppm, whereas the concentrations of red dye covered the range of about 0.055 to 0.55 ppm, the effect of DLA on the fouling rate was much less than the effect of red dye, while the effect of one of the FAME products appeared to have a very positive effect. The difference is not too surprising since DLA and FAME are surface-

active materials and could be establishing a protective coating that inhibits conventional thermal stability deposits.

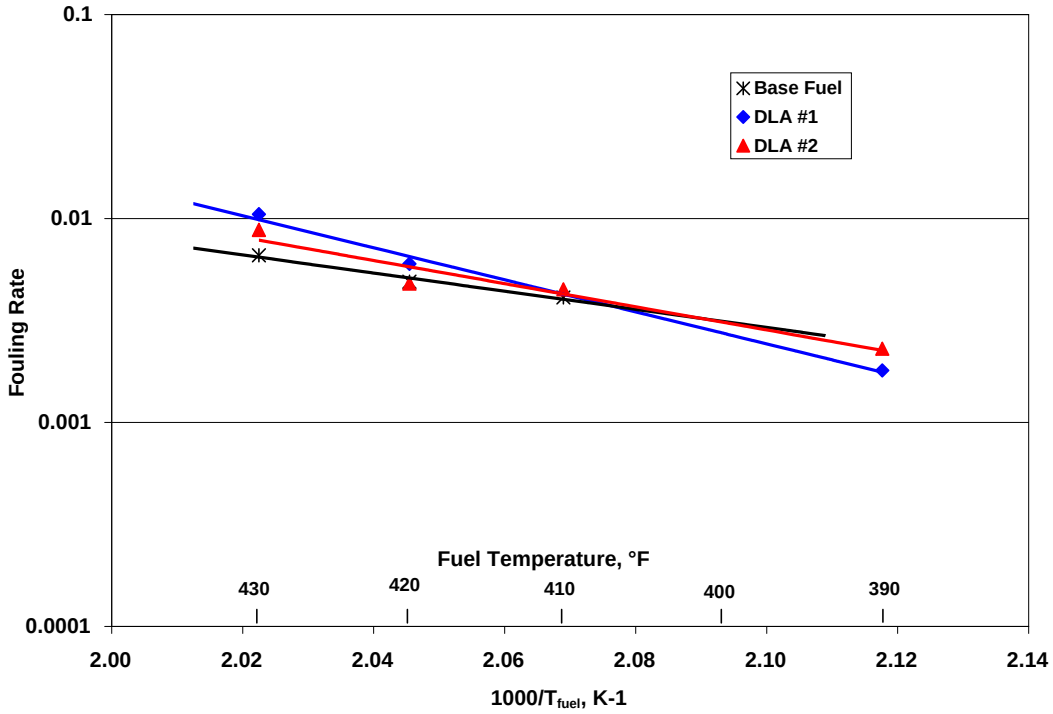

Figure J-6. Effect of Two DLAs at 100 ppm on Fuel Nozzle Fouling Rate

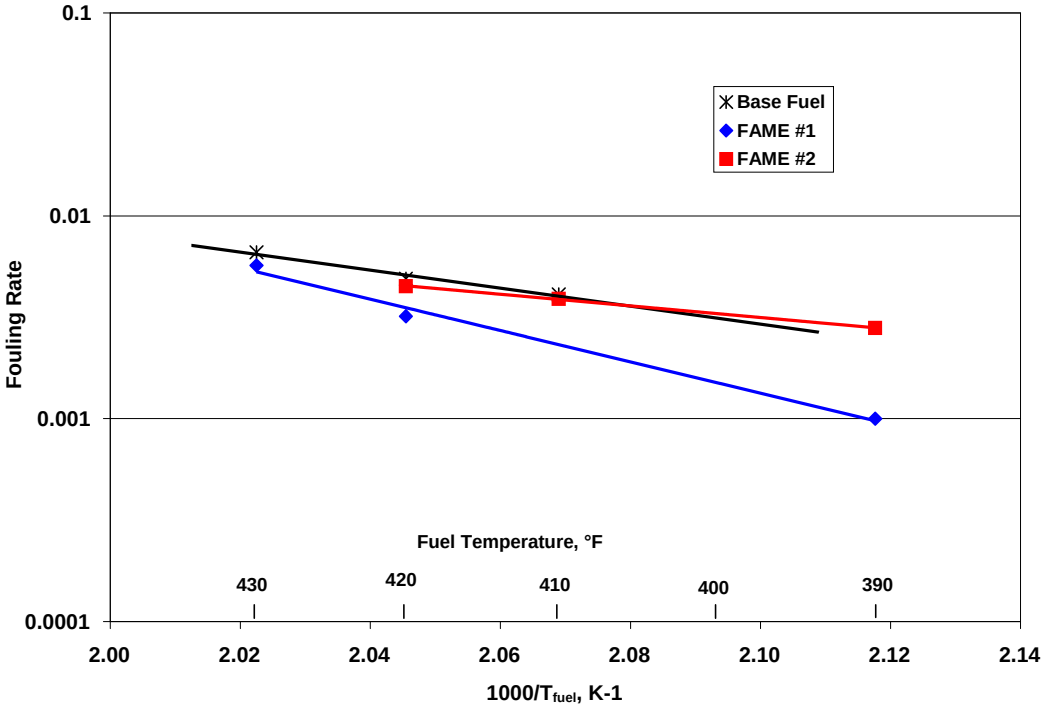

Figure J-7. Effect of two FAMEs at 100 ppm on Fuel Nozzle Fouling Rate

J.5 SUMMARY AND CONCLUSIONS.

In summary, the new data at red-dye concentrations of 0.055 and 0.14 mg/L confirm the linearity of the effect of red-dye contamination on the fouling rate of fuel nozzles found at higher concentrations in the earlier effort. The results and conclusions of the earlier effort are not changed by these new data.

The results on the effect of the diesel lubricity additives (DLA) and fatty-acid methyl esters (FAME) contaminations are to be considered preliminary, and no conclusions should be drawn. Over 100 tests have been conducted on the effects of red dye. As shown in figure J-1, the effects vary with different fuel nozzle types. This is the first data produced on the potential effects of DLA and FAME on fuel nozzle fouling. Also, there is effectively only one red dye, whereas there are several chemical types of DLA and several products of each type on the market. Furthermore, there are several different FAMEs available (e.g., from rape and soy).

Thus, not only is the chemistry involved in these additives and blending materials significantly different than the hydrocarbon chemistry of the fuel, there is a wide variety of chemistry involved within the various products marketed as DLA and for the various FAMEs available.

Further evaluations of the different DLA and FAME chemistries must be investigated with basic tests, such as the JFTOT as a screening tool, to be followed by a comprehensive evaluation with fuel nozzle fouling tests.

J.6 RECOMMENDATIONS.

It is recommended that the engine manufacturers use the new data provided on the effect of red-dye concentration fouling rates to develop an industry consensus on the minimum acceptable level of red-dye contamination in jet fuel.

It is recommended that further tests be conducted on several candidate chemistries of both DLA and FAME in one or more fuel nozzles that allow fouling rates to be measured at lower fuel temperatures than tested here. The design of fuel nozzle TN-C is such that the fuel temperatures necessary to get measurable fouling rates in test times of the order of 10 to 30 hours are much higher than most of the other nozzles tested. Since the presence of DLA and FAME infer potentially different chemical mechanisms leading to deposition, the results would be more meaningful if the fuel temperatures were closer to operational fuel temperatures, perhaps in the range of 300° to 350°F.